INVESTIGATION OF KOYULHİSAR (SİVAS) SETTLEMENT AREA IN TERMS OF SLOPE INSTABILITY

A THESIS SUBMITTED TO
THE GRADUATE SCHOOL OF NATURAL AND APPLIED SCIENCES
OF
MIDDLE EAST TECHNICAL UNIVERSITY

BY

OLGUN HATİBOĞLU

IN PARTIAL FULFILLMENT OF THE REQUIREMENTS
FOR
THE DEGREE OF MASTER OF SCIENCE
IN
GEOLOGICAL ENGINEERING

SEPTEMBER 2009

Approval of the thesis:

INVESTIGATION OF KOYULHİSAR (SİVAS) SETTLEMENT AREA IN TERMS OF SLOPE INSTABILITY

submitted by **OLGUN HATİBOĞLU** in partial fulfillment of the requirements for the degree of **Master of Science in Geological Engineering Department, Middle East Technical University** by,

Prof. Dr. Canan Özgen _____
Dean, Graduate School of **Natural and Applied Sciences**

Prof. Dr. M. Zeki Çamur _____
Head of Department, **Geological Engineering**

Prof. Dr. Tamer Topal _____
Supervisor, **Geological Engineering Dept., METU**

Examining Committee Members:

Prof. Dr. Vedat Doyuran _____
Geological Engineering Dept., METU

Prof. Dr. Tamer Topal _____
Geological Engineering Dept., METU

Prof. Dr. Vedat Toprak _____
Geological Engineering Dept., METU

Prof. Dr. Hüsnü Aksoy _____
Geological Engineering Dept., Hacettepe University

Assoc. Prof. Dr. M. Lütfi Süzen _____
Geological Engineering Dept., METU

Date: 01.09.2009

I hereby declare that all information in this document has been obtained and presented in accordance with academic rules and ethical conduct. I also declare that, as required by these rules and conduct, I have fully cited and referenced all material and results that are not original to this work.

Name, Last name: Olgun Hatiboğlu

Signature:

ABSTRACT

INVESTIGATION OF KOYULHİSAR (SİVAS) SETTLEMENT AREA IN TERMS OF SLOPE INSTABILITY

Hatiboğlu, Olgun

M.S., Department of Geological Engineering

Supervisor: Prof. Dr.Tamer Topal

September 2009, 175 pages

Koyulhisar settlement area is located on the northern flank of Kelkit valley which is seismically active and landslide-prone area. The settlement area was adversely affected from active landslides and some of the houses were evacuated. The purpose of this thesis is to delineate areas where slope instability exists within the Koyulhisar settlement area, and to investigate an active landslide by means of field observations, drilling, sampling, field and laboratory testing, and in-situ monitoring using inclinometer.

Based on the field studies, it is observed that flyschoidal sequence as bedrock and colluvium consisting clay and silt with some gravel are the main lithological units exposed in the study area. Two landslide affected areas are identified, the one investigated due to its adverse effect to some important governmental buildings, has a non-circular failure surface due to the existence of the flyschoidal sequence below the colluvium.

The inclinometer measurements reveal that the displacements are local and their velocities are generally less than 14 mm/year indicating that the landslide is an extremely slow landslide. In addition, high

groundwater table is observed as one of the major parameters in occurrence of landslide.

Keyword: Colluvium, flysch, inclinometer, landslide, Koyulhisar

ÖZ

KOYULHİSAR (SİVAS) YERLEŞİM ALANININ ŞEV DURAYSIZLIĞI AÇISINDAN İNCELENMESİ

Hatiboğlu, Olgun

Yüksek Lisans, Jeoloji Mühendisliği Bölümü

Tez Yöneticisi: Prof. Dr. Tamer Topal

Eylül 2009, 175 sayfa

Koyulhisar ilçe merkezi yerleşim alanı, sismik olarak aktif olan ve heyelanlı saha içerisinde bulunan Kelkit vadisinin kuzey yamacında bulunmaktadır. Yerleşim alanı heyelanlardan ciddi biçimde zarar görmüş olup, bazı evler boşaltılmıştır. Bu tezin amacı; Koyulhisar yerleşim alanında bulunan şev duraysızlığına sahip alanları tayin etmek ve sondaj, örnek alma, saha ve laboratuar deneyleri, ve inklinometre aracılığıyla aktif bir heyelanı incelenmektir.

Saha çalışmalarında, anakaya olarak filişli birimle beraber, kil, silt ve çakıldan oluşan kolüvyon yüzeylenmiş olan ana litolojik birimler olarak gözlemlenmiştir. Heyelandan etkilenmiş olan iki alan belirlenmiş olup, önemli idari binaları etkilemesi nedeniyle incelenen heyelanlardan biri, kolüvyum altında bulunan filişli birim nedeniyle dairesel olmayan bır yenilme karakteri sergilemektedir.

İnklinometre sonuçları deplasmanların yerel olduğunu göstermekte, heyelanın yıllık hız değerlerinin genel olarak 14 mm/yıl dan daha düşük olması, çok yavaş bir heyelan karakterine sahip olduğuna işaret etmektedir. Ayrıca heyelan olan bölgelerdeki yüksek su tablasının, heyelan oluşumunda önemli bir etken olduğu gözlemlenmiştir.

Anahtar Kelimeler: Kolüvyon, filiş, inklinometre, heyelan, Koyulhisar.

To My Family, Melis and Pluto

ACKNOWLEDGMENTS

I would like to express my appreciation to my supervisor Prof.Dr. Tamer Topal for his guidance, supervision and encouragements from the beginning of my Master program.

I would like to present my gratitude to Prof. Dr. Orhan Tatar from Cumhuriyet University for the inclinometer device provided and for the financial support of the project.

I would also like to thank the other members of my committee for their guidance and support.

I am grateful to Çağıl Kolat for her care and valuable helps in the TNT software usage.

This thesis would never be completed without the help of my father Ahmet Tahir Hatiboğlu who accompanied me in the field survey and provided a basis for the format of the thesis.

I am grateful to my brother Can Ulaş Hatiboğlu and my beloved Melis Doğru for their valuable contributions and support during the preparation of this thesis.

Finally, I would like to thank to my mother İpek Hatiboğlu for her love and trust.

TABLE OF CONTENTS

LIST OF TABLES

TABLES

LIST OF FIGURES

FIGURES

CHAPTER 1

INTRODUCTION

1.1. Purpose and Scope

Although landslides or similar slope instability events are considered as less hazardous disasters compare to earthquakes or floods, financial damages and loss of life realized in the past experiences have indicated the severity of this natural event. Individual landslides are not as costly as earthquakes and floods, however they are more widespread and the total financial loss due to slope failures is greater than most of the other geological hazards. Therefore, in planning urban growth, it is essential to assess slope stability and to identify situations where human intervention is likely to cause slope instability. Although many authorities have general restrictions prohibiting building on slopes exceeding a certain slope amount, other effects triggering slope instability should also be considered in landslide assessments to workout a complete urban growth plan.

In this manner, a multi disciplinary investigation is carried out by several research teams from different universities in Turkey under the project name of "Natural Disaster Risk Analysis of Settlements located along Kelkit River on North Anatolian Fault Zone". This investigation involves slope stability assessment of E-W trending Kelkit River area between Koyulhisar and Niksar which is seismically active and a landslide-prone area. Hereby thesis study is also a part of this investigation and has been conducted to delineate areas where slope instability exists within the Koyulhisar settlement area, and to investigate an active landslide by means of field observations, drilling, sampling, field and laboratory testing, and in-situ monitoring using inclinometer.

This study involves landslide assessment of Koyulhisar and the determination of boundaries where displacement has been measured. The investigation is carried out by one of the most accurate inclination measurement device, inclinometer, by taking the measurements in three periods. Beside the information of velocity, direction of displacement and potential threat of slope failure in the study area; inclinometer measurements have also provided useful and handy information in terms of urban growth and evacuation of the buildings.

1.2. Location and Accessibility

The study area is the urbanized section of Koyulhisar settlement area which is located in the eastern Black sea region at the north of E-W extending Kelkit river between latitude 40°17’ and 40°18’ and longitudes 37°48’ and 40°18’ (Figure 1.1). Surrounding settlements are Reşadiye (Tokat) in north west, Mesudiye (Ordu) in north, Suşehri (Sivas) in south east and Şebinkarahisar (Giresun) in east (Figure 1.1). The study area covers more than 0,45 square kilometres and it is included in the 1/25.000 topographic map sheets H39-b4 and H39-b3. Concerning the accessibility, E80 highway is located at the south of the study area next to the Kelkit River; the Koyulhisar road running across the settlement area is directly connected to this highway towards the south of the area. High scaled map showing the boundaries of study area within the settlement area is given in Figure 1.2.

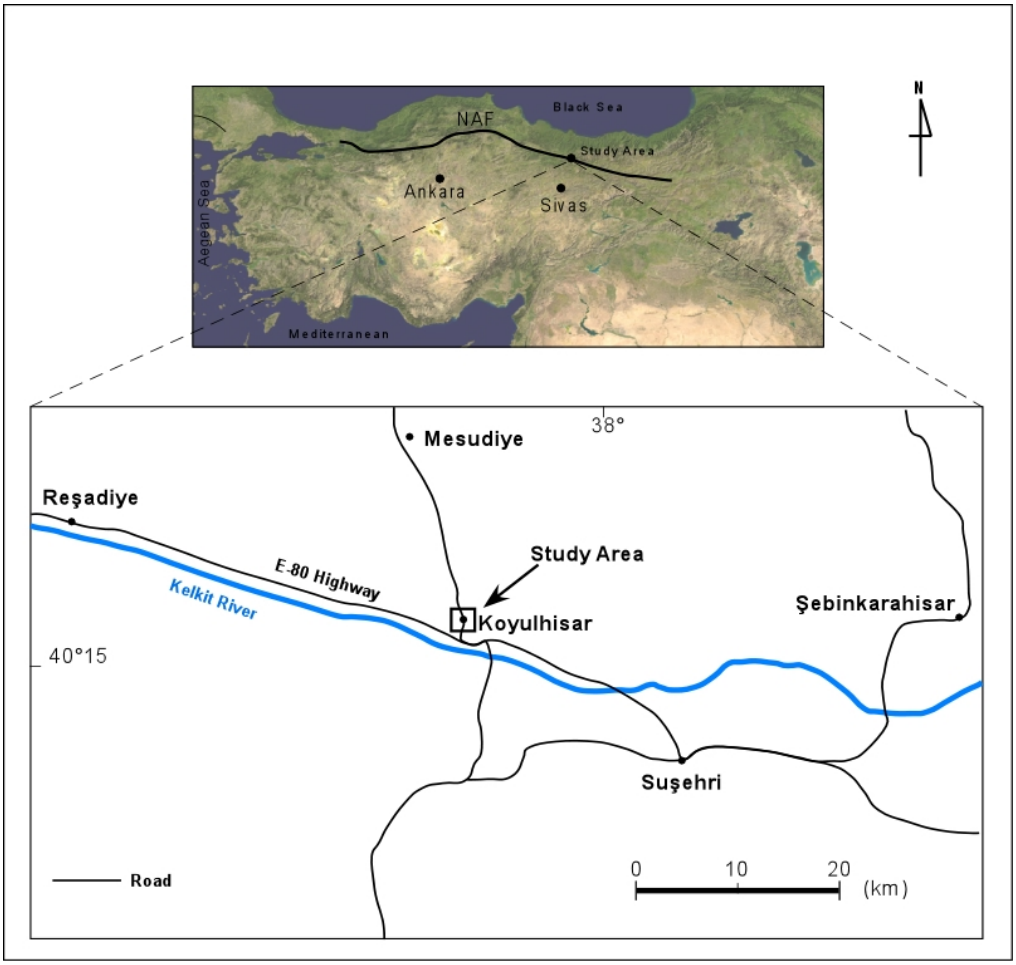

Figure 1.1. Location map of the study area

1.3. Topography

Digital elevation map (DEM) of the study area was constructed by using TNT software (Microimages, 2003) and the topography show an increase from south west through the north east of the settlement area (Figure 1.2). In addition, aspect map and slope map of the study area are prepared (Figure 1.3 and Figure 1.4) considering the significance of slope amount in instability of the slopes. Slope amount vary between 0° and 25° where the settlement is available however, in some parts of the study area, the slope amount seems very high but no structure or building exist at these areas (Figure 1.3). The slope directions are mostly

towards south and west at the study area while the slope direction is toward east at the east and south east of the study area (Figure 1.4).

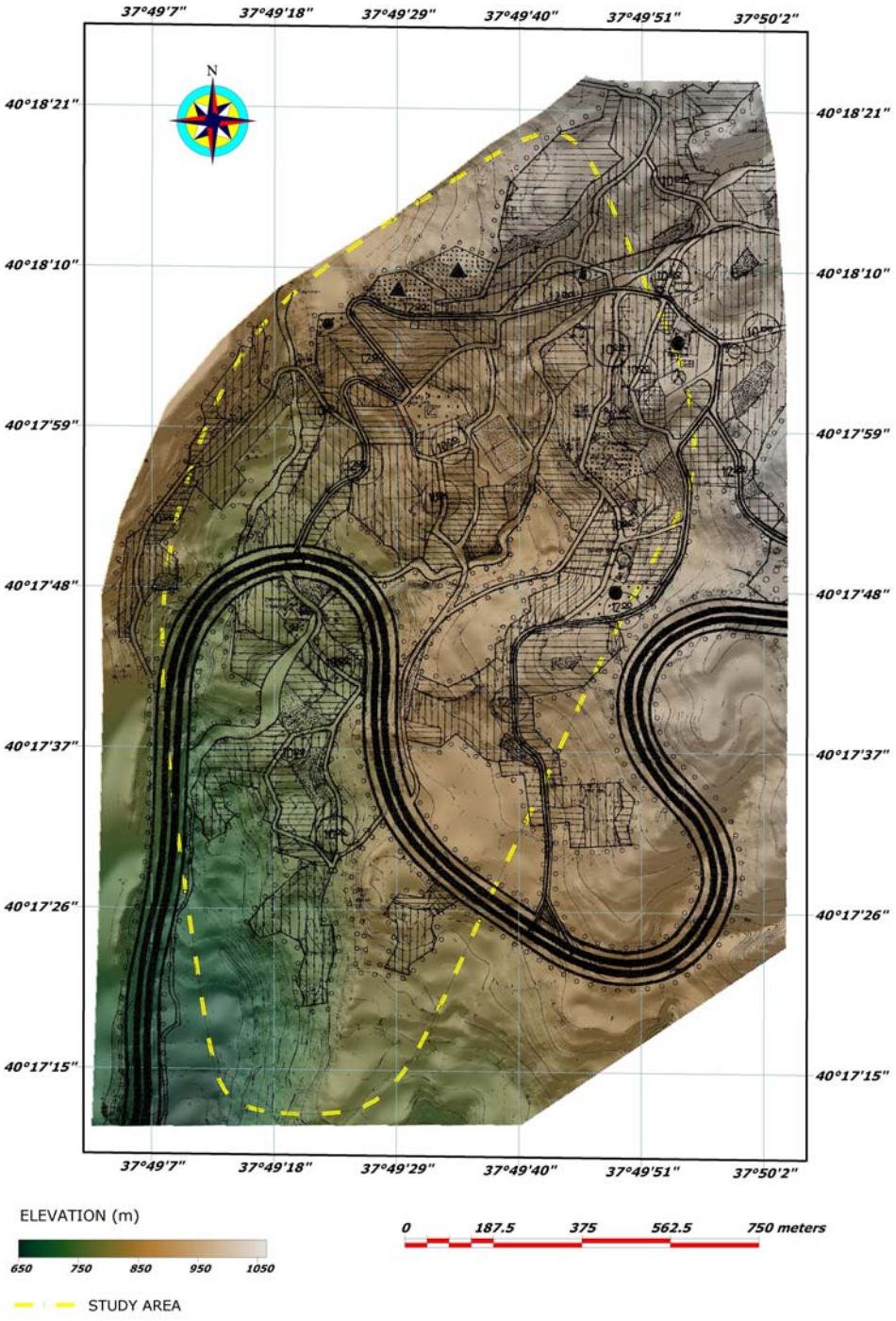

Figure 1.2 Digital elevation map (DEM) of the study area

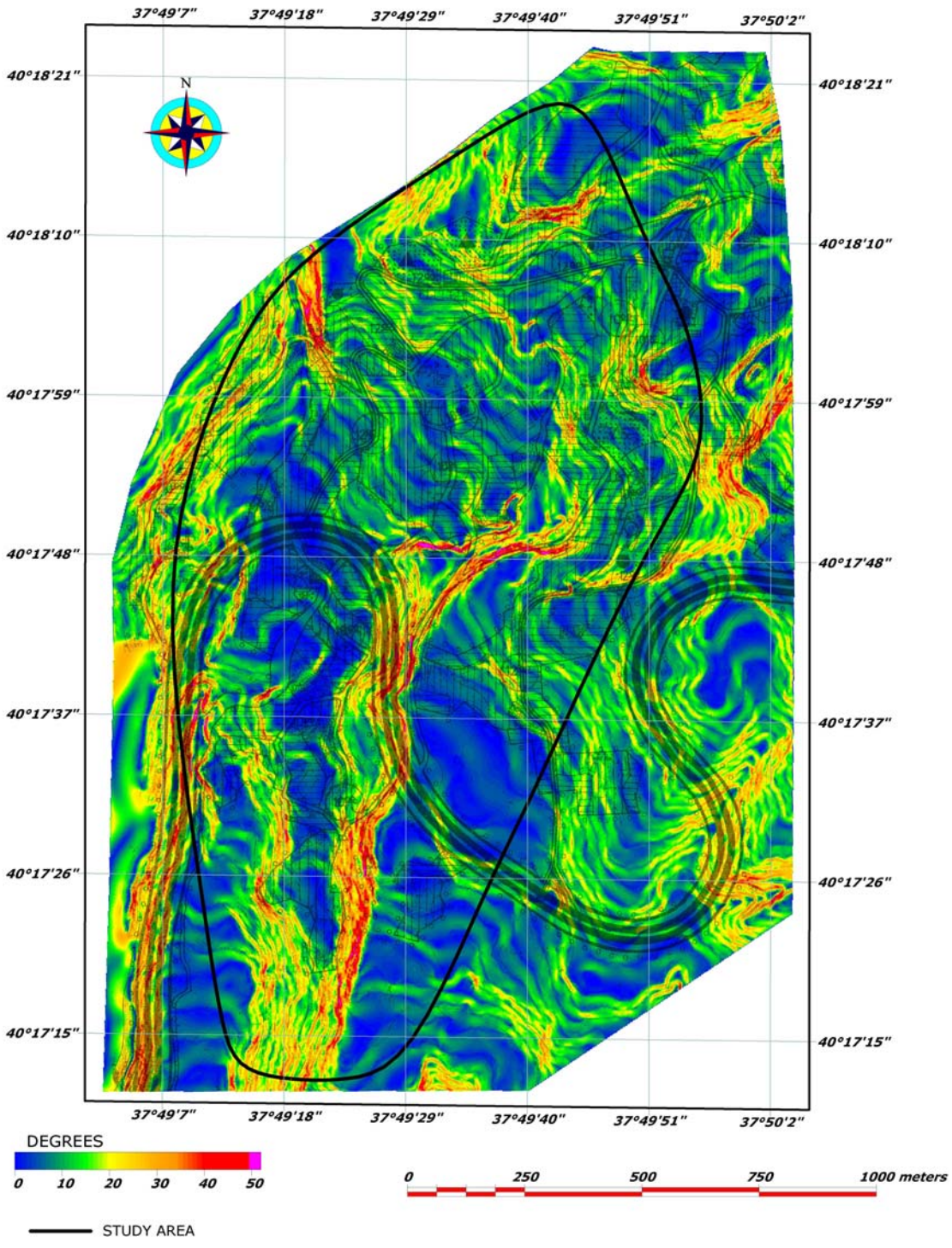

Figure 1.3 Slope map of the study area

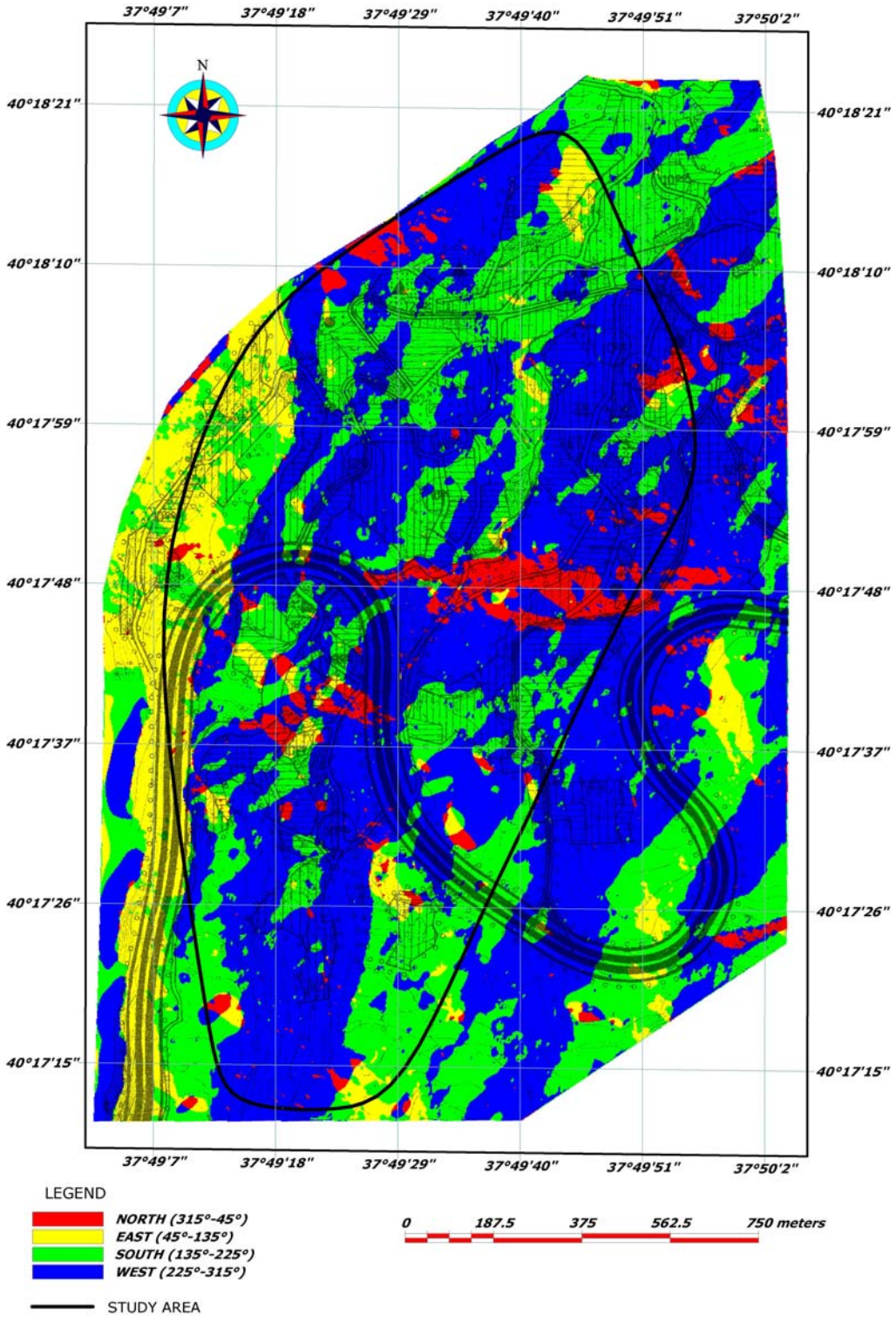

Figure 1.4 Aspect map of the study area

1.4. Climate

Although Sivas is located in Central Anatolia region, Koyulhisar settlement area falls in Eastern Black sea region where rainy and continental climate dominate. In summers, hot and dry weather with cool nights; in winters, cold weather with rain and snow exists. Since the rainfall is one of the most significant parameter in landslide occurrence, precipitation values of Koyulhisar are given in Figure 1.5 between the years 1950 and 1992. Mean annual rainfall in the area is approximately 400 mm and the most intensive period in terms of rainfall is known as May (DMİ, 2008). The minimum recorded value is 265,9mm in 1962 while the maximum value is recorded as 575.1 mm in 1983. On the other hand, the highest average temperature occurred in August with 20,6°C while the coldest occurred in January with -1.9°C through the year (DMİ, 2008). It is recorded that the meteorology station located in Koyulhisar was closed in 1992 after which no data have been received.

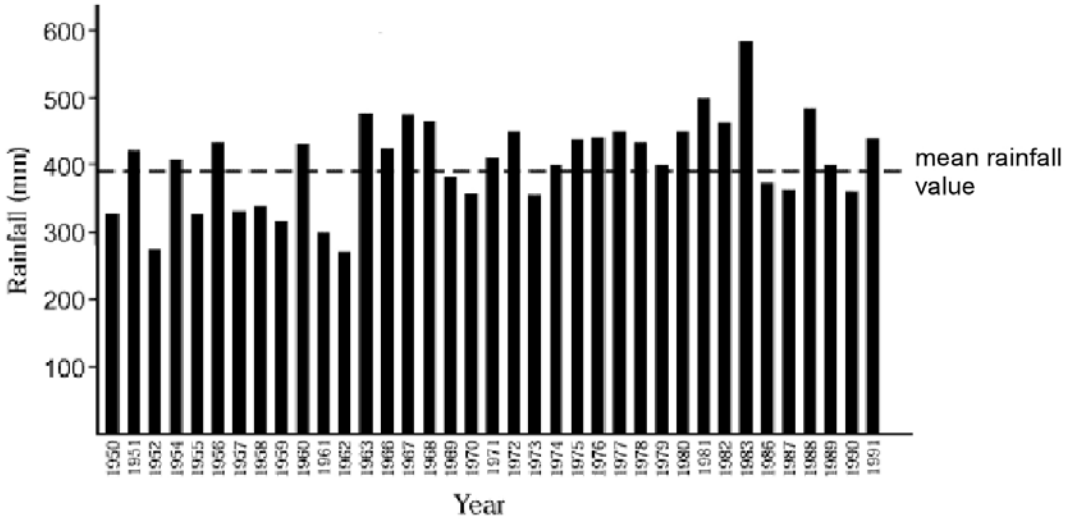

Figure 1.5. Precipitation distribution in Koyulhisar (DMİ, 2008 in Sendir and Yilmaz, 2002)

1.5. Previous Studies

There are a number of studies carried out in Koyulhisar region and in neighbouring area due to the important geological features of the region. Some of these features can be summarized as the presence of mineral deposits, presence of NAFZ and the tectonic evolution of the area. Although most of the papers cover more than one field like mineral deposits, structural geology and stratigraphy, a basic classification is made by dividing previous studies into three groups which are mineral deposits, general geological investigations and structural geology. Major studies carried out until today is summarized in Table 1.1;

Table 1.1. Summary table including all studies carried out in the close vicinity of Koyulhisar

	AUTHOR	YEAR	STUDY AREA	EXPLANATIONS
MINERAL DEPOSIT STUDIES	WESTRUM.H	1961	KOYULHİSAR	LEAD ZINC MINE STUDY IN SİVAS; KOYULHİSAR-SİSORTA AREA KANKOY MURADIN DISTRICT
	OVALIOĞLU.R	1964	KOYULHİSAR	STUDY EXPOSURE DETAIL OF PB ZN CU IN KOYULHİSAR-SİSORTA-MURADINKOY
	ILDIZ.T	1965	KOYULHİSAR	LEAD ZINC PROSPECT STUDY OF THE AREA BETWEEN KOYULHİSAR-SİSORTA-ŞEBİNKARAHİSAR
	PETRASCHECK.W	1967	KOYULHİSAR-SUŞEHRİ	LEAD-ZINC STUDY OF KOYULHİSAR-ŞEBİNKARAHİSAR-SUŞEHRİ; THE AREA LEFT BETWEEN SİVAS AND GİRESUN
	DURRICH.K	1967	KOYULHİSAR	LIGNITE PROSPECT IN SİVAS, KOYULHİSAR BASIN
	KAPTANOĞLU.H	1968	KOYULHİSAR	LEAD ZINC COPPER EXPOSURE AND RESERVE OF SİVAS, KOYULHİSAR-SİSORTA MURADIN VILLAGE
	HOLLICK.C	1971	KOYULHİSAR-SİSORTA	FLOTATION AMENABILITY TESTS ON KOYULHİSAR-SİSORTA PR ZN CU ORE
	AYIŞKAN.O	1971	KOYULHİSAR	BENEFICATION AND RECOVERY STUDIES OF ZINC ORE IN KOYULHİSAR-SİSORTA
	TAKASHIMA.K ET AL.	1974	KOYULHİSAR	GEOLOGY AND MINERALIZATION OF THE FIELD AROUND MENKA MINE, KOYULHİSAR
	ERGUN.A	1975	KOYULHİSAR	GENERAL STUDY REPORT OF POWDER CALCITE RAW MATERIAL IN KOYULHİSAR, SİVAS
	ÖZGÜNEYLİOĞLU.A and AOKABE.K	1981	KOYULHİSAR	LEAD ZINC COPPER ORE EXPLORATION IN SİVAS KOYULHİSAR-SİSORTA-KURŞUNLUKÖY AND ENVIRONS
	ÖZÇİÇEK.H	1986	NİKSAR	LEAD ZINC COPPER ORE IN SİVAS KOYULHİSAR-KURŞUNLU VILLAGE AND ENVIRONS
	AKBULUT.A	1991	REŞADİYE	BENTONITE PRE-PROSPECT REPORT OF NİKSAR-REŞADİYE-TOKAT-KOYULHİSAR AREA
	BOMBA.Z	1993	KOYULHİSAR	DIATOMITE PROSPECTING REPORT OF REŞADİYE-MESUDİYE-SUŞEHRİ-KOYULHİSAR
	ÇAKIR.M and KESKİN.Ö	1998	KOYULHİSAR	REPORT OF GOLD FIELD MINE GEOLOGY OF EVLİYAKENT-ORTAKENT-KOYULHİSAR SİVAS
	STCHEPINSKY.V	1940	KOYULHİSAR	GEOLOGY REPORT OF ZARA-KOYULHİSAR-SUŞEHRİ AREA
	BLUMENTHAL, M.	1950	TOKAT-ERBAA	GEOLOGY OF MIDDLE AND SOUTH YEŞİLIRMAK AREA INCLUDING TOKAT, AMASYA, ERBAA, NİKSAR.
	NEBERT, K.	1961	KELKİT AND KIZILIRMAK RIVER	GEOLOGY OF KELKIT AND KIZILIRMAK RIVERS REGION.
	NEBERT, K.	1964	KELKİT RIVER	GEOLOGY OF NORTH EAST ANATOLIA REGION RIVERS.
	UYGUR.İ	1969	KOYULHİSAR	GEOLOGY AND ORE DEP. EVALUATION OF OLIGOCENE AND MIOCENE FIELDS IN BETWEEN KOYULHİSAR-SUŞEHRİ-ŞEBİNKARAHİSAR
	ALP, D.	1972	AMASYA	GEOLOGY OF AMASYA REGION.

Table 1.1. (Continued)

	AUTHOR	YEAR	STUDY AREA	EXPLANATIONS
GEOLOGICAL STUDIES	SEYMEN, İ.	1975	KELKİT RIVER	GEOLOGICAL AND TECTONIC CHARACTERISTICS OF NAFZ ON KELKİT RIVER AREA
	TATAR, Y.	1978	GEREDE-ILGAZ (NAFZ)	GEOLOGICAL REVIEW IN GEREDE-ILGAZ SECTION OF NAFZ
	ARSLANPAY.D and İÇERLER.A	1979	KOYULHİSAR	GEOPHYSICAL STUDY IN SİVAS, KOYULHİSAR-ORTAKENT-SİSORTA-GÜZELYURT MADENCAMİ VE KURŞUNLU VILLAGE
	TERLEMEZ, İ. and YILMAZ, A.	1980	KOYULHİSAR	GEOLOGY OF THE AREA IN BETWEEN ÜNYE ORDU REŞADİYE KOYULHİSAR KARAÇAYIR HAFİK
	ÖZSAYAR ET AL.	1981	EAST PONTIDE	INTERPRETATION OF CRETECEOUS ROCK OF EASTERN PONTIDES
	PELİN ET AL.	1982	EAST PONTIDE	FORMATION OF RED BIOMICRITES IN EAST PONTIDES
	TUTKUN, S.Z. and İNAN, S.	1982	NİKSAR-ERBAA	GEOLOGY OF THE AREA BETWEEN NİKSAR AND ERBAA
	YILMAZ.A	1983	TOKAT-SİVAS	BASIC GEOLOGICAL PROPERTIES OF TOKAT AND SİVAS REGIONS AND THE ORIENTATION OF OPHIOLITIC MELANGE
	AKINCI, Ö.T.	1984	EAST PONTIDE	VOLCANO-SEDIMENTARY ROCK AND SULPHIDE DEPOSITS OF EASTERN PONTIDES.
	ERCAN, T. and GEDİK, A.	1984	EAST PONTIDE	VOLCANISM IN PONTIDES.
	TERZİOĞLU, M.N.	1985a	REŞADİYE	REVIEW OF EOCENE AGED HASANŞEYH PLATO-BASALTS LOCATED IN NORTH OF REŞADİYE
	TERZİOĞLU, M.N.	1985b	REŞADİYE	REVIEW OF HASANDEDE ANDESITS LOCATED IN NORTH-WEST OF REŞADİYE
	TOPRAK, G.M.V.	1989	KOYULHİSAR	DETAILED GEOLOGIC AND TECTONIC CHARACTERİSTİCS OF KOYULHİSAR
	UYSAL.S	1995	KOYULHİSAR	GEOLOGY OF KOYULHİSAR AREA IN SİVAS
	YILMAZ. I and SENDİR, H.	2002	KOYULHİSAR	STRUCTURAL, GEOMORPHOLOGICAL AND GEOMECHANICAL ASPECTS OF THE KOYULHISAR LANDSLIDES.
	YILMAZ, I. ET AL.	2005	KOYULHİSAR	KUZULU LANDSLIDE FAILURE AND FLOW DEVELOPMENT ANALYSIS
	ULUSAY, R. ET AL.	2007	KOYULHİSAR	GEOTECHNICAL ASSESSMENT OF THE 2005 KUZULU LANDSLIDE
	GÖKÇEOĞLU.C ET AL.	2005a	KOYULHİSAR	KUZULU LANDSLIDE REPORT DATED 17.03.2005 KOYULHİSAR, SİVAS
	GÖKÇEOĞLU.C ET AL.	2005b	KOYULHİSAR	EVALUATION OF THE 17 MARCH 2005 KUZULU LANDSLIDE AND LANDSLIDE-SUSCEPTIBILITY MAP OF ITS NEAR VICINITY.
	NEFESLİOĞLU, H.A. ET AL.	2008	KELKIT RIVER	LANDSLIDE SUSCEPTIBILITY MAPPING OF A PART OF KELKIT VALLEY
	YILMAZ, I.	2009	KOYULHİSAR	A CASE STUDY FROM KOYULHISAR (SIVAS-TURKEY) FOR LANDSLIDE SUSCEPTIBILITY MAPPING BY ARTIFICIAL NEURAL NETWORKS

Table 1.1. (Continued)

	AUTHOR	YEAR	STUDY AREA	EXPLANATIONS
STRUCTURAL GEOLOGY	ERGUVANLI, K.	1951	ZARA-ŞEBİNKARAHİSAR-MESUDİYE	GEOLOGY THE AREA BETWEEN ŞEBİNKARAHİSAR-ZARA-MESUDİYE
	KETİN, İ.	1966	NAFZ	TECTONIC UNITS OF ANATOLIA; ANATOLIDES AND PONTIDES.
	KETİN, İ.	1969	NAFZ	STUDIED THE NORTH ANATOLIAN FAULT ZONE
	AMBRASEYS, N.N.	1970	NAFZ	DISCUSS SOME CHARACTERISTIC OF NAFZ
	KETİN, İ.	1976	NAFZ	A COMPARISON BETWEEN SAN ANDREAS FAULT AND NORTH ANATOLIAN FAULTS.
	ŞENGÖR, A.M.C.	1979	NAFZ	THE AGE, OFFSET AND SIGNIFICANCE OF THE NORTH ANATOLIAN TRANSFORM FAULT.
	ALLEN, C.R.	1982	NAFZ	COMPARAISON BETWEEN NAFZ AND SAN ANDREAS FAULT IN CALIFORNIA
	ŞENGÖR, A.M.C. and CANITEZ, N.	1982	NAFZ	NORTH ANATOLAIN FAULT
	HANCOCK, P.L. and BARKA, A.A.	1982	NAFZ	DISCUSS EVIDENCES FOR LEFT-LATERAL DISPLACEMENT ON NAFZ DURING THE PLIO-PLEISTOCENE
	HEMPTON, M.R.	1982	NAFZ	STUDY ON NAFZ AND COMPLEXITIES OF CONTINENTAL ESCAPE.
	SİPAHİOĞLU, S.	1984	NAFZ	REVIEW OF HISTORICAL EARTHQUAKES BETWEEN 550 B.C. AND 1900 A.D.
	BARKA, A.A.	1984	NAFZ	TECTONIC EVOLUTION OF SOME NEOGEN-KUVARTERNER BASIN AROUND NAFZ
	BARKA, A.A. and HANCOCK, P.L.	1984	NAFZ	STUDIED THE AREA BETWEEN ERBAA AND ÇERKES AND DISCUSS THE NEOTECTONIC DEFORMATION PATTERN IN THE CONVEX-NORTHWARDS ARC OF NAFZ
	BEKTAŞ, O.	1984	EAST PONTIDE	GEOTECTONIC IMPORTANCE OF ŞOŞONİTİK VOLCANISM IN EAST PONTIDES
	ROJAY, B. F.	1985	NAFZ	TECHTONOSTRATIGRAPHIC CHARACTERSITICS OF KELKIT VALLEY.
	YILMAZ.A	1985	KELKIT RIVER	STRUCTURAL EVOLUTION AND GEOLOGY OF THE AREA BETWEEN MUNZUR MOUNTAINS AND KELKİT RIVER
	BARKA, A.A. and KADINSKY-CADE, K.	1988	NAFZ	REVIEW THE GEOMETRY OF STRIKE-SLIP FAULT IN TURKEY AND EVIDENCES FOR LARGE EARTHQUAKES .
	FRIEDMANN, H. ET AL	1988	NAFZ	EARTHQUAKE PREDICTION STUDY ALONG THE NAFZ
	KOÇYİĞİT, A.	1988a	SUŞEHRİ	STUDIED SUŞEHRİ SECTION OF NAFZ WITH GENERAL CHARACTERISTICS AND TOTAL OFFSET OF THE NAFZ
	KOÇYİĞİT, A.	1988b	GEVYE	TECTONIC SETTING OF THE GEYVE BASIN WITH THE AGE AND TOTAL DISPLACEMENT OF GEYVE FAULT ZONE
	KOÇYİĞİT, A.	1989	SUŞEHRİ	FORMATION AND EVALUTION OF SUŞEHRI BASIN WHICH IS AN ACTIVE FAULT-WEDGE BASIN ON THE NAFZ.

Considering the important remarks and conclusions included in some of the studies in terms of lithology, stratigraphy and the structural geology of the region, following major ones are explained with more details among them;

One of the first studies carried out in the study area are the Stchepinsky's study (1940) after the 1939 Erzincan earthquake. Stchepinsky mapped the Zara-Koyulhisar-Suşehri area and made a stratigraphic reconnaissance which specifies an unconformity between Paleozoic Metamorphics and younger sedimentary rocks. Beside these geological observations, he also implied some exposure of lignite in Şıhlar, Chromite in Suşehri and Copper in Zara.

One of the important studies including a basic tectonic outline and a stratigraphical frame work of the neighbouring area around Şebinkarahisar, Suşehri-Şiran is the Nebert's study (1961, 1964). In these studies, he classified the rock units according to the geosynclinal concept.

Ketin (1969) have first observed the basic trend of the fault zone with Ambraseys (1970) from North East Anatolian region to Marmara sea region. Besides observing some surface ruptures of recent earthquake, they have introduced some evidences for right-lateral movement.

Seymen (1975) has submitted two different stratigraphical columnar sections for north and south part of Kelkit River. According to Seymen (1975), Kelkit valley divides the area into two separate blocks which have different lithologies and stratigraphical sections. This difference has been observed by Blumenthal (1950) and Ketin (1966), and defined as Pontides and Anatolides for the north and south part of Kelkit River, respectively. However, Seymen (1975) has defined the blocks as Northern and Southern considering the tectonic properties of the NAFZ. Beside a new stratigraphical nomenclature defined differently from Blumenthal (1950), this study includes a rate of movement of 0,5-0,6 cm per year.

Tatar (1978) concentrated on faults and mechanical interpretation

of them which is carried out around the Erzincan - Refahiye portion of the NAFZ. He suggested that the initial age of the NAFZ is around Early or Middle Miocene, and the total displacement is about 50 km since its first formation.

Şengör (1979), and Şengör and Canıtez (1982) have gathered and evaluated all related information on the NAFZ according to the plate tectonics concept and also discuss the age and origin of the fault zone within the structural framework of Turkey.

Terlemez and Yılmaz (1980) mapped and studied an N-S oriented area which is bounded with Ordu-Fatsa from north and Kelkit valley from south. In this study, detailed stratigraphy of the region which can be applicable to whole Black Sea belt is studied, and the thicknesses of the units starting from Jurassic to Miocene-Pliocene are defined with the total observable thickness of 5525m. Basically, a new stratigraphic reconnaisance has been derived by comparing the observations and columnar sections of Westrum (1960) and Seymen (1975). According to Terlemez and Yılmaz (1980); Paleozoic metamorphics constitute the basement rock which is unconformably overlain by Late Jurassic-Early Cretaceous carbonate platform. This platform is represented as Zinav limestone according to Terlemez and Yılmaz (1980) and Hankırtepe-Kartepe formation according to Seymen (1975). Futhermore they have proved that Lower Cretaceous rocks are unconformably overlain by Upper Cretaceous volcano sedimentary units of volcanic origin, even though Seymen (1975) considers this boundary as a conformable boundary and refers them as Çaltepeleri Group. Eocene is also represented with a volcano-sedimentary sequence which includes conglomerate, sandy-gravelly limestone, andesite and basalt. This sequence is referred to Yeşilce formation according to Terlemez and Yılmaz (1980) and Kavaklıdere Group according to Seymen (1975). Lastly, this formation is overlaid by Miocene-Pliocene andesitic to basaltic volcanics represented as Erdembaba basalts and Canik formation (Terlemez and Yılmaz 1980).

Ercan and Gedik (1984) evaluated the volcanism and made a

correlation of volcanic rocks among all pontide belts. Volcanic occurrences and events have been classified according to their age between Carboniferous to Recent.

Barka (1984), and Barka and Hancock (1984) studied on the NAFZ and the formation of the basin in the region between Erbaa and Çerkes. They suggested a left lateral movement for the fault zone during Pliocene and Early Pleistocene on the basis of evidences gathered from this site.

Koçyiğit (1988a, 1989) studied the Erzincan-Suşehri region of the NAFZ and achieved some important conclusions such as; total offset of 35 km for the NAFZ, 5.5m to 7.5m lateral offset of Erzincan 1939 earthquake, and active fault-wedge character and evolutionary model of the Suşehri basin. Beside this, Koçyiğit (1988b) has studied Geyve basin and defined the total displacement and age of Geyve fault zone.

Toprak (1989) gathered the stratigraphic sequence of all previous works, and made a correlation table which covers a wide E-W trending area of East Pontide. A detailed map of the area is prepared and it is defined that the age of flyschoidal sequence exposed at the North of Kelkit valley between Koyulhisar and Reşadiye is Late Maastrchtien instead of Eocene. Contrary to Terlemez and Yılmaz (1980), a transitional boundary including a thick and coarsening-upward sequence between Upper Creteceaous and Paleocene is identified. Their composition, lithofacies, fossil content and internal structures suggest that the flyschoidal sequence was deposited by a southward retreating sea. Concerning the structural geology of the area, he subdivided the Koyulhisar segment of the NAFZ into five sets. It is defined that two of them, Koyulhisar and Kelkit fault sets make a right-step over and result in the development of a small scale pull-apart basin around Koyulhisar.

Some recent studies related with slope instability around the study area have been carried out by Yılmaz and Sendir (2002) and Yılmaz et al. (2005). First study is mainly concentrated on structural, geomorphological and geomechanical aspects of Koyulhisar landslides while the latter study represents a real case happened in 2005 in Kuzulu

district of Koyulhisar. This paper describes and analyses the results of the detailed surveys in accordance with field and laboratory measurements. According to them, limestone and surficial water and groundwater circulation due to the heavy rainfall are the major causes of this hazard. In addition to these studies, Ulusay et al. (2007) and Gökçeoğlu et al. (2005a) have also studied the same landslide in 2005 and Nefeslioğlu et al. (2008) have prepared landslide susceptibility map of Kelkit valley area. Lastly, Yılmaz (2009) has constructed a landslide susceptibility map by using neural networks. It is recommended to use this method for planners and engineers in the initial assessment of landslide susceptibility.

1.5.1. Reports of General Directorate of Natural Disasters

In order to obtain specific information concerning the landslide mechanism available in the study area and the velocity of the current displacements; reports acquired from "General Directorate of Natural Disasters" are examined and summarized in Table 1.2.

Table 1.2. Summary table of all "General Directorate of Natural Disasters" reports since 1985

AUTHOR	ASSESSMENTS AND EXPLANATIONS
Yılmaz and Yılmaz (1985)	- Stated that the sloping area located at the north of the road (Cumhuriyeti Avenue) cause a landslide due to the water exposed through this field. - Local landslides was observed. - Although no damage on buildings was recorded, ten houses were denominated which seems to be affected by these landslides unless precautions or measures are taken.
Özkan and Demirbaş (1994)	- Same sloping area having a slope of 10 % approximately and located at the north of Cumhuriyet avenue has been investigated. - Artificial and natural water leakages have been observed at the slope. The source of this water might be derived from both rains and water storage tank. - Beside the above mentined factors, it was stated that sewerage system located near the house no.2 has failed several times within this year, this system might be a possible reason for these leakages. - As a result of investigations, it was stated that; 10 houses were indicated as to be affected by landslide and no.2 and no.7 houses should be evacuated. - Lastly, it was stated that remedial measures to reduce water level should be taken by municipality to prevent the displacement.
Öztaşkın and Ataytür (1997)	- Similar comments were made with the report dated 1994. - Cracks and settlements were observed at the same 10 houses and one of the major reason was specified as the wrong foundation construction of these houses. - As in the previous reports, only local sildes were observed and it is emphasized that remedial measures should be taken by municipality to remove the water from the area.
Alkan and Körpe (1998)	- After studying stratigraphy of the area, 3 layers suceptible to landslides were defined which are Miocene and Eocene clayly layers. - It was stated that Paleo landslides were observed throughout the village and circulaire failure mechanism were obsersed in these landslides. - In addition, it was mentioned that all village are settled on a paleo landslide area which have a circulare failure geometry having a 150 meters scarp, 1,5km width and 2 km length. - It was estimated that this mass slides on a lower Miocene clay layer and the sliding surface is located approximately 200 meters depths. - It was stated that this landslide continue its activity not as a mass movement, but local landslides occured on the village surfaces. - Another landslide event located at 2 km North of Koyulhisar (Dumanlı Tepe) was explained and the scarp is specified as 350 meters. - Totally 44 houses have been evacuated (28 Houses from Temi/Subasi district and 28 Houses from Aklan District) due to the creep event occured at Dumanlı Tepe.
Alacahan and Ataytür (2000)	- It was reported that the creep was continuing through Temi and Aklan Mahalle and emphasized the necessity of evacuation as soon as possible.
Kayakıran and Kızıltuğ (2002)	- A detailed previous studies section was included in the report. - Police station, religious school, community center,jail construction were effected from the landslide which prove that the slide continue at the same area since 1985.
Kızıltuğ and Gündoğdu (2005)	- This report was kept further to Kuzulu landslide occured on 17.03.2005. - This year a significant amount of movement was recorded due to the high precipitation rate. - After a detailed examination the structures throughout the village, damaged building and areas affected from landslide are defined in the following three points; **a)** Orta District-Atatürk Avenue.: Cracks with 1-2 cm apertures were observed in five houses and these building are evacuted. Orta District-Tozar street: Breaks in structural columns, cracks with 1-2 cm apertures were observed at this area having a steep slope. Five houses were evacuted. **b)** Camiikebir District-Kızılyeri street: Beside ten houses mentioned in reports dated 07.03.1985, 12.07.1994 and 18.03.1997, three more houses were considered as damaged from landslide. One of them was evacuated due to the serious damage. **c)** Aklan Mahallesi: One more house was decided to be evacuated in addition to the list stated in 25.09.1998.
Şeren and Yılmaz (2006)	- Two houses were added to the damaged building list at Orta District which corresponds to the south of the study area of this thesis. - Landslide boundary was corrected according to this modification.
İleri and Aktan (2007)	- This report include additional investigation on the estimated landslide boundary defined in previous projects. - Two buildings were examined and minor damage was recorded, so no evacuations have been decided. - It was reported that except the area which had been settled on a paleo landslide, there was not any additional active landslide near area.
Eraslan and Uluç (2008)	- It was stated that any new landslide movement was not available except the houses for which the transfer had been requested in previous reports. - As in the previous reports, two buildings were examined and it was decided not to be evacuated although minor damages were available which also confirm the slow velocity and prove the boundaries of local landslide.

1.5.2. Landslide Displacement Measurements Using PSInSAR and GPS Methods

Generally, methods of landslide monitoring can be divided into two main group; surface measurements and subsurface measurements. Inclinometer and rod extensometers are some of the major monitoring methods of sub-surface deformation while cracks and joint measurements, tape extensometers, tiltmeters are in-situ methods to measure surface deformation. In addition to these surface measurement techniques, remote sensing methods are widely used in measuring displacement of landslides and provide significant information on the landslide activity by means of recent technological advances in satellite remote sensing and geographic information system (GIS) techniques. Remote sensing tools, such as satellite images, Global Positioning System (GPS) and interferometry are used in all phases of landslide assessment like detection and classification, monitoring activity of existing landslides, and analysis and prediction of slope failures. Although these methods do not provide subsurface deformations and have lower accuracies compared to inclinometer measurement, these methods are also included in this thesis to evaluate all information available on the deformation in the study area. To sum up, three (3) methods including interferometry, GPS and inclinometer are evaluated together and the differences in terms of resolution, advantages and disadvantages are discussed by checking the similar studies from the literature. In addition, presence of these studies within the same project gives a chance to compare the results with inclinometer measurements.

1.5.2.1. Interferometry and PSInSAR Method

One of these studies is carried out by Çakır (2009) in which a wider area including both northern and southern part of NAFZ has been studied, and the deformation along the fault has been examined. Basically, this method uses phase differences of two satellite images

taken in different dates. This phase difference shows the distance variation between the satellite and the earth surface. In this method, there are four main factors which cause phase difference; 1) Topography, 2) Different view angle, 3) Atmospheric influences and 4) Earth surface movements. First two factors are eliminated by using DEM of the area and detailed positioning information of the satellite. Although some details including annual offset of NAFZ etc. has been considered in the study, it is concluded that it is not possible to measure the deformation along the fault due to the atmospheric effects. However, this study also includes another investigation in Koyulhisar settlement area realized with Permanent Scatterers (PsInSAR) method (Figure 1.6). This method includes finding the pixels having same amount of reflection and the comparison of phase variation in these pixels against time. This method is effective in urban areas where building and man made structures are abundant since these structures are used as the permanent scatterers and make this method useful for the landslide assessment of Koyulhisar.

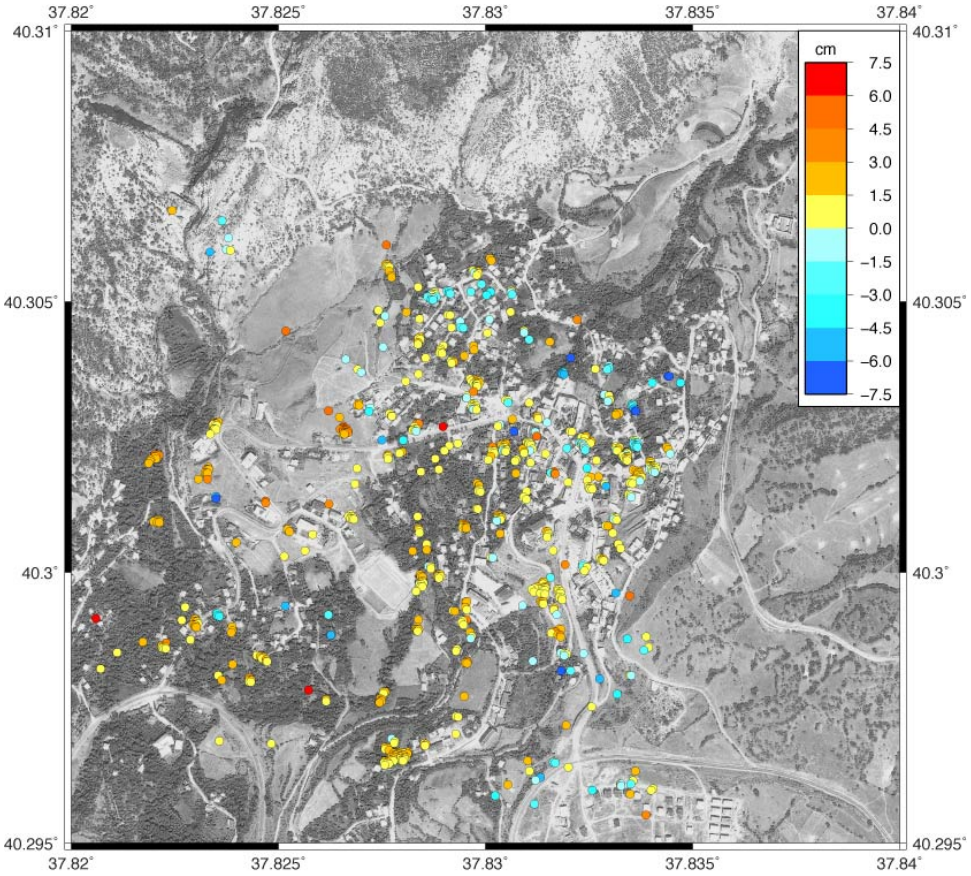

Figure 1.6. Output map constructed by PsInSAR method showing the annual displacement around Koyulhisar (Çakır, 2009)

In order realize a healthy comparison between inclinometer and permanent scatterers method, similar studies in the literature including landslide investigation by both PsInSAR method and inclinometer are examined. In Farina et al. (2006), deformation velocity is measured as 3,4 mm/year by inclinometer while it is found as an average value of 9,5 mm/year by PSInSAR method at the same area. These differences between two sets were arisen by the types of movement (superficial vs. deep deformations) and the low sensitivity of PS measurements to horizontal movements (Farina et al., 2006). Besides, Ferreti et al.(2005) state that there is a good agreement between the two methods in terms of qualitative behaviour which means that the displacement directions and velocity difference between the toe and head of a landslide are

similar. However, the velocities are measured as 9 cm/year and 4,5 cm/year by inclinometer while the deformation on the same points are measured as 4 cm/year and 2,5 cm/year, respectively. So, it is obvious that there is a big difference in the velocity amounts. According to Colesanti et al. (2003), PS method is well suited for wide area and provides low cost monitoring on a high benchmark grid. However, it is emphasized that the usage of other techniques together with PS method increases the reliability.

In Çakır (2009) which is carried out by PsInSAR method, the displacement directions are not specified and the distribution of the deformation throughout the Koyulhisar settlement area does not follow a systematical variation. For example, a very big deformation (60 mm) is available next a small deformed area (15 mm) (Figure 1.6). So, it is not possible to predict a deformation rate of a specific point where displacement information is not available. However, displacements have been calculated in many points distributed around the settlement area and cover almost all the area. The results show a random distribution with a peak value of 6-7.5 cm/year in some parts (Figure 1.6).

1.5.2.2. Global Positioning System (GPS) Method

Hastaoğlu (2009) includes landslide investigation with global positioning system (GPS) method which provides the displacements in three dimensions. The primary objective of this study is to examine an occurred landslide which is located at 2 km in the north of Koyulhisar settlement area center, to confirm its boundaries and to observe the effects of this landslide near area. 12 control points are used, two of them (KH07 and KH10) are located in the landslide and remaining points are located near the boundary and in Koyulhisar (Figure 1.7).

Figure 1.7 Control points used in GPS method for the measurement of annual displacement (Hastaoğlu, 2009)

The results obtained from the measurements taken between April 2007 and November 2008 are as follows (Table 1.3);

Table 1.3. GPS method results for displacement measurement in 11 control points (Hastaoğlu, 2009)

	DISPLACEMENT VALUES MEASURED BY GPS METHOD (mm/year)		
Point no	**NORTH (mm)**	**EAST (mm)**	**HEIGHT (mm)**
KH01	-1.4 ± 6.3	1.1 ± 4.4	-6.9 ± 12.9
KH02	-1.0 ± 6.1	1.5 ± 2.4	0.6 ± 12,3
KH03	-3.4 ± 5.0	4.2 ± 2.6	-9.9 ± 12.0
KH04	-8.6 ± 4.4	-2.0 ± 2.7	-17.0 ± 11.9
KH05	0.5 ± 3.8	6.3 ± 2.6	-2.8 ± 11.8
KH06	-13.7 ± 2.9	-3.7 ± 2.8	-0.3 ± 10.8
KH07	-60.2 ± 2.9	-55.4 ± 3.8	3.8 ± 12.2
KH09	-1.7 ± 4.2	-4.3 ± 4.6	4.5 ± 14.6
KH10	-.1.2 ± 3.25	-2.2 ± 3.9	0.3 ± 12.7
KH11	-0.4 ± 3.35	-16.3 ± 2.8	-4.2 ± 12.0

After the regression analysis of displacement values by evaluating the standard deviations of each control point measurements, above red indicated values are considered valid. So, it is concluded that the remaining results do not provide a significant and certain conclusion except three points which are KH06, KH07 and KH11.

Similar to the interferometry method, related studies which involve an obvious comparison between inclinometer and GPS method are researched and three studies are selected as example. First study carried out by Noferini et al. (2007) indicates a perfect match between GPS and inclinometer measurement in terms of velocity and trend of displacement vs. time curve. Secondly, according to Mora et al. (2003), a conformable result is observed after a comparison between inclinometer and GPS measurements which are 1.63 and 1.57, respectively. Lastly, according

to the study of Gili et al. (2000), a difference of 2 to 3 cm is observed between the two methods, and it is interpreted that GPS values fit well within their own error bar.

1.6. Method of Study

Basically, the studies carried out in this research can be divided into four sections as follows: (1) Available data collection related to the study area; (2) Data collection through field testing and, monitoring and laboratory testing; (3) Analysis of the gathered information using a software and interpretation of the results; (4) Discussions, comparison with other techniques, conclusions with basic recommendation for remedial solutions.

First stage is the office work which contains the collection of background information about the study area. This stage includes literature survey on geology of the area, the collection of information regarding the other studies carried out with different techniques, the seismicity and the climatic conditions of the study area. In addition, reports of "General Directorate of Natural Disasters" are examined to observe the degree and the progression of damages occurred at the study area.

The second step is the field data acquisition and laboratory test stage. Totally 22 drillings were made around the study area and casings were installed in 13 of them to carry out inclinometer measurements while 9 of them are used to measure the depth of groundwater table and to carry out standard penetration test (SPT). SPT test was performed at every 1 meter and totally 181 (58 from groundwater monitoring boreholes and 123 from inclinometer boreholes) disturbed samples were collected during the field study and laboratory tests such as particle size distribution, moisture content, atterberg limits tests were carried out by a service provider company in order to define the soil parameters which will be used in the slope stability analysis. Besides, 11 undisturbed samples

were collected by shelby tubes and unit weight and specific gravity were determined, and UU direct shear test and consolidation test were carried out on these samples. Inclinometer measurements were taken in three periods between 10-11 May 2008, 01-03 November 2008 and 16-18 May 2009.

Third stage involves the interpretation of all data gathered from the first and second sections. Inclinometer measurements were studied by drawing displacement diagrams, and cross sections on which the back-analysis have been conducted, were prepared by using TNT-Mips software by Microimages (2004). Inclinometer results were evaluated to determine the annual velocity of deformation and the boundaries of landslide. In addition, Slide software of Rocscience (2004) is used in order to carry out back-analysis and make an assessment of the soil parameters calculated from laboratory studies.

Finally, based on the evaluations and the characteristics of landslide movement like velocity and the affected zones; current circumstance of the landslide is determined by specifying the boundaries, major triggering factors and risks available in the settlement area. Annual displacement values measured in the same area by INSAR and GPS methods are compared with the values obtained in this study. Then, recommendations were made considering possible threat of the landslide.

CHAPTER 2

GEOLOGY

2.1. Regional Geology

Although the study area covers the urbanized section of Koyulhisar depression (Toprak, 1989) which is a relatively small area compared to the other previous geological studies, brief information on rock associations exposed in the region has been provided in this section.

Basically, the area comprises from the following sequences; the oldest unit is a volcano-sedimentary sequence of Late Cretaceous age which comprises thin bedded, deformed and jointed limestone including interbeds of sandstone, claystone and sandy clay. Paleocene is represented with this volcano-sedimentary unit which has a partly transitional boundary between Upper Cretaceous and Paleocene with a coarsening upward sequence (Toprak, 1989). Eocene is represented by another volcano-sedimentary sequence which overlies Cretaceous-Paleocene rocks with an unconformity. This Eocene sequence involves conglomerate, sandy gravely limestone, basalt, andesite and pyroclastics and overlain by Pliocene continental volcanics. This volcanic sequence comprises mostly basalt, dacite and andesite, and is overlain by younger colluviums of Plio-Quaternary age (Toprak, 1989). Based on the formation of a small scale pull-apart basin around Koyulhisar, the area is filled with the Plio-Quaternary colluviums (Toprak, 1989) and comprises mostly talus and fluvial conglomerates. Lastly, the final sequence is the recent alluviums which are formed by Kelkit River. (Figure 2.1).

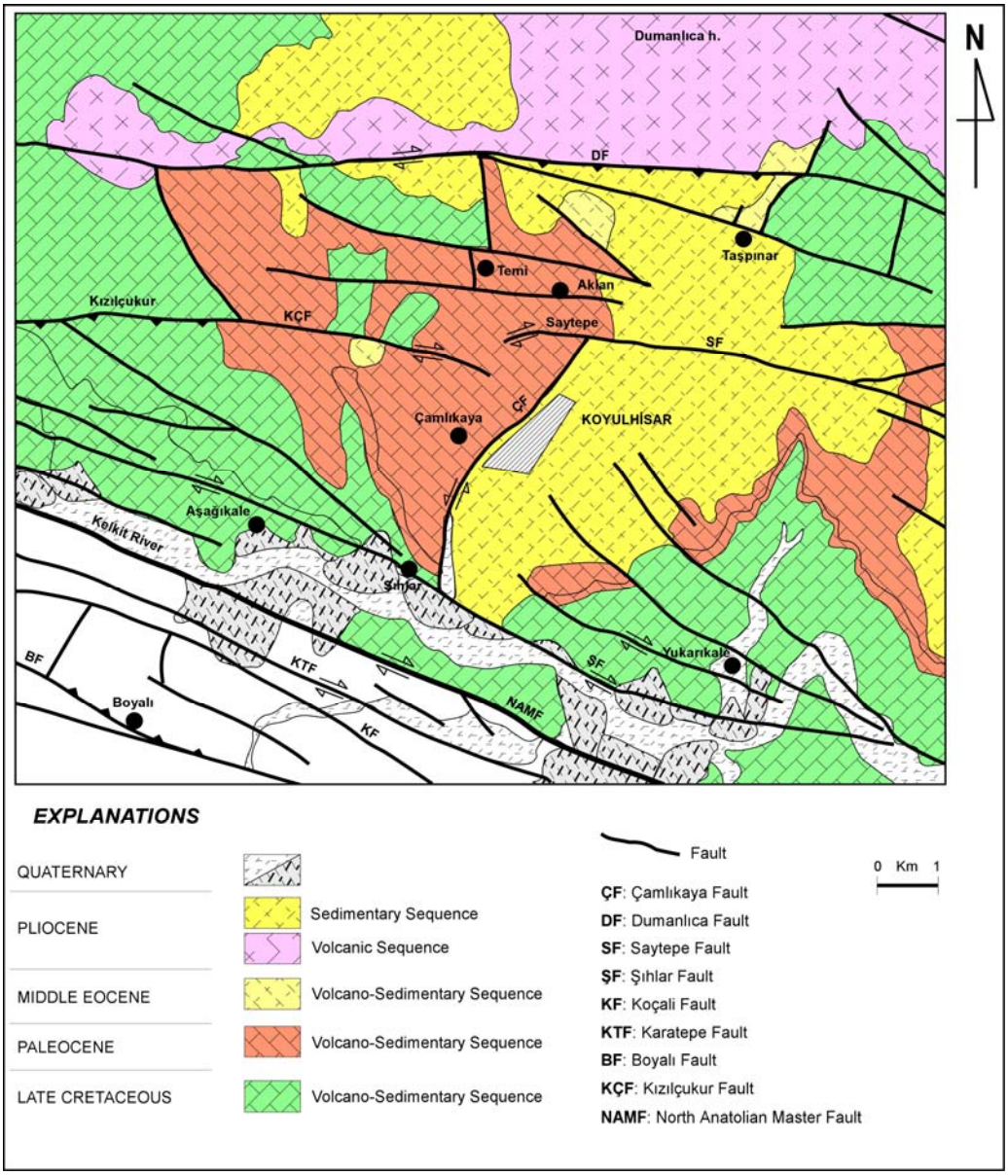

Figure 2.1. Regional geological map of the study area (modified from Toprak, 1989)

Concerning the structural geology and geomorphology of the region; the study area is located in the North Anatolian Fault Zone, so typical active fault zone morphology is observed at the study area. Deep erosion of Kelkit River and perpendicular minor valleys are formed due to the current neotectonic activity, as a result of this, a steep topography has been formed at the north and south of east-west trending Kelkit

River. The Koyulhisar segment of NAFZ is divided into several fault sets and following faults are included near Koyulhisar settlement area (Toprak, 1989). The master fault or the principal displacement zone is the North Anatolian Master Fault (NAMF) along which the great displacements have been observed. Koyulhisar fault set which is located at the north-west part of the study area contains several faults including right lateral east-west trending Dumanlıca fault and Saytepe faults and Kızılçukur fault which forms the southern part of the Koyulhısar fault set. Şıhlar fault set is located at the south of Koyulhisar and it is oriented parallel to the master fault. This single fault bifurcates into a number a short fault segments and converts into a fault set. Kuruçay fault set is located at the southwest of the area, on the southern block of NAMF. It is formed of several short and long fault segments oriented in about 290^{o} direction which is nearly parallel to master fault and include, from north to south, Karatepe, Koçali and Karatepe faults (Toprak, 1989). Lastly Çamlıkaya fault is exposed to the east of Çamlıkaya village and defines the western margin of the Koyulhisar depression. (Toprak, 1989)

2.2. Site Geology

One of the most detailed study concerning the geology of Koyulhisar settlement area has been carried out by Toprak (1989) who prepared a 1/25.000 scaled geological map of this area. Thus, this section of the thesis and the detailed geological map of the region have been prepared based on Toprak's study by combining the field observations of this thesis study and making a comparison between the rock classification of Terlemez and Yılmaz (1980), Seymen (1975) and Toprak (1989).

The details of basement rock associations have been studied in the previous works and these studies have been collected in the correlation chart of Toprak (1989). In the light of this information, following considerations can be done even though these units are not exposed in

our study area; the basement rock is the Paleozoic aged metamorphics which are unconformably overlain by Liassic flyschoidal sequence. Late Jurassic-Lower Cretaceous is represented by platform carbonates which are defined as Zinav limestone according to Terlemez and Yılmaz (1980).

These units are unformably overlain by Upper Cretaceous Volcano-Sedimentary sequence of island arc origin (Toprak, 1989) and defined as Mesudiye and Reşadiye formations according to Terlemez and Yılmaz (1980). However, these formations are reclassified by Toprak (1989) under the Akçaağıl Group which consists of Aşağıkale, Kapaklı, Kızıltepe and Gökçebel formations. The Aşağıkale formation can be observed near Koyulhisar as seen in Figure 2.2. This formation is composed of basaltic lava flow and agglomerate alternation with thin green tuff and sandstone intercalations.

The Late Maastrichtien is represented by İğdir formation (Toprak, 1989) which is characterized by white and yellowish, medium to thick bedded fossiliferous sandy limestone. This formation can be observed in a very small area located at the southwest of the study area. The presence of Paleocene deposits is recorded for the first time in Toprak's (1989) study and these units are divided into three formations as Düdenyaylası, Yalnıztepe and Şıhlar formations from younger to older, respectively. Two formations exposed in the study area are Düdenyaylası and Şıhlar formation which comprise sandstone, conglomerate and limestone with siltstone, mudstone, gypsum intercalations.

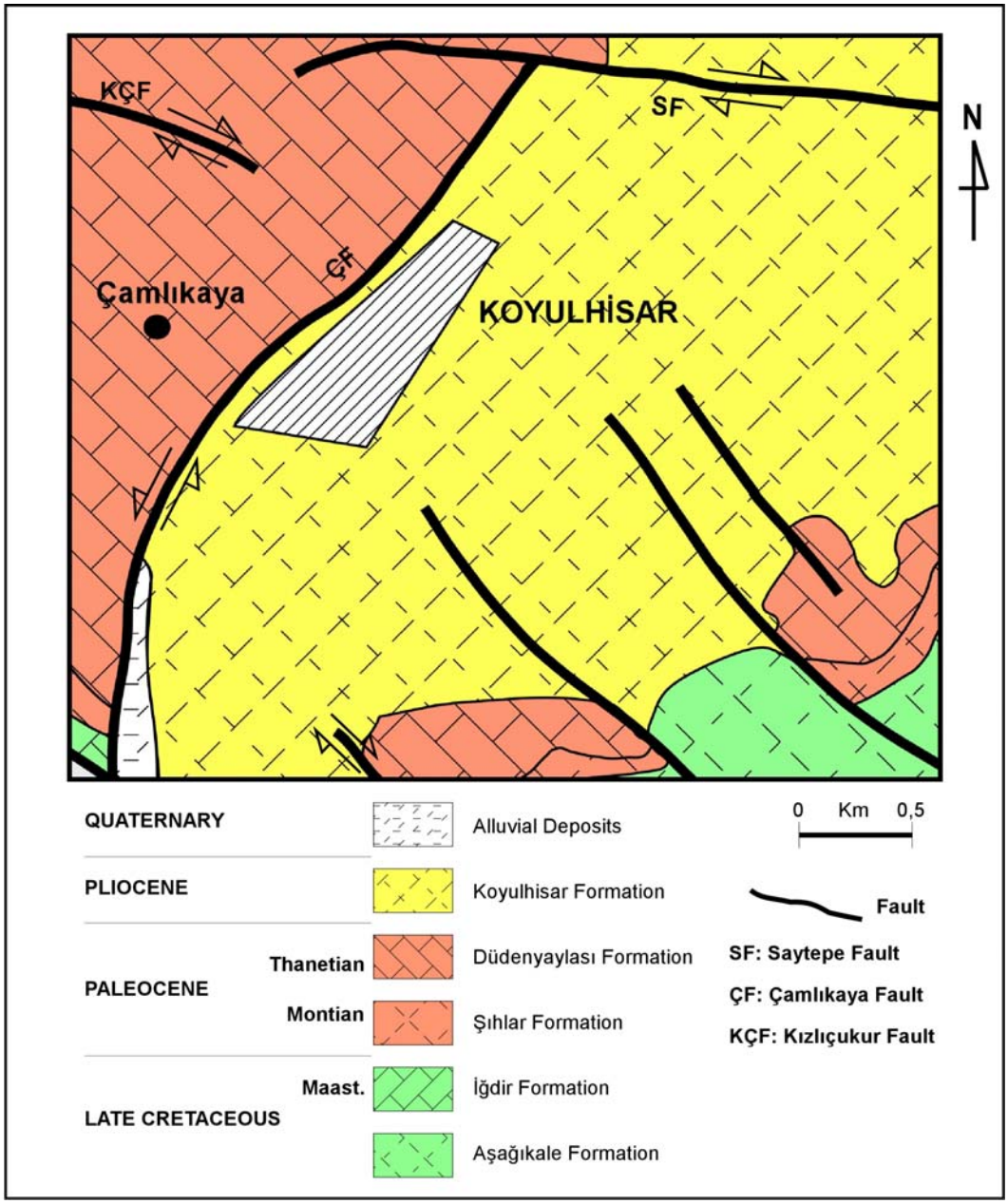

Figure 2.2. Site geology map (Modified from Toprak, 1989)

In the study area, totally two units are observed which are; 1) flyscoidal sequence within the Düdenyaylası formation and 2) colluvium within the Koyulhisar formation. The yellowish-white flyschoidal sequence which includes mostly claystone and mudstone interbedded with sandstone alternations are exposed at the west part of Koyulhisar (Figure

2.3). At the field exposures, the general bedding direction is measured as N23°W/24°NE and bed confined joints are observed at the road cuts. This sequence is composed of Upper Maastrichtien volcano-clastics and the Early Paleocene shallow marine to continental clastics (Toprak, 1989) and involved in the Düdenyaylası formation.

Figure 2.3. A view from flyschoidal sequence

All of the above mentioned rock associations and Pliocene volcanic rocks mentioned in the regional geology section are overlain by younger colluviums which are defined as Koyulhisar formation of Plio-Quaternary age (Toprak, 1989). This unit is the second unit observed in the study area and it is belong to Koyulhisar formation. This formation comprises mostly talus and fluvial conglomerates which have been derived from Pliocene volcanic rocks, and faulted and has erosional contact with older

units. The youngest units are the recent alluviums which are mostly seen in the northern side of Kelkit valley (Figure 2.2). These are clastic materials accumulated from weathering, erosion and mass movements and comprised brownish sandy and silty clay.

2.3. Seismicity of the Region

Koyulhisar is located within the North Anatolian Fault Zone where several subsequent fault zones have been developed. Nearby faults are Şıhlar fault in the south, Çamlıkaya fault in the west and Saytepe fault in the north (Figure 2.1). Koyulhisar is about 3 km away from the master fault which is able to produce an earthquake of magnitude 8 according to Richter scale. The study area is included in the first degree earthquake zone where the peak horizontal ground acceleration is expected to be greater than 0.4g (Kandilli Observatory, 2008). The epicenters of the earthquakes greater than 4 in Richter magnitude since 1900 are shown in Figure 2.4. The earthquakes occurred before 1970 are added to the database by converting the intensity to the related magnitude. The epicenter information are acquired from Kandilli Observatory (2008) while the seismic zones are determined based on the classification of General Directorate of Natural Disasters.

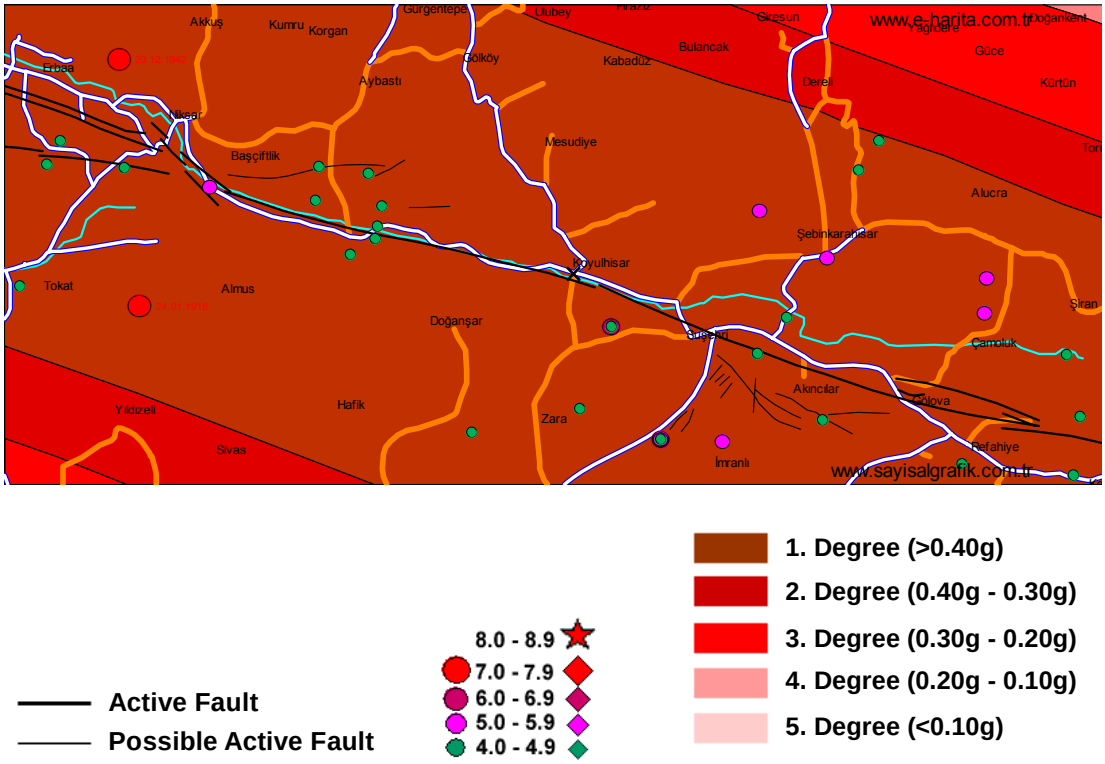

Figure 2.4. Zone of seismic acceleration with epicenters greater than 4 around study area (Kandilli Observatory, 2008)

CHAPTER 3

FIELD AND LABORATORY STUDIES

Koyulhisar is situated on a landslide-prone area. It is settled in a valley and surrounded by a range of mountains higher than 1500 meters. Since the main scope of the study is the landslide assessment of whole Koyulhisar settlement area, this thesis area covers a relatively wider area compared to the other similar studies which examine a specific slope or a local area where a landslide event has been occurred. Therefore, detailed visual examination and accurate estimation of the landslide area become more important to find out the critical points to be examined considering the extensive dimensions of the study area. In this manner, observation of landslide effects on buildings and houses constitute the first stage of the field investigation. At the same time, 1/1000 and 1/5000 scaled topographic map of the county have been acquired from the related division of the municipality and corresponding cross-sections have been prepared. Based on the gathered information and field observations, borehole locations have been defined and a total of 22 drilling have been realized. Some boreholes are used to define water level, take distributed samples and to carry out common in-situ test such as SPT while remainings are used for sampling and inclinometer measurements. Totally 181 disturbed and undisturbed samples were gathered from all of these boreholes, and laboratory tests including determination of unit weight, specific gravity, particle size, moisture content, atterberg limits, consolidation test and direct shear tests were carried out by a service provider company which is "ZEMAR Zemin Araştırma ve Geoteknik" according to the related standards and additional instructions. However, inclinometer measurements and the interpretation of the results constitute one of the major objective of this thesis study, so in this

section, particular interest will be given to the monitoring method.

3.1. Field Studies

3.1.1. Visual Inspection

As the first stage of the investigation, the actual conditions of the buildings and houses were observed and the presence of tension cracks and fissures in the houses and on the ground were checked. The locations of these damages are shown in Figure 3.1 and the photographs taken from these points showing the landslide affected structures are presented in Figure 3.2 thru Figure 3.9. Considering these details including locations and damages of the buildings and roads, Figure 3.10 has been prepared indicating the boundaries of critical areas which are affected from the landslides. Based on this site survey and Figure 3.10, it can be inferred that the instability mostly occurs in certain slopes, not throughout whole settlement area.

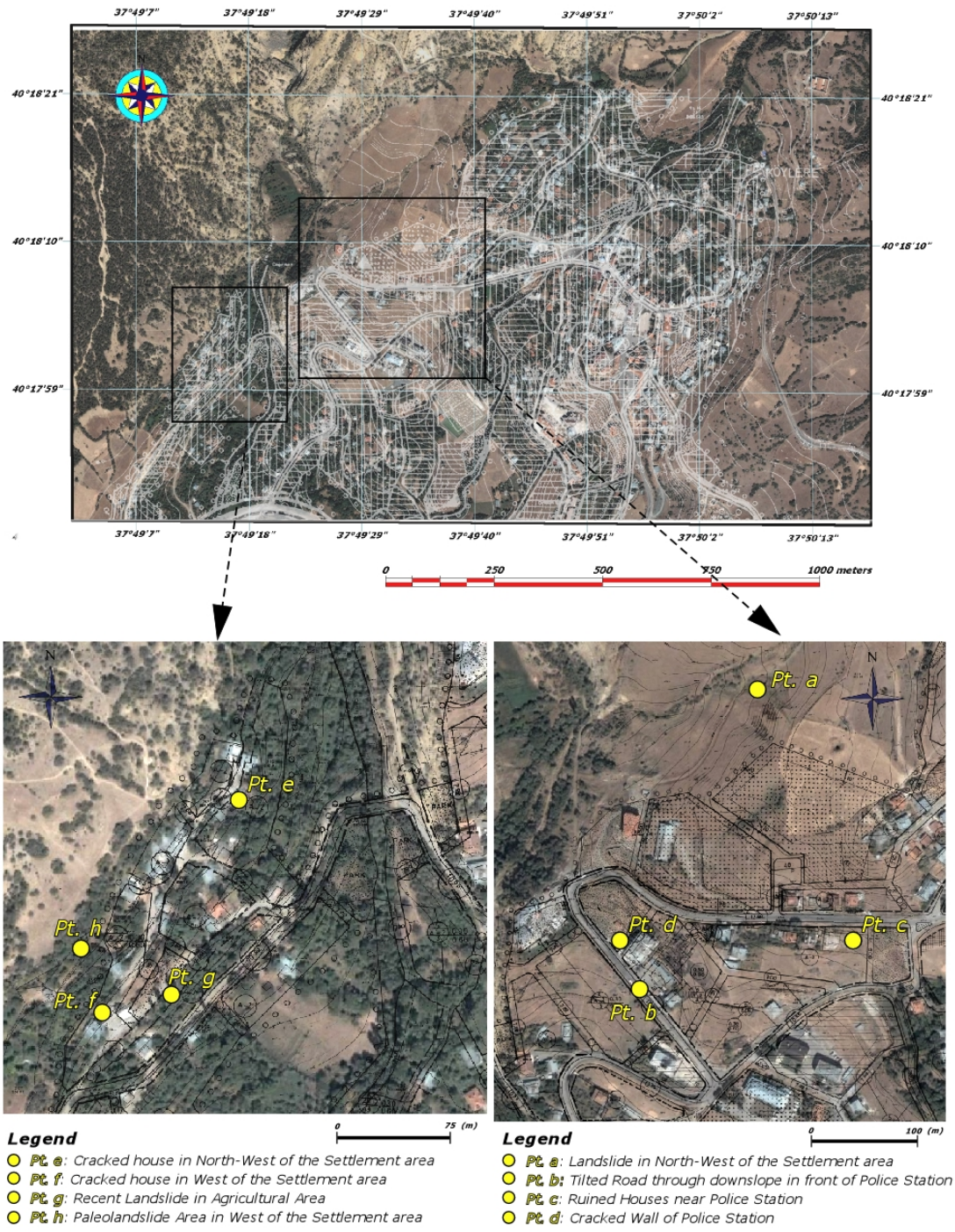

Figure 3.1. Detailed map of areas where damaged buildings exist in Koyulhisar settlement area

Figure 3.2. Landslide occurred in north-west of the settlement area which falls out of the study area (photo taken from point a in Figure 4.1)

Figure 3.3. Deformed road moving toward south direction (photo taken from point b in Figure 4.1)

Figure 3.4. Ruined houses in the settlement area (photo taken from point c in Figure 4.1)

Figure 3.5. Cracks on wall near Police Station (photo taken from point d in Figure 4.1)

Figure 3.6. Cracks on the wall of house located at west of settlement area (photo taken from point e in Figure 4.1)

Figure 3.7 Cracks and fissures on the wall of house (photo taken from point f in Figure 4.1)

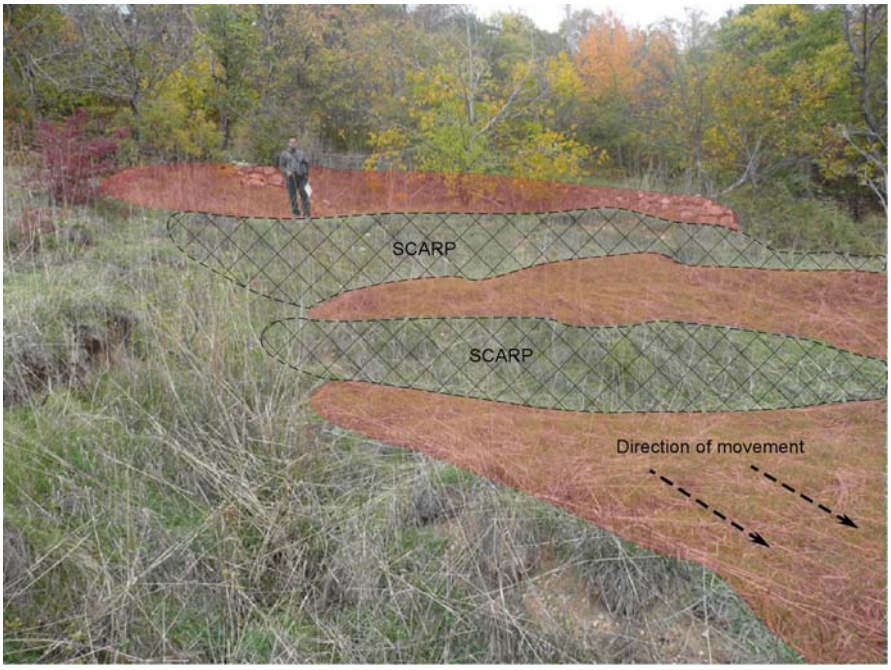

Figure 3.8. Recent landslide effect on topography (photo taken from point g in Figure 4.1)

Figure 3.9. Paleolandslide area at west of the settlement area (photo taken from point h in Figure 4.1)

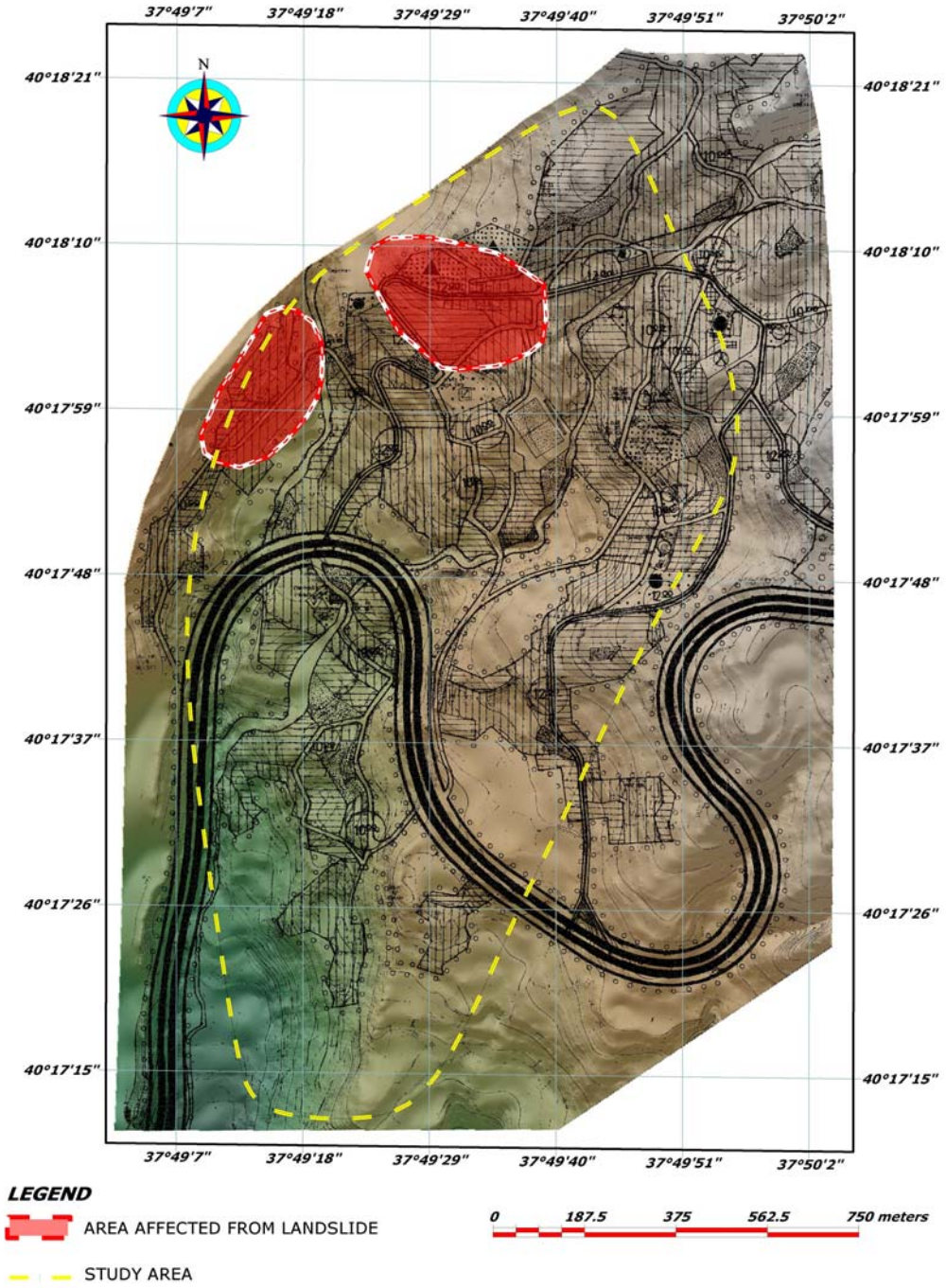

Figure 3.10. Landslide area delineated on the basis of field inspection

When evaluating the landslide affected areas with the constructed slope and aspect map, it can be observed that the slope amount is very

high at the selected area located at the west of study area and the slope direction is mostly toward south and east. However, this selected area is out of urban growth plan of municipality. On the other hand, for the second landslide affected area where important buildings are available like police station and military office, the slope amount is relatively high for a settlement area and the slope direction is mostly south and west at some parts.

3.1.2. Boreholes, In-situ Tests and Sampling

Based on the preliminary survey and future settlement plan of Koyulhisar municipality, critical areas are defined and the locations of boreholes are decided accordingly (Figure 3.11).

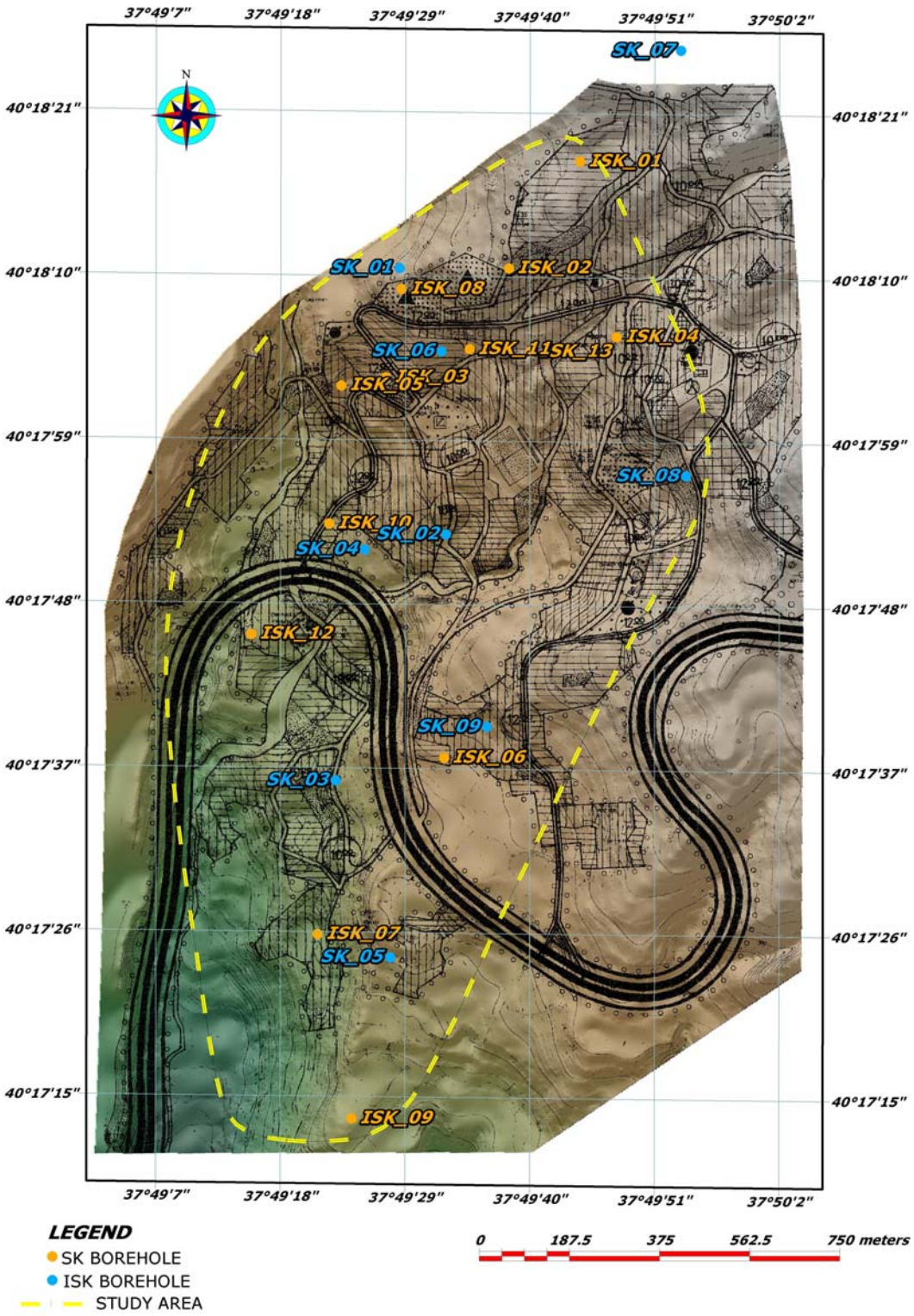

Figure 3.11. Borehole locations in the study area

Depths and coordinate details of all boreholes shown in Figure 3.11 are summarized in Table 3.1. The boreholes are divided into two categories according to the investigation type. ISK boreholes, in which inclinometer casings have been installed, are used to acquire inclinometer measurement in addition to other investigation methods while SK boreholes are used to take samples, define water levels and to carry out common soil tests such as SPT. Totally, 13 ISK and 9 SK boreholes have been drilled by "ZEMAR Zemin Araştırma ve Geoteknik" and standard penetration test (SPT) have been carried out in all boreholes at every 1 meter intervals. In addition, undisturbed samples have been acquired by Shelby tubes from several depths, preferably at every 1 meter intervals where sampling is possible. Thus, a continuous soil profile is achieved.

Table 3.1. Coordinates and depths of SK and ISK boreholes

	Borehole	Coordinates		Borehole Depth	Casing Depth	Elevation
		Latitude/Longitude		(m)	(m)	(m)
WATER BOREHOLES	SK-1	N 40 18 10.499	E 37 49 22.483	22,5	N.A.	894
	SK-2	N 40 17 52.703	E 37 49 32.576	15		833
	SK-3	N 40 17 36.269	E 37 49 21.008	24		796
	SK-4	N 40 17 51.636	E 37 49 25.407	18		818
	SK-5	N 40 17 24.340	E 37 49 27.678	15		820
	SK-6	N 40 18 04.968	E 37 49 32.196	12		875
	SK-7	N 40 18 23.094	E 37 49 48.634	22,5		977
	SK-8	N 40 17 56.816	E 37 49 53.809	21		914
	SK-9	N 40 17 39.843	E 37 49 36.190	15,1		857
INCLINOMETER BOREHOLES	ISK-1	N 40 18 17.763	E 37 49 44.422	20,5	14,5	955
	ISK-2	N 40 18 10.570	E 37 49 38.078	30,2	28,5	924
	ISK-3	N 40 18 03.203	E 37 49 27.292	28,8	26,5	856
	ISK-4	N 40 18 06.063	E 37 49 47.657	13,5	12	907
	ISK-5	N 40 18 02.594	E 37 49 23.390	9,5	8,5	845
	ISK-6	N 40 17 37.739	E 37 49 32.443	9,8	8,5	850
	ISK-7	N 40 17 25.821	E 37 49 21.311	9,6	5	770
	ISK-8	N 40 18 09.122	E 37 49 28.696	18,8	17	893
	ISK-9	N 40 17 13.523	E 37 49 24.310	15,6	12,5	795
	ISK-10	N 40 17 53.346	E 37 49 22.271	21	19,5	807
	ISK-11	N 40 18 05.156	E 37 49 34.697	30,5	29	875
	ISK-12	N 40 17 45.886	E 37 49 15.456	23	21	795
	ISK-13	N 40 18 05.005	E 37 49 40.026	41,5	40	892

As one of the most important parameter in slopes' stability, water level measurements have been taken in the same periods together with the inclinometer measurements (Table 3.2). Highest groundwater level is observed in May 2009, during the last inclinometer measurements when the average water level is peak due to the high infiltration rate after a snowy and rainy season. The measurements taken at this season are considered during the analysis since the highest level of the water table represents the worst case in the stability of slopes which makes it suitable for an accurate analysis in long term. Groundwater table map is prepared based on the gathered groundwater levels (Figure 3.12).

Table 3.2. Groundwater table depths measured in three periods

	Borehole	Casing depth	Groundwater table depths		
			May-08	Nov-09	May-09
		(m)	(m)	(m)	(m)
WATER BOREHOLES	SK-1	N.A.	19,6	21,2	17,2
	SK-2		-	-	-
	SK-3		20,4	23,7	18,1
	SK-4		-	-	-
	SK-5		-	-	-
	SK-6		-	-	10,6
	SK-7		-	-	-
	SK-8		-	-	-
	SK-9		-	-	-
INCLINOMETER BOREHOLES	ISK-1	14,5	10,5	12,2	8,7
	ISK-2	28,5	16,1	18,7	14,7
	ISK-3	26,5	5,6	7,5	2,1
	ISK-4	12	-	-	-
	ISK-5	8,5	-	-	8,8
	ISK-6	8,5	-	-	-
	ISK-7	5	4,5	-	3,4
	ISK-8	17	5,7	6,5	4,6
	ISK-9	12,5	9,5	12,3	8,4
	ISK-10	19,5	4,2	6,5	2,3
	ISK-11	29	8,5	10,6	6,4
	ISK-12	21	5,6	8,7	4,2
	ISK-13	40	21,2	24,3	20,1

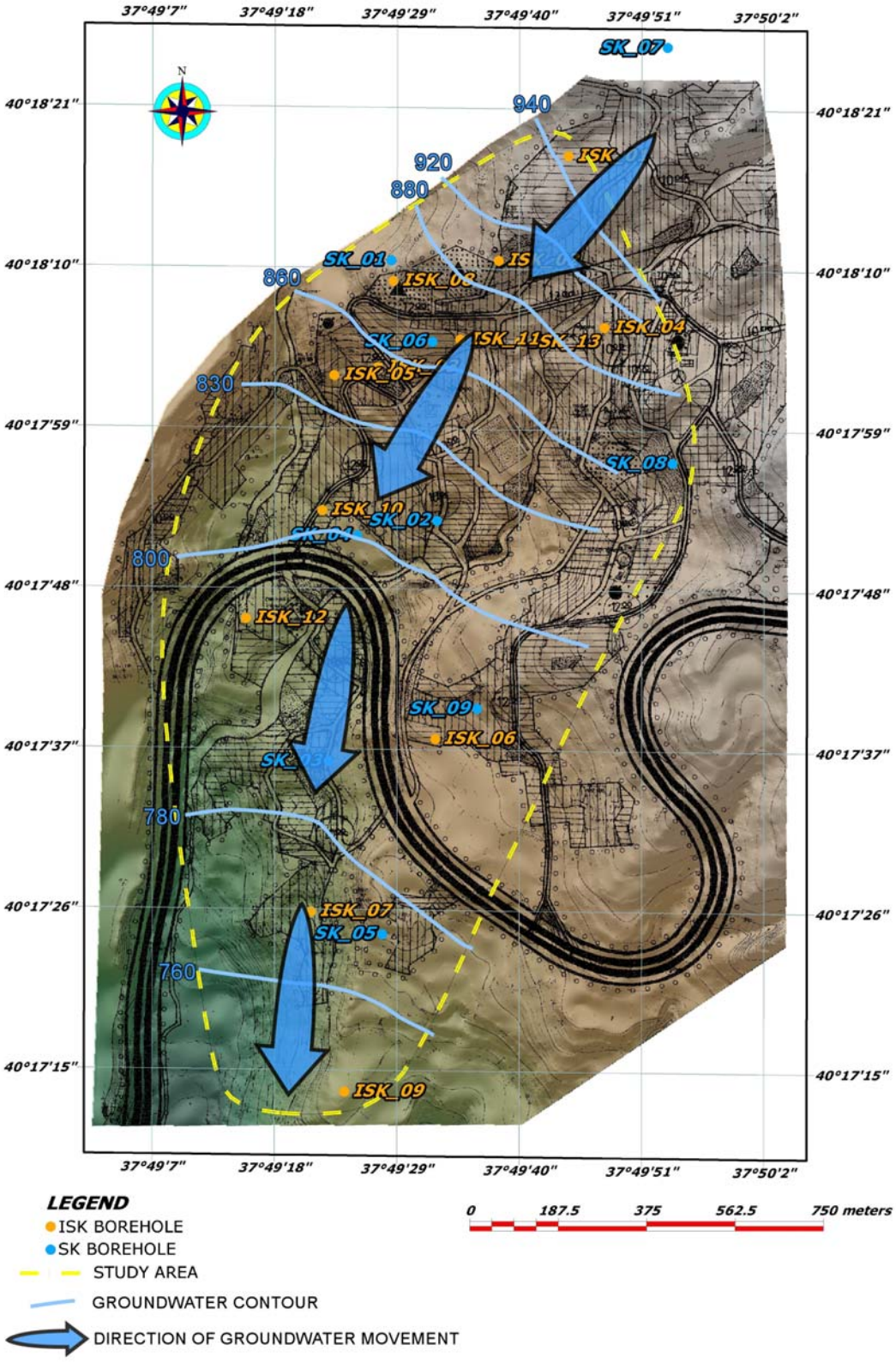

Figure 3.12. Groundwater contour map

As seen from Table 3.2, groundwater level is very shallow in some parts of the study area, especially the depth from the ground surface reaches to 2 and 3 meters in the landslide affected area. Based on the Figure 3.12, the groundwater table follows the topography, beginning from high altitude area through the valley plain which is located at the south of settlement area.

Resulting logs of ISK and SK boreholes including the SPT results and other soil parameters are prepared as shown in Figure 3.13 and logs of all SK and ISK boreholes are supplied in Appendix A.

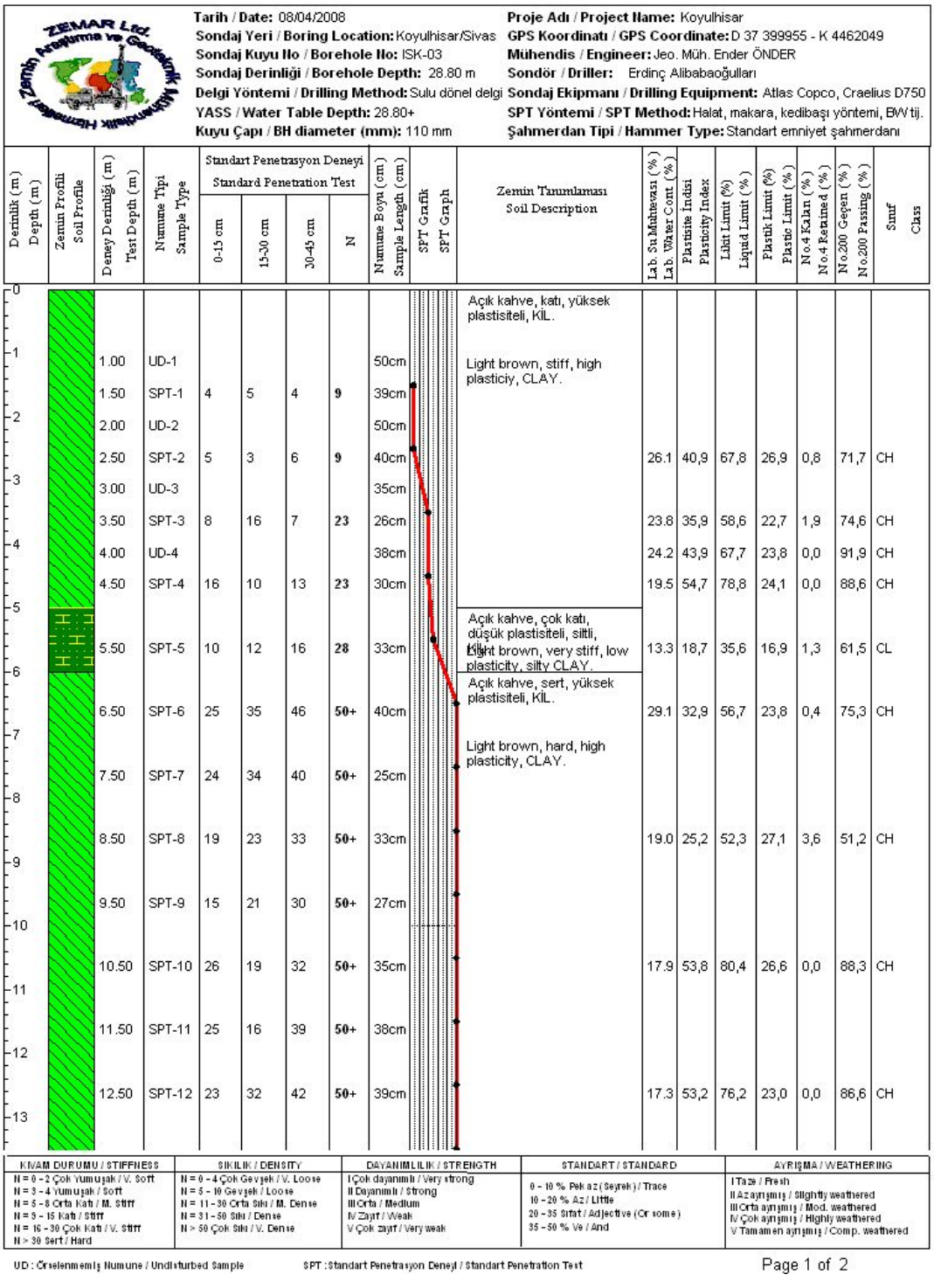

Deney Derinliği (m) Test Depth (m)	Numune Tipi Sample Type	0-15 cm	15-30 cm	30-45 cm	N	Numune Boyu (cm) Sample Length (cm)	Lab. Su Muhtevası (%) Lab. Water Cont. (%)	Plastisite İndisi Plasticity Index	Likit Limit (%) Liquid Limit (%)	Plastik Limit (%) Plastic Limit (%)	No.4 Kalan (%) No.4 Retained (%)	No.200 Geçen (%) No.200 Passing (%)	Sınıf Class
1.00	UD-1					50cm							
1.50	SPT-1	4	5	4	9	39cm							
2.00	UD-2					50cm							
2.50	SPT-2	5	3	6	9	40cm	26.1	40,9	67,8	26,9	0,8	71,7	CH
3.00	UD-3					35cm							
3.50	SPT-3	8	16	7	23	26cm	23.8	35,9	58,6	22,7	1,9	74,6	CH
4.00	UD-4					38cm	24.2	43,9	67,7	23,8	0,0	91,9	CH
4.50	SPT-4	16	10	13	23	30cm	19.5	54,7	78,8	24,1	0,0	88,6	CH
5.50	SPT-5	10	12	16	28	33cm	13.3	18,7	35,6	16,9	1,3	61,5	CL
6.50	SPT-6	25	35	46	50+	40cm	29.1	32,9	56,7	23,8	0,4	75,3	CH
7.50	SPT-7	24	34	40	50+	25cm							
8.50	SPT-8	19	23	33	50+	33cm	19.0	25,2	52,3	27,1	3,6	51,2	CH
9.50	SPT-9	15	21	30	50+	27cm							
10.50	SPT-10	26	19	32	50+	35cm	17.9	53,8	80,4	26,6	0,0	88,3	CH
11.50	SPT-11	25	16	39	50+	38cm							
12.50	SPT-12	23	32	42	50+	39cm	17.3	53,2	76,2	23,0	0,0	86,6	CH

Figure 3.13. Sample Log of ISK-03 (See Appendix A for complete logs)

In the study area, flyschoidal sequence is observed as bedrock and it is overlain by colluvium which consists of clay, silt, sand and gravel. On the other hand, both units mostly constitute clay, silt and gravel sized particles and involve sand and clay alternations. SPT values and the variation with the depth indicate the boundary between flyschoidal sequence and colluvium. The levels, where SPT refusal was encountered and continues consistently down to the bottom of the borehole, correspond to the flyschoidal sequence. However, SPT values obtained in shallow depths where colluvium exists are smaller and vary between 25 and 40 number of blow (N). In general, the boundary between the units is mostly observed between 3 to 10 meters depths according to the logs (Appendix A).

3.1.3. Inclinometer Measurements

A portable inclinometer, produced by Soil Instruments Co. and provided by Cumhuriyet University is used as the primary instrument for the displacement monitoring of the ground. This instrument is widely used in determining the magnitude, rate, direction, depth, and the type of landslide movement. Basically, it monitors deformations of the casing which provides a profile of subsurface horizontal deformation. As movement along the slip surface occurs, the vertical casing deforms in the direction of movement and causes to move the casing with ground motion from its initial position. The rate, depth, and magnitude of this displacement can be calculated by comparing the initial survey data with the subsequent surveys.

In consequence of the preliminary prospect, 13 inclinometer casings specified as ISK boreholes are installed to the suspected zones with the guidance of the municipality where lateral movement may occur or a strong indication of displacement might be available. Measurements have been taken in three different periods which are 10-11 May 2008, 01-03 November 2008 and 16-18 May 2009 respectively. These dates are

decided according to the precipitation amount in different seasons. Last measurements were taken in May 2009 after winter when high rate of rain and snow melts are expected. By this way, it was possible to observe the effects and influences of ground water to the instability of the slopes.

3.1.3.1. Quality Factors Affecting Inclinometer Data

The slope inclinometer installation and measuring processes involve several important factors affecting the measurement results. As one of the most important factor, the bottom of the inclinometer must be located well below the potential zone of movement. The inclinometer will not capture the total amount of movement in case the inclinometer casing does not pass through the failure surface. In other words, the borehole will be too shallow to distinguish the failure and can cause confusion about the failure depth of the slide (Figure 3.14). Because of this reason, it was decided to drill the inclinometer boreholes deep enough.

Beside this factor, the direction of casing slots should also oriented preferably parallel to the direction of the estimated landslide movement so that the displacement can be obtained in one component of the displacement vector, otherwise the total vector should be calculated from the two components of the displacement vector. In this study, the slot directions are mostly oriented toward the downhill which is the most probable direction for a potential movement.

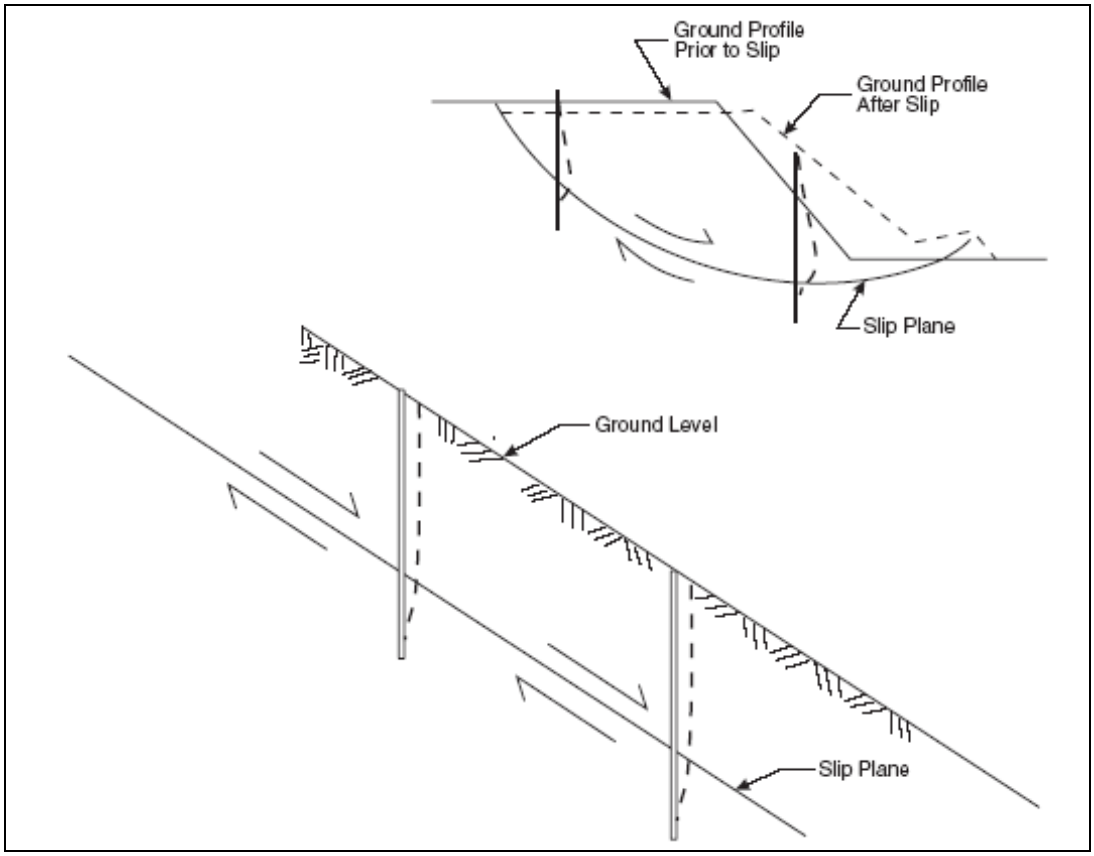

Figure 3.14 Critical casing level examples which are deeper than failure surface (Slope Indicator, 2008)

3.1.3.2. Inclinometer Data and Interpretation

The inclinometer probe does not measure the horizontal movement of the casing directly. As shown in Figure 3.15, the probe measures the tilt of the casing then this parameter is converted to the horizontal displacement by the relation;

Horizontal displacement (Deviation from vertical) = L x sin θ;

where the angle θ is the angle of tilt measured by the inclinometer probe and L is the measurement interval which is taken as 0,5 meters in this study.

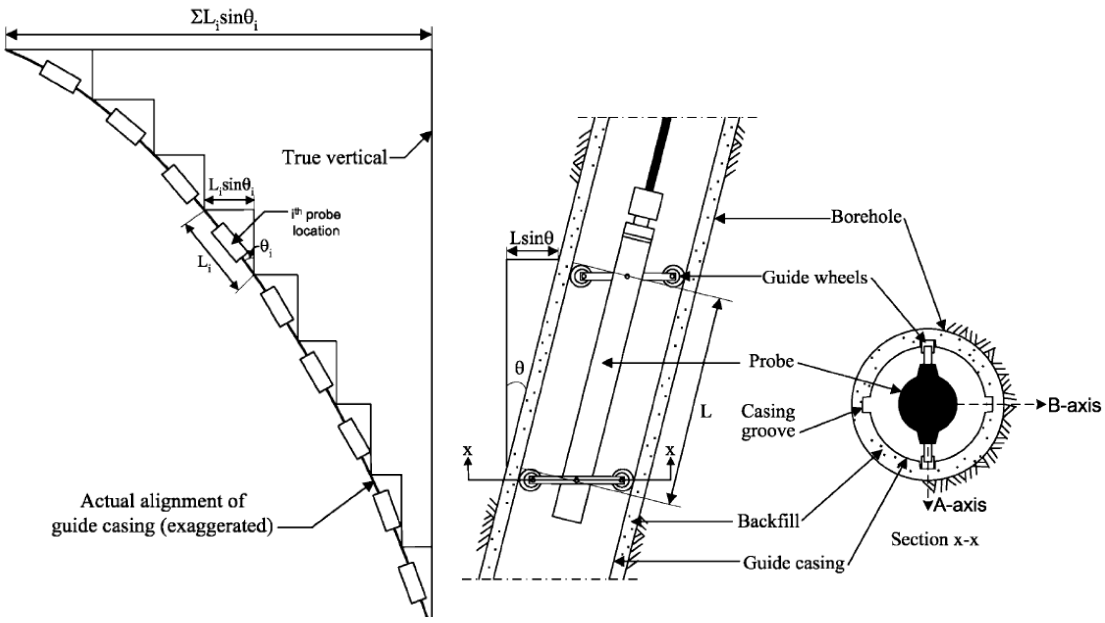

Figure 3.15. Measured parameters in inclinometer measurements (Stark and Choi, 2008)

The total horizontal displacement described as cumulative displacement is derived by summing the individual lateral deviations from bottom to top of casing. As seen in Figure 3.16 a, the cumulative horizontal displacement profile provides a representation of the actual deformation pattern of the casing. However, incremental displacements versus depth variations are also plotted to show movement at each measurement interval. This plot is useful to figure out the location of a potential deformation zone, a sudden change in this trend indicates the location of movement and the failure plane (Figure 3.16 b). Therefore, the incremental deflection and cumulative horizontal displacement profiles of each borehole are provided in Appendix B. Among three measurements which have been taken in 10-11th of May 2008, 01-03th of November 2008 and 16-18th of May 2009, the first one is indicated as a vertical line which is the reference one for the subsequent readings.

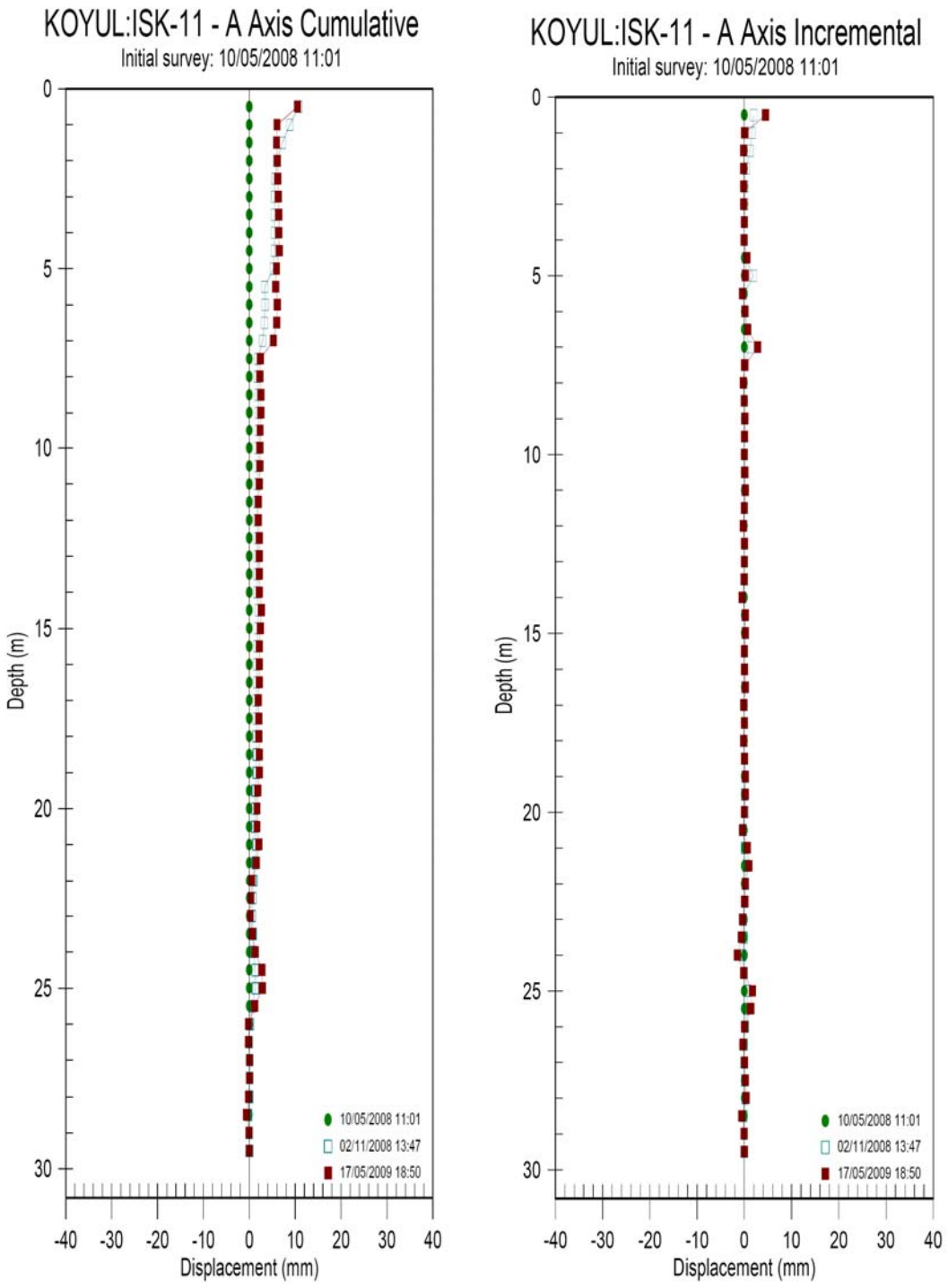

(a) (b)

Figure 3.16 Inclinometer data plotted in terms of (a) cumulative displacement and (b) incremental deflection

Based on the cumulative and incremental plots, following results for each borehole are obtained (Table 3.3);

Table 3.3. Results of inclinometer measurements

CASING BOREHOLES	A0 DIRECTIONS	EXPLANATIONS /INTERPRETATIONS
ISK-1	115°	No displacement has been observed.
ISK-2	195°	No displacement has been observed.
ISK-3	240°	Approximately 5mm displacements have been observed at the depths of 3, 16 and 25 meters.
ISK-4	170°	Approximately 3mm of smooth displacement has been observed along the casing starting from 11th meter depth.
ISK-5	170°	Smooth displacement (up to 6mm) has been observed starting at the 4th meter from the surface.
ISK-6	175°	No displacement has been observed.
ISK-7	195°	Minor displacement of 1-2mm has been observed, can be considered negligible.
ISK-8	150°	Approximately 4-5 mm of smooth displacement has been observed starting from the 11th meter of depth.
ISK-9	250°	Approximately 2.5-3 mm of displacement has been observed along the B-axis, perpendicular to slope direction.
ISK-10	230°	Approximately 2.5-3 mm of displacement has been observed at the 12th meter depth from the surface.
ISK-11	183°	Approximately 7-8 mm and 10 mm of sudden displacements have been observed at the 1st and 7th meter depths respectively.
ISK-12	220°	No significant displacement has been observed
ISK-13	215°	Approximately 7-8 mm of sudden displacements have been observed at the depths of 13, 17 and 32 meters.

Above interpretations are made according to the cumulative displacement behaviour of A0 axis corresponding to the the slope direction, the resultant displacements are calculated by the vector summation of both direction A0 and B0.

When the inclinometer results and logs of the boreholes are examined together, it is observed that the displacements occurred both; 1) between two units, colluvium and flyschoidal sequence, and 2) within

the colluvium. In some boreholes such as ISK-08 and ISK-05, failure levels mostly point out the depths where SPT values become refusal which corresponds to lower boundary of colluvium. On the other hand, displacement is also observed in clayey and silty layer. Based on this interpretation, it is inferred that the failure developed within the study area has a non-circular geometry.

In addition to the above mentioned plots, plan views of displacement axis are also provided in Appendix B to show the direction of displacement vectors (Figure 3.17). By this interpretation, we are able to see the orientation of displacement vectors involving both A and B axis components. Indication of these vectors on the map gives important clues concerning the direction of displacement in certain slopes of the settlement area (Figure 3.18).

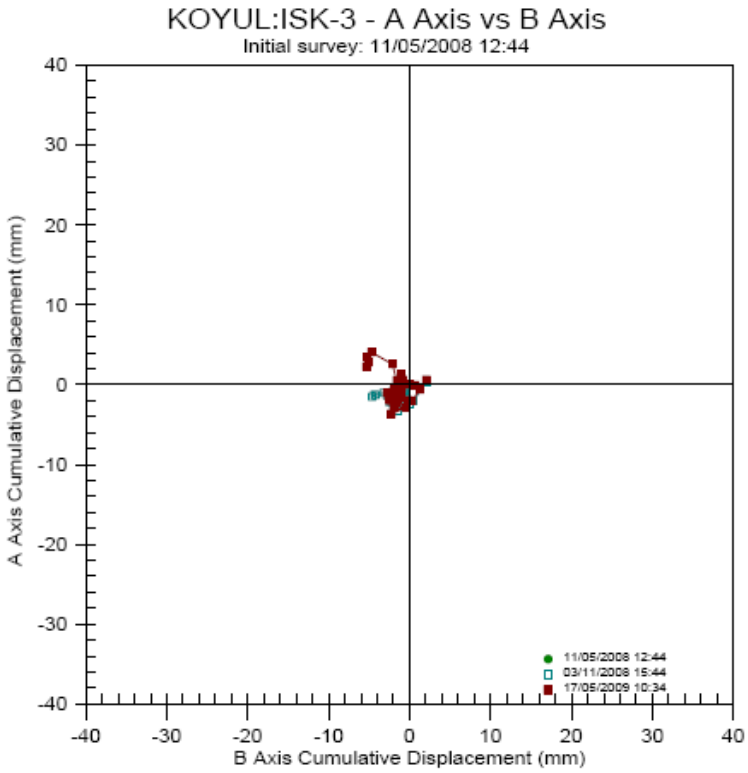

Figure 3.17. Inclinometer output of ISK-11 in plan view

Based on the above plan representation, displacement vectors are calculated considering both components and they are indicated in the Figure 3.18 and the annual displacement velocities for each borehole where deformation is available are shown in Table 3.4. The movement directions are mostly through downhill as estimated in the previous stages. However, the reason of the movement observed in ISK-09 is explained as insufficient waiting time for automatic temperature compensation of the probe. Some small variations can be observed in this method due to this reason.

Table 3.4. Calculated annual displacement velocities in ISK borehole points

CASING BOREHOLES	ANNUAL DISPLACEMENT VELOCITIES (mm/year)
ISK-1	-
ISK-2	-
ISK-3	7 mm
ISK-4	3,6 mm
ISK-5	6,7 mm
ISK-6	-
ISK-7	-
ISK-8	7,8 mm
ISK-9	-
ISK-10	-
ISK-11	14,1 mm
ISK-12	-
ISK-13	8,4 mm

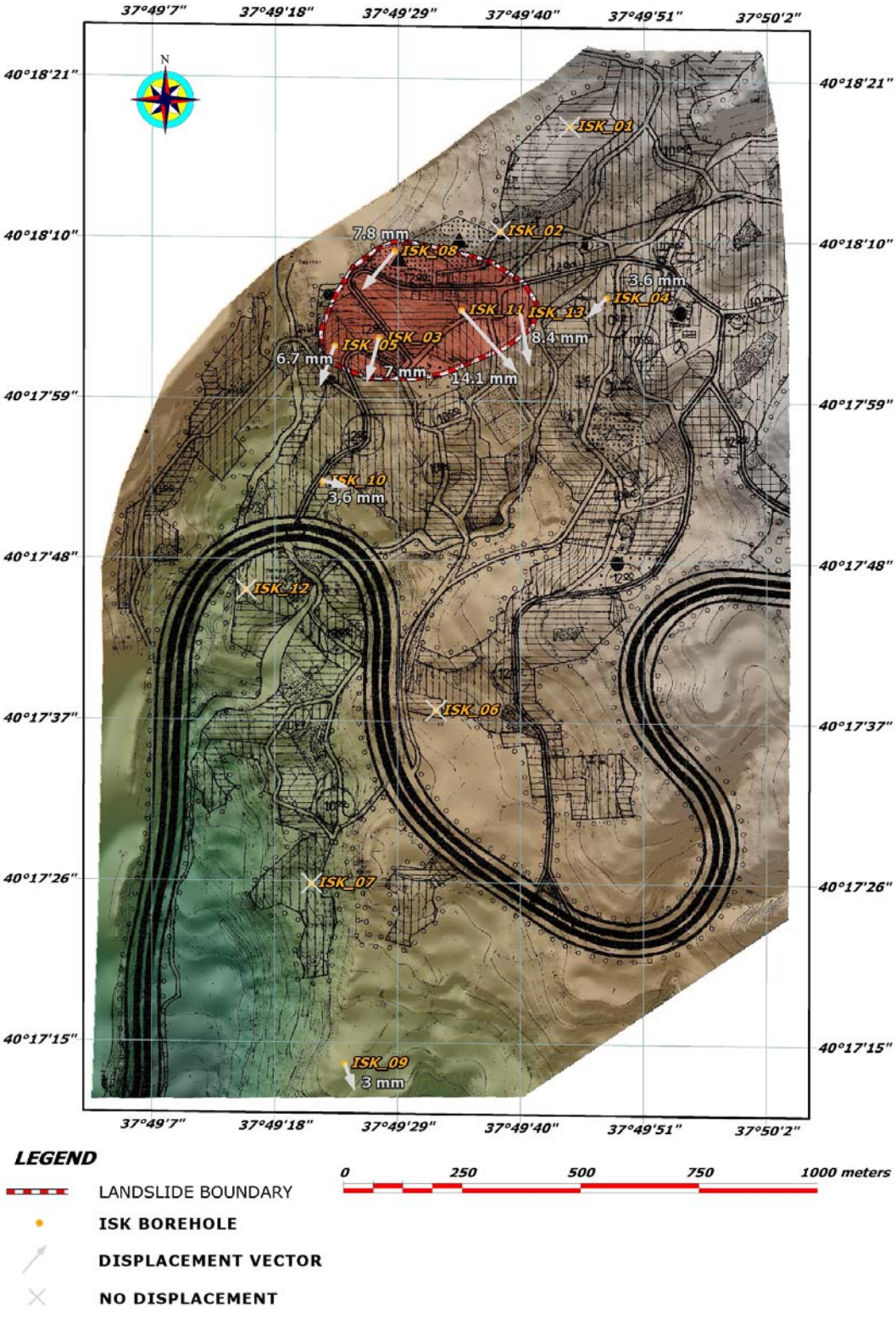

Figure 3.18. Displacement vectors derived from inclinometer data

3.2. Laboratory Studies

Soil laboratory tests including sieve analysis, atterberg limits and moisture content are carried out on all samples gathered from SK and ISK boreholes. On the other hand, unit weight, specific gravity and consolidation tests are performed on undisturbed samples which have been taken from boreholes SK-1, SK-8, SK-9, ISK-2, ISK-3, ISK-4, ISK-5, ISK-7 and ISK-8. In addition to these tests, direct shear test is carried out under consolidated-drained conditions in order to determine the shear strength parameters of the soil. All tests are carried out in the laboratory of "AKADEMİ Zemin - Jeolojik Jeoteknik Ltd. Şti." company. Brief information concerning these tests is provided in this section and the results are supplied in "Logs" and "Laboratory Test Results" in Appendix A and Appendix C, respectively.

3.2.1. Specific Gravity and Moisture Content

Unit weights of the samples are given in the Table 3.5. Dry densities of the samples are determined by the simple pycnometer device according to the ASTM D 854 (2004) standard and the results gathered from these tests are presented in the following table (Table 3.6);

Table 3.5 Unit weights of the samples

Borehole No.	Sample No.	Depth (m)	Unit Weight (kN / m3)	Average Unit Weight (kN / m3)
SK-1	UD-3	3,50	17,81	17,86
SK-1	UD-9	9,50	17,58	
SK-1	UD-12	12,50	17,47	
SK-1	UD-15	15,50	17,67	
SK-7	UD-3	3,50	18,08	
SK-7	UD-6	6,50	17,90	
ISK-3	UD-4	4,00	17,81	
ISK-4	UD-2	2,00	18,10	
ISK-5	UD-3	3,00	17,88	
ISK-7	UD-3	3,00	18,15	
ISK-8	UD-3	3,00	17,95	

Table 3.6. Specific gravity of the samples

Specimen No	Specimen Depth	Mass of Pycnometer	Mass of Pycnometer + Soil Specimen	Mass of Pycnometer + Soil Specimen + Water	Mass of Pycnometer + Water	Specific Gravity (Gs)
	(m)	(g)	(g)	(g)	(g)	Gs
SK-1 / UD-3	3,5	135,25	285,25	765,49	672,07	2,65
SK-1 / UD-9	9,5	141,69	291,69	768,02	674,52	2,65
SK-1 / UD-12	12,5	130,76	280,76	764,55	670,74	2,67
SK-1 / UD-15	15,5	123,93	273,93	757,09	662,43	2,71
SK-7 / UD-3	3,5	135,25	285,25	766,32	672,07	2,69
SK-7 / UD-6	6,5	141,69	291,69	768,9	674,52	2,7
ISK-2 / UD-7	7	134,09	284,09	762,53	671,36	2,55
ISK-3 / UD-4	4	83,42	233,42	680,02	585,27	2,71
ISK-4 / UD-2	2	127,91	277,91	719,91	626,28	2,66
ISK-5 / UD-3	3	135,25	285,25	766,52	672,07	2,7
ISK-7 / UD-3	3	141,69	291,69	768,05	674,52	2,66
ISK-8 / UD-3	3	130,76	280,76	764,95	670,74	2,69

As it can be observed form Table 3.5, average unit weight value is calculated as 17,86 kN/m^3. Beside, as per in the Table 3.6, the determined specific gravity values of the samples range between 2,55 and 2,71. The average value of specific gravity is calculated as 2,67 and the standard deviation is determined as 0,044 accordingly. The variation among the calculated values is very small except the specimen taken by ISK-2 borehole which is 2,55.

Moisture content of the samples was determined according to ASTM D 2216 (2004). Basically, this is the percentage ratio of water in the sample to the dry weight of the sample. Moisture content values are calculated from 196 disturbed and undisturbed samples which have been taken from different boreholes. The average moisture content is calculated as 19,2 % and the standard deviation is determined as 3,73 %. It is observed that there is not any specific relation among the depth of the specimen and its moisture content (Table 3.7). The percentages of each specimen are also specified in Laboratory Test Results (Appendix C).

Table 3.7. Moisture content values of the samples

ISK Boreholes	Moisture Content	SK Boreholes	Moisture Content
	%		%
ISK-1	18,27	SK-1	19,01
ISK-2	18,95	SK-2	-
ISK-3	22,81	SK-3	26,10
ISK-4	16,12	SK-4	10,45
ISK-5	18,10	SK-5	16,89
ISK-6	13,10	SK-6	23,30
ISK-7	12,78	SK-7	17,22
ISK-8	20,84	SK-8	18,30
ISK-9	14,37	SK-9	19,60
ISK-10	20,90		
ISK-11	19,89		
ISK-12	16,79		
ISK-13	21,78		

3.2.2. Particle Size Determination

Particle size distribution of each sample was determined by using the classical sieve and hydrometer method in accordance with the related standards (ASTM D 422-63, 2007) and unified soil classification system (ASTM D 2487). Basically, a set of sieve stack constituted by No.4, 10, 20, 40, 60, 160 and 200 were used in this study. No.200 sieve was used

as the bottom sieve and the particles which pass through this sieve are defined as fine-grained particles. Hydrometer analysis is used for this remaining fraction which has already passed through the 0.075mm (No.200) sieve. In this study, hydrometer analysis is carried out for the soil samples of which 50 % of its particles are fine grained. Lastly, all test results of hydrometer and mechanical analysis (sieve analysis) were combined on a plot where the vertical axis represents the weight percentage of particles and the horizontal axis represents the particle size on a logarithmic scale (Figure 3.19).

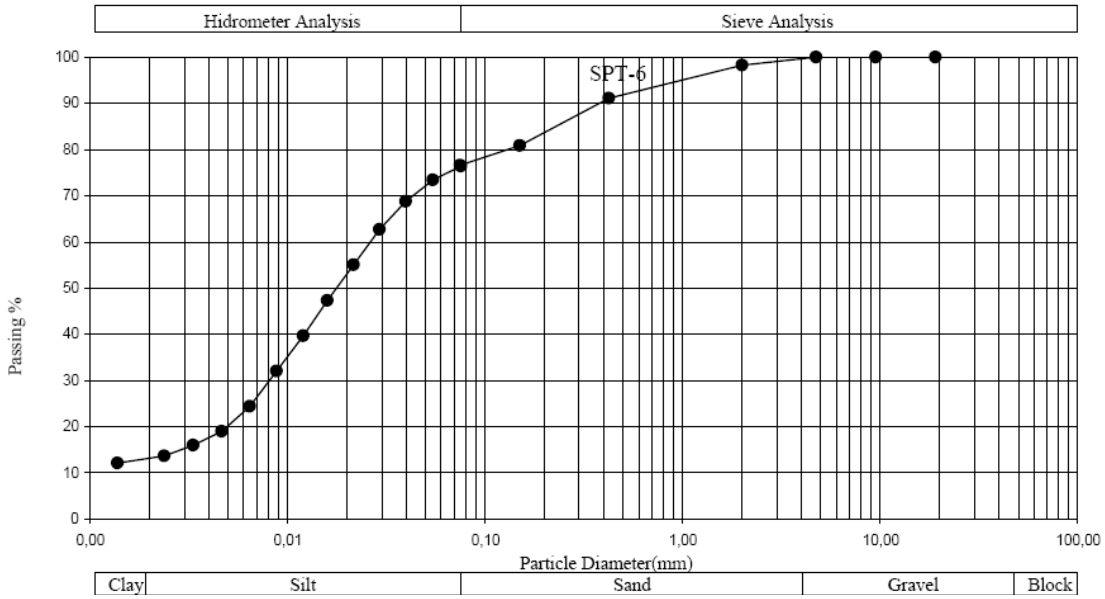

Figure 3.19. Particle size distribution of SPT-6 sample of ISK-07 borehole

Based on the general characteristics of the particle size distribution, it can be inferred that the samples are dominantly fine grained and mainly consist of clay and silt sized particle. Therefore, it is concluded that the soils analyzed belong to matrix of the colluvium.

3.2.3. Atterberg Limits

The term "consistency" is referred as the resistance to flow of a soil-water mixture which is related to the force of attraction between particles. According to the decreasing moisture content, soil shows different phase behaviours like liquid, plastic, semi solid and solid state respectively. The boundaries between these states are expressed as the Atterberg limits and used extensively in the classification of fine-grained soils.

In this study, atterberg limits of the samples were determined by Casagrande method according to the ASTM D 4318 (2004) standard. The test results of each sample including liquid limit, plastic limit, and plasticity index of soil specimens are given in Appendix C. Their plots on plasticity chart and activity chart are indicated in Figure 3.20 and Figure 3.21, respectively.

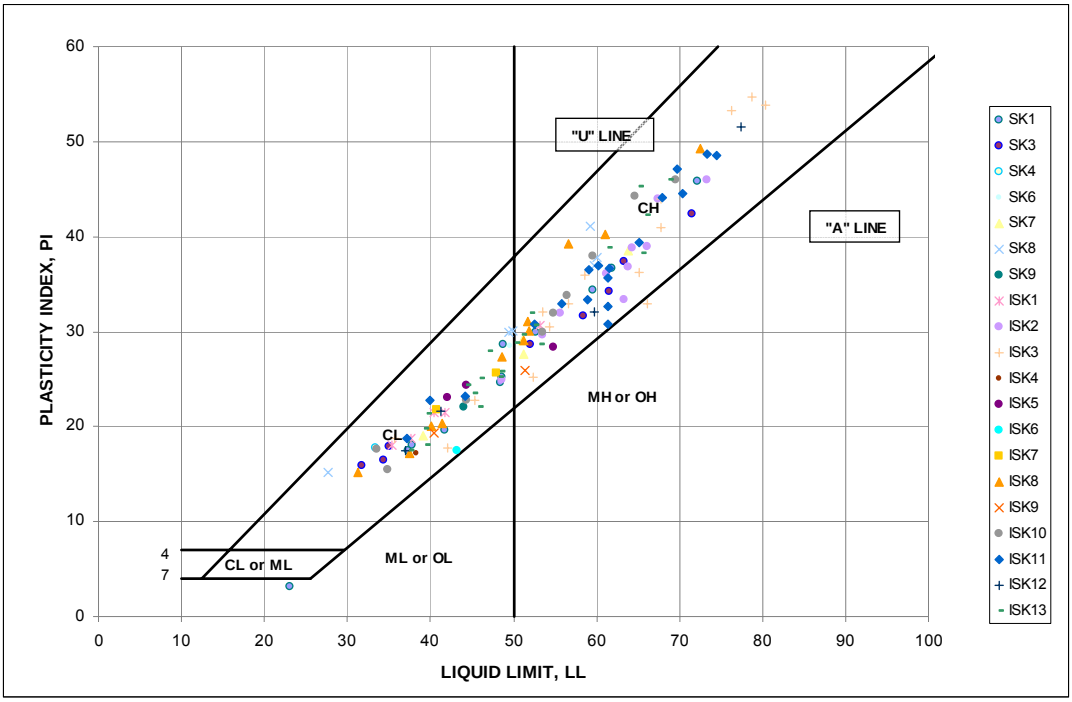

Figure 3.20. Plasticity Chart distributed according to the boreholes

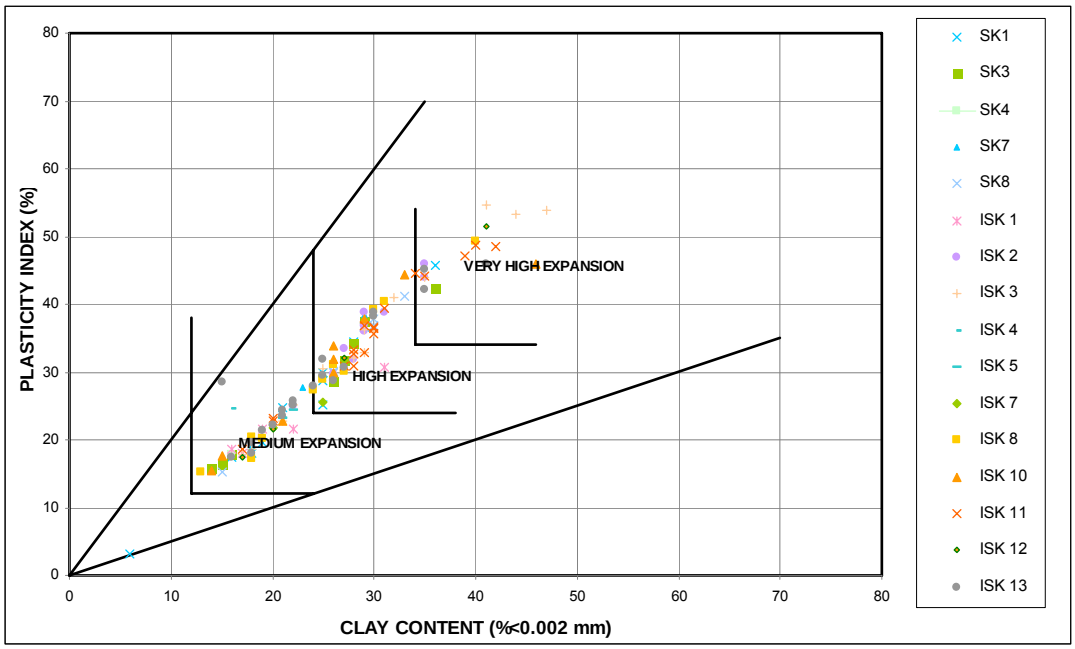

Figure 3.21. Activity chart indicating the swelling potential

As it is seen from the figures, the samples yield clays with high and low plasticity in line with the logs. For each borehole, soil types determined from samples taken from different depths are changing between CH and CL. However, there is not any certain relationship among them and since the results are very heterogene, it is not possible to define the zones based on the depth or regional variation. On the other hand, although regional variation throughout the settlement area could not be observed, it can be inferred that clay with low to high plasticity is dominant around landslide affected area.

The swelling potential of the soils is examined for each sample which is calculated by using the activity chart which is the plot of clay content (%) versus plasticity index (%). As can be observed from this graph (Figure 3.21), the values vary within the medium to very high expansion classes. However, since the obtained activities are distributed among the boreholes and depths, it is not possible to designate the activity of each borehole or catch a specific relation according to the

depth.

On the other hand, considering that almost all samples yield low to high plasticity clay and show high to very high expansion characteristics in terms of activity, it can be interpreted that the superficial damages observed in the landslide affected area might be the result of swelling and shrinkage effect in addition to the landslide influences. Although inclinometer results indicate the presence of a movement at deep levels like 5 to 10 meters, the possible damage of swelling and shrinkage which can be observed at 1^{st} to 2^{nd} meters depths from the ground surface, should not be ignored also together the effect of landslide.

3.2.4. Direct Shear Test

Compared to the widely used UU (Unconsolidated-Undrained) direct shear method, a more complicated and longer procedure is applied in this study. The main objective is to simulate identical conditions with the in-situ soil conditions and find out the corresponding soil parameters under these conditions. For this reason, ASTM D3080 (2004) test standard, which is the direct shear test procedure for samples under consolidated-drained (CD) conditions, has been followed.

In the first stage of the procedure, the sample was subjected to consolidation test according to ASTM D2435 (2004) until completion of primary consolidation. In CD conditions, the specimen should be sheared at a relatively slow rate so that no excess pore pressure would exist at failure. Consolidation test was carried out to find the exact loading rate which will be used in the direct shear test. As a first step, t_{50} is determined as per in the standard which is the time required to complete 50 % of total consolidation. T_{50} can be calculated by drawing the consolidation rate versus time graph on a semi-logarithmic plot and finding the correspondent value of time at 50 % consolidation. However, in this thesis study t_{90} is calculated by using Taylor's square root of time fitting method at the first stage, then t_{50} is derived by using the relation

$t_{50} = t_{90}/4{,}28$. The representative plot (4 kg load) for the first sample is shown in Figure 3.22, all consolidation test reports of first experiment for all different loads are presented in Appendix D;

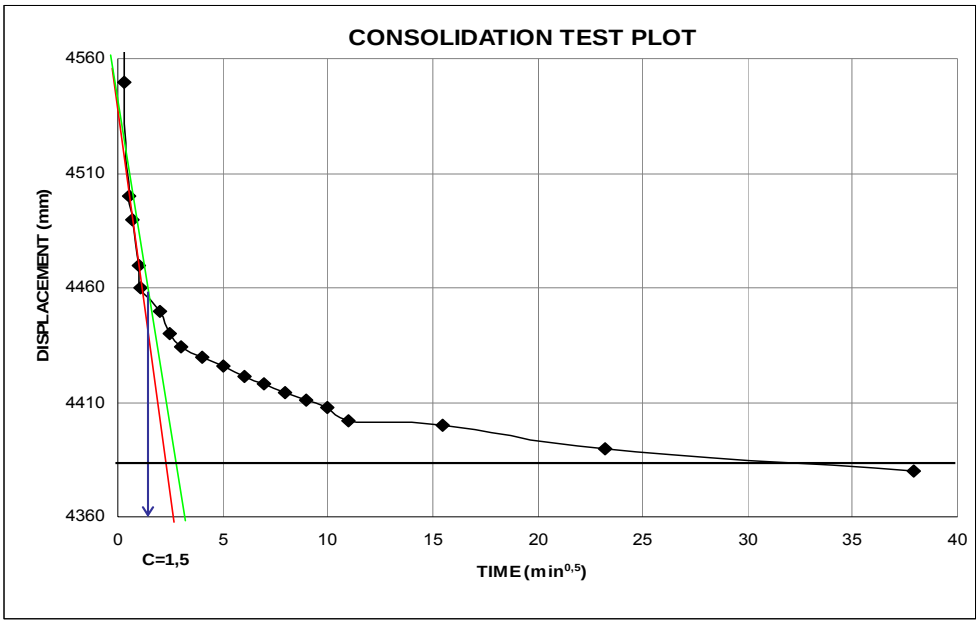

Figure 3.22. Consolidation plot of undisturbed specimen for CD direct shear test

After the calculation of t_{50}, appropriate displacement rate is selected by using the following equations.

$t_f=50.t_{50}$ and $d_r=d_f/t_f$

where;

d_r = displacement rate (in./min, mm/min),

d_f = estimated horizontal displacement at failure (in., mm),

t_f = total estimate elapsed time to failure, min.

Since the test sample is similar to consolidated fine-grained soil, the magnitude of the estimated displacement at failure is taken as 0.5 inch (12 mm).

After the above mentioned first stage, the test is carried out with

the calculated speed until the failure of the sample is achieved. The results are expressed in a typical shear stress versus deformation graph. After this stage, the sample is moved forward and backward in the shear box to simulate the soil conditions in the failure plane as explained in the previous section and by this way we were able to reach the minimum residual values. The same procedure is repeated with the same speed and a new shear stress versus deformation graph is obtained. This experiment is applied for two specimens collected from 3rd and 6th meters of ISK-03 borehole for three different normal loads which are 4, 8 and 16 kg. Three different loads which are 4, 8 and 16 kg, in other words 111,1, 222,2 and 444,4 kN/m2, respectively are calculated according to the corresponding load at 5th, 10th and 20th meters soil thickness above the failure surface in the field. These plots for different loads (4 kg, 8 kg and 16 kg) of the first experiment are shown in Figure 3.23 thru Figure 3.25, the post-failure plot has smaller shear stress values than the first experiment.

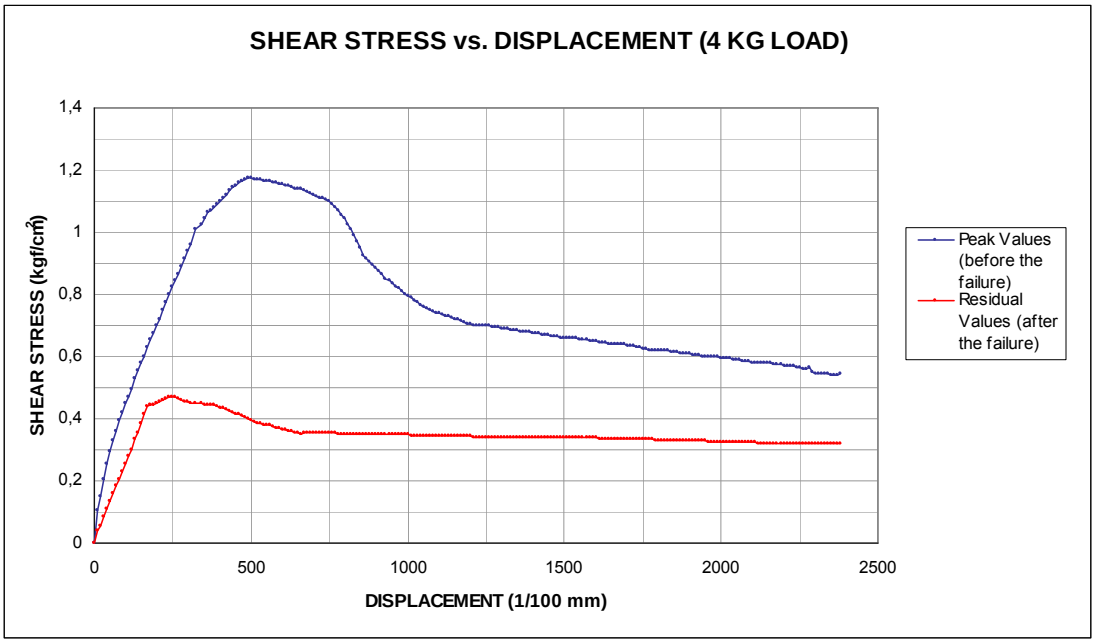

Figure 3.23 Shear stress vs. displacement plot with 4 kg normal load

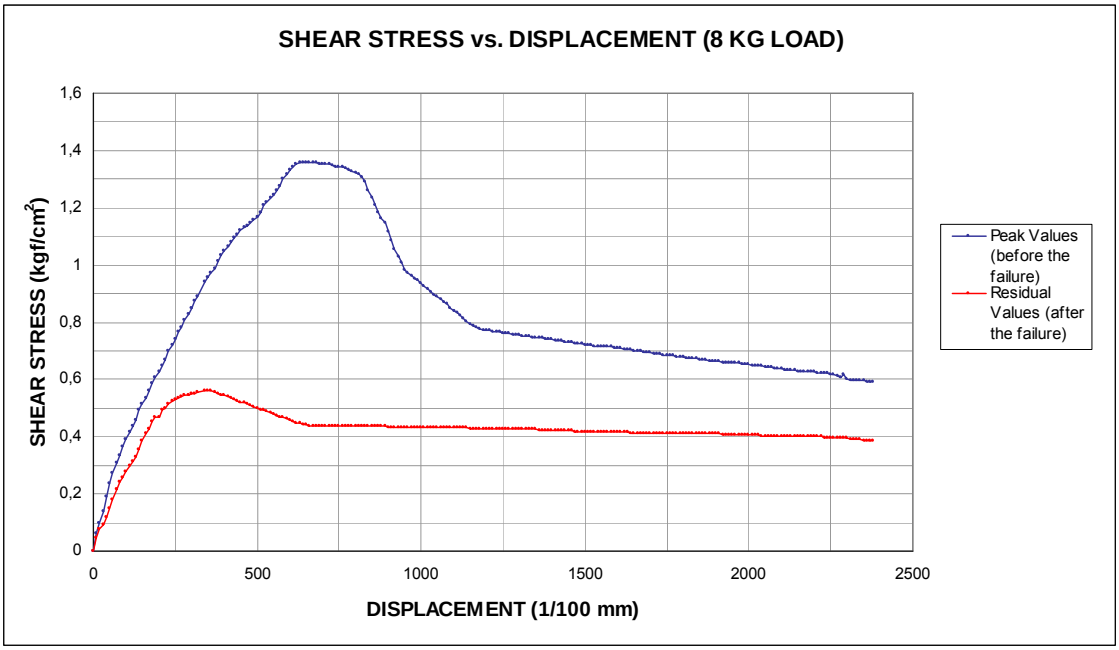

Figure 3.24. Shear stress vs. displacement plot with 8 kg normal load

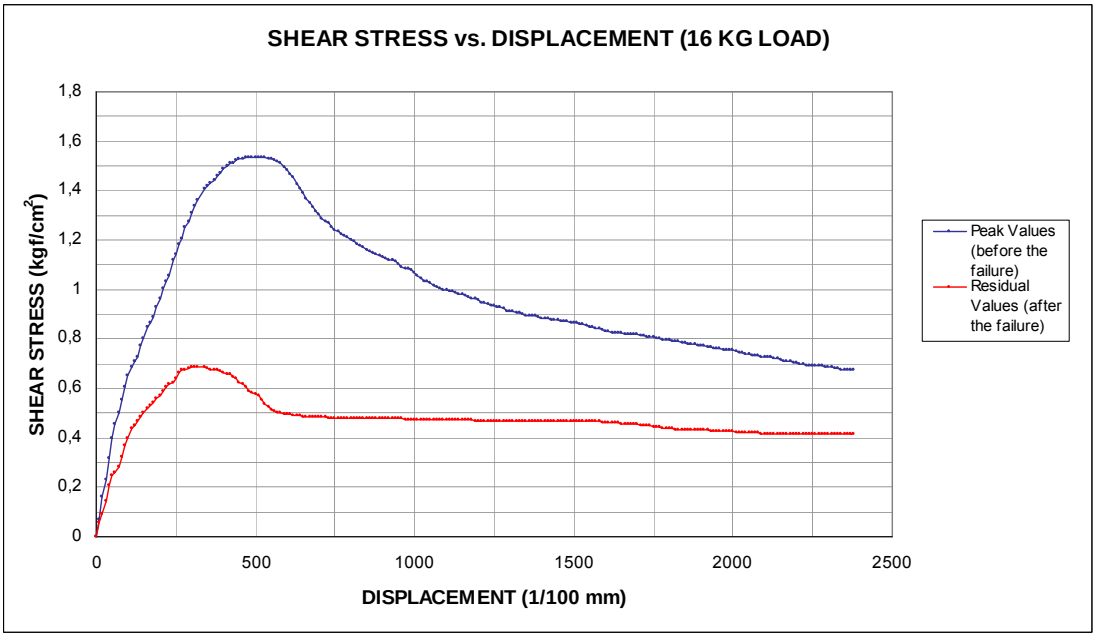

Figure 3.25. Shear stress vs. displacement plot with 16 kg normal load

Each of these peak and residual values represent a single point in

shear stress versus normal stress graph, so it is possible to define a failure envelope by applying the same tests in different loads and by drawing the best line for the peak and residual values. Shear stress versus normal stress plots of the 1st experiment and the best lines fitted according to the residual and peak values are presented in Figure 3.26 and Figure 3.27;

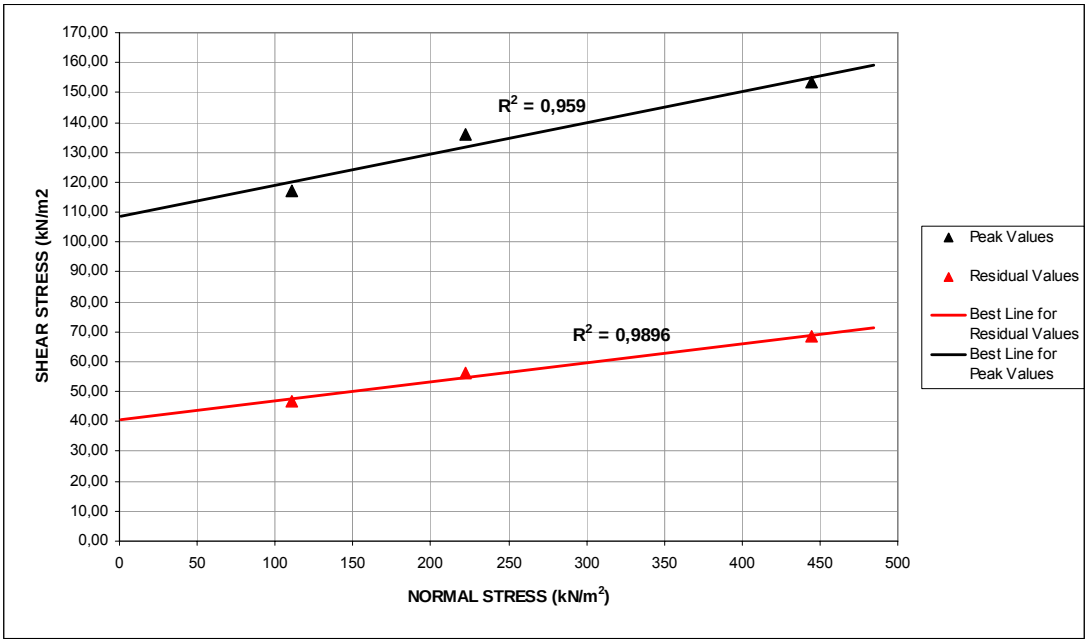

Figure 3.26. Pre-failure shear stress vs. normal stress plot

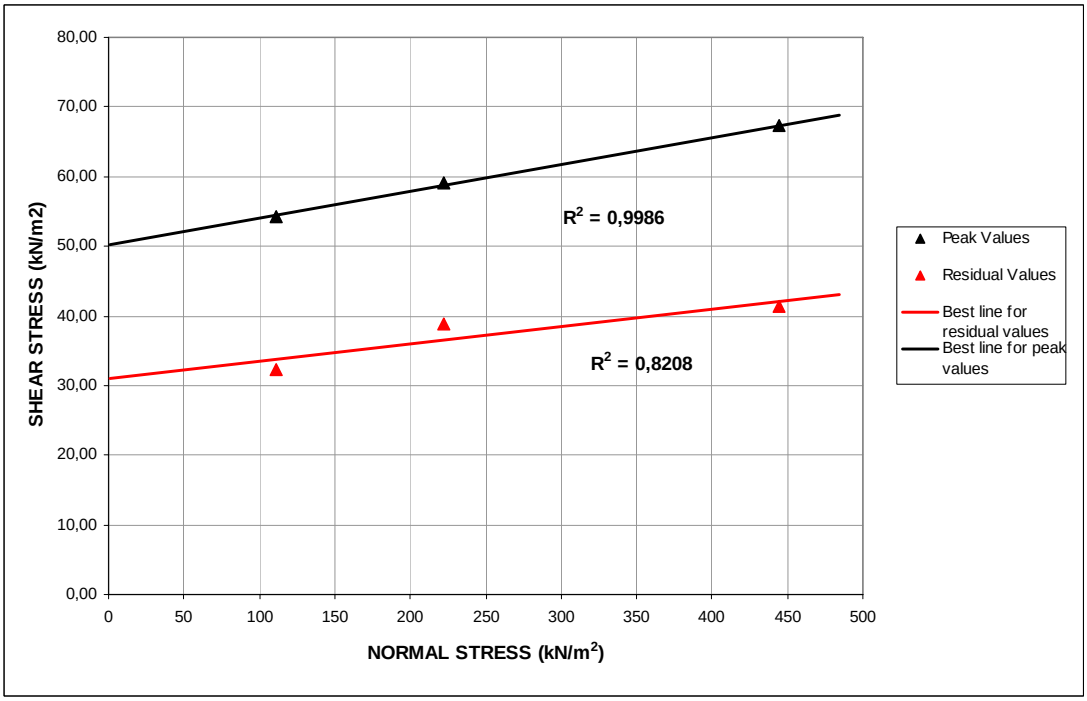

Figure 3.27. Post-failure shear stress vs. normal stress plot

The summary tables which involve all results of shear stress parameters calculated after both tests are given in Table 3.8 and Table 3.9.

Table 3.8. Direct shear test result of the 1st experiment

	Parameter	c (kN / m²)	Phi (degree)
Before Failure	Peak	109	5,9
	Residual	40	3,8
After Failure	Peak	50	2,3
	Residual	32	1,3

Table 3.9. Direct shear test result of the 2nd experiment

	Parameter	c (kN/m^2)	Phi (degree)
Before Failure	Peak	102	10,8
	Residual	61	1,2
After Failure	Peak	54	2,2
	Residual	33	0,3

The above results calculated by both experiments are not as expected from a clay dominant material. Especially, the cohesion values are much higher than expected and residual parameters should have smaller cohesion values. Considering the obtained cohesion values, it can be interpreted that forward and backward movement of the machine was applied only once during the experiment.

CHAPTER 4

ASSESSMENT OF SHEAR STRENGTH PARAMETERS

In this chapter, all information and results acquired from both laboratory and field studies are gathered together and interpreted to reach a final decision about the soil parameters. In order to do this, the slopes which are susceptible to landslide and the critical regions where displacement have been observed, are examined. The area for the analysis is selected by considering the significance of the region for municipality in terms of urbanization, remaining area was not taken into consideration. The analysis has been realized by a computer software SLIDE (Rocscience, 2004) by taking account surface topography, unit weight, water table level and failure surface geometry. The soil parameters calculated by laboratory tests involves several disadvantages like sample heterogenity and soil disturbance. Because of this reason, back analysis is carried out to compare the values of soil parameters determined through laboratory tests. Although this method provides relatively correct information concerning shear strength parameters of the slope forming material, the most accurate values may be obtained by incorporating both laboratory and back analysis results. Therefore, suitable shear strength parameters are decided with the above mentioned comparison. Contrary to the most slope stability studies in which back analysis is carried out in an already failed slope, an obvious failed slope is not available in this study. So, the analysis is made based on the findings on failure surface geometry and the use of inclinometer data. Because of this reason, it is out of the scope of this thesis to carry out the analysis in order to stabilize the slopes by considering the earthquake effect, and recommending the remedial measures.

4.1. Back Analysis of the Landslide

Back analysis of the landslide (Sancio 1981; Chandler 1977; Turner and Schuster 1996; Teoman et al. 2004; Topal and Akin, 2008) where critical structure such as police station exist, is carried out along three sections which have been selected according to the inclinometer results where displacement is available. The selected cross-sections are indicated in Figure 4.1. For the analysis, variation of the shear strength parameters (c' and ϕ') of the landslide material satisfying a factor of safety (FS) of 1, which corresponds to the limit equilibrium condition, was determined for different shear strength pairs. The analysis was carried out for non-circular slide, using the Janbu's method by means of SLIDE software (Rocscience, 2004).

A 1/1000 scale topographic map of the landslide area, the latest groundwater measurements corresponding to highest water level, and failure depths observed from the inclinometer results were used for assessing the shear strength parameters governing the landslide activity. Basically, the failure surface was determined by assuming a non-circular failure due to the boundary between two units which are colluvium and flyschoidal sequence (Figure 4.2). Although a thin layer of soil was available above the main material, this layer is ignored since the failure points were located in the underlying main material. Therefore, unique material parameters were used in the back analysis with two different unit weights as 17,8 kN/m^3 and 16 kN/m^3 for saturated and unsaturated unit weights, respectively.

Concerning the used limit equilibrium method; Janbu's simplified and corrected methods are based on the force equilibrium condition which is particularly useful in composite shear surfaces such as layered soils. In this method, an ideal solution can be obtained if the shear surface is plane where the sliding takes place without any inter-slice movements (Aryal, 2006). On the other hand, Janbu (1973) later proposed a complicated formulation which is more tedious in

computation. When the factor of safety from the simplified method is multiplied with this correction factor, the result will be close to that from the analysis which takes into account both forces and moment equilibrium (Cheng and Lau, 2008). For instance, while the Simplified Janbu procedure without the correction factor underestimates the factor of safety by about 7%, the corrected version agrees within 1% with the value of the factor of safety calculated using methods that satisfy moment equilibrium (Duncan and Wright, 1996). Therefore, considering the shape of slip surface observed in study area, Janbu's corrected method with 25 slices was chosen for the back analysis based on the suitability of this method to our case. These cross-sections together with the sliding surfaces and groundwater table for the analysis are indicated in Figure 4.3 thru Figure 4.5.

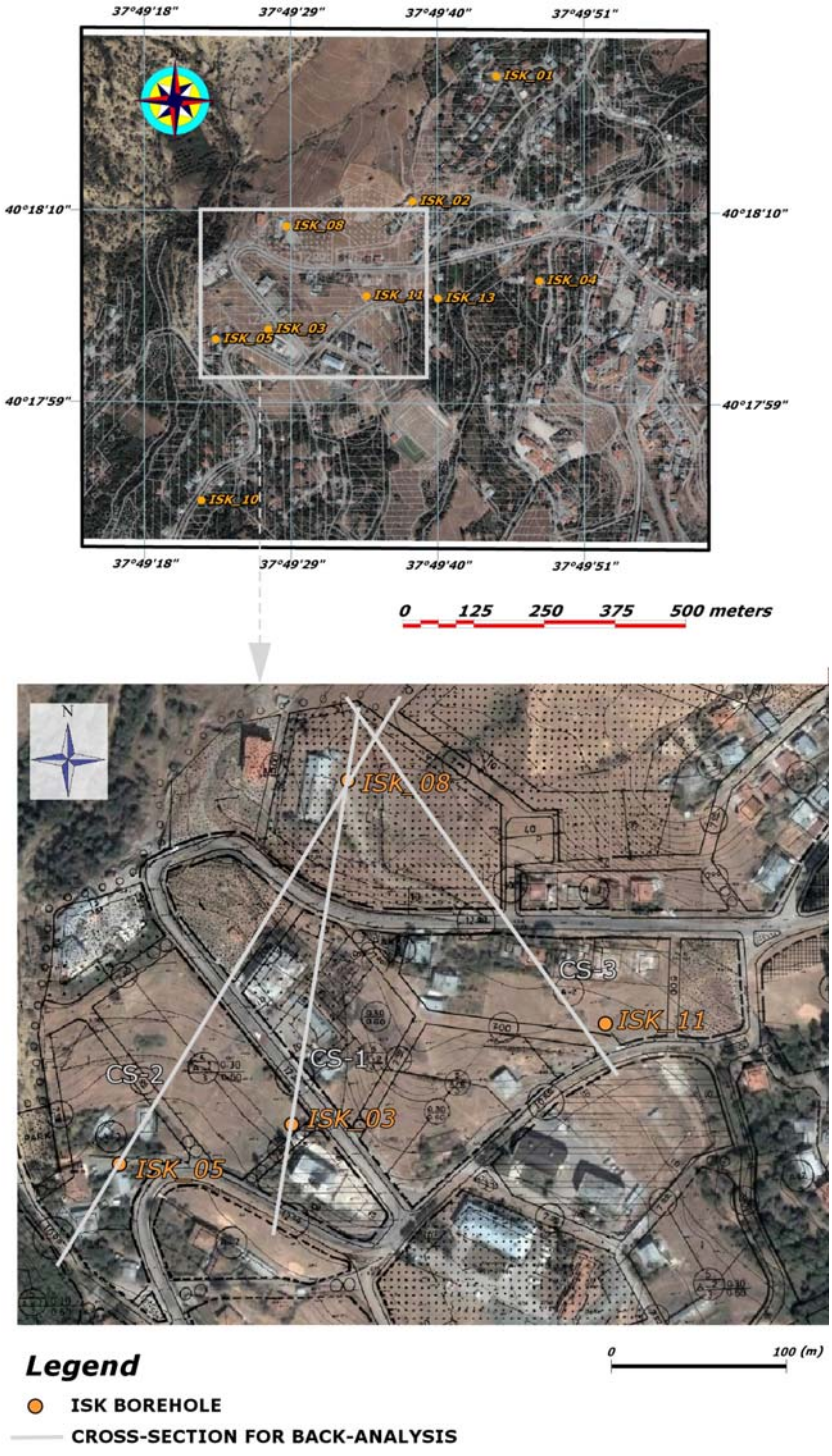

Figure 4.1. Locations of cross-sections (CS) for the back-analysis

Figure 4.2 Flysch exposed in the study area

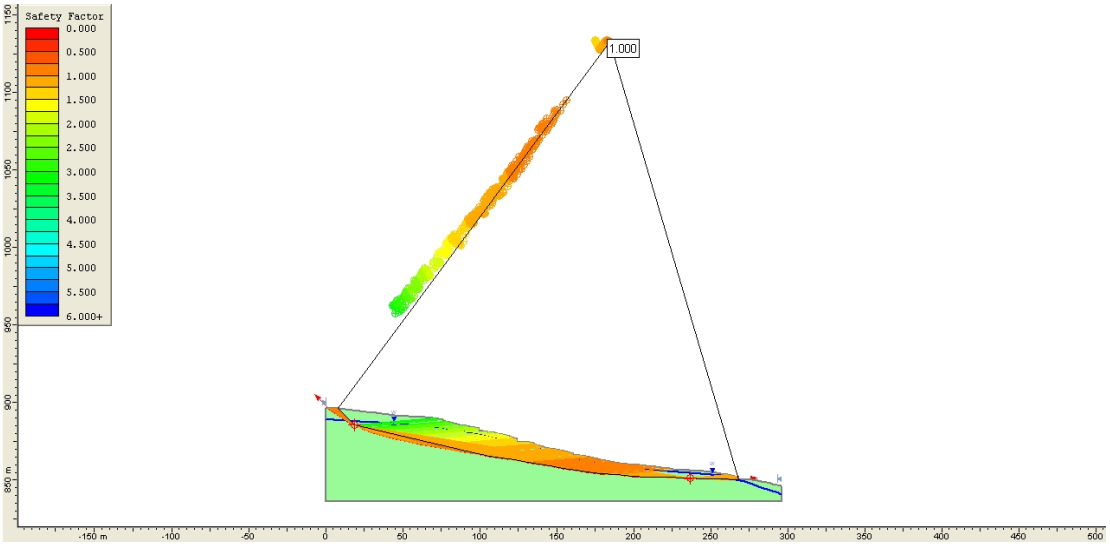

Figure 4.3. Back analysis output along cross section 1 (between ISK-8 and ISK-3)

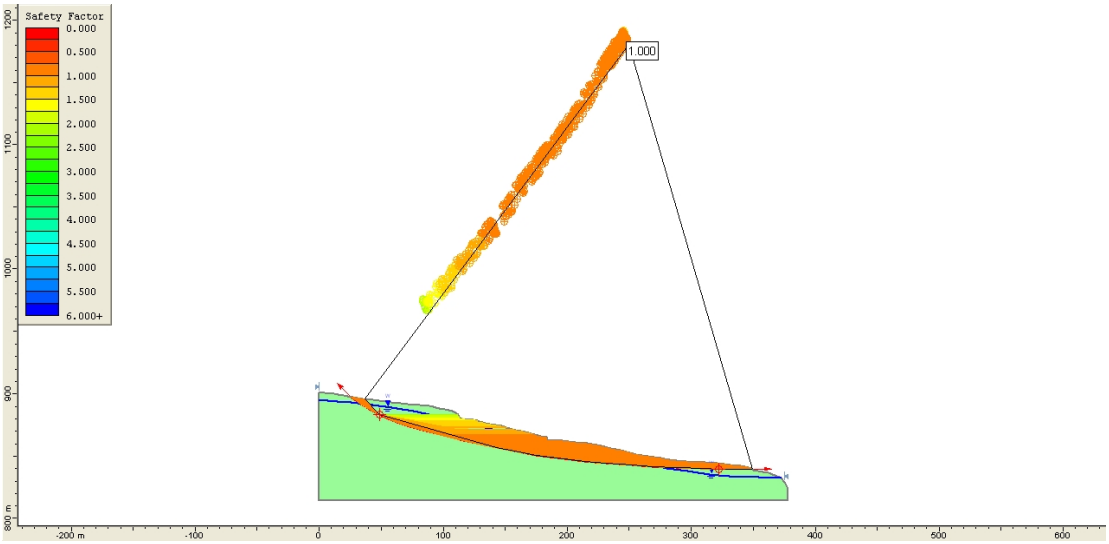

Figure 4.4. Back analysis output along cross section 2 (between ISK-8 and ISK-5)

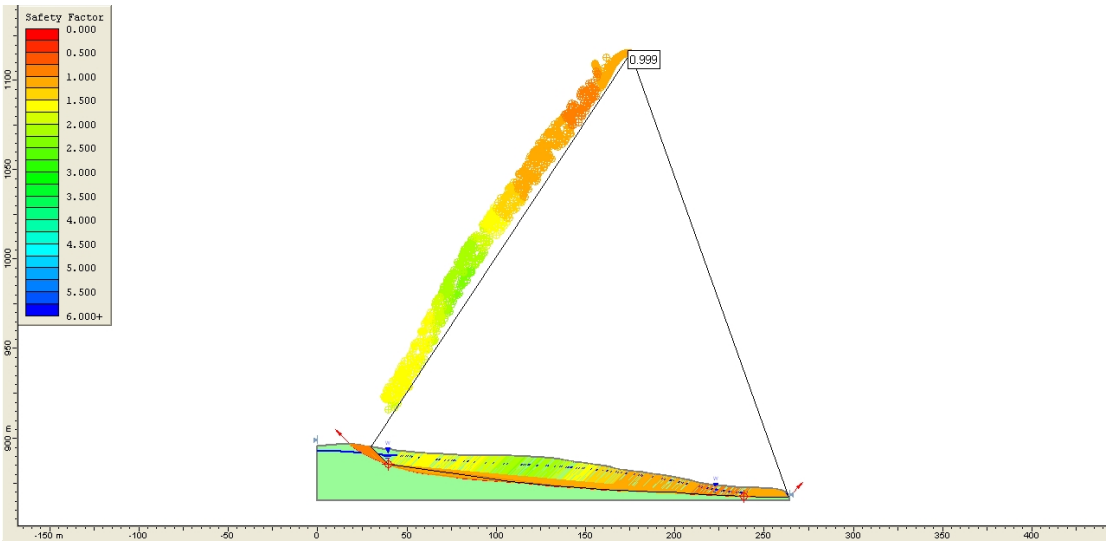

Figure 4.5. Back analysis output along cross section 3 (between ISK-8 and ISK-11)

For each section, three different simulations were carried out during the analysis. Respectively, 1 kPa, 5 kPa and 10 kPa cohesion values are assigned in each simulation and corresponding friction angles were obtained for these cohesion values at the time when the factor of safety is one (1.0). Then, these results are interpreted in cohesion versus friction angle plot based on the Sancio's multiple solution approach (Sancio, 1981). This method includes usage of different cross-sections of a slide and determination of c-ϕ pairs in limiting equilibrium conditions. According to the acquired results, the values are plotted in a c-ϕ graph (Figure 4.6) and the intersections of these lines yield approximate values for soil parameters.

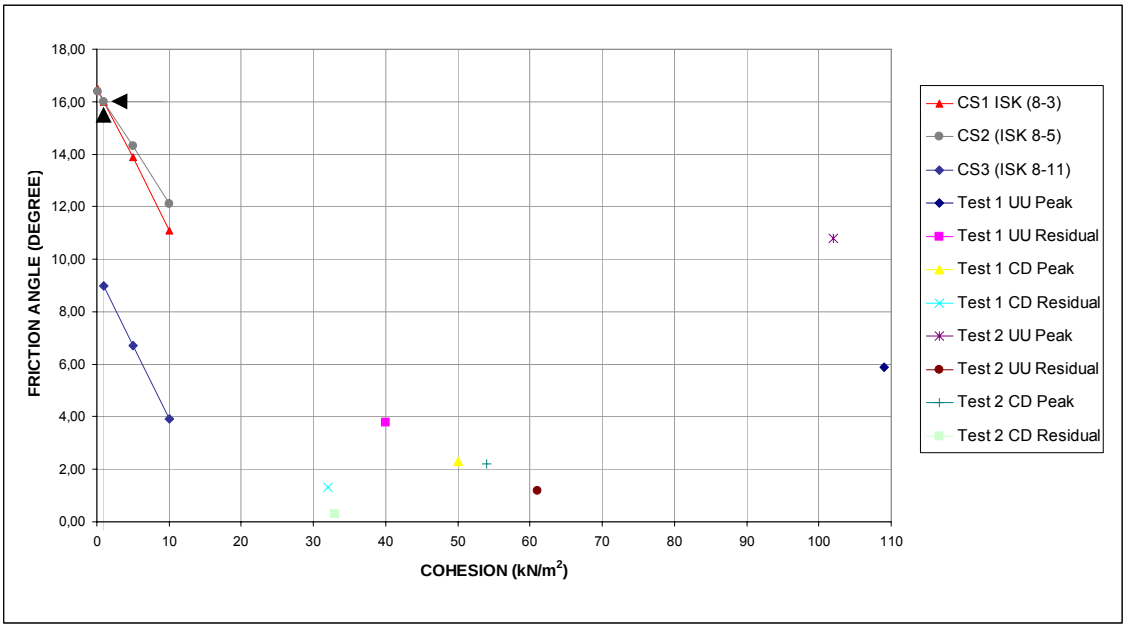

Figure 4.6. Friction angle vs. cohesion plot of three sections and points of test results obtained from the back-analysis

As seen from the above plot (Figure 4.6), line of each section is determined according to the limiting equilibrium conditions and the values obtained from laboratory results fall very far from the lines

obtained from laboratory results. Although all three lines do not intersect with each other, CS1 and CS2 intersect at approximately 1 kPa cohesion and 16° friction angle which enable us to make estimation for soil parameters. Since much lower cohesion values is expected from a failed clay dominant material, it can be inferred that back analysis has been provided more consistent results than the laboratory results (Table 4.1).

Table 4.1 Comparison of back analysis and direct shear test results.

Parameter		**Cohesion (kPa)**		**Friction Angle (°)**	
		Test 1	*Test 2*	*Test 1*	*Test 2*
Direct Shear Test	**Pre-failure (peak)**	109	102	5,9	10,8
	Pre-failure (residual)	40	61	3,8	1,2
	Post-failure (peak)	50	54	2,3	2,2
	Post-failure (residual)	32	32	1,3	0,3
Back Analysis (for FS=1)		1		16	

CHAPTER 5

DISCUSSIONS

Based on the information acquired from reports and data obtained from this thesis study, following evaluations are noted;

1) In order to make a comparison with PSInSAR method, each displacement value of corresponding inclinometer point is summarized in Table 5.1.

Table 5.1. Comparison of PSInSAR method versus inclinometer results in terms of landslide displacement

INCLINOMETER BOREHOLES	DEFORMATION RESULTS WITH PsInSAR METHOD (mm/year)	INCLINOMETER RESULTS (mm/year)
ISK-1	15-30 mm (-)	-
ISK-2	0-15 mm	-
ISK-3	30-45 mm	7 mm
ISK-4	0-30 mm	3,6 mm
ISK-5	60-75 mm (-)	6,7 mm
ISK-6	N.A.	-
ISK-7	N.A.	-
ISK-8	N.A.	7,8 mm
ISK-9	N.A.	-
ISK-10	N.A.	-
ISK-11	0-15 mm	14,1 mm
ISK-12	N.A.	-
ISK-13	0-15 mm	8,4 mm

It is obvious that these results are very different and unconformable with the inclinometer measurements specified in this thesis study. Although the results partially match to each other at some

points like ISK-4, ISK-11 and ISK-13, there are some significant differences in ISK-1, ISK-3 and ISK-5 boreholes in terms of the deformation amounts with the inclinometer results. Since the location of the points where the measurements have been taken are not exactly same and the measurement intervals are different, a perfect match is not expected between these two methods. However, considering the resolution of inclinometer system which is 0,01 mm and the difference amount between the results; it can be concluded that approximately 6-7,5 cm/year of deformation obtained from PsInSAR method might be inconsistent.

2) Regarding the GPS method, in Hastaoğlu (2009) only two points, KH07 and KH10, are located within the study area of this thesis. So, the only one control point evaluable in this study is KH07 and it has a much higher displacement value than the nearest inclinometer point ISK-03 which is 65 meters away from the control point. According to the GPS method, a displacement of 60.2 ± 2.9 mm/year in north-south direction and 55.4 ± 3.8 mm/year in east-west direction is calculated while it is observed approximately 7 mm/year with inclinometer device (Table 5.2). Although the borehole and control point do not totally coincide in terms of location and there is a one (1) year difference between the measurement periods, a difference like this were not expected. Considering the damages occurred on buildings and the reports held by "General Directorate of Natural Disasters" since 1985, it can be inferred that this amount of deformation is not consistent with the field indications. This high amount might be occurred because of incorrect control point appointment or high rate of superficial movement due to the overlying soil material.

Table 5.2 Comparison of GPS and inclinometer measurements for landslide displacement

	DISPLACEMENT VALUES MEASURED BY GPS METHOD (mm/year)			INCLINOMETER RESULTS (mm/year)
Point no	**NORTH (mm)**	**EAST (mm)**	**HEIGHT (mm)**	**ISK-3**
KH01	-1.4 ± 6.3	1.1 ± 4.4	-6.9 ± 12.9	-
KH02	-1.0 ± 6.1	1.5 ± 2.4	0.6 ± 12,3	-
KH03	-3.4 ± 5.0	4.2 ± 2.6	-9.9 ± 12.0	-
KH04	-8.6 ± 4.4	-2.0 ± 2.7	-17.0 ± 11.9	-
KH05	0.5 ± 3.8	6.3 ± 2.6	-2.8 ± 11.8	-
KH06	-13.7 ± 2.9	-3.7 ± 2.8	-0.3 ± 10.8	-
KH07	-60.2 ± 2.9	-55.4 ± 3.8	3.8 ± 12.2	7
KH09	-1.7 ± 4.2	-4.3 ± 4.6	4.5 ± 14.6	-
KH10	-.1.2 ± 3.25	-2.2 ± 3.9	0.3 ± 12.7	-
KH11	-0.4 ± 3.35	-16.3 ± 2.8	-4.2 ± 12.0	-

3) High precipitation rate available in the study area is mentioned several times in previous sections of this study, correspondingly in 1955, 8 houses located near valley plain are totally damaged in Ortamahalle due to the flood. Related reports acquired from General Directorate of Disaster Affairs (GDDA) are not explained in details since this subject is considered irrelevant within the context of this thesis. Therefore, based on the field observations and GDDA reports (Yılmaz and Yılmaz, 1985; Özkan and Demirbaş, 1994; Öztaşkın and Ataytür, 1997; Kızıltuğ and Gündoğdu, 2005), it can be stated that high water level is one of most important parameter causing instability of the slopes. If it is drained, the stability of slopes would be significantly improved.

4) Based on the inclinometer results, the deformation has been observed only in a local area (Figure 3.18). A negligible or very minor amount of displacement has been observed in remaining boreholes. So, it

can be concluded that the movements take place only as local landslides, not big a scale slide containing whole settlement area. In addition, GDDA reports (Yılmaz and Yılmaz, 1985; Öztaşkın and Ataytür, 1997; Alkan and Korpe, 1998) state that the settlement area has been partly settled on an active sliding mass and it is interpreted that this activity take place with local landslides. Therefore, this comment also support and confirm the availability of local landslide in the studied area proposed by this thesis.

5) It is possible that the superficial damages observed in the landslide affected area might be the result of swelling and shrinkage effect in addition to the landslide influences considering the results of the samples in terms of activity and plasticity. However, sub-surface deformations have been observed by inclinometer results and the resultant failure geometry shows a non-circular geometry due to the flyschoidal sequence beneath the colluvium.

6) Without any exception, in all GDDA reports, pre-existing and progressive damages have been observed on houses in Camiikebir area which is the most important part of this thesis study area (Figure 5.1). Ten (10) critical houses which have been indicated in Figure 5.1 (houses no 1 to 10), are recorded as damaged due to the landslide (Yılmaz and Yılmaz, 1985; Özkan and Demirbaş, 1994; Öztaşkın and Ataytür, 1997) together with the Police station, Religious school, Community center and Jail construction (Alkan and Korpe, 1998; Kayakıran and Kızıltuğ, 2002). In addition to 10 houses, three more houses (no. 11, 12 and 13) (Figure 5.1) were added to this list as damaged buildings (Kızıltuğ and Gündoğdu, 2005). In the following study dated 2007 (İleri and Aktan), no landslide indication has been observed in the settlement area except Camiikebir district. Beside damaged 13 houses, two more houses located next to police station and near ISK-2 borehole were investigated and minor damages were recorded. Report prepared by Eraslan and Uluç (2008) includes the same observations and conclusions with İleri and

Aktan's report (2007). In the light of the above information interpreted from GDDA reports; it is indicated that the landslide event is observed in the same critical area which is also supported with the thesis study including inclinometer measurements and new field observations. In addition, as confirmed in last GDDA reports (İleri and Aktan, 2007) and (Eraslan and Uluç, 2008), further new landslides are not observed around the settlement area which strictly define the boundary of the landslide affected area in compliance with the findings of this thesis and it confirms that landslide exist only at this area, not in different locations around settlement area.

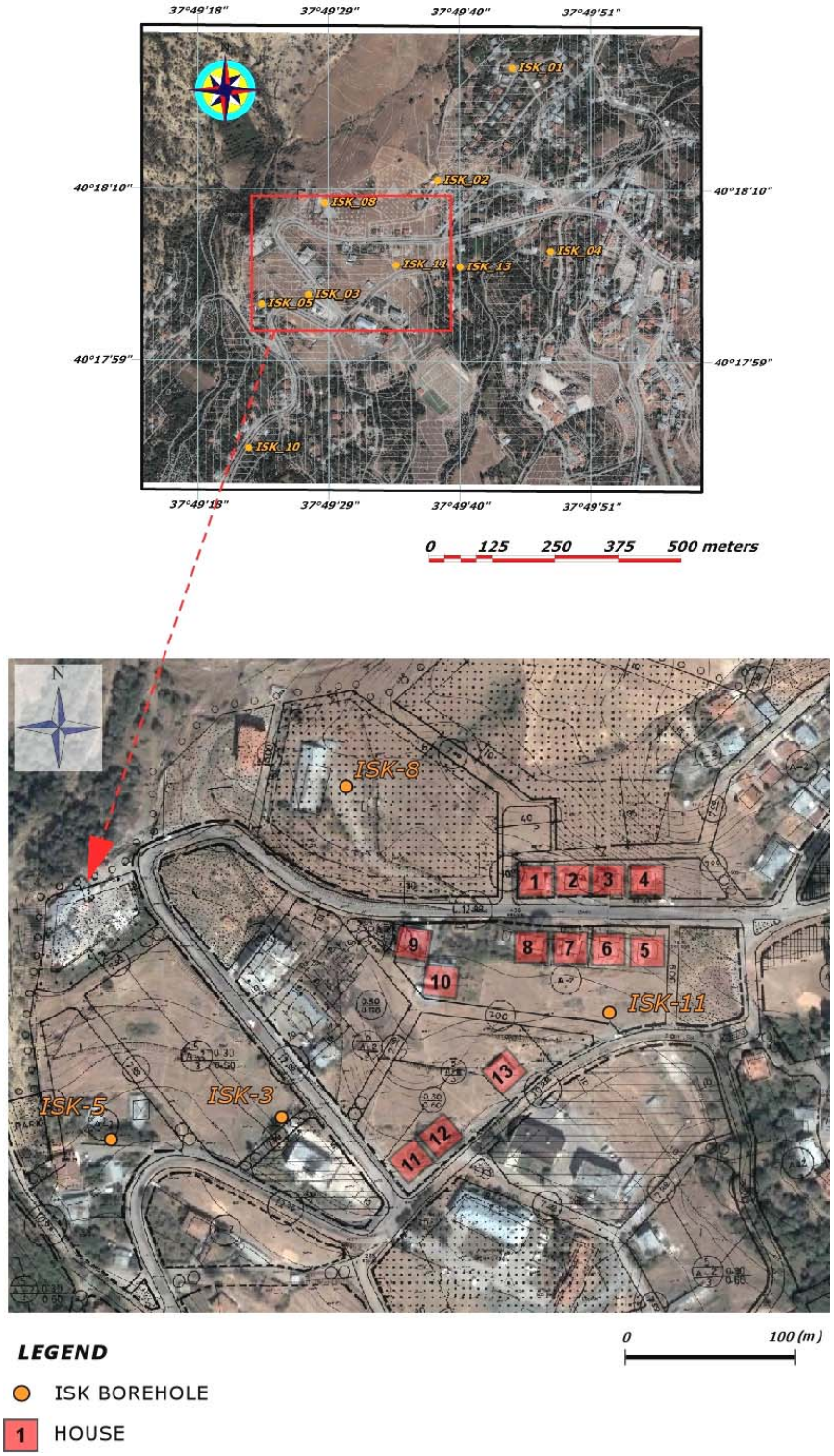

Figure 5.1. Camiikebir district and landslide affected houses indicated in GDDA reports

7) The occurrence of landslide event since 1985 and the amount of damages on the houses recorded in the reports are important indications and evidences concerning the velocity of the landslide. Considering that the landslide continues its activity since 1985 and damaged houses were evacuated in 2005, it can be stated that a creep like movement occurs in the area instead of a landslide having a velocity exceeding 5-6 cm/year. The velocity values obtained from the inclinometer measurements are classified as extremely slow (Table 5.3) (WP – WLI, 1995) which is the slowest classification according to Union of Geological Sciences Working Group on Landslides. So, according to Castelli et al. (2009), these types of phenomena considered in this category may be either slides that have experienced progressive displacements for many hundreds or thousands of years or that may have experienced a fast episode of movement in the past and now are only affected by residual movements. Considering that a similar movement velocity is available at the study area, it can be concluded that the landslide takes place in the form of extremely slow landslide as estimated above.

Table 5.3. Classification of landslide on the basis of velocity (WP – WLI, 1995)

Velocity Class	Velocity Description	Velocity Limits
7	Extremely Rapid	>5m/sec
6	Very Rapid	3m/min – 5m/sec
5	Rapid	1.8m/hr – 3m/min
4	Moderate	13m/month – 1.8m/hr
3	Slow	1.6m/year – 13m/month
2	Very Slow	16mm/year – 1.6m/year
1	Extremely Slow	<16mm/year

CHAPTER 6

CONCLUSIONS AND RECOMMENDATIONS

Concerning the slope instability assessment of Koyulhisar, further to the findings and corresponding results obtained in this thesis where the yellowish-white flyschoidal sequence and colluvium are the main lithological units exposed respectively, following conclusions can be attained;

1) Inclinometer measurements taken in 3 periods reveal that local movement velocity around Camiikebir district is 3,6 to 14,1 mm/year approximately. Negligible or no movement has been recorded at the remaining parts. Contrary to interferometry and Global Positioning System (GPS) survey methods, inclinometer measurements yield much slower velocity values than other studies. Considering the progressive damage amount of the buildings in Camiikebir district and availability of this continuous damage since 1985; the results of other methods is concluded to be inconsistent. So, the inclinometer measurements are considered valid and the landslide is classified as extremely slow landslide.

3) The landslide is only observed in Camiikebir area where police station, military school, community center and other structures are located. Inclinometer measurements indicate the lack of movement at the remaining part of the settlement area.

4) The failure geometry shows a non-circular shape due to the bedded layers which correspond to the flyschoidal sequence.

5) The movement observed at Camiikebir area requires some precautions; this deformation does not take place as sudden landslide and does not cause enormous mass destruction due to the velocity and the mechanism of the movement. Instead of this, the effect of the available deformation will be seen in long term. Correspondingly, it is concluded that it is necessary to continue the inclinometer measurements in next seasons and stability analysis should be carried out within the scope of this data which will be supported with the new readings. For further analysis, earthquake effect may also be considered and based on the results of longterm inclinometer readings and stability analysis, an effective remedial measure can be planned.

REFERENCES

Akbulut, A., 1991. "Niksar-Reşadiye-Koyulhisar Sivas yöresi Bentonit Ön Arama Raporu" , M.T.A., Rp.No:9264

Akıncı, Ö.T., 1984. "The Eastern Pontide volcano-sedimentary belt and associated massive sulphide deposits", in Dixon, J.E, and Robertson, A.H.F., eds. The Geological Evolution of the Eastern Mediterranean, Geological Society of London, Special Publication, No:17, 415-428.

Alacahan, H., Ataytür, H. 2000. "Jeolojik Etüd Raporu" AFET İŞLERİ GENEL MÜDÜRLÜĞÜ.

Alkan, M., Korpe, G. 1998. "Jeolojik Etüd Raporu" AFET İŞLERİ GENEL MÜDÜRLÜĞÜ.

Allen, C.R., 1982. "Comparisons between the North Anatolian Fault of Turkey and the San Andreas Fault of California", in Işıkara, A.M. and Vogel, A., eds., Multidisciplinary approach to Earthquake Prediction: Wiesbaden, Friedrich, Vieweg and Sohn, 67-85.

Alp, D., 1972, "Amasya yöresinin jeolojisi", İ.Ü. Fen Fak. Monogr., No.22, İstanbul.

Ambraseys, N.N., 1970. "Some characteristic features of the North Anatolian Fault Zone", Tectonophysics, 9, 143-165.

Arslanpay, D. and İçerler, A., 1979. "Sivas Koyulhisar-Ortakent (Sisorta) Güzelyurt Madencami ve Kurşunlu Köyü Jeofizik Etüdü", M.T.A., Rp.No:6502

Aryal, K. (2006): Slope stability evaluation by LE and FE methods . Ph D thesis, Norwegian University of Science and Technology, NTNU:

ASTM D 2487-06e1, 2006, "Standard Test Method for Particle-Size Analysis of Soils", Annual Book of ASTM Standards, Soil and Rock, Vol 04.08, ASTM, Philadelphia

ASTM D 422-63, 2007, "Standard Test Method for Particle-Size Analysis of Soils", Annual Book of ASTM Standards, Soil and Rock, Vol 04.08, ASTM, Philadelphia

ASTM D 854, 2004, "Standard Test Methods for Specific Gravity of Soil Solids by Water Pycnometer", Annual Book of ASTM Standards, Soil and Rock, Vol 04.08, ASTM, Philadelphia

ASTM D 2216, 2004, "Standard Test Method for Laboratory Determination of Water (Moisture) Content of Soil and Rock by Mass", Annual Book of ASTM Standards, Soil and Rock, Vol 04.08, ASTM, Philadelphia

ASTM D 4318, 2005, "Standard Test Methods for Liquid Limit, Plastic Limit, and Plasticity Index of Soils", Annual Book of ASTM Standards, Soil and Rock, Vol 04.08, ASTM, Philadelphia

ASTM D2435, 2004, "Standard Test Methods for One-Dimensional Consolidation Properties of Soils Using Incremental Loading", Annual Book of ASTM Standards, Soil and Rock, Vol 04.08, ASTM, Philadelphia

ASTM D3080-04, 2004, "Standard test method for Direct Shear Test of Soils under Consolidated Drained Conditions", Annual Book of ASTM Standards, Soil and Rock, Vol 04.08, ASTM, Philadelphia

Ayışkan, O., 1971. "Koyulhisar-Sisorta Çinko Cevherinin Ön Zenginleştirme Etütleri" , M.T.A., Rp.No:4569

Barka, A.A. and Hancock, P.L., 1984. "Neotectonic deformation patterns in the convex-northwards arc of the North Anatolian Fault Zone", in Dixon, J.E. and Robertson, A.H.F., eds. The Geological Evolution of the Eastern Mediterranean, Geological Society of London, Special Publication, No: 17, 285-296.

Barka, A.A. and Kadinsky-Cade, K., 1988. "Strike-slip fault geometry in Turkey and its influence on earthquake activity", Tectonics, 7, 3, 663-684.

Barka, A.A., 1984. "Kuzey Anadolu Fay Zonundaki bazı Neojen-Kuvaterner havzalarının jeolojisi ve tektonik evrimi", Ketin Sempozyumu, T.J.K. Bull., 209-227.

Bektaş, O., 1984. "Doğu Pontidlerde Üst Kretase yaşlı şoşonitik volkanizma ve jeotektonik önemi", K.Ü. Bull., Jeoloji, 3, 1-2, 53-62.

Blumenthal, N.M., 1950. "Orta ve Aşağı Kızılırmak Bölgelerinin (Tokat, Amasya, Havza, Erbaa, Niksar) Jeolojisi Hakkında", MTA Yayınları, Seri D, No: 4, Ankara.

Bomba, Z., 1993. "Reşadiye-Mesudiye-Suşehri-Koyulhisar Diyatomit Prospeksiyon Rapor" , M.T.A., Rp.No:9479

Çakır, M. And Keskin, Ö., 1998. "Evliyakent-Ortakent-Koyulhisar Sivas Altin Yatağı Maden Jeolojisi Raporu", M.T.A., Rp.No:10217

Çakır, Z., 2009. "Kelkit Vadisinde Yapay Açıklık Radar İnterferometrisi (InSAR) Yöntemiyle Heyelan ve Tektonik Hareketlerin İncelenmesi", Bölüm 7, 10p.

Castelli, M., Scavia, C., Bonnard, C., Laloui, L., 2009. "Mechanics and velocity of large landslides" Engineering Geology doi: 10.1016/j.enggeo.2009.07.009

Chandler, R.J., 1977. "Back analysis techniques for slope stabilisation works: a case record", Géotechnique, Volume 27, pages 479–495.

Cheng, Y.M., Lau, C.K., 2008, Slope Stability Analysis and Stabilization: New methods and insight", Routledge_ Taylor & Francis, New York, 241p.

Colesanti, C., Ferretti, A., Prati, C. and Rocca, F., 2003. "Monitoring landslides and tectonic motions with the Permanent Scatterers Technique" Engineering Geology, Volume 68, Issues 1-2, Pages 3-14

DMİ, 2008, Devlet Meteoroloji İşleri Genel Müdürlüğü - Ankara Meteoroloji Bölge Müdürlüğü, http://ankara.meteor.gov.tr/ (Accessed: 12.11.2008).

Duncan, J. M. and Wright, S. G., 1996, "Soil Strength and Slope Stability.", John Wiley & Sons, Hoboken, New York. …p

Durrich, K., 1967. "Sivas Koyulhisar Havzasinin Linyit Etüdü" , M.T.A., Rp.No:6048

Eraslan, F., Uluç, Z. M., 2008. "Jeolojik Etüd Raporu" AFET İŞLERİ GENEL MÜDÜRLÜĞÜ, 3 p.

Ercan, T. and Gedik, A., 1984. "Pontidlerdeki volkanizma", Jeoloji Mühendisliği, 18, 3-22.

Ergun, A., 1975. "Koyulhisar Sivas Toz Kireci Hammaddesi Umumi Prospeksiyon Raporu" , M.T.A., Rp.No:5316

Erguvanlı, K., 1951. "Zara-Şebinkarahisar-Mesudiye Arasindaki Bölgenin Jeolojisi Hakkinda Rapor", M.T.A., Rp.No:1926

Farina, P., Colombo D., Fumagalli A., Marks F.and Moretti S., 2006."Permanent Scatterers for landslide investigations: outcomes from the ESA-SLAM project", Engineering Geology, Volume 88, Issues 3-4, Pages 200-217

Ferretti, A., Prati, C., Rocca, F., Casagli, N., Farina, P.,Young, B., 2005. "Permanent Scatterers technology: a powerful state of the art tool for historic and future monitoring of landslides and other terrain instability phenomena." Proc. of 2005 International Conference on Landslide Risk Management. A.A. Balkema, Vancouver, Canada, CD-Rom.

Friedmann, H., Aric, K., Gutdeutsch, R., King, C.Y. and Altay, C., 1988. "Radon measurements for earthquake prediction along the North Anatolian Fault Zone: a progress report", Tectonophysics, 152, 209-214.

Gili, J. A., Corominas, J., Rius, J., 2000, "Using Global Positioning System Techniques in Landslide Monitoring" Engineering Geology, Volume 55, pages 167-192.

Gökçeoğlu, C., Nefeslioğlu, H.A., Sönmez, H. and Duman, T., 2005a. "17.03.2005 Kuzulu Sivas, Koyulhisar Heyelanı", M.T.A., Rp.No:10718

Gökçeoğlu, C., Nefeslioğlu, H.A., Sönmez, H., Duman, T. and Can, T., 2005b. "The 17 March 2005 Kuzulu landslide (Sivas, Turkey) and landslide-susceptibility map of its near vicinity", Engineering Geology, Volume 81, Issue 1, 65-83.

Hancock, P.L. and Barka, A.A., 1982. "Structural evidence for left-lateral displacement on the North Anatolian Fault Zone during the Plio-Pleistocene", in Işıkara, A.M. and Vogel, A., eds., Multidisciplinary approach to Earthquake Prediction: Wiesbaden, Friedrich, Vieweg and Sohn, 43-44.

Hastaoğlu, K. O., 2009. "Koyulhisar Heyelanının GPS ile İzlenmesi", DPT Proje Raporu, 45 p.

Hempton, M.R., 1982. "The north Anatolian Fault and complexities of continental escape", Journal of Structural Geology, 4, 502-504.

Hollick, C., 1971. "Flotation Amenability Tests On Koyulhisar-Sisorta Pr-Zn-Cu-Ore", M.T.A., Rp.No:4564

Ildız, T., 1965. "Koyulhisar Sisorta-Şebinkarahisar Arasindaki Sahanin Kurşun Çinko Prospeksiyonu", M.T.A., Rp.No:3821

İleri, N. H., I., Aktan, M. 2007. "Jeolojik Etüd Raporu" AFET İŞLERİ GENEL MÜDÜRLÜĞÜ, 4 p.

Janbu, N., 1973. "Slope stability computations, in Embankment-Dam Engineering: Casagrande Volume", R. C. Hirschfeld and S. J. Pouros, Eds., Wiley, Hoboken, NJ, pp. 47–86.

Kandilli Observatory, Sayısal Grafik San. Ve Tic. Ltd. Şti., 2008, Türkiye Deprem Sitesi-Deprem Haritası, http://www.sayisalgrafik.com.tr/deprem/tr_frames.htm, (Connected in: 01.12.2008).

Kaptanoğlu, H., 1968. "Sivas Koyulhisar-Sisorta Muradin Köy Kurşun-Çinko-Bakir Zuhurlari Ve Rezerv durumu", M.T.A., Rp.No:3953

Kayakıran, I., Kızıltuğ, A. 2002. "Jeolojik Etüd Raporu" AFET İŞLERİ GENEL MÜDÜRLÜĞÜ, 3 p.

Ketin, İ., 1966. "Anadolunun Tektonik Birlikleri", M.T.A. Bull., 66, 20-34.

Ketin, İ., 1969. "Kuzey Anadolu Fayı Hakkında", M.T.A. Bull., 72, 1-27.

Ketin, İ., 1976. "San Andreas ve Kuzey anadolu Fayları arasında bir karşılaştırma", T.J.K. Bull., 19, 149-154.

Kızıltuğ, A., Gündoğdu, I. 2005. "Jeolojik Etüd Raporu" AFET İŞLERİ GENEL MÜDÜRLÜĞÜ, 24 p.

Koçyiğit, A., 1988a. "Basic geological characteristics and total offset of North Anatolian Fault Zone in Suşehri area, NE Turkey", M.E.T.U. J. and Pure Appl. Sc., 22, 3, 43-68.

Koçyiğit, A., 1988b. "Tectonic setting of the Geyve basin: Age and total displacement of the Geyve fault zone", M.E.T.U. J. Pure and Appl. Sc., 21, 1-3, 81-104.

Koçyiğit, A., 1989. "Suşehri basin: an active fault-wedge basin on the North Anatolian Fault Zone, Turkey", Tectonophysics, Volume 167, 13–29.

Microimages, 2003, "TNT-MIPS, Scientific Sofware-The Map and Image Processing System", Version 6.9, Microimages Inc., USA.

Mora P., Baldi P., Casula G., Fabris M., Ghirotti M.,Mazini E., Pesci A., 2003. "Global Positioning Systems and digital photogrammetry for the monitoring of mass movements: application to the Ca' di Malta landslide (northern Apennines, Italy)" Engineering Geology Volume 68 pages 103–121

Nebert, K., 1961. "Kelkit çayı ve Kızılırmak (Kuzeydoğu Anadolu) nehirleri mecra bölgelerinin jeolojik yapısı", M.T.A. Bull., 57, 1-49.

Nebert, K., 1964. "Şiran güneybatısındaki (Kuzeydoğu Anadolu) Kelkit çayı üst mecrasının jeolojisi hakkında", M.T.A. Bull., 68, 41-58.

Nefeslioğlu, H.A., Duman, T. and Durmaz, S., 2008. "Landslide susceptibility mapping for a part of tectonic Kelkit Valley (Eastern Black Sea region of Turkey)", Geomorphology, Volume 94, Issues 3-4, 401-418.

Noferini, L., Pieraccini, M., Mecatti, D., Macaluso, G., Atzeni, C., Mantovani, M., Marcato, G., Pasuto, A., Silvano S. and Tagliavini F., 2007. "Using GB-SAR technique to monitor slow moving landslide" Engineering Geology, Volume 95, Issues 3-4, Pages 88-98

Ovalıoğlu, R., 1964. "Koyulhisar Sisorta-Muradinkoy Pb-Zn-Cu Zuhurlari Detay Etüdü" , M.T.A., Rp.No:3799

Özçiçek, H., 1986. "Sivas Koyulhisar Kurşunlu Köy ve civari Kurşun-Çinko-Bakir Madenleri" , M.T.A., Rp.No:7980

Özgüneylioğlu, A. And Aokabe, K. , 1981. "Sivas Koyulhisar-Sisorta-Kurşunluköy Ve Civari Kurşun-Çinko-Bakir Madeni A.", M.T.A., Rp.No:7625

Özkan, F., Demirbaş, E. 1994. "Jeolojik Etüd Raporu" AFET İŞLERİ GENEL MÜDÜRLÜĞÜ, 3 p.

Özsayar, T., Pelin, S. and Gedikoğlu, A., 1981. "Doğu Pontidlerde Kretase", K.T.Ü. Yerbilimleri derg., 1, 2, 65-114.

Öztaşkın, H., Ataytür, H. 1997. "Jeolojik Etüd Raporu" AFET İŞLERİ GENEL MÜDÜRLÜĞÜ, 7 p.

Pelin, S., Özsayar, T., Gedikoğlu, A. and Tülümen, E., 1982. "Doğu Pontidlerde Üst Kretase yaşlı kırmızı biyomikritlerin oluşumu", K.T.Ü. Yerbilimleri Derg., 2, 1-2, 69-79.

Petrascheck, W., 1967. "Sivas İle Giresun Arasindaki Koyulhisar-Şebinkarahisar-Suşehri Kurşun-Çinko Prospeksiyonu", M.T.A., Rp.No:3908

Rocscience, 2004, "Slide, Scientific Software-2D limit equilibrium slope stability for soil and rock slopes", Version 5.014, Rocscience Inc., Canada.

Rojay, B.F., 1985. "Tectonostratigraphic characteristics of the Kelkit valley subzone of the North Anatolian Fault", Ms.Thesis, M.E.T.U., Ankara.

Sancio, R.T., 1981. "The use of back-calculations to obtain shear and tensile strength of weathered rocks", Proc. Int. Symp. on Weak Rock, Vol.2, Tokyo, pages 647-652.

Şengör, A.M.C. and Canıtez, N., 1982. "The North Anatolain Fault", Alpine Mediterranean Geodynamics: American Geophysical Union Geodynamics Series, 7, 205-216.

Şengör, A.M.C., 1979. "The North Anatolain transform fault: its age, offset and significance", Jour. Geol. Soc. of London, 136, 269-282.

Şeren, I., Yılmaz, S. 2006. "Jeolojik Etüd Raporu" AFET İŞLERİ GENEL MÜDÜRLÜĞÜ, 5 p.

Seymen, İ., 1975. "Kelkit vadisi kesiminde Kuzey Anadolu Fay Zonunun tektonik özelliği", İ.T.Ü. Maden Fak. Yayın., İstanbul.

Sipahioğlu, S., 1984, "Kuzey anadolu Fay zonu ve çevresinin deprem etkinliğinin incelenmesi", Deprem Araştırma Bülteni, 45, 1-139.

Slope Indicator (2008) Citing online sources: advice on online citation formats [online].http://www.slopeindicator.com (Connected in: 23.02.2009).

Stark, T. D., Choi, H., 2008. "Slope inclinometers for landslides" Landslides, Volume 5, Issue 3, pages 339-350, Springer Berlin.

Stchepinsky, V., 1940. "Zara-Koyulhisar-Suşehri Mintikasinin Jeolojisi Hakkinda Rapor" , M.T.A., Rp.No:1094

Takashima, K., Hakari, N. And Kawada, K., 1974. "Menka Madeni Etrafindaki Sahanin Jeolojisi Ve Mineralizasyon Koyulhisar Sivas", M.T.A., Rp.No:5148

Tatar, Y., 1978. "Kuzey Anadolu Fay Zonunun Erzincan-Refahiye arasındaki bölümü üzerinde tektonik incelemeler", H.Ü. Yerbilimleri Dergisi, 4, 1-2, 201-236.

Teoman, M.B., Topal, T., and Işık, N.S., 2004, "Assessment of slope stability in Ankara clay: a case study along E90 highway", Environmental Geology, volume 45, issue 7, pages 963-977.

Terlemez, I. and Yilmaz, A., 1980. "Ünye-Ordu-Resadiye-Koyulhisar-Karaçayır-Hafik arasında kalan bölgesinin jeolojisi", M.T.A. Rp. No: 6671.

Terzioğlu, M.N., 1985a. "Reşadiye (Tokat) kuzeyindeki Eosen yaşlı Hasanseyh platobazaltlarının mineralojik-petrografik ve jeokimyasal incelemesi", C.Ü. Müh. Fak. Yer Bilimleri Derg., 2, 1, 105-134.

Terzioğlu, M.N., 1985b. "Reşadiye (Tokat) kuzeybatısındaki Hasandede andezitinin mineralojik-petrografik ve jeokimyasal incelemesi", C.Ü. Müh. Fak. Yer Bilimleri Derg., 2, 1, 105-134.

Topal, T., Akin, M., 2008, "Geotechnical assessment of a landslide along a natural gas pipeline for possible remediations (Karacabey-Turkey)" Environmental Geology (in press)

Toprak, G. M. V., 1989. "Tectonic and stratigraphic characteristics of the Koyulhisar segment of North Anatolian Fault", Ph. D. Thesis, M.E.T.U., Ankara.

Turner, K.A., Schuster, R.L., 1996, "Landslides: Investigation and mitigation", National Academy Press, 672 p.

Tutkun, S.Z. and İnan, S., 1982. "Niksar-Erbaa (Tokat) yöresinin jeolojisi", Karadeniz Üniv., Yerbilimleri Derg., 2, 1-2, 51-68.

Ulusay, R., Aydan, Ö. and Kılıç, R., 2007. "Geotechnical assessment of the 2005 Kuzulu landslide (Turkey)", Engineering Geology, Volume 89, Issues 1-2, 112-128.

Uygur, İ., 1969. "Koyulhisar-Suşehri-Şebinkarahisar Arasinda Kalan Oligosen Ve Miyosen Sahaları", M.T.A., Rp.No:4620

Uysal, S., 1995. "Koyulhisar (Sivas) yöresinin jeolojisi", M.T.A. Rp No: 9838.

Westrum, H., 1961. "Sivas Koyulhisar-Sisorta-Nahiyesi Kankoy-Muradin Mahallesi Kurşun Çinko Maden Prospeksiyonu" , M.T.A., Rp.No:3413

WP – WLI. 1995. A suggested method for describing the rate of movement of a landslide. International Union of Geological Sciences Working Group on Landslides. Bulletin of the International Association of Engineering Geology, Vol. 52, N° 1, pp.75-78.

Yılmaz, A., 1983. "Tokat (Dumanlıdağ) ile Sivas (Çeltekdağı) dolaylarının temel jeoloji özellikleri ve ofiyolitli karışığın konumu", M.T.A. Bull., 99-100, 1-18.

Yılmaz, A., 1985. "Yukarı Kelkit çayı ile Munzur dağları arasının temel jeoloji özellikleri ve yapısal evrimi", TJ.K. Bull., 28, 2, 79-92.

Yılmaz, B. and Yılmaz, M., 1985. "Jeolojik Etüd Raporu" AFET İŞLERİ GENEL MÜDÜRLÜĞÜ, 3 p.

Yılmaz, I and Sendir, H., 2002. "Structural, geomorphological and geomechanical aspects of the Koyulhisar landslides in the North Anatolian Fault Zone (Sivas-Turkey)". Env Geol 42(1):52–60.

Yılmaz, I., 2009. "A Case Study From Koyulhisar (Sivas-Turkey) For Landslide Susceptibility Mapping By Artificial Neural Networks", Bull. Eng. Geol. Environ., Springer

Yılmaz, I., Ekemen, T., Yıldırım, M., Keskin, İ. and Özdemir, G., 2005. "Failure and flow development of a collapse induced complex landslide: the 2005 Kuzulu (Koyulhisar, Turkey) landslide hazard", Environmental Geology, Volume 49, 467-476.

APPENDIX A

LOGS OF ISK AND SK BOREHOLES

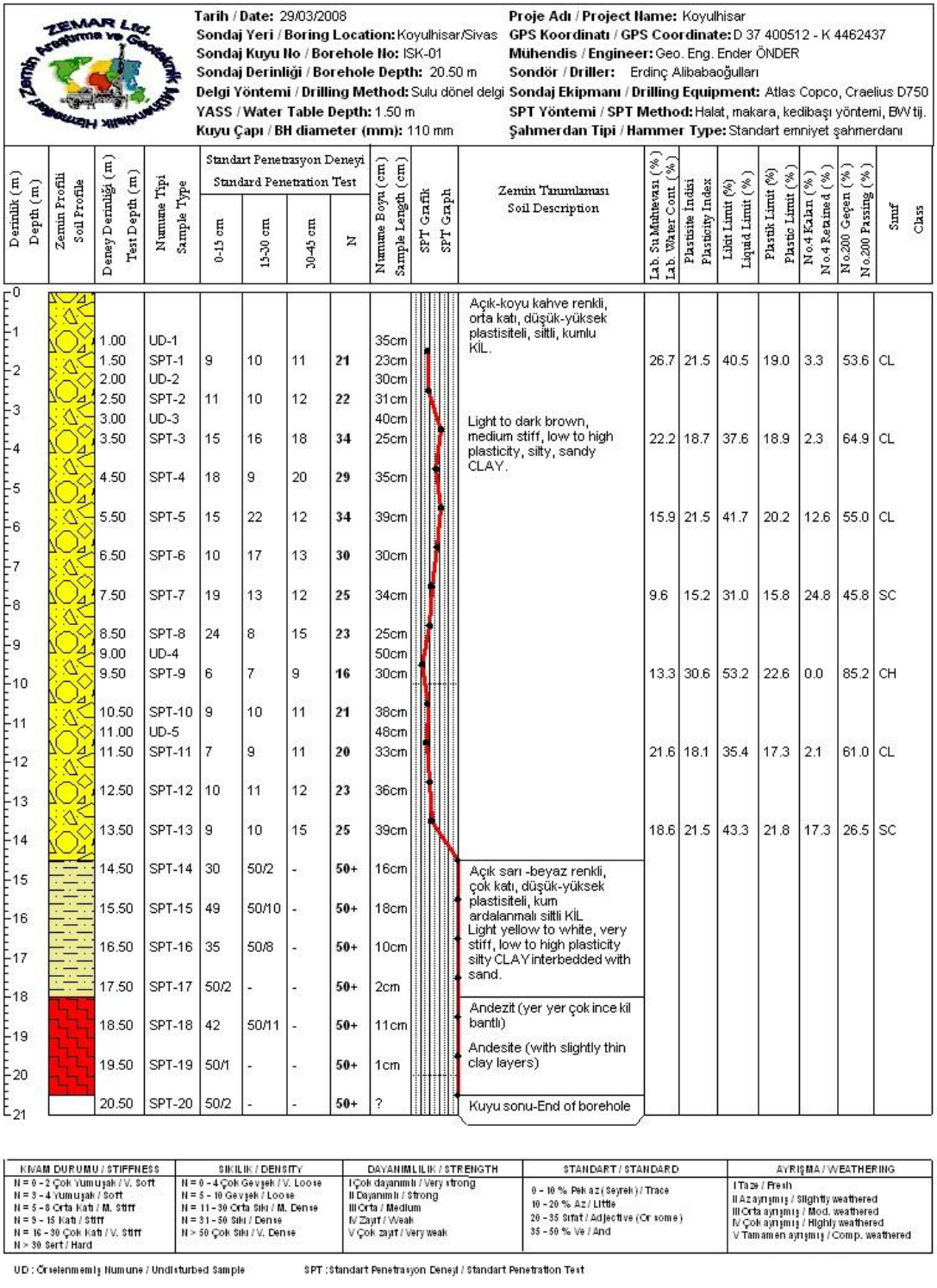

Figure A.1 Log of ISK-1 borehole.

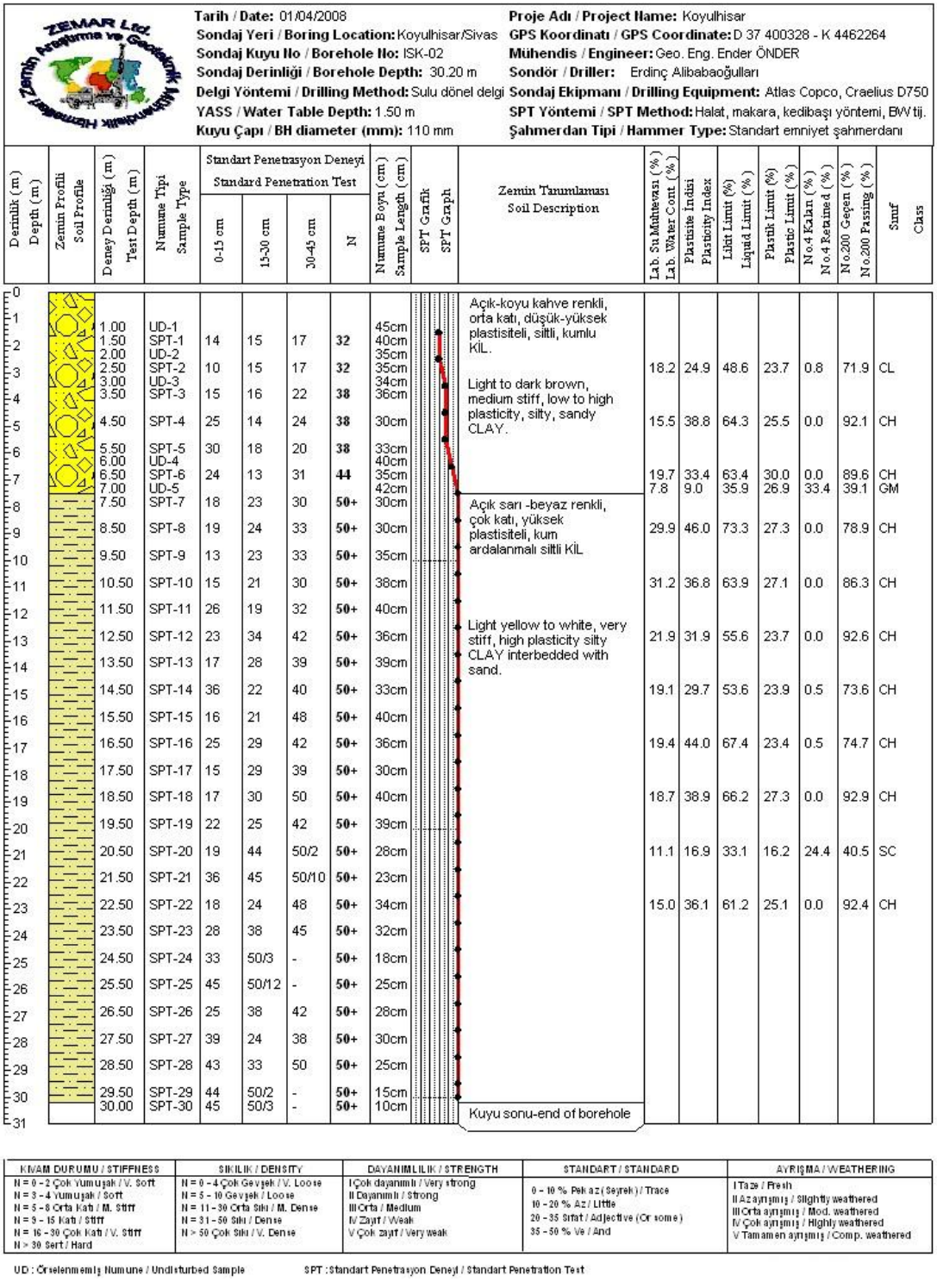

Test Depth (m)	Sample Type	0-15 cm	15-30 cm	30-45 cm	N	Sample Length (cm)	Lab. Water Cont (%)	Plasticity Index	Liquid Limit (%)	Plastic Limit (%)	No.4 Retained (%)	No.200 Passing (%)	Class
1.00	UD-1					45cm							
1.50	SPT-1	14	15	17	32	40cm							
2.00	UD-2					35cm							
2.50	SPT-2	10	15	17	32	35cm	18.2	24.9	48.6	23.7	0.8	71.9	CL
3.00	UD-3					34cm							
3.50	SPT-3	15	16	22	38	36cm							
4.50	SPT-4	25	14	24	38	30cm	15.5	38.8	64.3	25.5	0.0	92.1	CH
5.50	SPT-5	30	18	20	38	33cm							
6.00	UD-4					40cm							
6.50	SPT-6	24	13	31	44	35cm	19.7	33.4	63.4	30.0	0.0	89.6	CH
7.00	UD-5					42cm	7.8	9.0	35.9	26.9	33.4	39.1	GM
7.50	SPT-7	18	23	30	50+	30cm							
8.50	SPT-8	19	24	33	50+	30cm	29.9	46.0	73.3	27.3	0.0	78.9	CH
9.50	SPT-9	13	23	33	50+	35cm							
10.50	SPT-10	15	21	30	50+	38cm	31.2	36.8	63.9	27.1	0.0	86.3	CH
11.50	SPT-11	26	19	32	50+	40cm							
12.50	SPT-12	23	34	42	50+	36cm	21.9	31.9	55.6	23.7	0.0	92.6	CH
13.50	SPT-13	17	28	39	50+	39cm							
14.50	SPT-14	36	22	40	50+	33cm	19.1	29.7	53.6	23.9	0.5	73.6	CH
15.50	SPT-15	16	21	48	50+	40cm							
16.50	SPT-16	25	29	42	50+	36cm	19.4	44.0	67.4	23.4	0.5	74.7	CH
17.50	SPT-17	15	29	39	50+	30cm							
18.50	SPT-18	17	30	50	50+	40cm	18.7	38.9	66.2	27.3	0.0	92.9	CH
19.50	SPT-19	22	25	42	50+	39cm							
20.50	SPT-20	19	44	50/2	50+	28cm	11.1	16.9	33.1	16.2	24.4	40.5	SC
21.50	SPT-21	36	45	50/10	50+	23cm							
22.50	SPT-22	18	24	48	50+	34cm	15.0	36.1	61.2	25.1	0.0	92.4	CH
23.50	SPT-23	28	38	45	50+	32cm							
24.50	SPT-24	33	50/3	-	50+	18cm							
25.50	SPT-25	45	50/12	-	50+	25cm							
26.50	SPT-26	25	38	42	50+	28cm							
27.50	SPT-27	39	24	38	50+	30cm							
28.50	SPT-28	43	33	50	50+	25cm							
29.50	SPT-29	44	50/2	-	50+	15cm							
30.00	SPT-30	45	50/3	-	50+	10cm							

Figure A.2 Log of ISK-2 borehole.

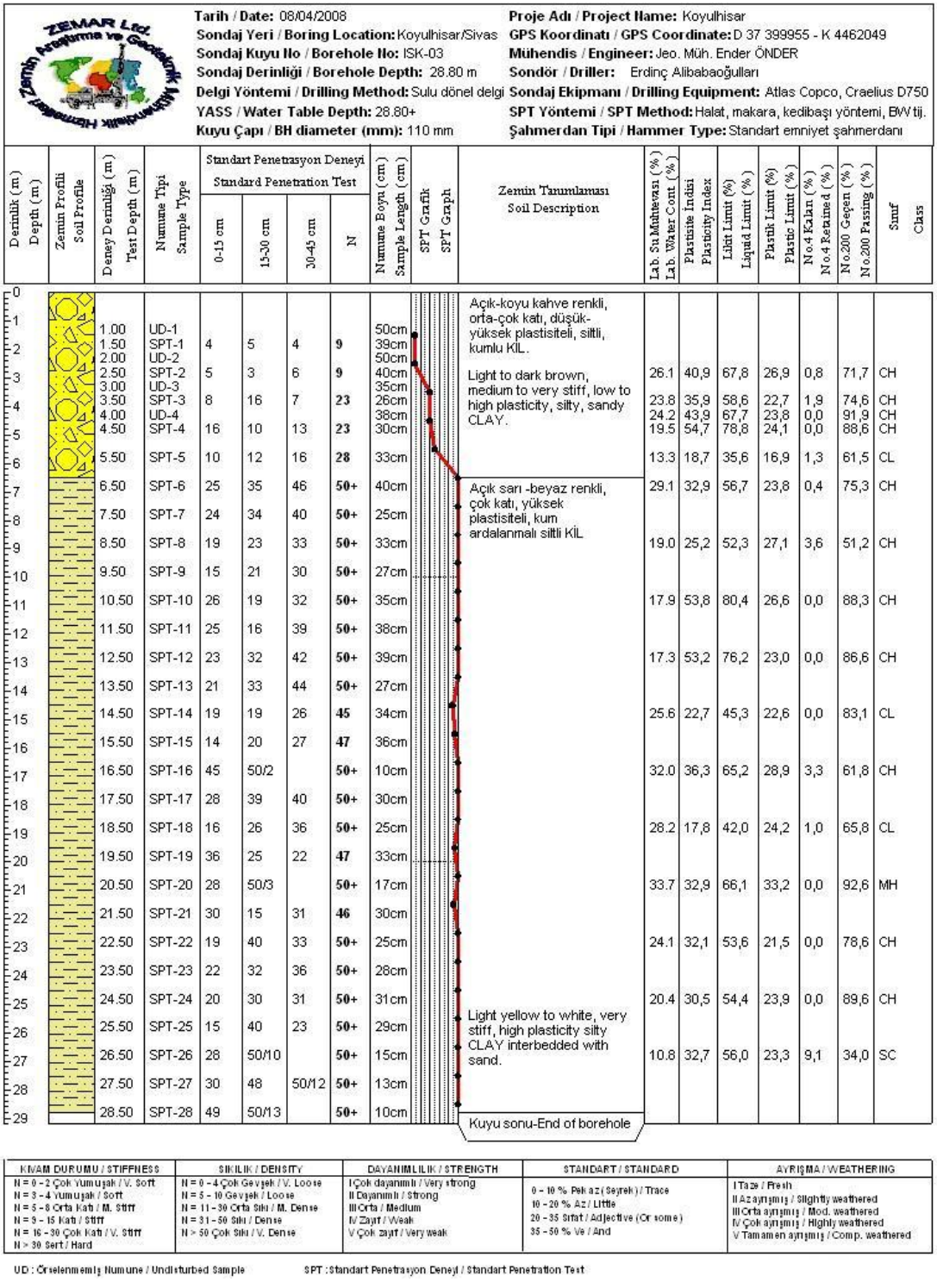

Derinlik (m)	Deney Derinliği (m)	Numune Tipi	0-15 cm	15-30 cm	30-45 cm	N	Numune Boyu (cm)	Zemin Tanımlaması	Lab. Su Muhtevası (%)	Plastisite İndisi	Likit Limit (%)	Plastik Limit (%)	No.4 Kalan (%)	No.200 Geçen (%)	Sınıf
1	1.00	UD-1					50cm	Açık-koyu kahve renkli, orta-çok katı, düşük-yüksek plastisiteli, siltli, kumlu KİL.							
2	1.50	SPT-1	4	5	4	9	39cm								
	2.00	UD-2					50cm								
3	2.50	SPT-2	5	3	6	9	40cm		26.1	40,9	67,8	26,9	0,8	71,7	CH
	3.00	UD-3					35cm	Light to dark brown, medium to very stiff, low to high plasticity, silty, sandy CLAY.							
4	3.50	SPT-3	8	16	7	23	26cm		23.8	35,9	58,6	22,7	1,9	74,6	CH
	4.00	UD-4					38cm		24.2	43,9	67,7	23,8	0,0	91,9	CH
5	4.50	SPT-4	16	10	13	23	30cm		19.5	54,7	78,8	24,1	0,0	88,6	CH
6	5.50	SPT-5	10	12	16	28	33cm		13.3	18,7	35,6	16,9	1,3	61,5	CL
7	6.50	SPT-6	25	35	46	50+	40cm	Açık sarı -beyaz renkli, çok katı, yüksek plastisiteli, kum ardalanmalı siltli KİL	29.1	32,9	56,7	23,8	0,4	75,3	CH
8	7.50	SPT-7	24	34	40	50+	25cm								
9	8.50	SPT-8	19	23	33	50+	33cm		19.0	25,2	52,3	27,1	3,6	51,2	CH
10	9.50	SPT-9	15	21	30	50+	27cm								
11	10.50	SPT-10	26	19	32	50+	35cm		17.9	53,8	80,4	26,6	0,0	88,3	CH
12	11.50	SPT-11	25	16	39	50+	38cm								
13	12.50	SPT-12	23	32	42	50+	39cm		17.3	53,2	76,2	23,0	0,0	86,6	CH
14	13.50	SPT-13	21	33	44	50+	27cm								
15	14.50	SPT-14	19	19	26	45	34cm		25.6	22,7	45,3	22,6	0,0	83,1	CL
16	15.50	SPT-15	14	20	27	47	36cm								
17	16.50	SPT-16	45	50/2		50+	10cm		32.0	36,3	65,2	28,9	3,3	61,8	CH
18	17.50	SPT-17	28	39	40	50+	30cm								
19	18.50	SPT-18	16	26	36	50+	25cm		28.2	17,8	42,0	24,2	1,0	65,8	CL
20	19.50	SPT-19	36	25	22	47	33cm								
21	20.50	SPT-20	28	50/3		50+	17cm		33.7	32,9	66,1	33,2	0,0	92,6	MH
22	21.50	SPT-21	30	15	31	46	30cm								
23	22.50	SPT-22	19	40	33	50+	25cm		24.1	32,1	53,6	21,5	0,0	78,6	CH
24	23.50	SPT-23	22	32	36	50+	28cm								
25	24.50	SPT-24	20	30	31	50+	31cm		20.4	30,5	54,4	23,9	0,0	89,6	CH
26	25.50	SPT-25	15	40	23	50+	29cm	Light yellow to white, very stiff, high plasticity silty CLAY interbedded with sand.							
27	26.50	SPT-26	28	50/10		50+	15cm		10.8	32,7	56,0	23,3	9,1	34,0	SC
28	27.50	SPT-27	30	48	50/12	50+	13cm								
29	28.50	SPT-28	49	50/13		50+	10cm	Kuyu sonu-End of borehole							

Figure A.3 Log of ISK-3 borehole.

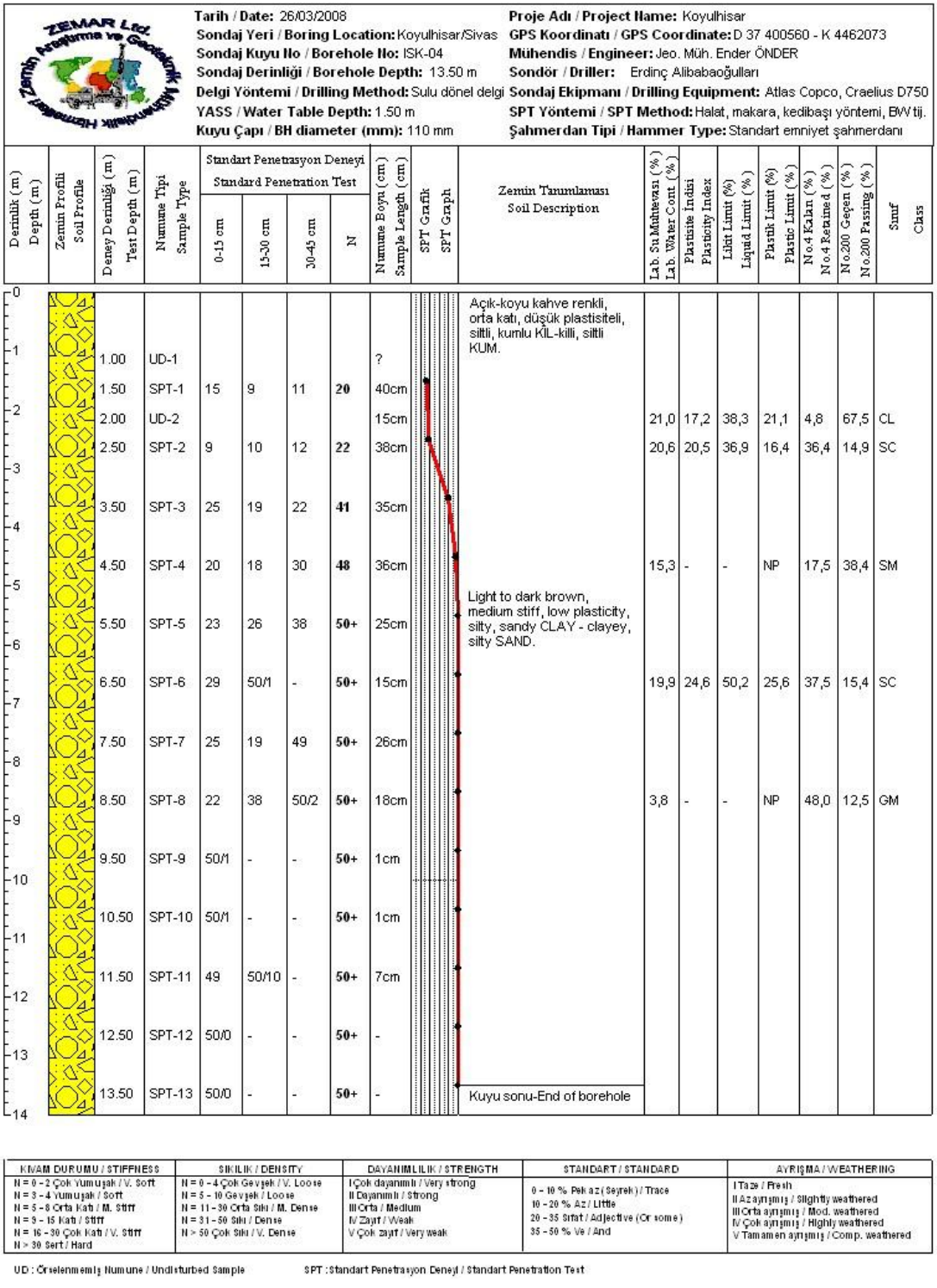

Figure A.4 Log of ISK-4 borehole.

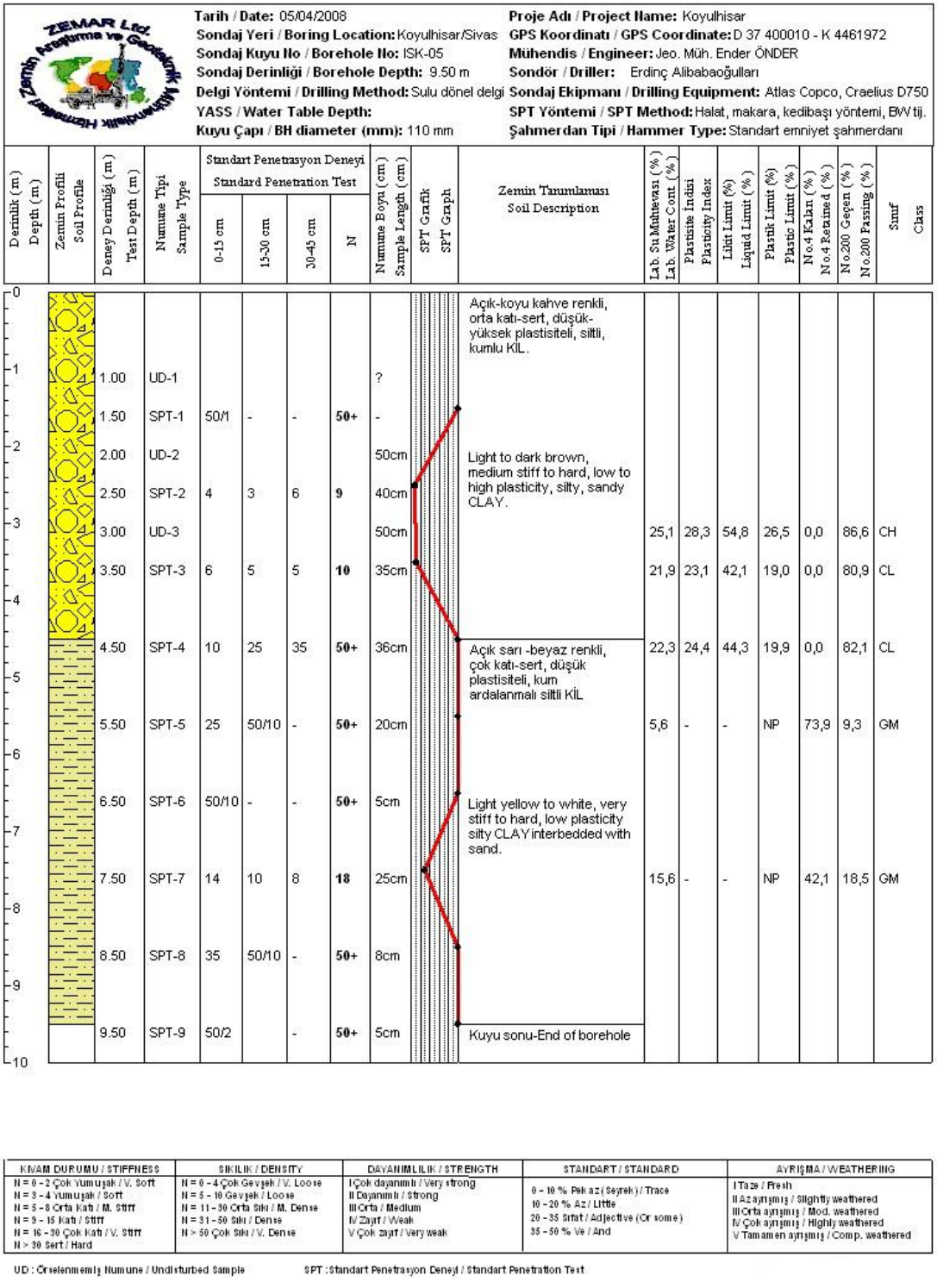

Figure A.5 Log of ISK-5 borehole.

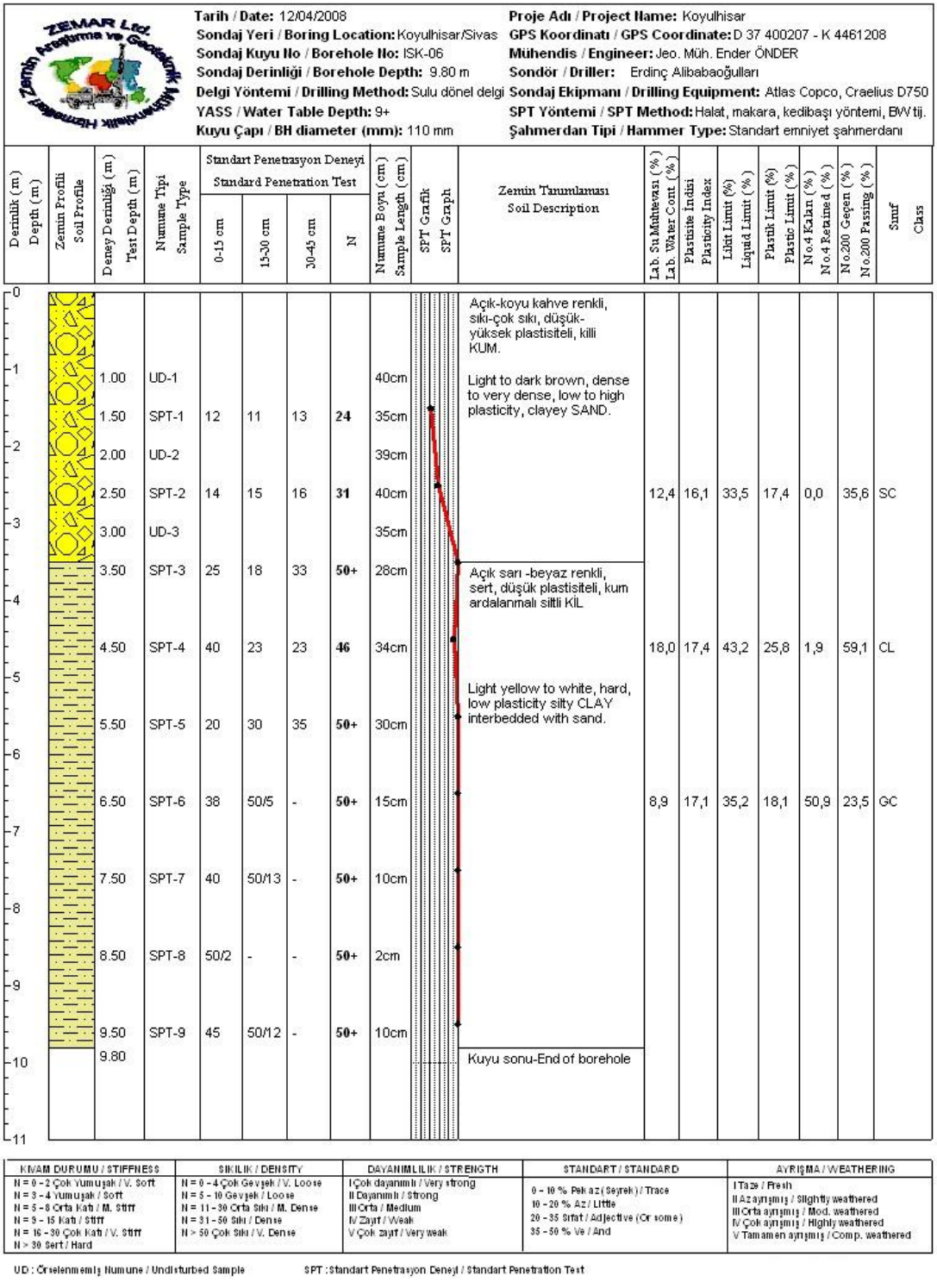

Test Depth (m)	Sample Type	0-15 cm	15-30 cm	30-45 cm	N	Sample Length (cm)	Lab. Water Cont (%)	Plasticity Index	Liquid Limit (%)	Plastic Limit (%)	No.4 Retained (%)	No.200 Passing (%)	Class
1.00	UD-1					40cm							
1.50	SPT-1	12	11	13	24	35cm							
2.00	UD-2					39cm							
2.50	SPT-2	14	15	16	31	40cm	12,4	16,1	33,5	17,4	0,0	35,6	SC
3.00	UD-3					35cm							
3.50	SPT-3	25	18	33	50+	28cm							
4.50	SPT-4	40	23	23	46	34cm	18,0	17,4	43,2	25,8	1,9	59,1	CL
5.50	SPT-5	20	30	35	50+	30cm							
6.50	SPT-6	38	50/5	-	50+	15cm	8,9	17,1	35,2	18,1	50,9	23,5	GC
7.50	SPT-7	40	50/13	-	50+	10cm							
8.50	SPT-8	50/2	-	-	50+	2cm							
9.50	SPT-9	45	50/12	-	50+	10cm							
9.80													

Figure A.6 Log of ISK-6 borehole.

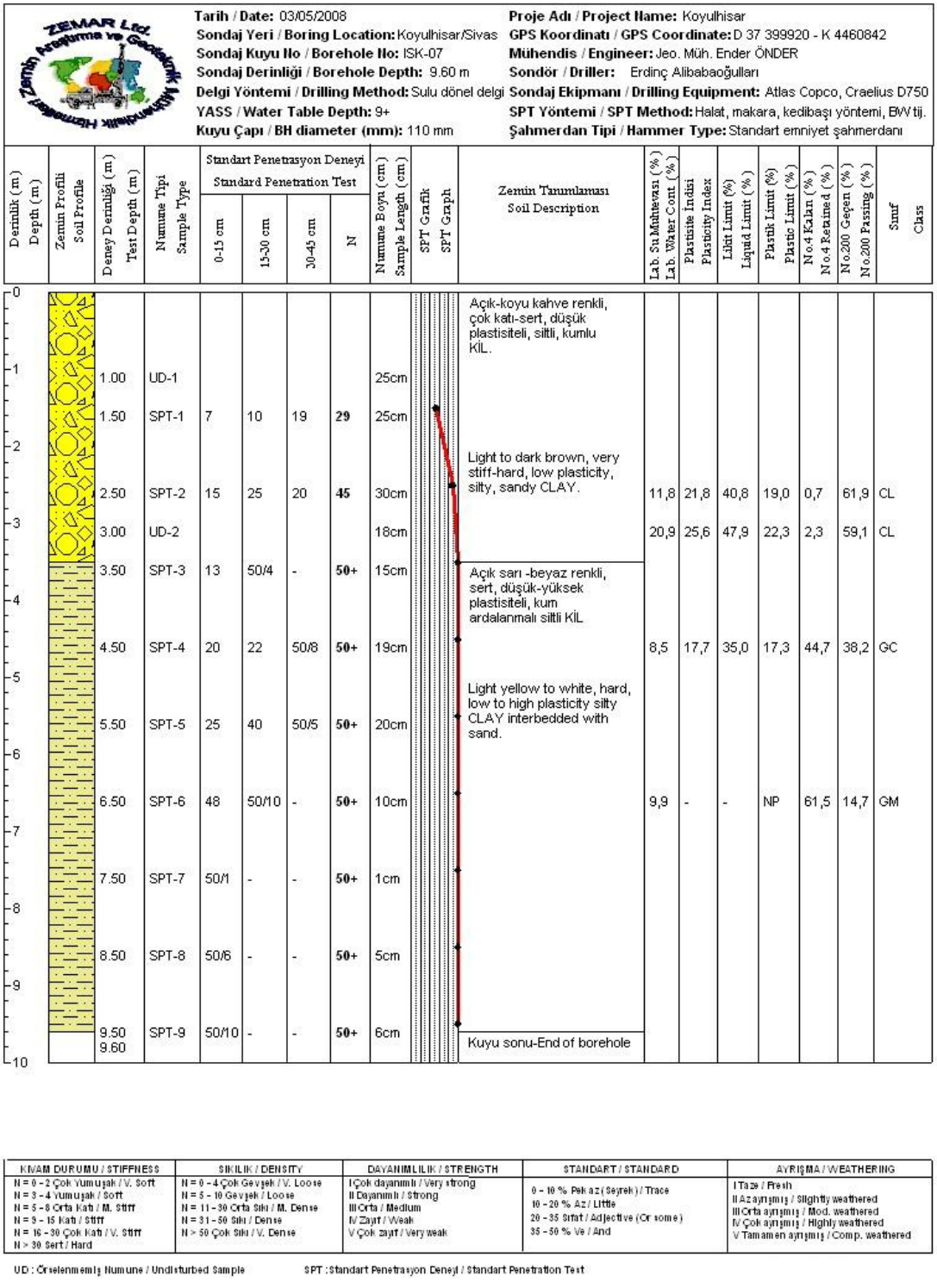

Figure A.7 Log of ISK-7 borehole.

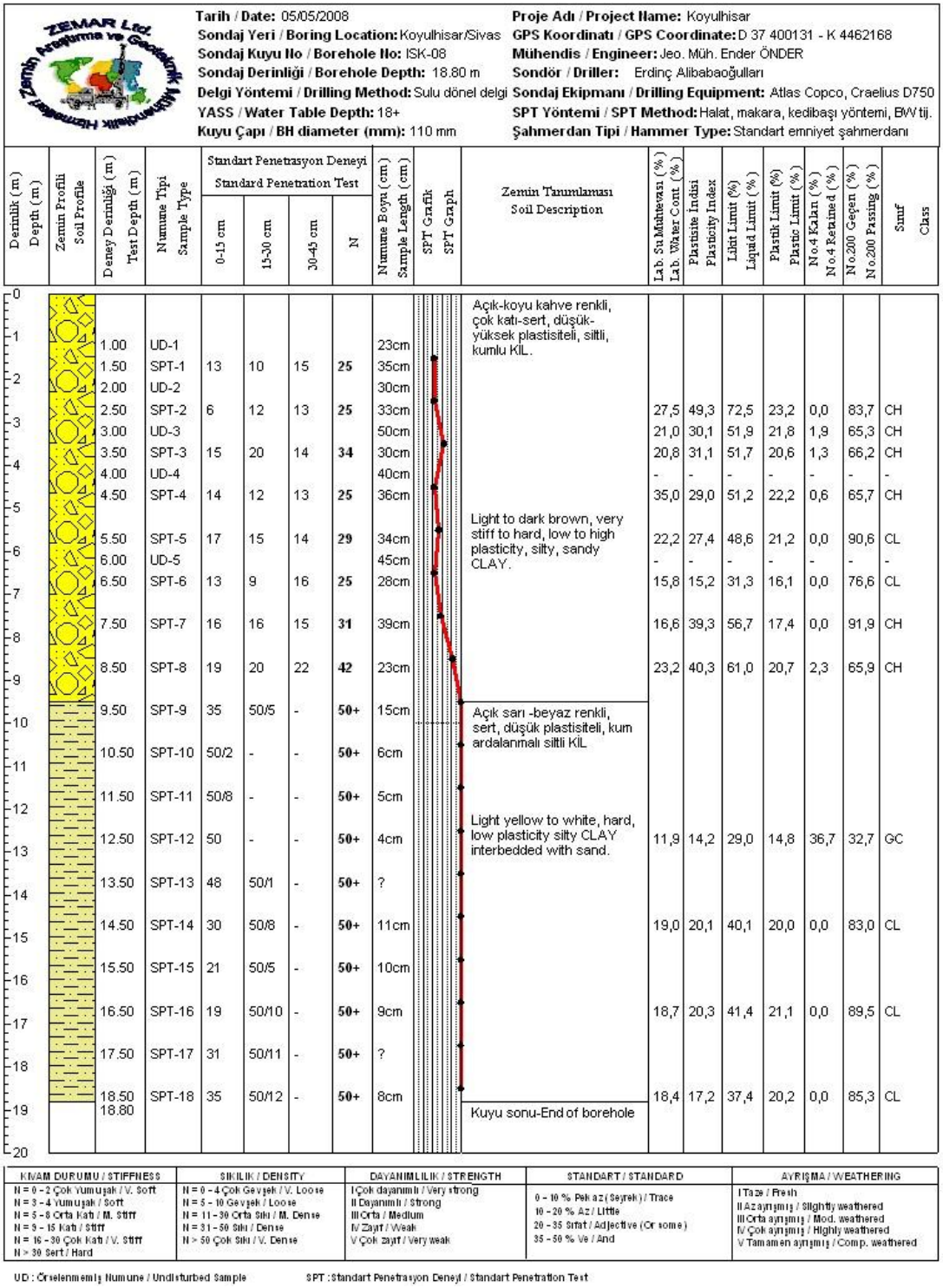

Test Depth (m)	Sample Type	0-15 cm	15-30 cm	30-45 cm	N	Sample Length (cm)	Lab. Water Cont (%)	Plasticity Index	Liquid Limit (%)	Plastic Limit (%)	No.4 Retained (%)	No.200 Passing (%)	Class
1.00	UD-1					23cm							
1.50	SPT-1	13	10	15	25	35cm							
2.00	UD-2					30cm							
2.50	SPT-2	6	12	13	25	33cm	27,5	49,3	72,5	23,2	0,0	83,7	CH
3.00	UD-3					50cm	21,0	30,1	51,9	21,8	1,9	65,3	CH
3.50	SPT-3	15	20	14	34	30cm	20,8	31,1	51,7	20,6	1,3	66,2	CH
4.00	UD-4					40cm	-	-	-	-	-	-	-
4.50	SPT-4	14	12	13	25	36cm	35,0	29,0	51,2	22,2	0,6	65,7	CH
5.50	SPT-5	17	15	14	29	34cm	22,2	27,4	48,6	21,2	0,0	90,6	CL
6.00	UD-5					45cm	-	-	-	-	-	-	-
6.50	SPT-6	13	9	16	25	28cm	15,8	15,2	31,3	16,1	0,0	76,6	CL
7.50	SPT-7	16	16	15	31	39cm	16,6	39,3	56,7	17,4	0,0	91,9	CH
8.50	SPT-8	19	20	22	42	23cm	23,2	40,3	61,0	20,7	2,3	65,9	CH
9.50	SPT-9	35	50/5	-	50+	15cm							
10.50	SPT-10	50/2	-	-	50+	6cm							
11.50	SPT-11	50/8	-	-	50+	5cm							
12.50	SPT-12	50	-	-	50+	4cm	11,9	14,2	29,0	14,8	36,7	32,7	GC
13.50	SPT-13	48	50/1	-	50+	?							
14.50	SPT-14	30	50/8	-	50+	11cm	19,0	20,1	40,1	20,0	0,0	83,0	CL
15.50	SPT-15	21	50/5	-	50+	10cm							
16.50	SPT-16	19	50/10	-	50+	9cm	18,7	20,3	41,4	21,1	0,0	89,5	CL
17.50	SPT-17	31	50/11	-	50+	?							
18.50	SPT-18	35	50/12	-	50+	8cm	18,4	17,2	37,4	20,2	0,0	85,3	CL
18.80													

Figure A.8 Log of ISK-8 borehole.

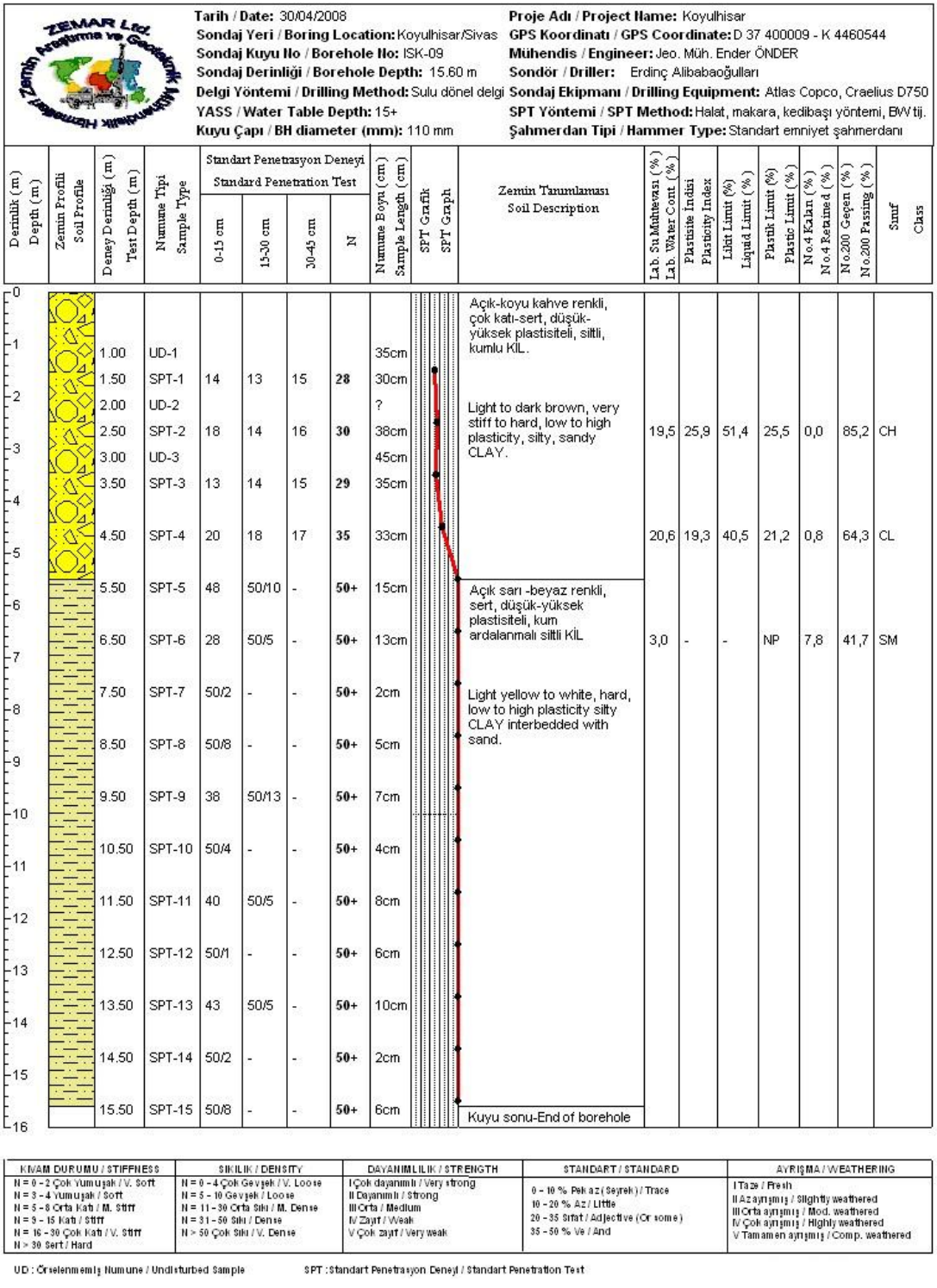

Figure A.9 Log of ISK-9 borehole.

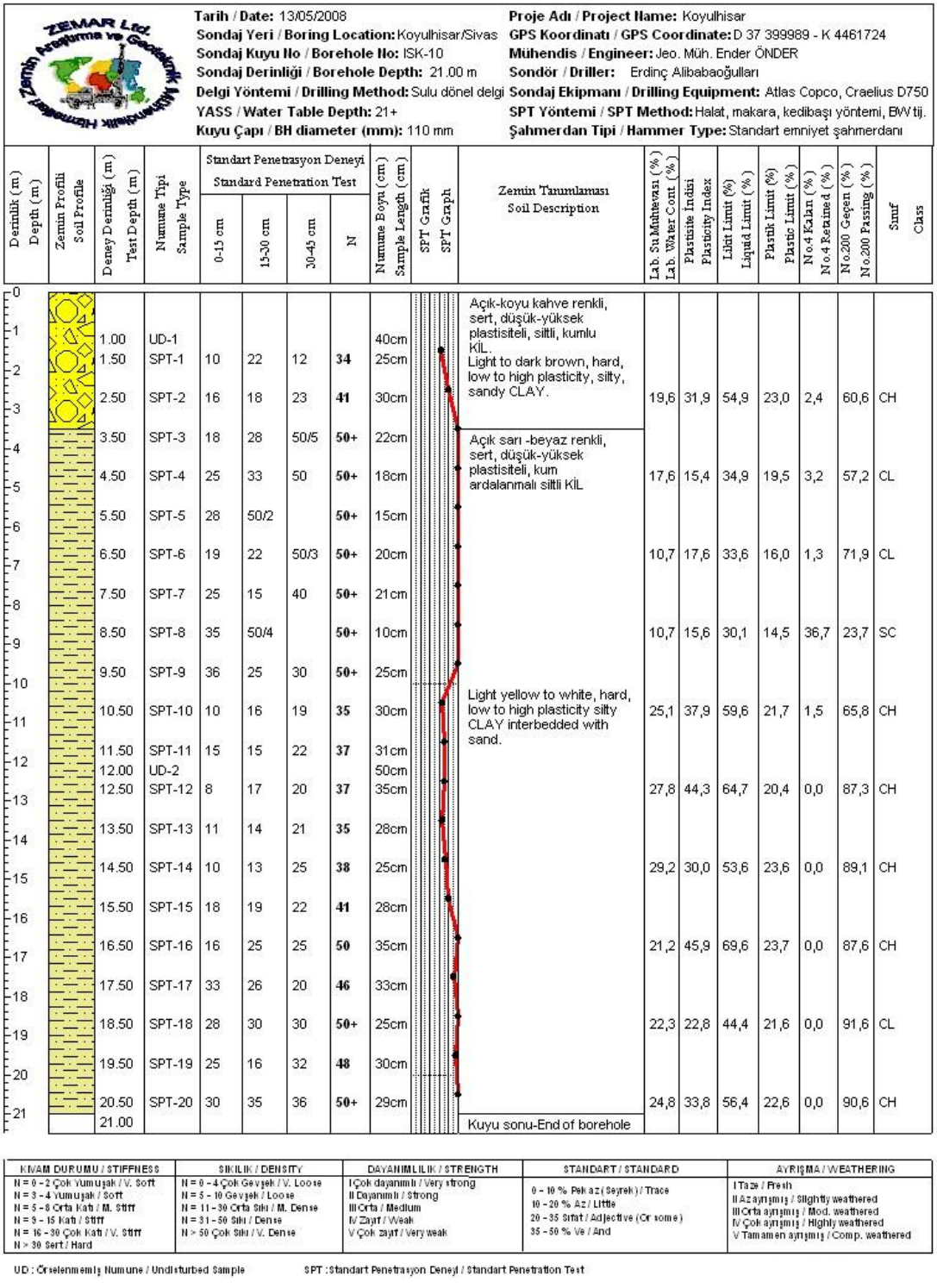

Depth (m)	Sample Type	Test Depth (m)	0-15 cm	15-30 cm	30-45 cm	N	Sample Length (cm)	Lab. Water Cont (%)	Plasticity Index	Liquid Limit (%)	Plastic Limit (%)	No.4 Retained (%)	No.200 Passing (%)	Class
1.00	UD-1						40cm							
1.50	SPT-1	10	22	12	34		25cm							
2.50	SPT-2	16	18	23	41		30cm	19,6	31,9	54,9	23,0	2,4	60,6	CH
3.50	SPT-3	18	28	50/5	50+		22cm							
4.50	SPT-4	25	33	50	50+		18cm	17,6	15,4	34,9	19,5	3,2	57,2	CL
5.50	SPT-5	28	50/2		50+		15cm							
6.50	SPT-6	19	22	50/3	50+		20cm	10,7	17,6	33,6	16,0	1,3	71,9	CL
7.50	SPT-7	25	15	40	50+		21cm							
8.50	SPT-8	35	50/4		50+		10cm	10,7	15,6	30,1	14,5	36,7	23,7	SC
9.50	SPT-9	36	25	30	50+		25cm							
10.50	SPT-10	10	16	19	35		30cm	25,1	37,9	59,6	21,7	1,5	65,8	CH
11.50	SPT-11	15	15	22	37		31cm							
12.00	UD-2						50cm							
12.50	SPT-12	8	17	20	37		35cm	27,8	44,3	64,7	20,4	0,0	87,3	CH
13.50	SPT-13	11	14	21	35		28cm							
14.50	SPT-14	10	13	25	38		25cm	29,2	30,0	53,6	23,6	0,0	89,1	CH
15.50	SPT-15	18	19	22	41		28cm							
16.50	SPT-16	16	25	25	50		35cm	21,2	45,9	69,6	23,7	0,0	87,6	CH
17.50	SPT-17	33	26	20	46		33cm							
18.50	SPT-18	28	30	30	50+		25cm	22,3	22,8	44,4	21,6	0,0	91,6	CL
19.50	SPT-19	25	16	32	48		30cm							
20.50	SPT-20	30	35	36	50+		29cm	24,8	33,8	56,4	22,6	0,0	90,6	CH
21.00														

Figure A.10 Log of ISK-10 borehole.

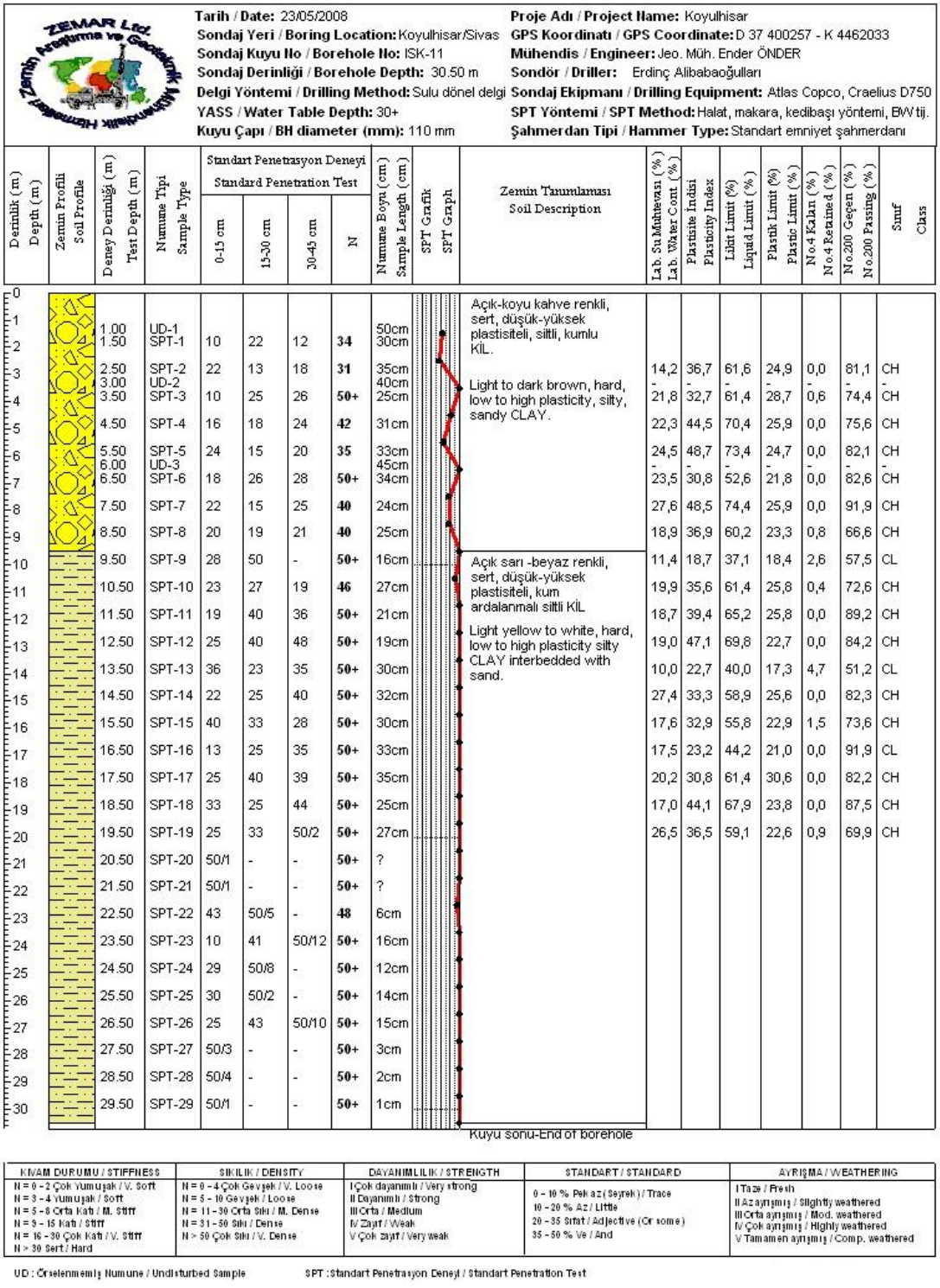

Depth (m)	Test Depth (m)	Sample Type	0-15 cm	15-30 cm	30-45 cm	N	Sample Length (cm)	Lab. Water Cont (%)	Plasticity Index	Liquid Limit (%)	Plastic Limit (%)	No.4 Retained (%)	No.200 Passing (%)	Class
1.00	1.00	UD-1					50cm							
1.50	1.50	SPT-1	10	22	12	34	30cm							
2.50	2.50	SPT-2	22	13	18	31	35cm	14,2	36,7	61,6	24,9	0,0	81,1	CH
3.00	3.00	UD-2					40cm	-	-	-	-	-	-	-
3.50	3.50	SPT-3	10	25	26	50+	25cm	21,8	32,7	61,4	28,7	0,6	74,4	CH
4.50	4.50	SPT-4	16	18	24	42	31cm	22,3	44,5	70,4	25,9	0,0	75,6	CH
5.50	5.50	SPT-5	24	15	20	35	33cm	24,5	48,7	73,4	24,7	0,0	82,1	CH
6.00	6.00	UD-3					45cm	-	-	-	-	-	-	-
6.50	6.50	SPT-6	18	26	28	50+	34cm	23,5	30,8	52,6	21,8	0,0	82,6	CH
7.50	7.50	SPT-7	22	15	25	40	24cm	27,6	48,5	74,4	25,9	0,0	91,9	CH
8.50	8.50	SPT-8	20	19	21	40	25cm	18,9	36,9	60,2	23,3	0,8	66,6	CH
9.50	9.50	SPT-9	28	50	-	50+	16cm	11,4	18,7	37,1	18,4	2,6	57,5	CL
10.50	10.50	SPT-10	23	27	19	46	27cm	19,9	35,6	61,4	25,8	0,4	72,6	CH
11.50	11.50	SPT-11	19	40	36	50+	21cm	18,7	39,4	65,2	25,8	0,0	89,2	CH
12.50	12.50	SPT-12	25	40	48	50+	19cm	19,0	47,1	69,8	22,7	0,0	84,2	CH
13.50	13.50	SPT-13	36	23	35	50+	30cm	10,0	22,7	40,0	17,3	4,7	51,2	CL
14.50	14.50	SPT-14	22	25	40	50+	32cm	27,4	33,3	58,9	25,6	0,0	82,3	CH
15.50	15.50	SPT-15	40	33	28	50+	30cm	17,6	32,9	55,8	22,9	1,5	73,6	CH
16.50	16.50	SPT-16	13	25	35	50+	33cm	17,5	23,2	44,2	21,0	0,0	91,9	CL
17.50	17.50	SPT-17	25	40	39	50+	35cm	20,2	30,8	61,4	30,6	0,0	82,2	CH
18.50	18.50	SPT-18	33	25	44	50+	25cm	17,0	44,1	67,9	23,8	0,0	87,5	CH
19.50	19.50	SPT-19	25	33	50/2	50+	27cm	26,5	36,5	59,1	22,6	0,9	69,9	CH
20.50	20.50	SPT-20	50/1	-	-	50+	?							
21.50	21.50	SPT-21	50/1	-	-	50+	?							
22.50	22.50	SPT-22	43	50/5	-	48	6cm							
23.50	23.50	SPT-23	10	41	50/12	50+	16cm							
24.50	24.50	SPT-24	29	50/8	-	50+	12cm							
25.50	25.50	SPT-25	30	50/2	-	50+	14cm							
26.50	26.50	SPT-26	25	43	50/10	50+	15cm							
27.50	27.50	SPT-27	50/3	-	-	50+	3cm							
28.50	28.50	SPT-28	50/4	-	-	50+	2cm							
29.50	29.50	SPT-29	50/1	-	-	50+	1cm							

Figure A.11 Log of ISK-11 borehole.

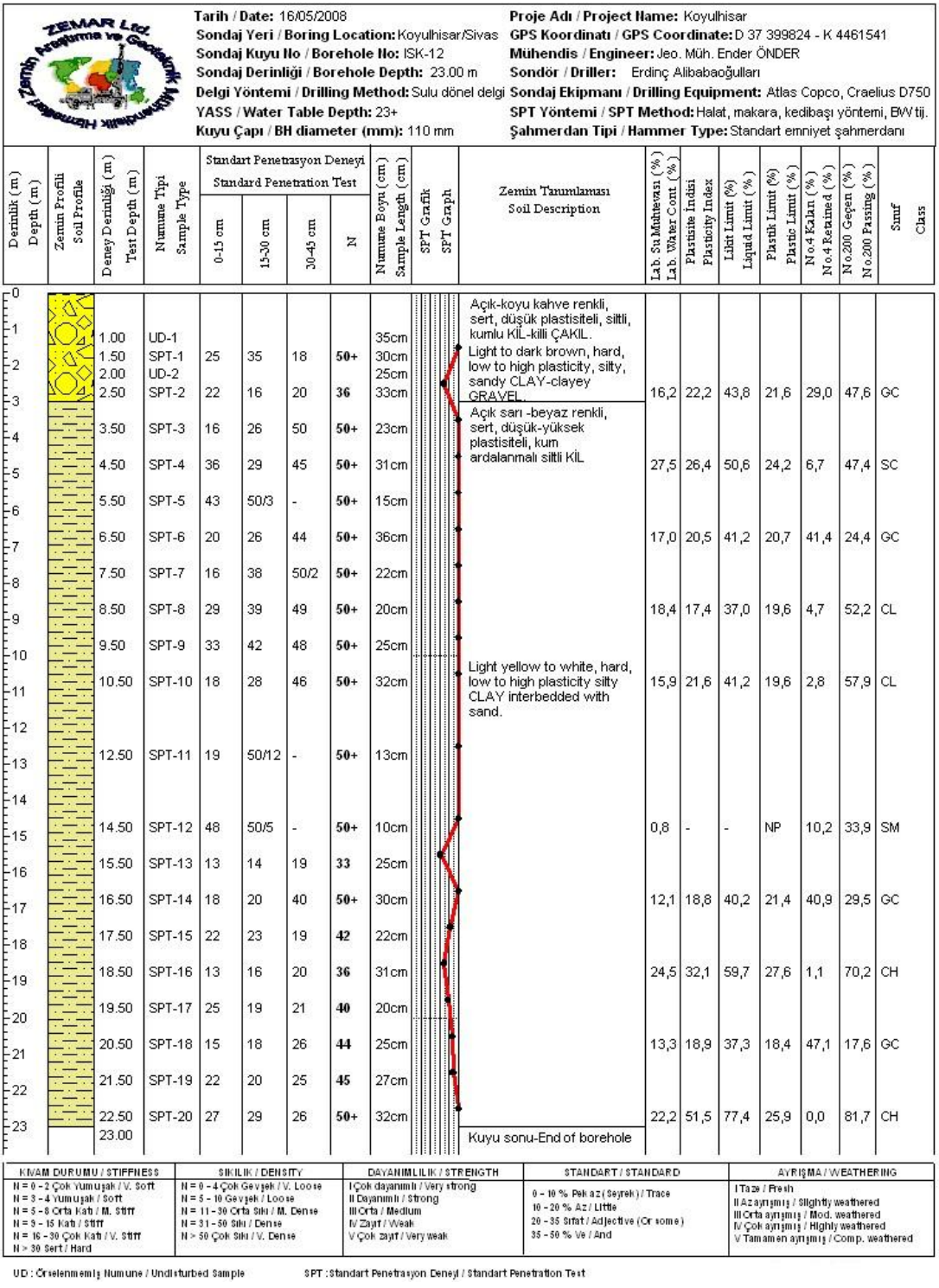

Depth (m)	Sample Type	Test Depth (m)	0-15 cm	15-30 cm	30-45 cm	N	Sample Length (cm)	Lab. Water Cont (%)	Plasticity Index	Liquid Limit (%)	Plastic Limit (%)	No.4 Retained (%)	No.200 Passing (%)	Class
1.00	UD-1						35cm							
1.50	SPT-1		25	35	18	50+	30cm							
2.00	UD-2						25cm							
2.50	SPT-2		22	16	20	36	33cm	16,2	22,2	43,8	21,6	29,0	47,6	GC
3.50	SPT-3		16	26	50	50+	23cm							
4.50	SPT-4		36	29	45	50+	31cm	27,5	26,4	50,6	24,2	6,7	47,4	SC
5.50	SPT-5		43	50/3	-	50+	15cm							
6.50	SPT-6		20	26	44	50+	36cm	17,0	20,5	41,2	20,7	41,4	24,4	GC
7.50	SPT-7		16	38	50/2	50+	22cm							
8.50	SPT-8		29	39	49	50+	20cm	18,4	17,4	37,0	19,6	4,7	52,2	CL
9.50	SPT-9		33	42	48	50+	25cm							
10.50	SPT-10		18	28	46	50+	32cm	15,9	21,6	41,2	19,6	2,8	57,9	CL
12.50	SPT-11		19	50/12	-	50+	13cm							
14.50	SPT-12		48	50/5	-	50+	10cm	0,8	-	-	NP	10,2	33,9	SM
15.50	SPT-13		13	14	19	33	25cm							
16.50	SPT-14		18	20	40	50+	30cm	12,1	18,8	40,2	21,4	40,9	29,5	GC
17.50	SPT-15		22	23	19	42	22cm							
18.50	SPT-16		13	16	20	36	31cm	24,5	32,1	59,7	27,6	1,1	70,2	CH
19.50	SPT-17		25	19	21	40	20cm							
20.50	SPT-18		15	18	26	44	25cm	13,3	18,9	37,3	18,4	47,1	17,6	GC
21.50	SPT-19		22	20	25	45	27cm							
22.50	SPT-20		27	29	26	50+	32cm	22,2	51,5	77,4	25,9	0,0	81,7	CH
23.00														

Figure A.12 Log of ISK-12 borehole.

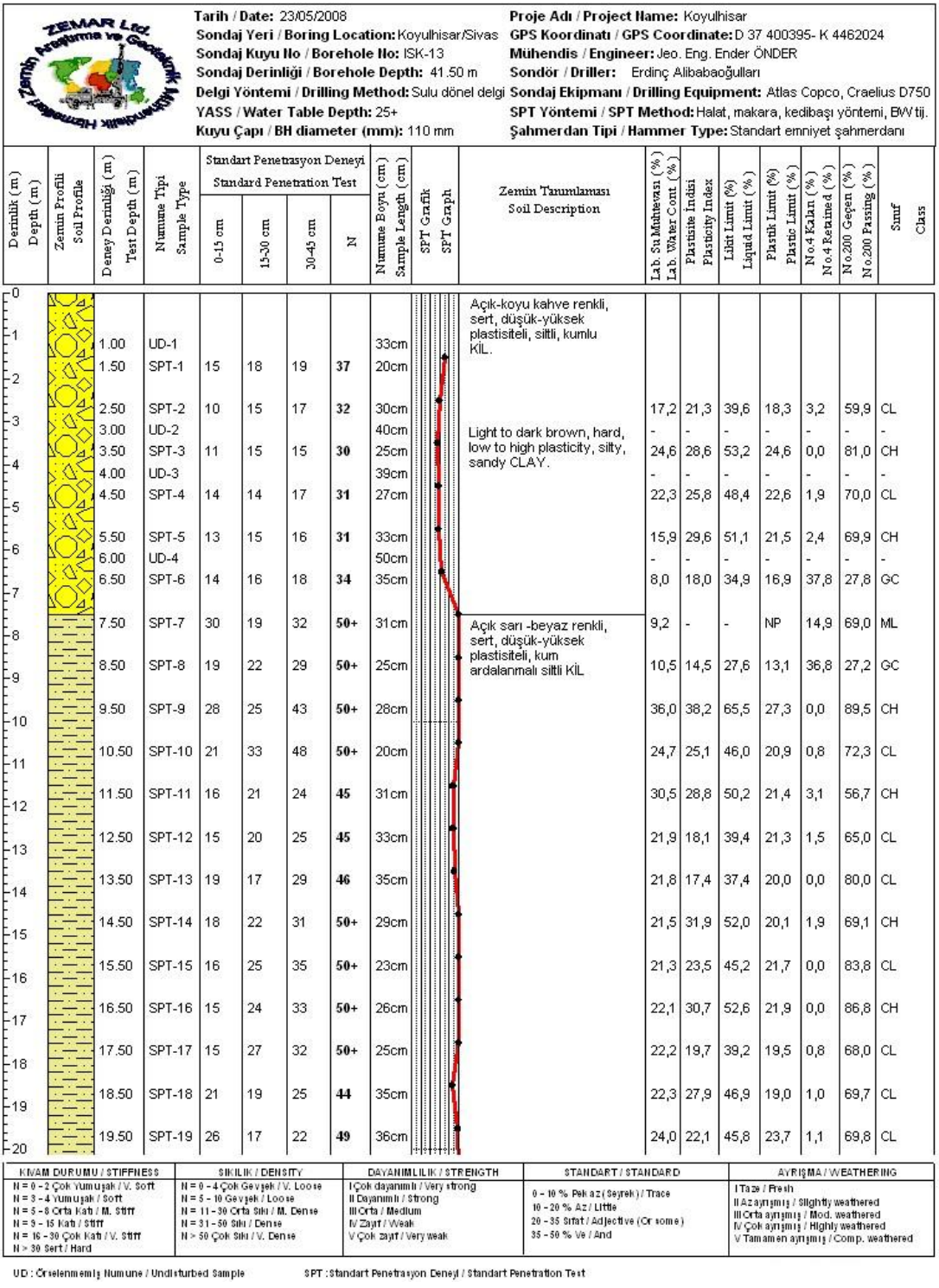

Depth (m)	Test Depth (m)	Sample Type	0-15 cm	15-30 cm	30-45 cm	N	Sample Length (cm)	Soil Description	Lab. Water Cont (%)	Plasticity Index	Liquid Limit (%)	Plastic Limit (%)	No.4 Retained (%)	No.200 Passing (%)	Class
1	1.00	UD-1					33cm	Açık-koyu kahve renkli, sert, düşük-yüksek plastisiteli, siltli, kumlu KİL.							
1	1.50	SPT-1	15	18	19	37	20cm								
2	2.50	SPT-2	10	15	17	32	30cm		17,2	21,3	39,6	18,3	3,2	59,9	CL
3	3.00	UD-2					40cm	Light to dark brown, hard, low to high plasticity, silty, sandy CLAY.	-	-	-	-	-	-	-
3	3.50	SPT-3	11	15	15	30	25cm		24,6	28,6	53,2	24,6	0,0	81,0	CH
4	4.00	UD-3					39cm		-	-	-	-	-	-	-
4	4.50	SPT-4	14	14	17	31	27cm		22,3	25,8	48,4	22,6	1,9	70,0	CL
5	5.50	SPT-5	13	15	16	31	33cm		15,9	29,6	51,1	21,5	2,4	69,9	CH
6	6.00	UD-4					50cm		-	-	-	-	-	-	-
6	6.50	SPT-6	14	16	18	34	35cm		8,0	18,0	34,9	16,9	37,8	27,8	GC
7	7.50	SPT-7	30	19	32	50+	31cm	Açık sarı -beyaz renkli, sert, düşük-yüksek plastisiteli, kum ardalanmalı siltli KİL	9,2	-	-	NP	14,9	69,0	ML
8	8.50	SPT-8	19	22	29	50+	25cm		10,5	14,5	27,6	13,1	36,8	27,2	GC
9	9.50	SPT-9	28	25	43	50+	28cm		36,0	38,2	65,5	27,3	0,0	89,5	CH
10	10.50	SPT-10	21	33	48	50+	20cm		24,7	25,1	46,0	20,9	0,8	72,3	CL
11	11.50	SPT-11	16	21	24	45	31cm		30,5	28,8	50,2	21,4	3,1	56,7	CH
12	12.50	SPT-12	15	20	25	45	33cm		21,9	18,1	39,4	21,3	1,5	65,0	CL
13	13.50	SPT-13	19	17	29	46	35cm		21,8	17,4	37,4	20,0	0,0	80,0	CL
14	14.50	SPT-14	18	22	31	50+	29cm		21,5	31,9	52,0	20,1	1,9	69,1	CH
15	15.50	SPT-15	16	25	35	50+	23cm		21,3	23,5	45,2	21,7	0,0	83,8	CL
16	16.50	SPT-16	15	24	33	50+	26cm		22,1	30,7	52,6	21,9	0,0	86,8	CH
17	17.50	SPT-17	15	27	32	50+	25cm		22,2	19,7	39,2	19,5	0,8	68,0	CL
18	18.50	SPT-18	21	19	25	44	35cm		22,3	27,9	46,9	19,0	1,0	69,7	CL
19	19.50	SPT-19	26	17	22	49	36cm		24,0	22,1	45,8	23,7	1,1	69,8	CL

Figure A.13 Log of ISK-13 borehole from 0 to 19,5 meters depth.

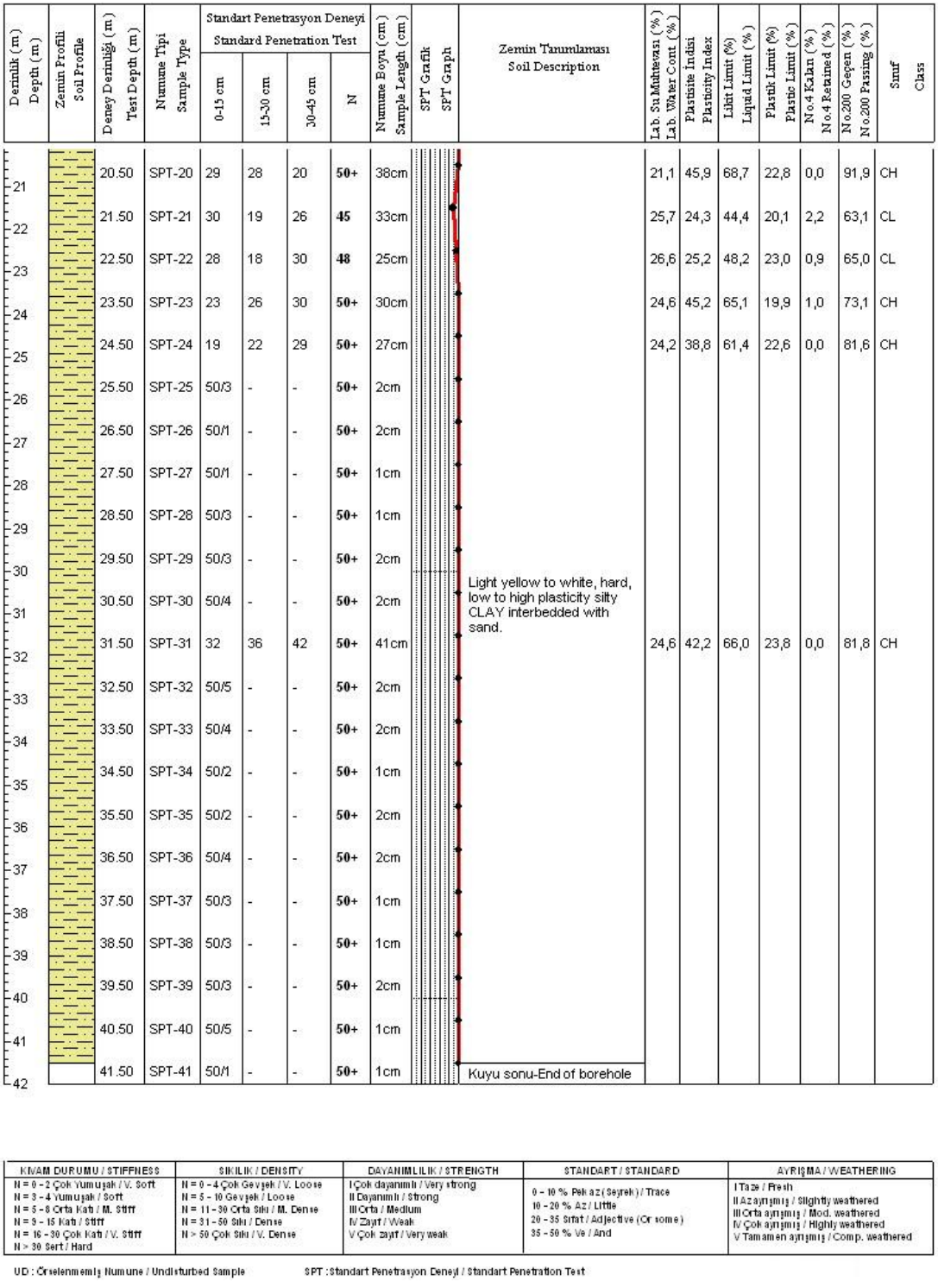

Figure A.14 Log of ISK-13 borehole from 20,5 to 41,5 meters depth.

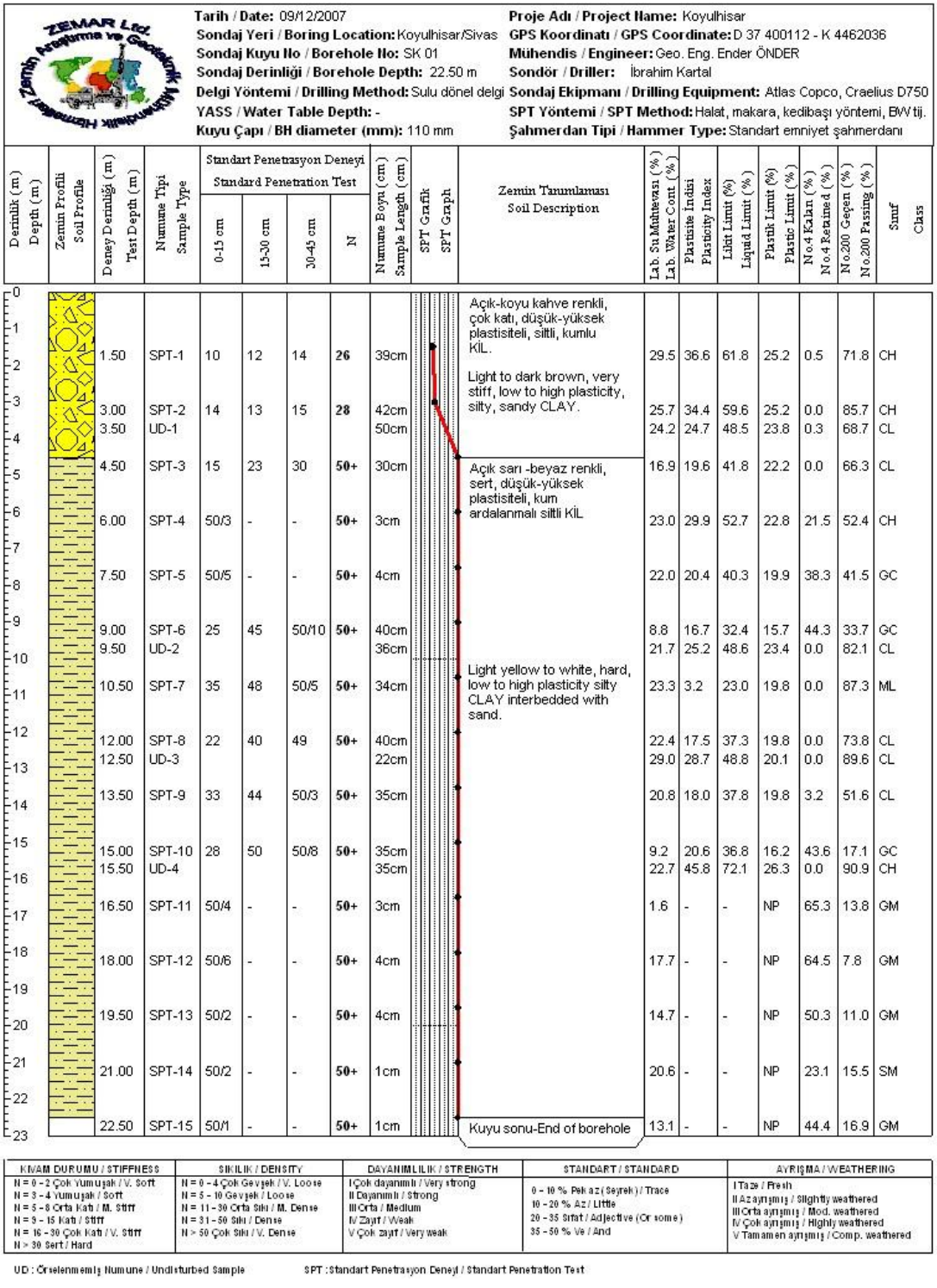

Depth (m)	Test Depth (m)	Sample Type	0-15 cm	15-30 cm	30-45 cm	N	Sample Length (cm)	Lab. Water Cont (%)	Plasticity Index	Liquid Limit (%)	Plastic Limit (%)	No.4 Retained (%)	No.200 Passing (%)	Class
1.50	SPT-1	10	12	14	**26**	39cm	29.5	36.6	61.8	25.2	0.5	71.8	CH
3.00	SPT-2	14	13	15	**28**	42cm	25.7	34.4	59.6	25.2	0.0	85.7	CH
3.50	UD-1					50cm	24.2	24.7	48.5	23.8	0.3	68.7	CL
4.50	SPT-3	15	23	30	**50+**	30cm	16.9	19.6	41.8	22.2	0.0	66.3	CL
6.00	SPT-4	50/3	-	-	**50+**	3cm	23.0	29.9	52.7	22.8	21.5	52.4	CH
7.50	SPT-5	50/5	-	-	**50+**	4cm	22.0	20.4	40.3	19.9	38.3	41.5	GC
9.00	SPT-6	25	45	50/10	**50+**	40cm	8.8	16.7	32.4	15.7	44.3	33.7	GC
9.50	UD-2					36cm	21.7	25.2	48.6	23.4	0.0	82.1	CL
10.50	SPT-7	35	48	50/5	**50+**	34cm	23.3	3.2	23.0	19.8	0.0	87.3	ML
12.00	SPT-8	22	40	49	**50+**	40cm	22.4	17.5	37.3	19.8	0.0	73.8	CL
12.50	UD-3					22cm	29.0	28.7	48.8	20.1	0.0	89.6	CL
13.50	SPT-9	33	44	50/3	**50+**	35cm	20.8	18.0	37.8	19.8	3.2	51.6	CL
15.00	SPT-10	28	50	50/8	**50+**	35cm	9.2	20.6	36.8	16.2	43.6	17.1	GC
15.50	UD-4					35cm	22.7	45.8	72.1	26.3	0.0	90.9	CH
16.50	SPT-11	50/4	-	-	**50+**	3cm	1.6	-	-	NP	65.3	13.8	GM
18.00	SPT-12	50/6	-	-	**50+**	4cm	17.7	-	-	NP	64.5	7.8	GM
19.50	SPT-13	50/2	-	-	**50+**	4cm	14.7	-	-	NP	50.3	11.0	GM
21.00	SPT-14	50/2	-	-	**50+**	1cm	20.6	-	-	NP	23.1	15.5	SM
22.50	SPT-15	50/1	-	-	**50+**	1cm	13.1	-	-	NP	44.4	16.9	GM

Figure A.15 Log of SK-1 borehole.

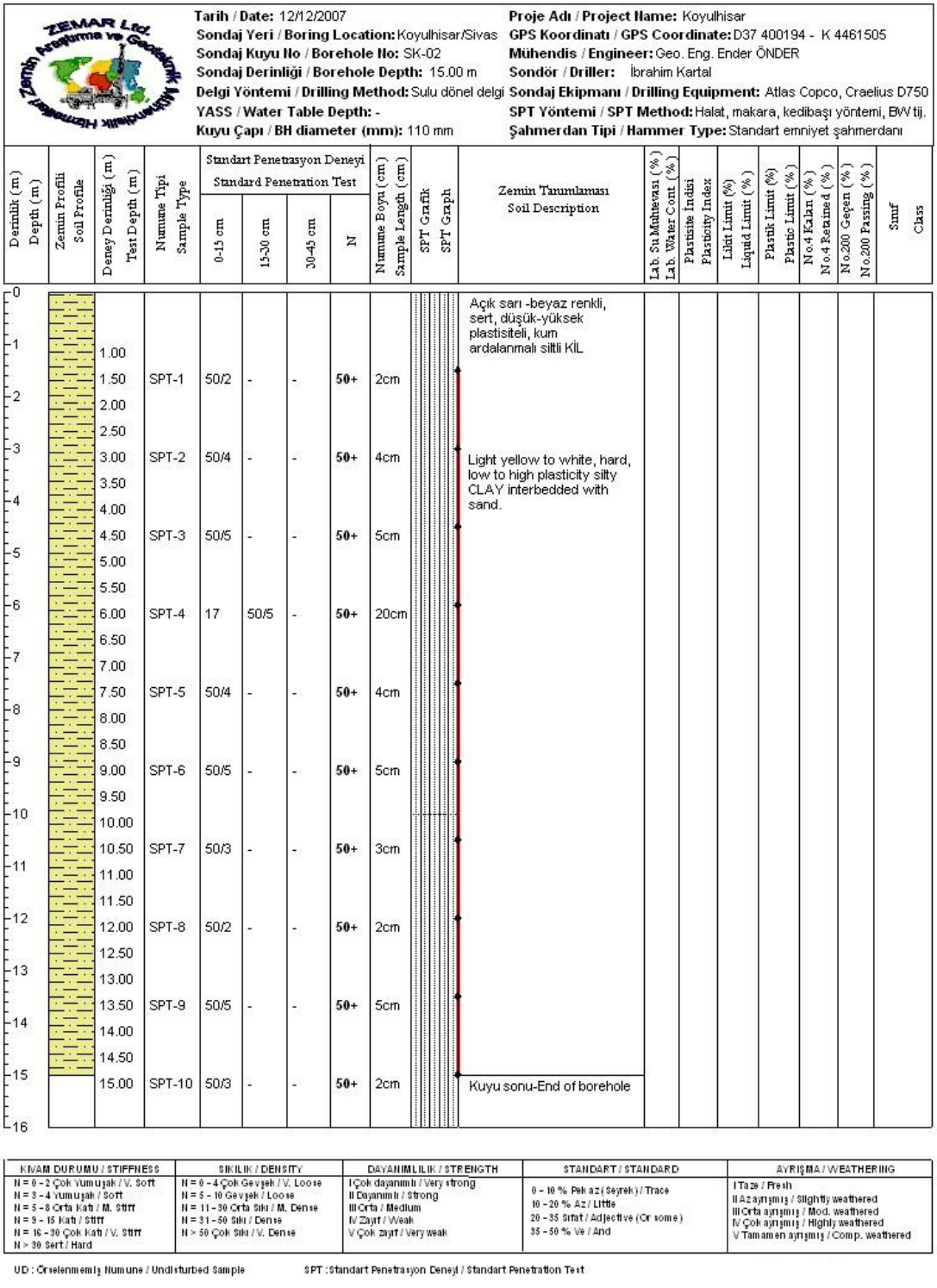

Figure A.16 Log of SK-2 borehole.

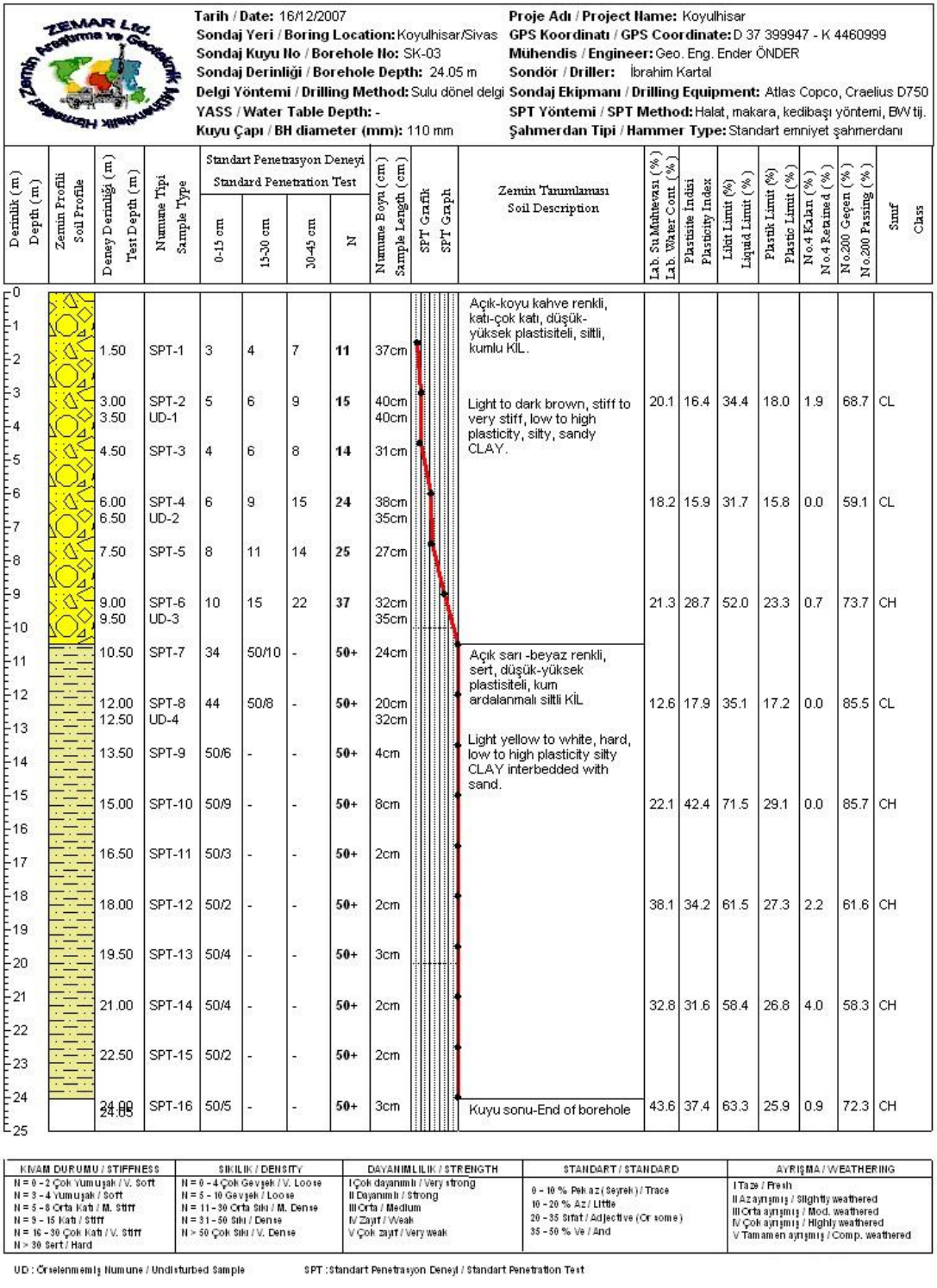

Figure A.17 Log of SK-3 borehole.

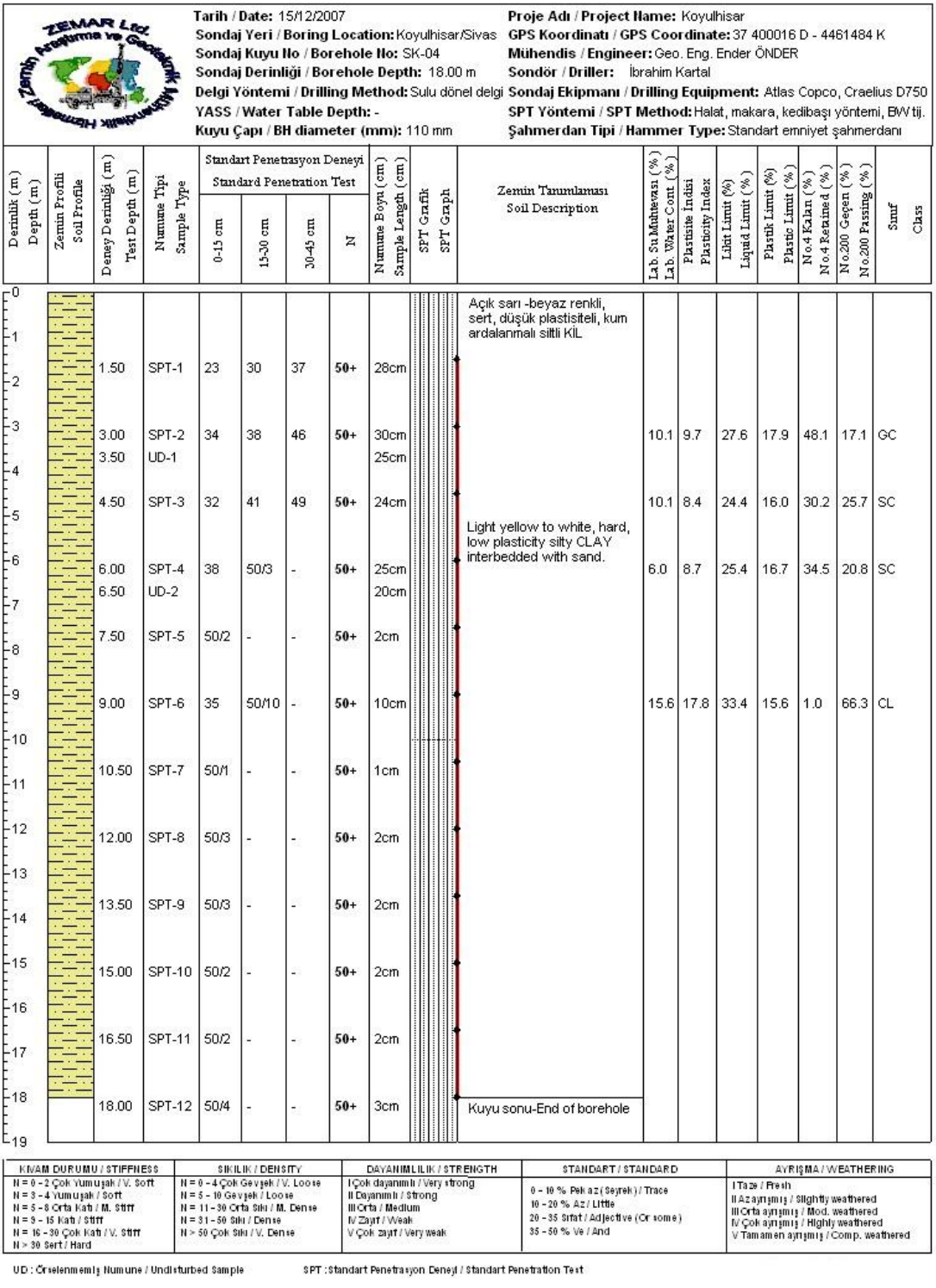

Derinlik (m) Depth (m)	Deney Derinliği (m) Test Depth (m)	Numune Tipi Sample Type	0-15 cm	15-30 cm	30-45 cm	N	Numune Boyu (cm) Sample Length (cm)	Lab. Su Muhtevası (%) Lab. Water Cont (%)	Plastisite İndisi Plasticity Index	Likit Limit (%) Liquid Limit (%)	Plastik Limit (%) Plastic Limit (%)	No.4 Kalan (%) No.4 Retained (%)	No.200 Geçen (%) No.200 Passing (%)	Sınıf Class
1	1.50	SPT-1	23	30	37	50+	28cm							
3	3.00	SPT-2	34	38	46	50+	30cm	10.1	9.7	27.6	17.9	48.1	17.1	GC
	3.50	UD-1					25cm							
5	4.50	SPT-3	32	41	49	50+	24cm	10.1	8.4	24.4	16.0	30.2	25.7	SC
6	6.00	SPT-4	38	50/3	-	50+	25cm	6.0	8.7	25.4	16.7	34.5	20.8	SC
	6.50	UD-2					20cm							
7	7.50	SPT-5	50/2	-	-	50+	2cm							
9	9.00	SPT-6	35	50/10	-	50+	10cm	15.6	17.8	33.4	15.6	1.0	66.3	CL
10	10.50	SPT-7	50/1	-	-	50+	1cm							
12	12.00	SPT-8	50/3	-	-	50+	2cm							
13	13.50	SPT-9	50/3	-	-	50+	2cm							
15	15.00	SPT-10	50/2	-	-	50+	2cm							
16	16.50	SPT-11	50/2	-	-	50+	2cm							
18	18.00	SPT-12	50/4	-	-	50+	3cm							

Figure A.18 Log of SK-4 borehole.

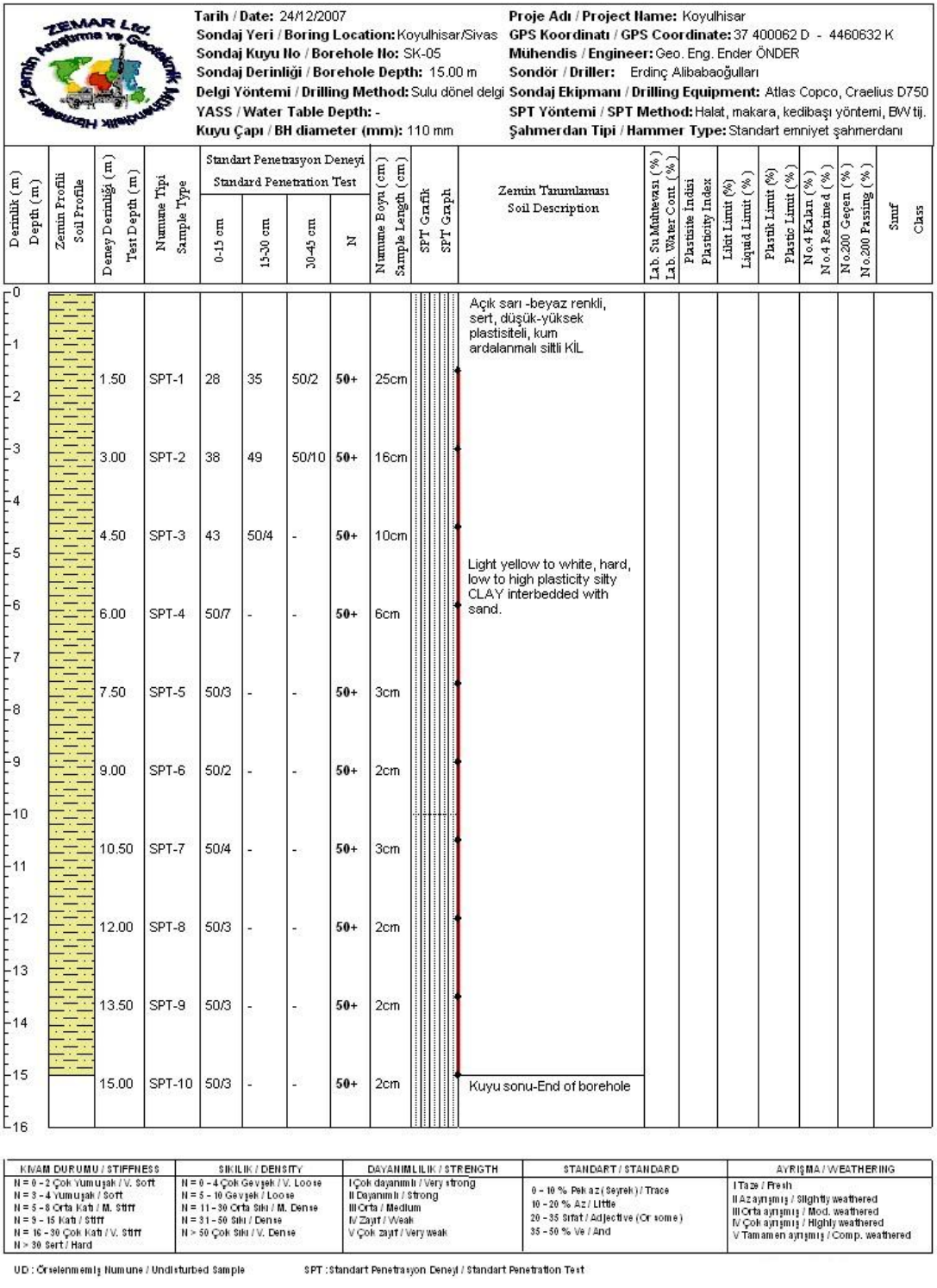

Figure A.19 Log of SK-5 borehole.

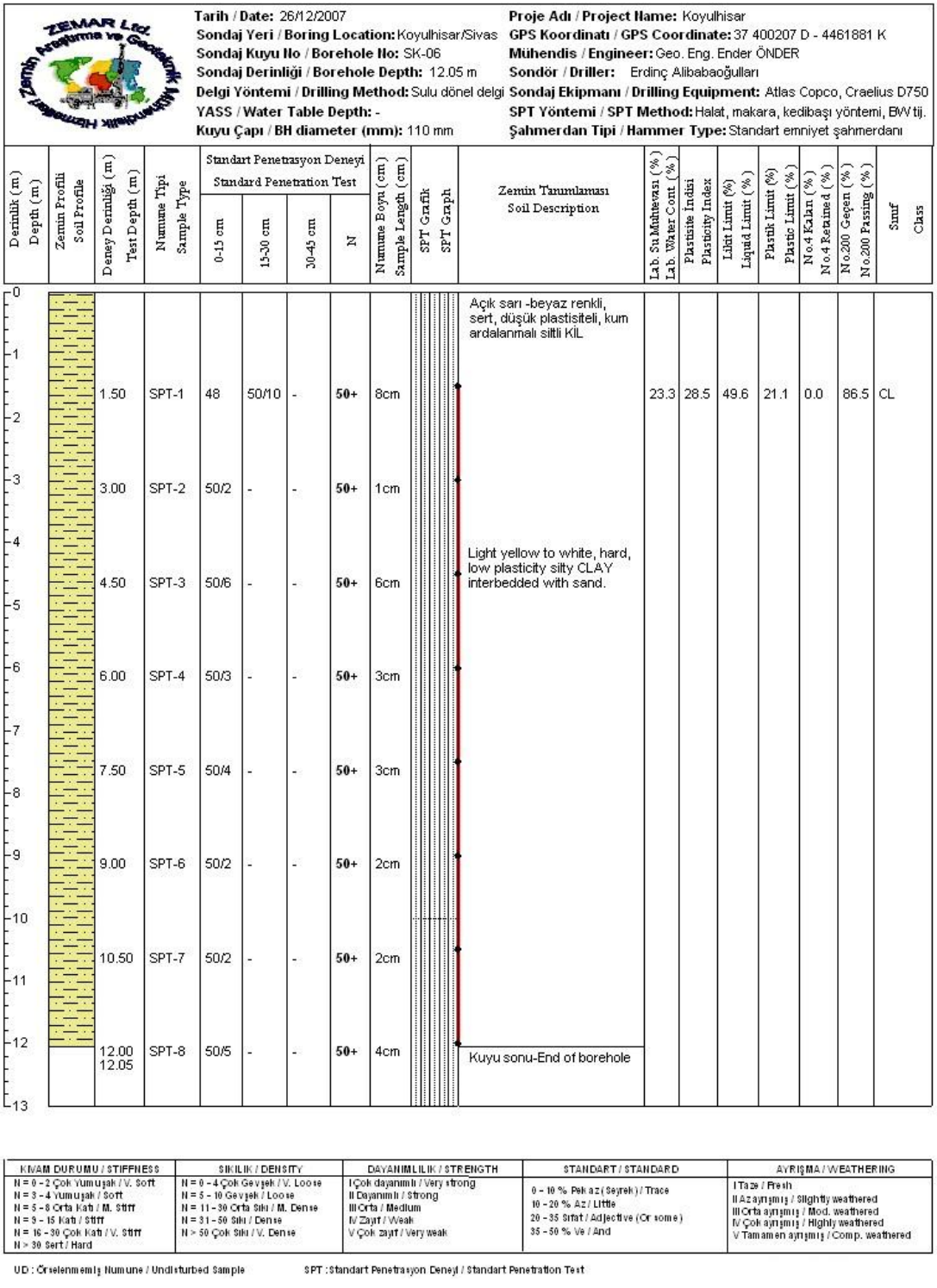

Figure A.20 Log of SK-6 borehole.

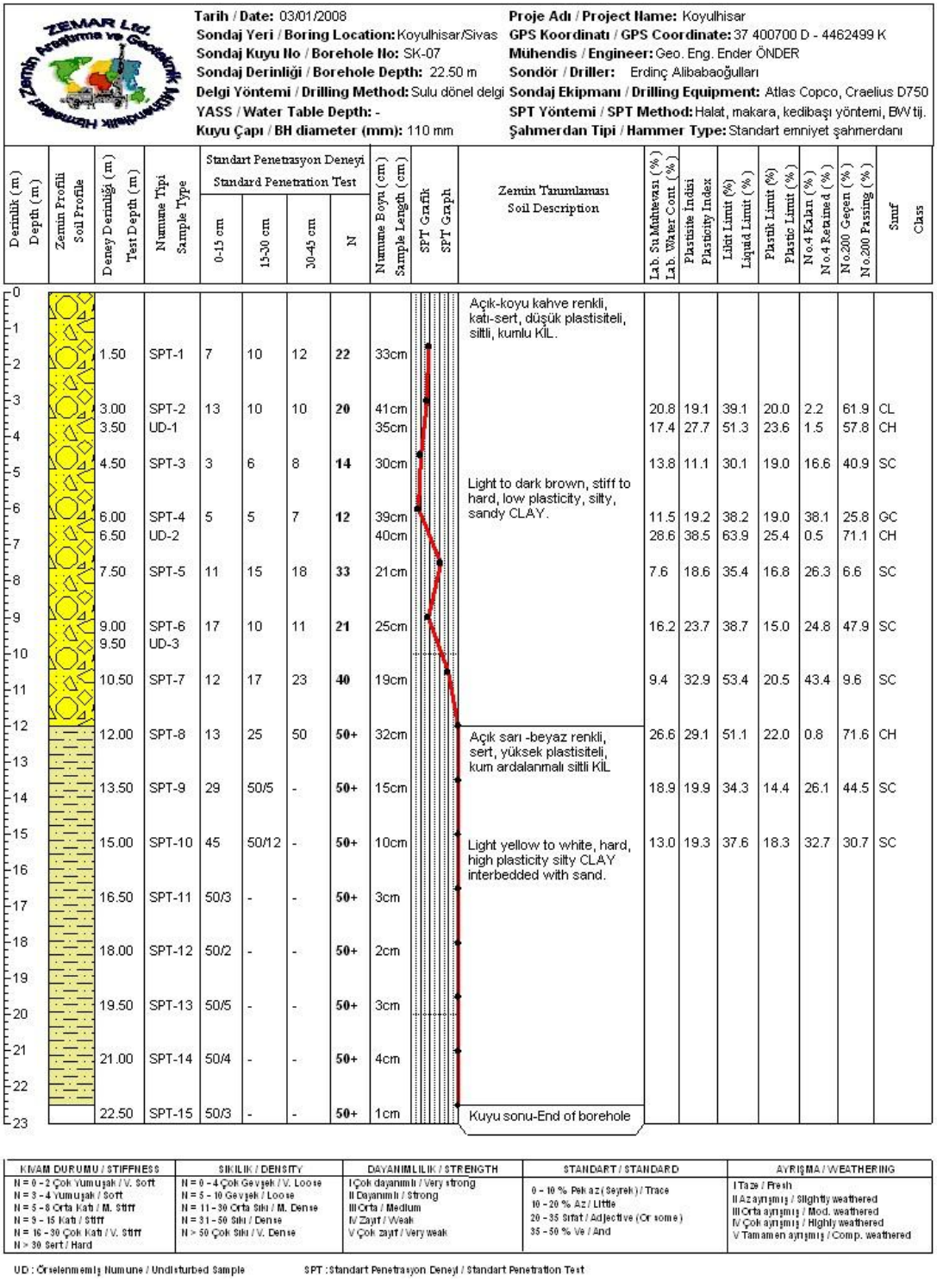

Depth (m)	Test Depth (m)	Sample Type	0-15 cm	15-30 cm	30-45 cm	N	Sample Length (cm)	Lab. Water Cont (%)	Plasticity Index	Liquid Limit (%)	Plastic Limit (%)	No.4 Retained (%)	No.200 Passing (%)	Class
	1.50	SPT-1	7	10	12	22	33cm							
	3.00	SPT-2	13	10	10	20	41cm	20.8	19.1	39.1	20.0	2.2	61.9	CL
	3.50	UD-1					35cm	17.4	27.7	51.3	23.6	1.5	57.8	CH
	4.50	SPT-3	3	6	8	14	30cm	13.8	11.1	30.1	19.0	16.6	40.9	SC
	6.00	SPT-4	5	5	7	12	39cm	11.5	19.2	38.2	19.0	38.1	25.8	GC
	6.50	UD-2					40cm	28.6	38.5	63.9	25.4	0.5	71.1	CH
	7.50	SPT-5	11	15	18	33	21cm	7.6	18.6	35.4	16.8	26.3	6.6	SC
	9.00	SPT-6	17	10	11	21	25cm	16.2	23.7	38.7	15.0	24.8	47.9	SC
	9.50	UD-3												
	10.50	SPT-7	12	17	23	40	19cm	9.4	32.9	53.4	20.5	43.4	9.6	SC
	12.00	SPT-8	13	25	50	50+	32cm	26.6	29.1	51.1	22.0	0.8	71.6	CH
	13.50	SPT-9	29	50/5	-	50+	15cm	18.9	19.9	34.3	14.4	26.1	44.5	SC
	15.00	SPT-10	45	50/12	-	50+	10cm	13.0	19.3	37.6	18.3	32.7	30.7	SC
	16.50	SPT-11	50/3	-	-	50+	3cm							
	18.00	SPT-12	50/2	-	-	50+	2cm							
	19.50	SPT-13	50/5	-	-	50+	3cm							
	21.00	SPT-14	50/4	-	-	50+	4cm							
	22.50	SPT-15	50/3	-	-	50+	1cm							

Figure A.21 Log of SK-7 borehole.

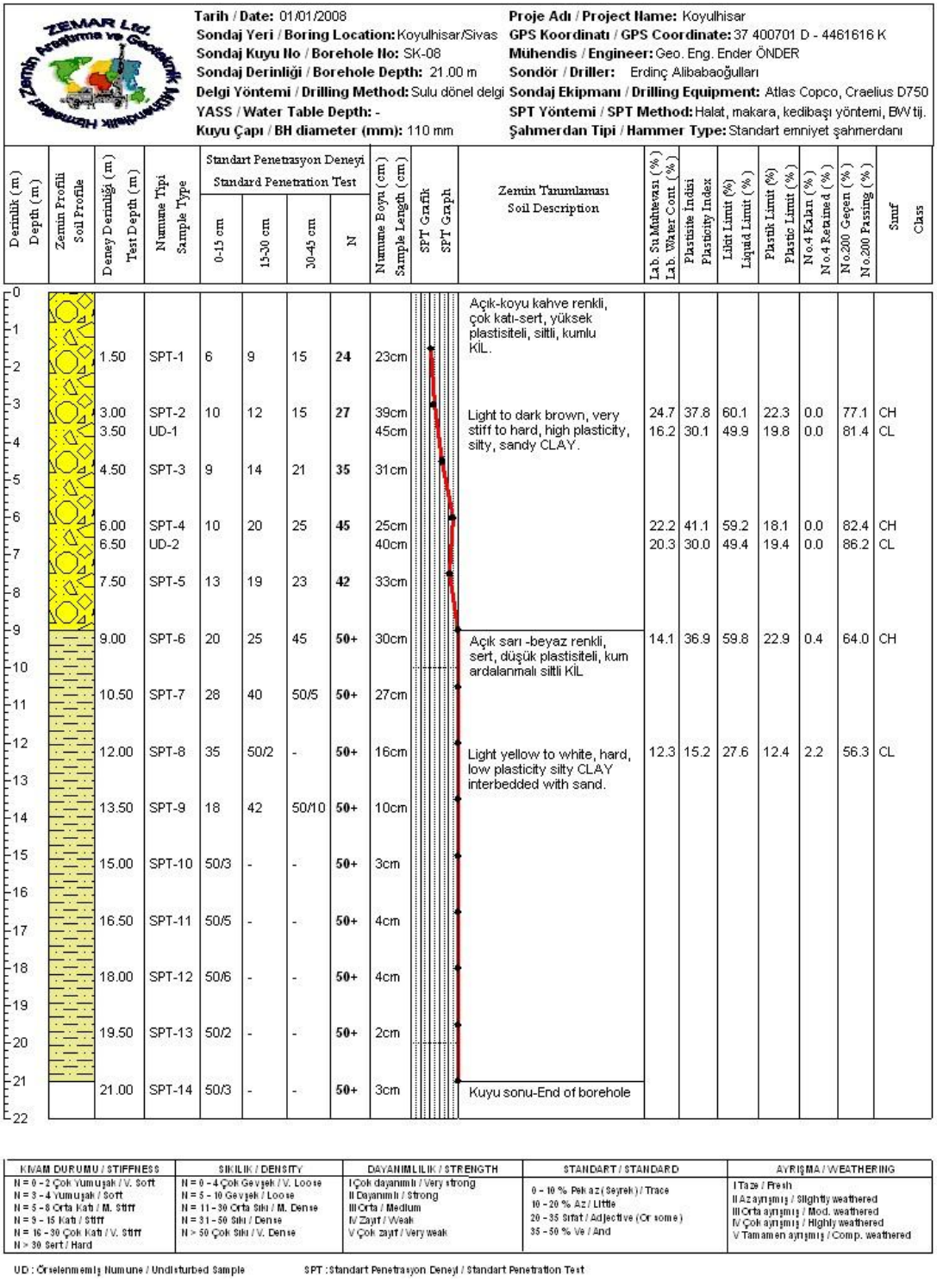

Figure A.22 Log of SK-8 borehole.

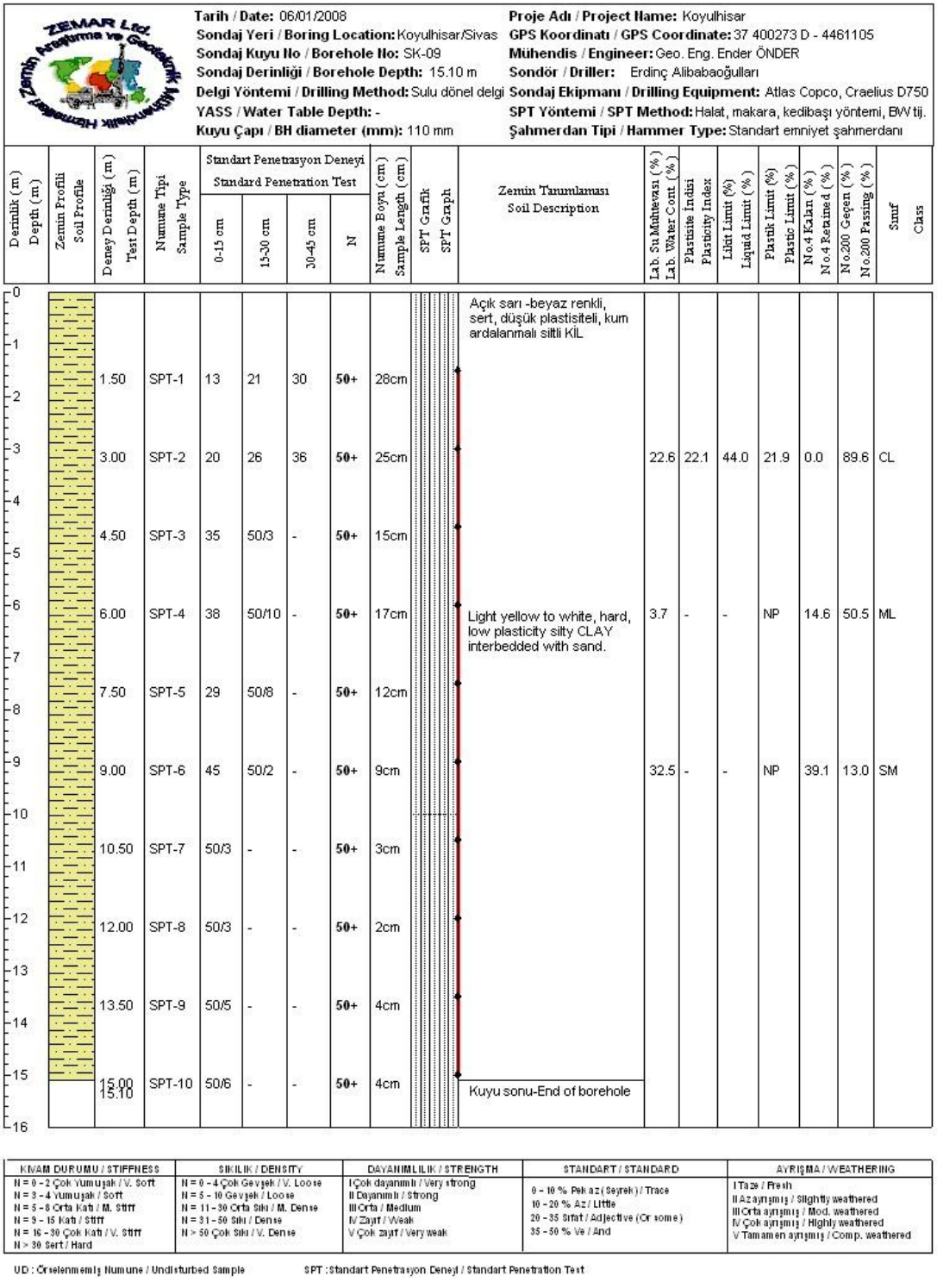

Figure A.23 Log of SK-9 borehole.

APPENDIX B

INCLINOMETER MEASUREMENTS OF ISK BOREHOLES

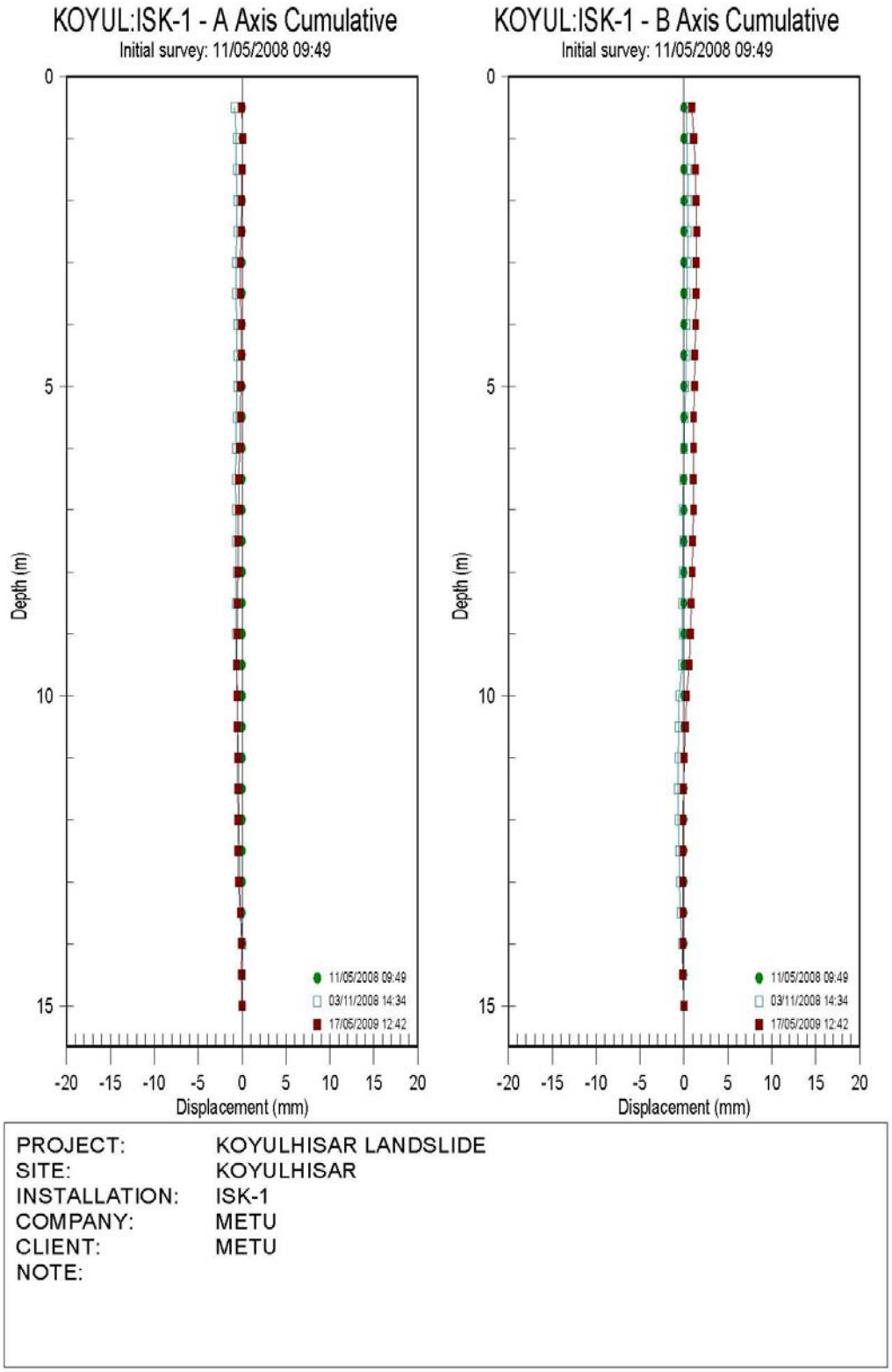

Figure B.1 Cumulative plot of ISK-1 borehole.

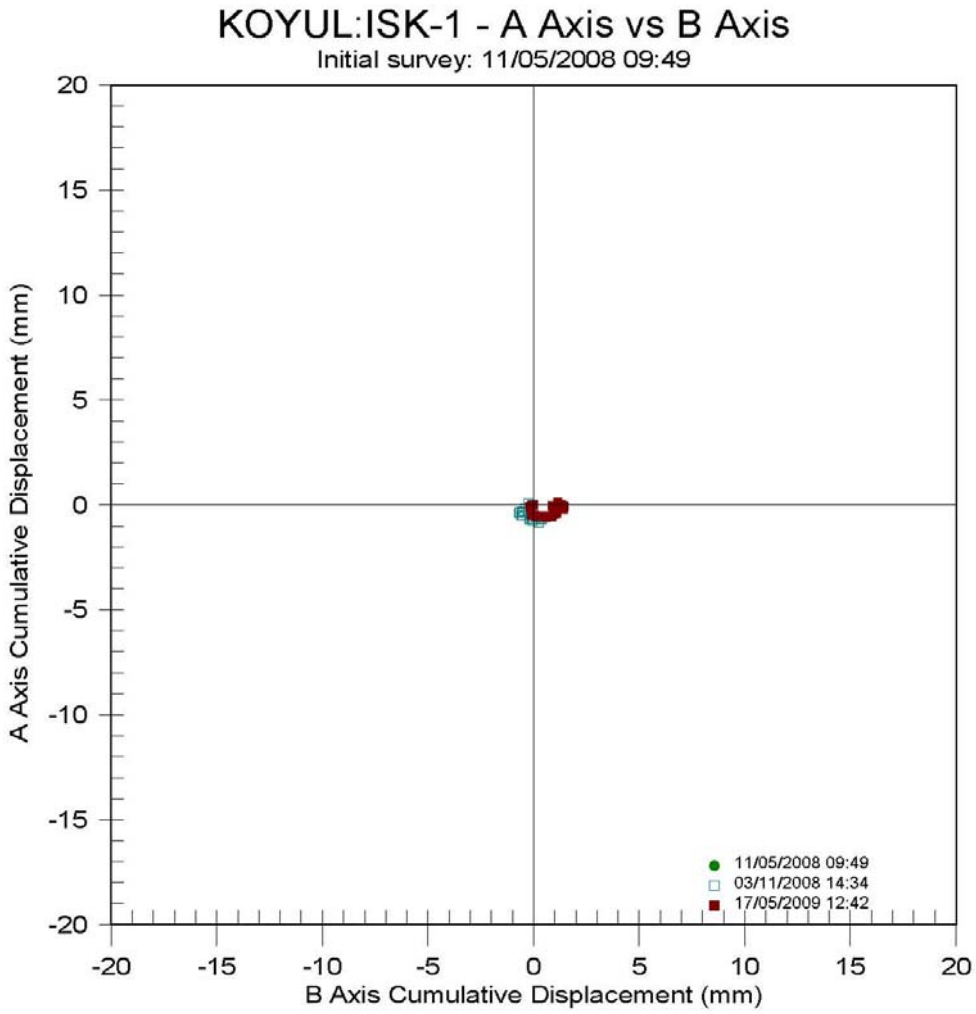

PROJECT:	KOYULHISAR LANDSLIDE
SITE:	KOYULHISAR
INSTALLATION:	ISK-1
COMPANY:	METU
CLIENT:	METU
NOTE:	

Figure B.2 Plan view plot of ISK-1 borehole

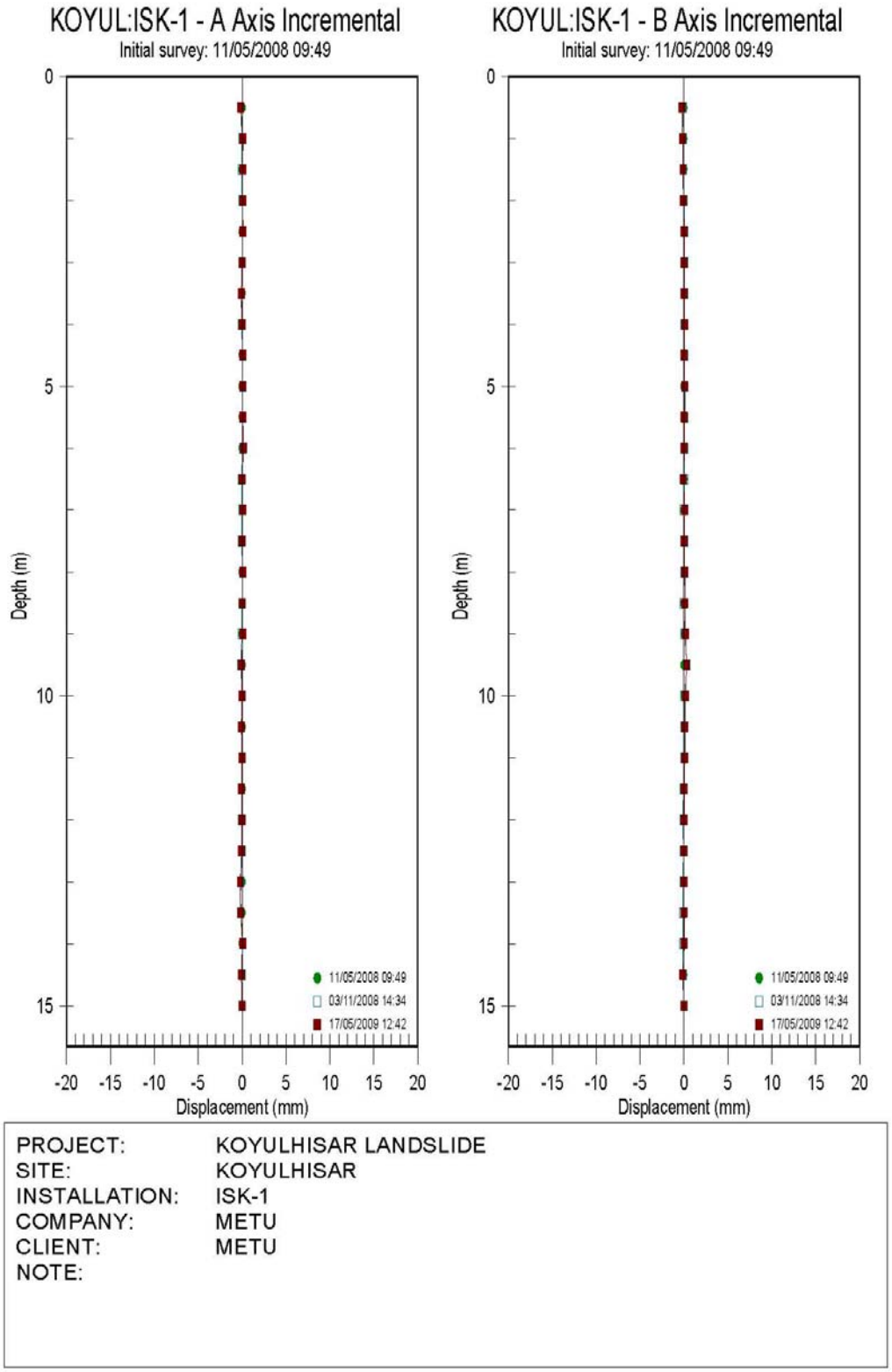

Figure B.3 Incremental plot of ISK-1 borehole

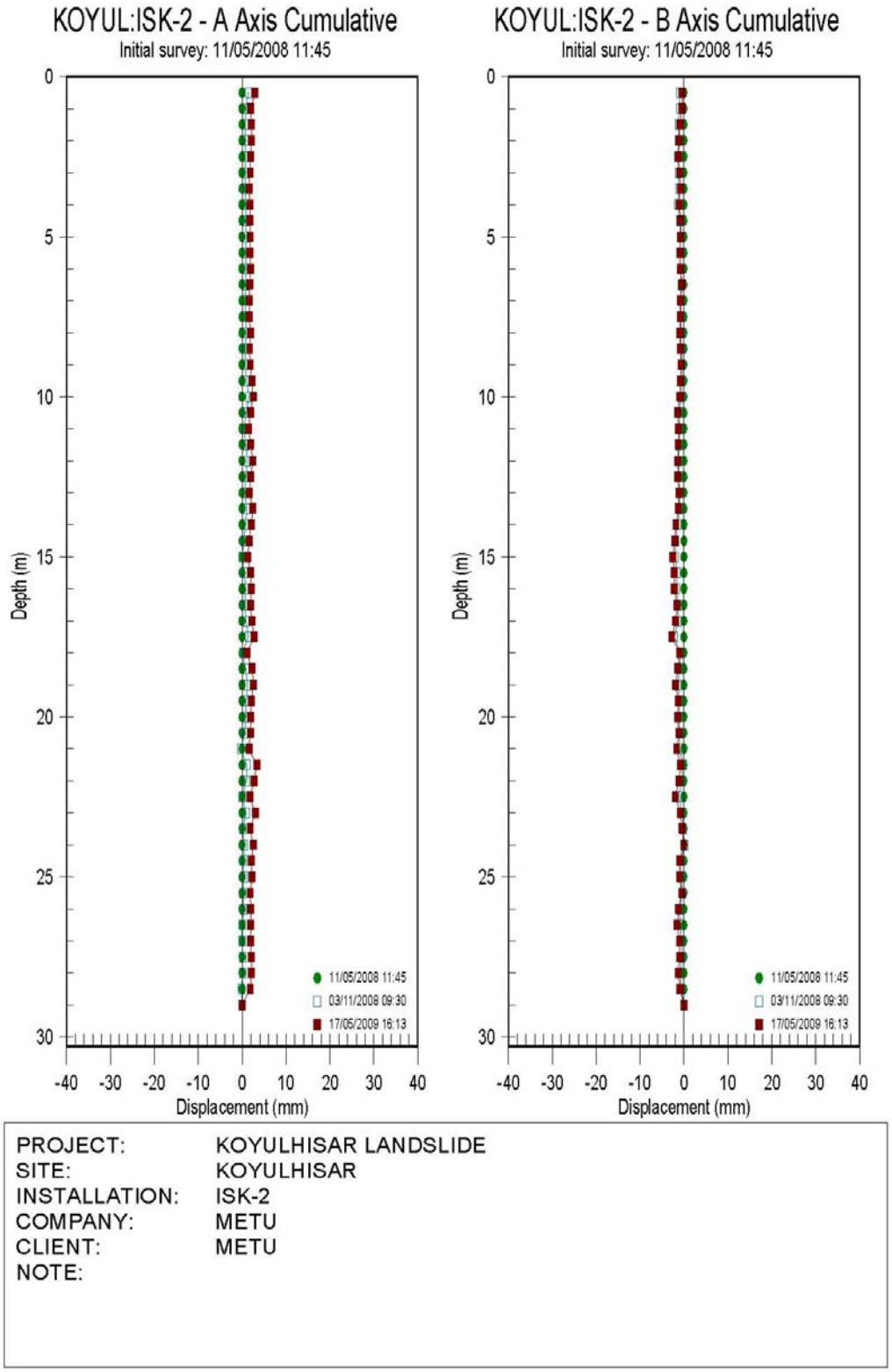

Figure B.4 Cumulative plot of ISK-2 borehole

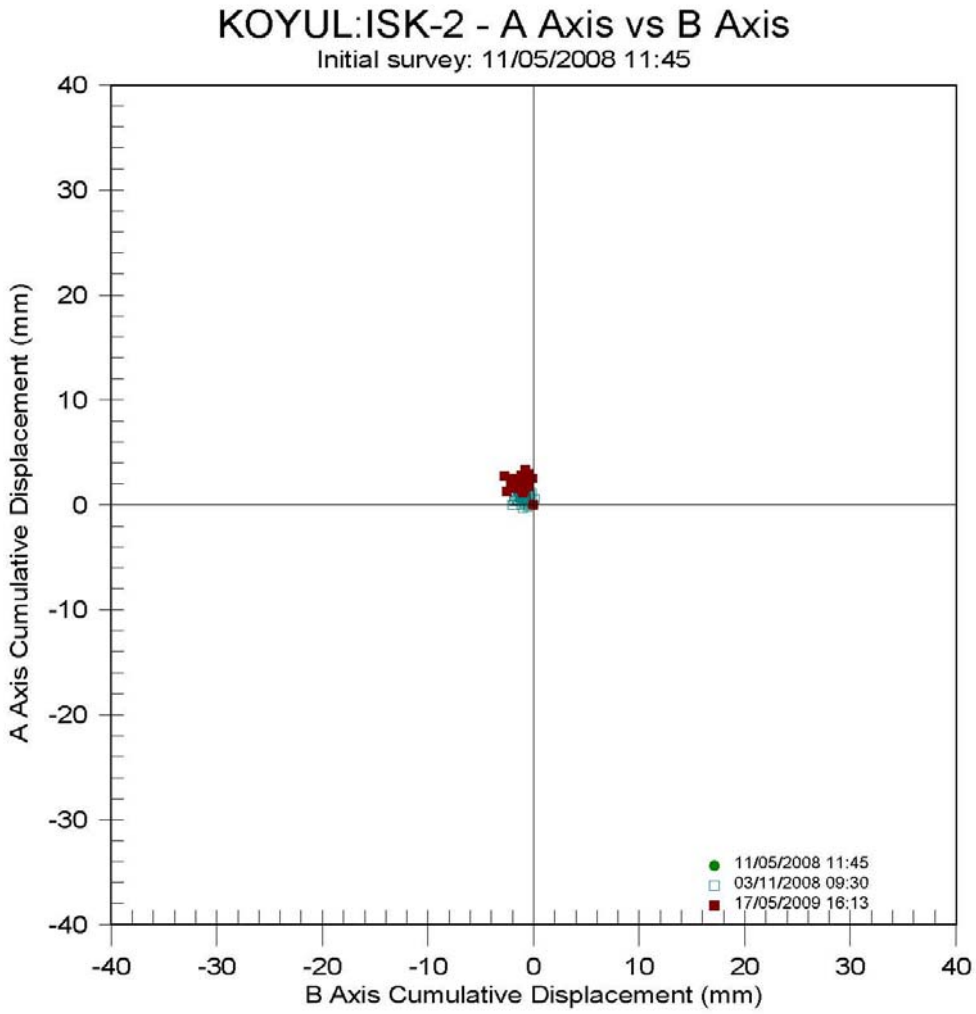

PROJECT:	KOYULHISAR LANDSLIDE
SITE:	KOYULHISAR
INSTALLATION:	ISK-2
COMPANY:	METU
CLIENT:	METU
NOTE:	

Figure B.5 Plan view plot of ISK-2 borehole

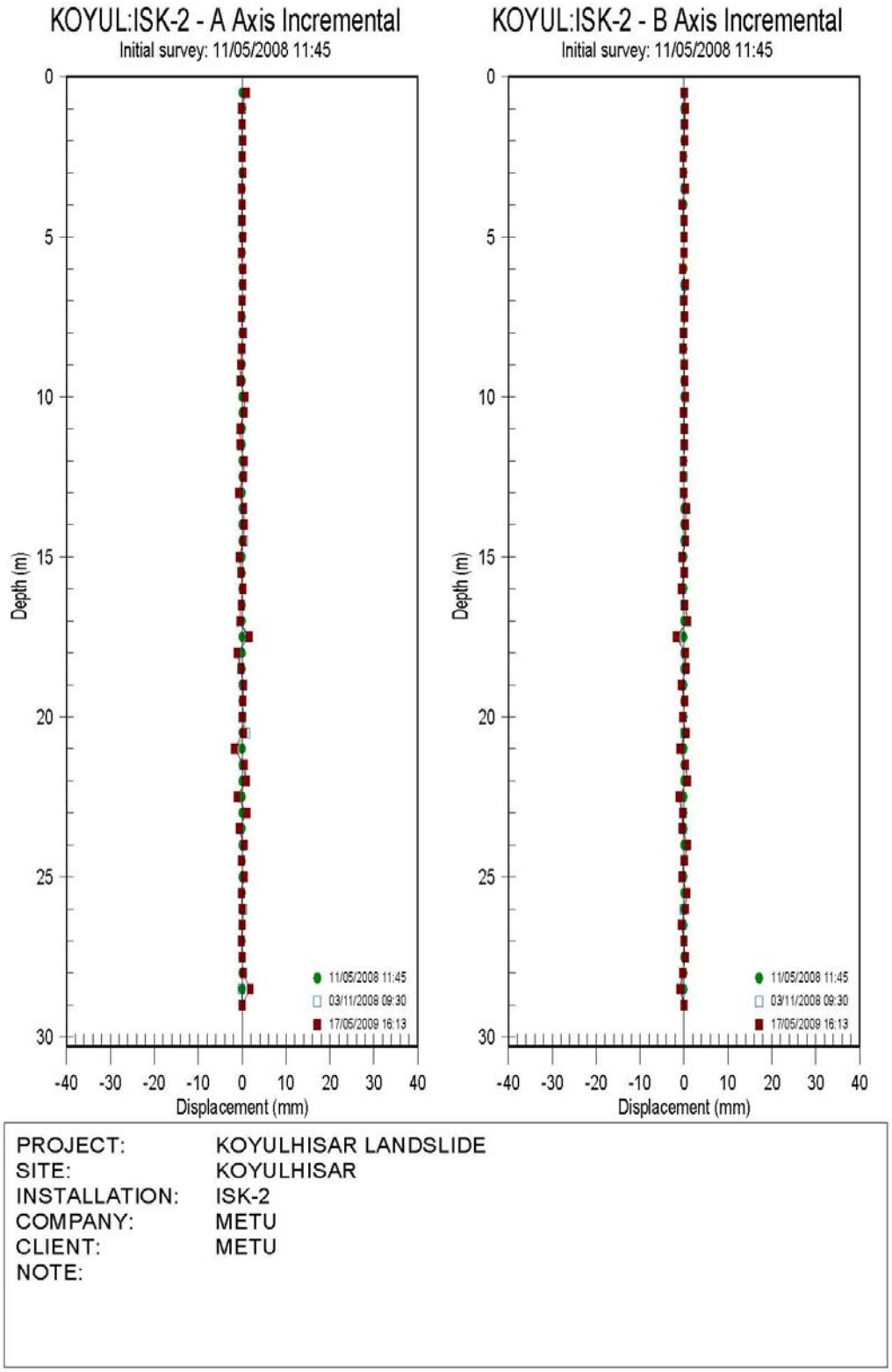

Figure B.6 Incremental plot of ISK-2 borehole

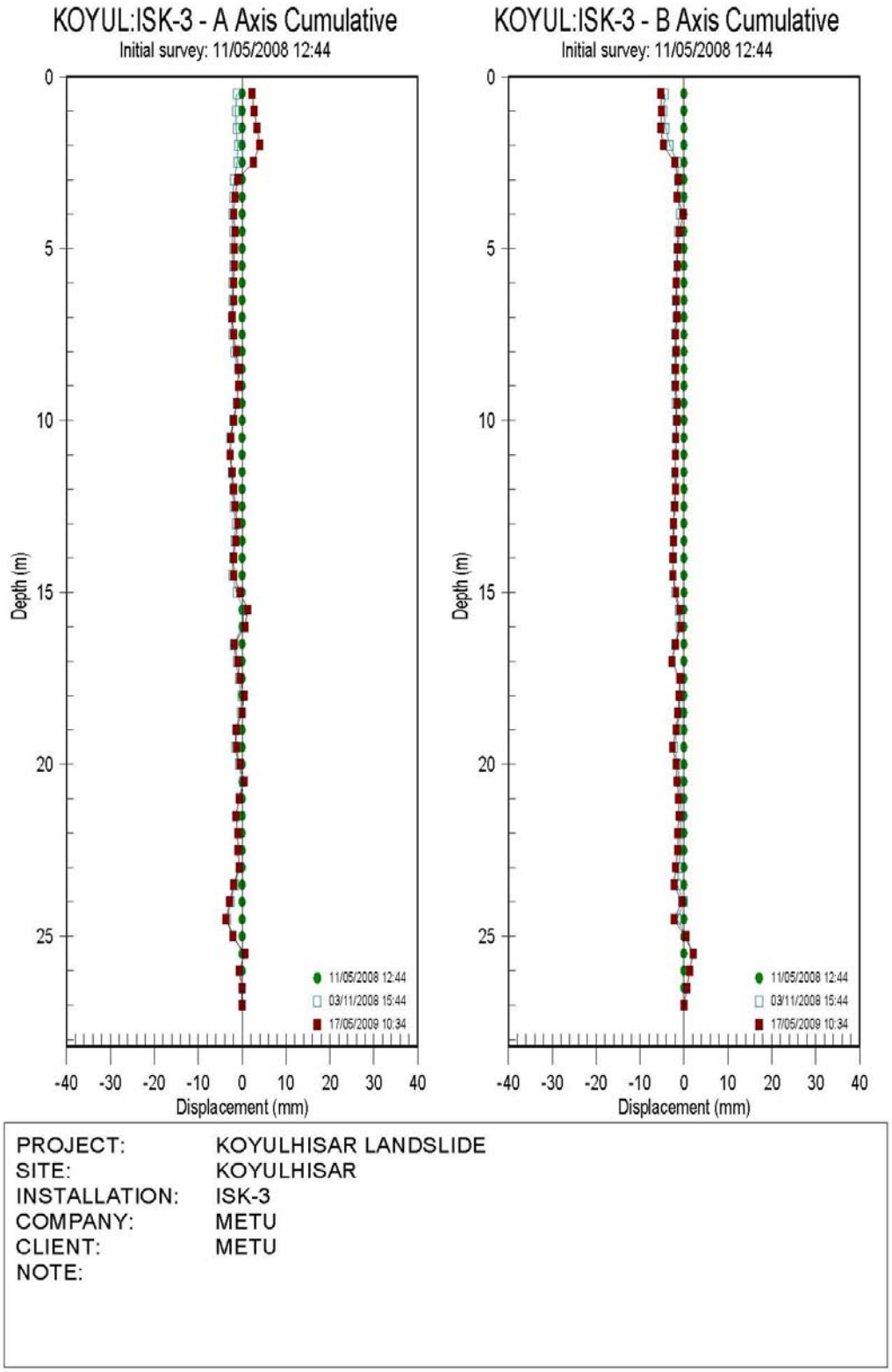

Figure B.7 Cumulative plot of ISK-3 borehole

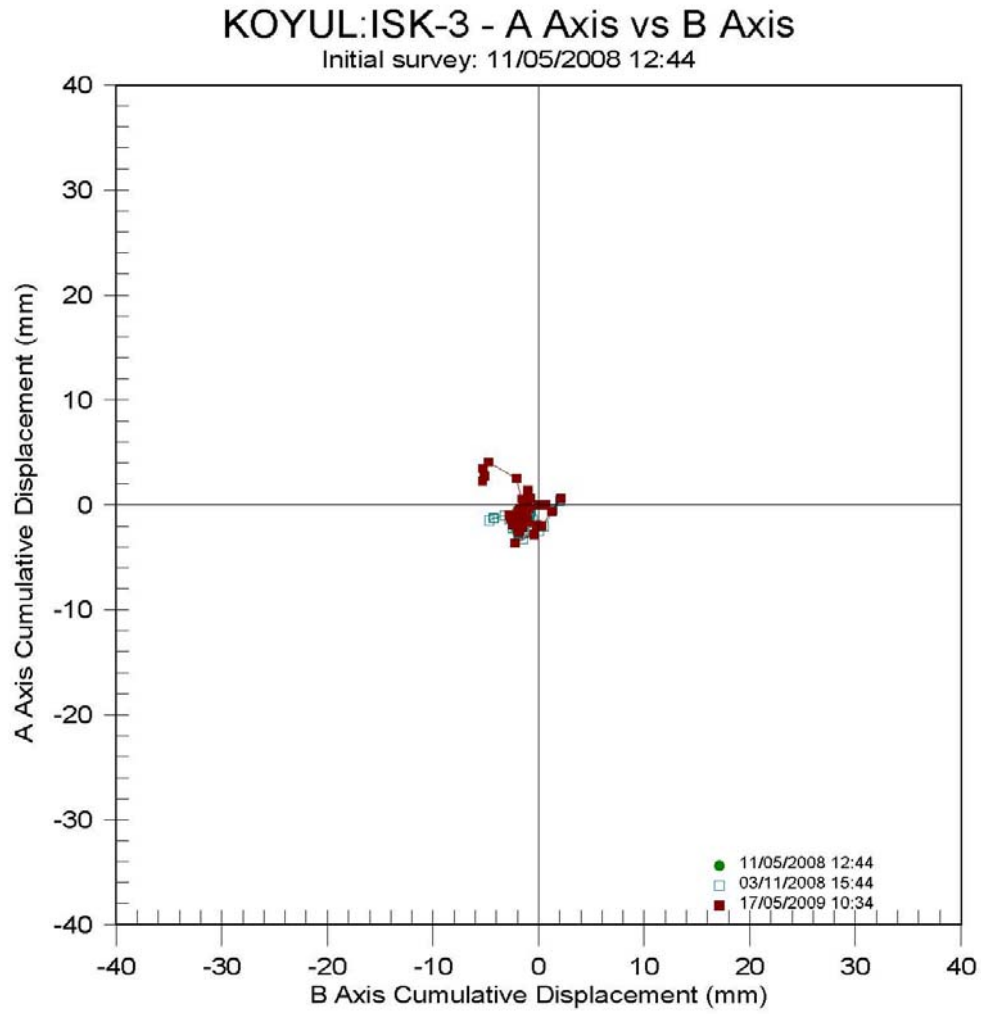

PROJECT:	KOYULHISAR LANDSLIDE
SITE:	KOYULHISAR
INSTALLATION:	ISK-3
COMPANY:	METU
CLIENT:	METU
NOTE:	

Figure B.8 Plan view plot of ISK-3 borehole

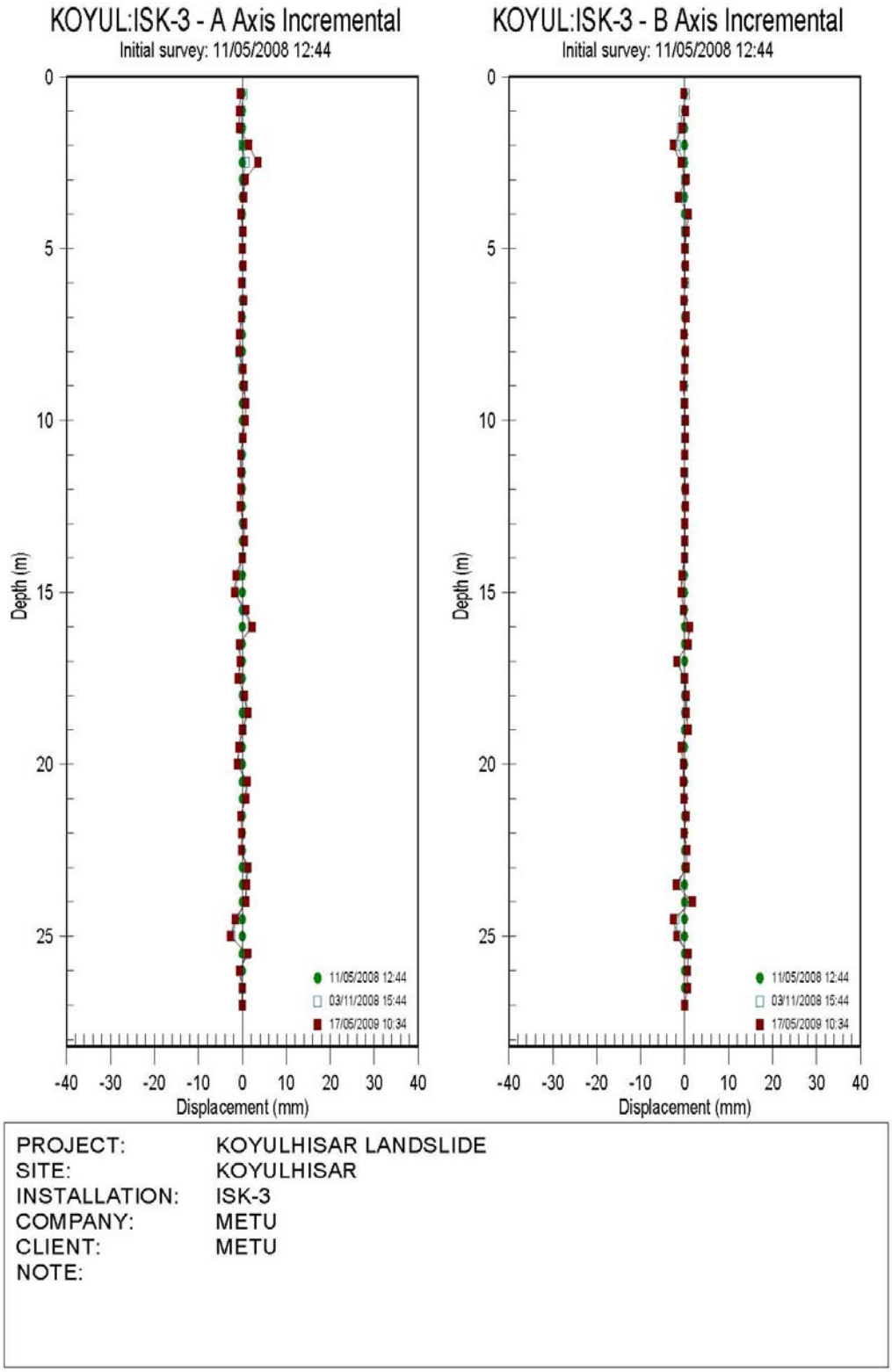

Figure B.9 Incremental plot of ISK-3 borehole

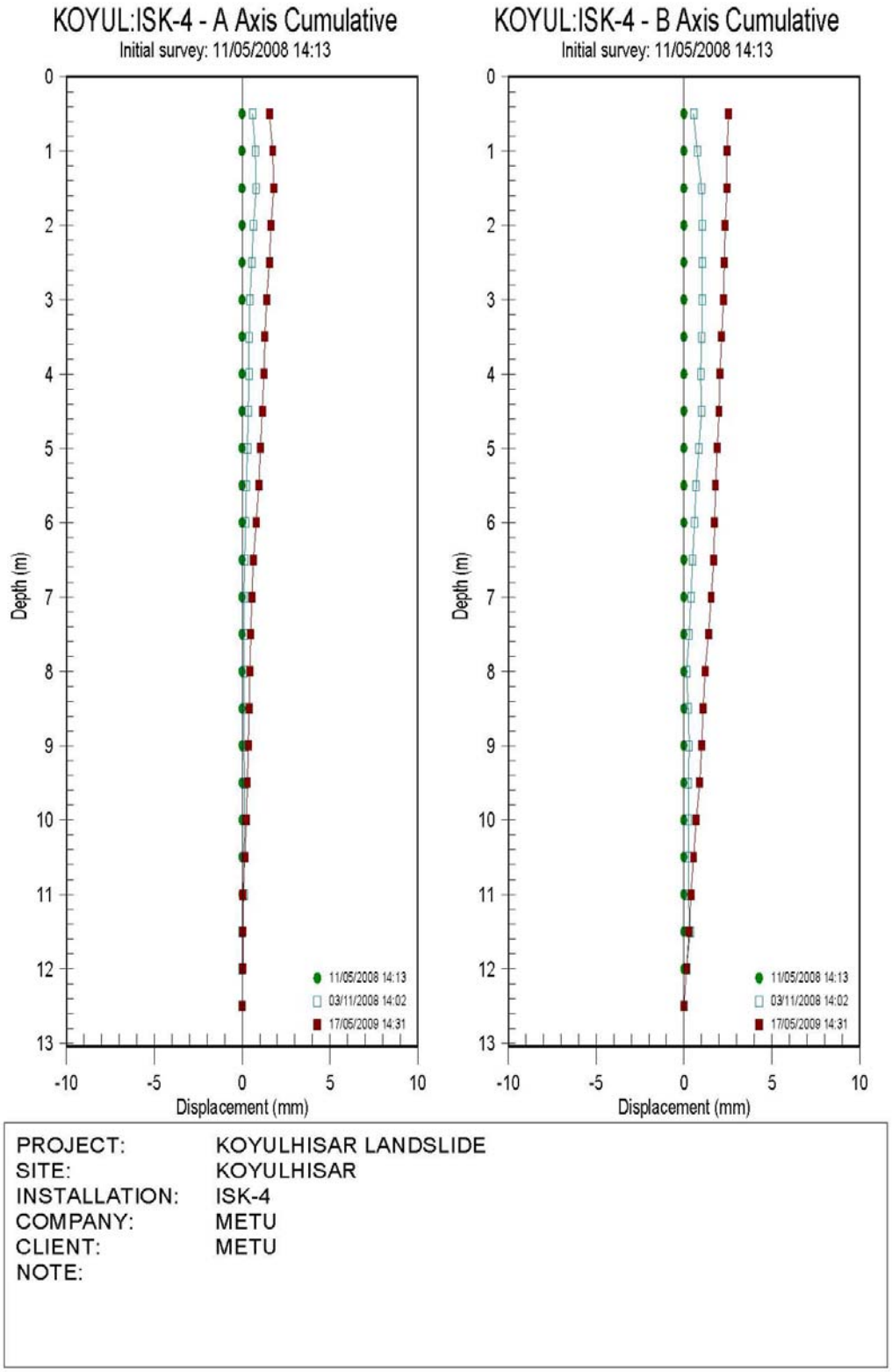

Figure B.10 Cumulative plot of ISK-4 borehole

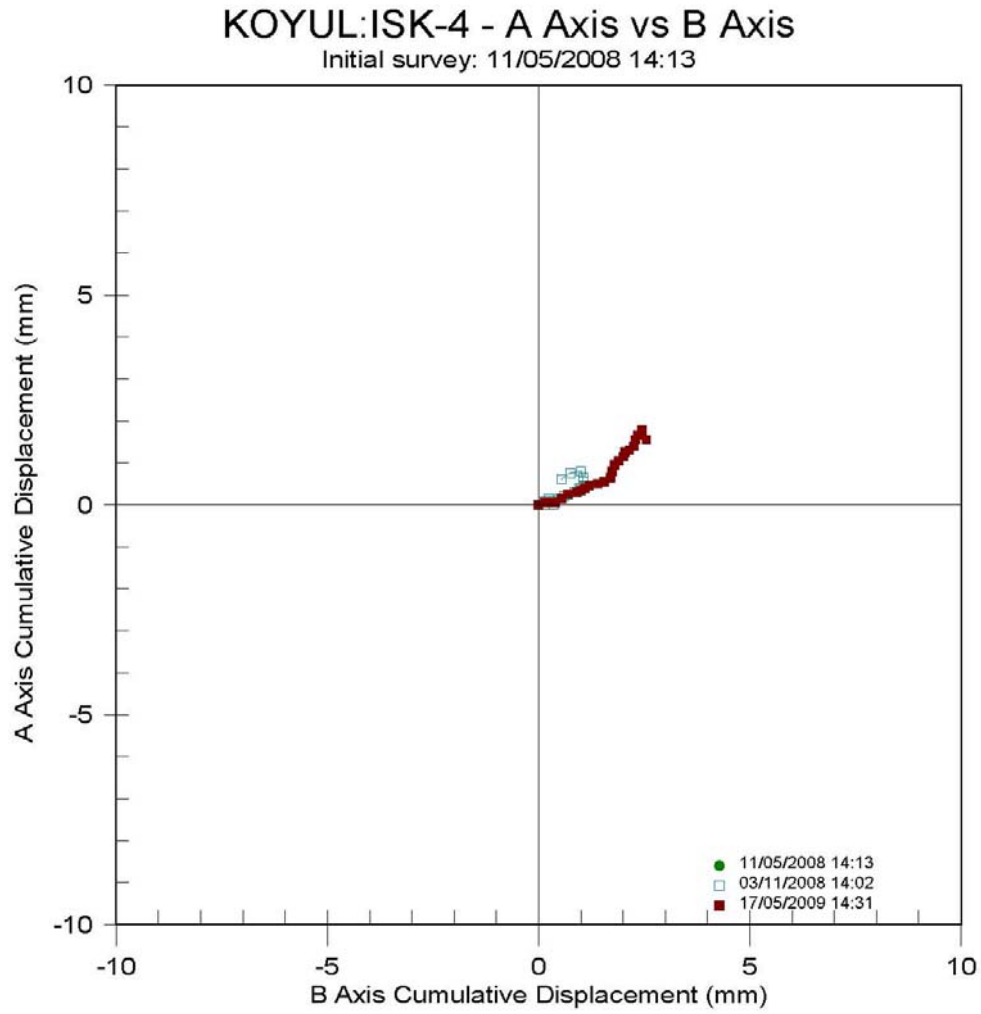

PROJECT:	KOYULHISAR LANDSLIDE
SITE:	KOYULHISAR
INSTALLATION:	ISK-4
COMPANY:	METU
CLIENT:	METU
NOTE:	

Figure B.11 Plan view plot of ISK-4 borehole

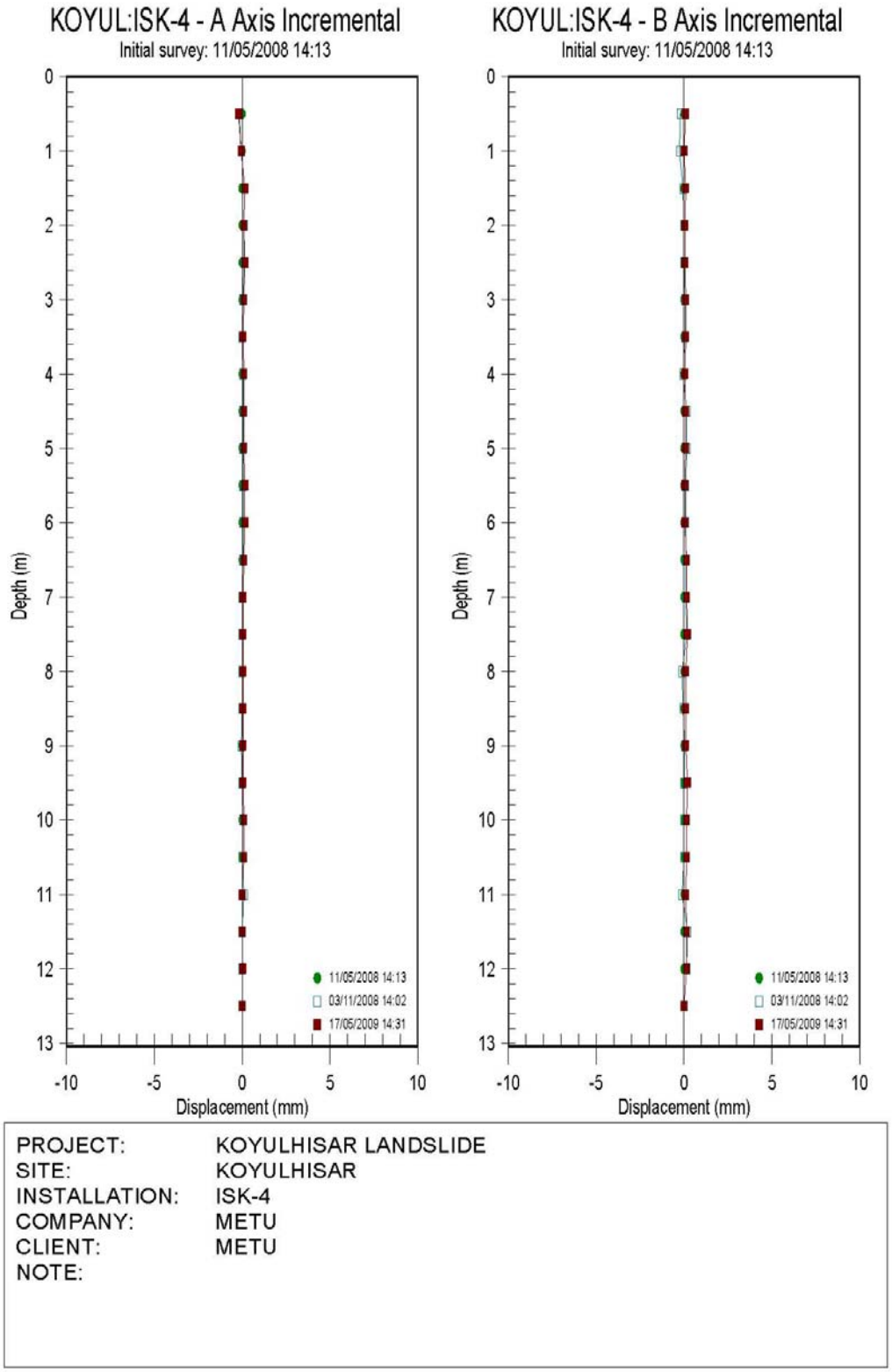

Figure B.12 Incremental plot of ISK-4 borehole

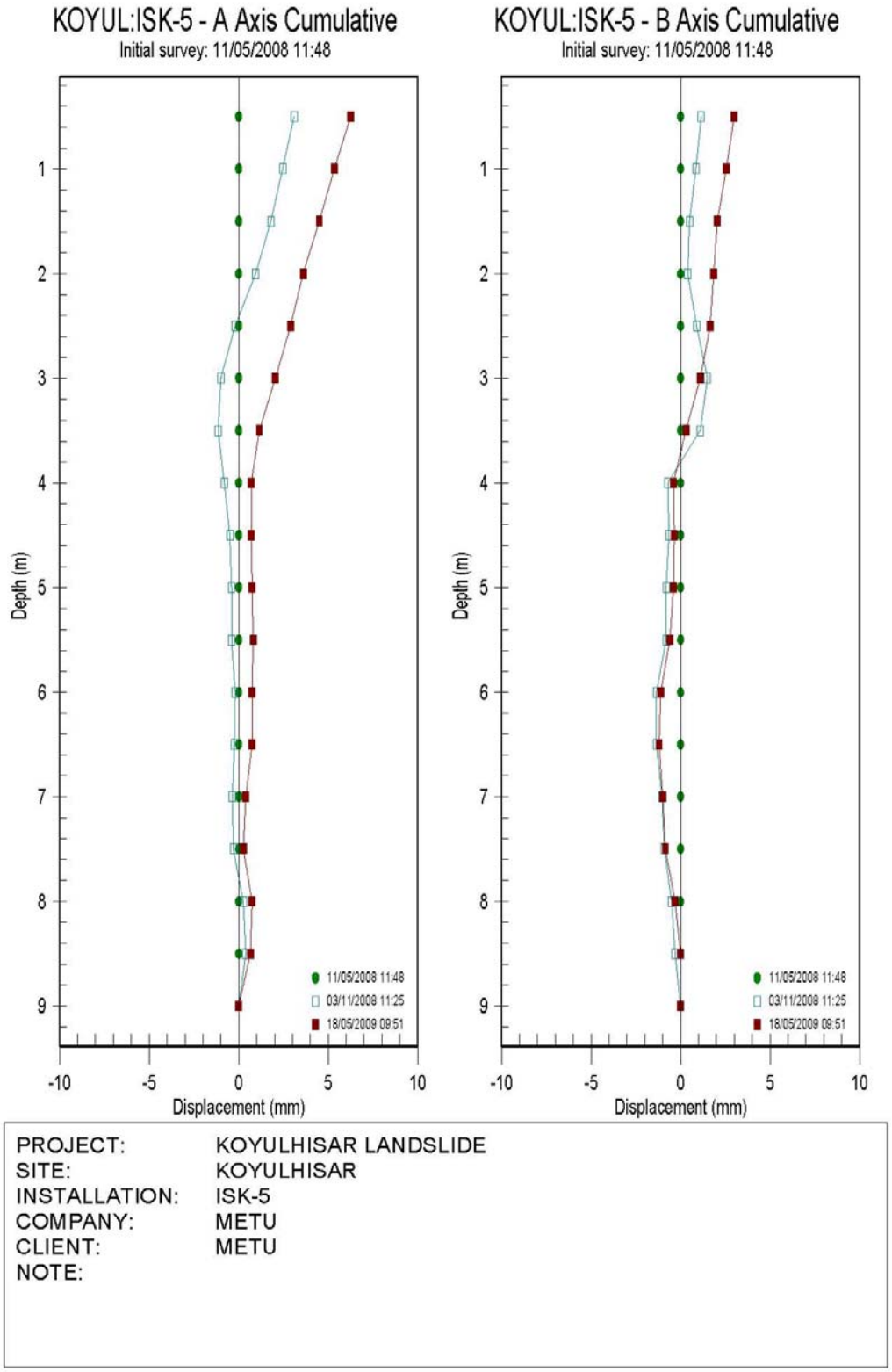

Figure B.13 Cumulative plot of ISK-5 borehole

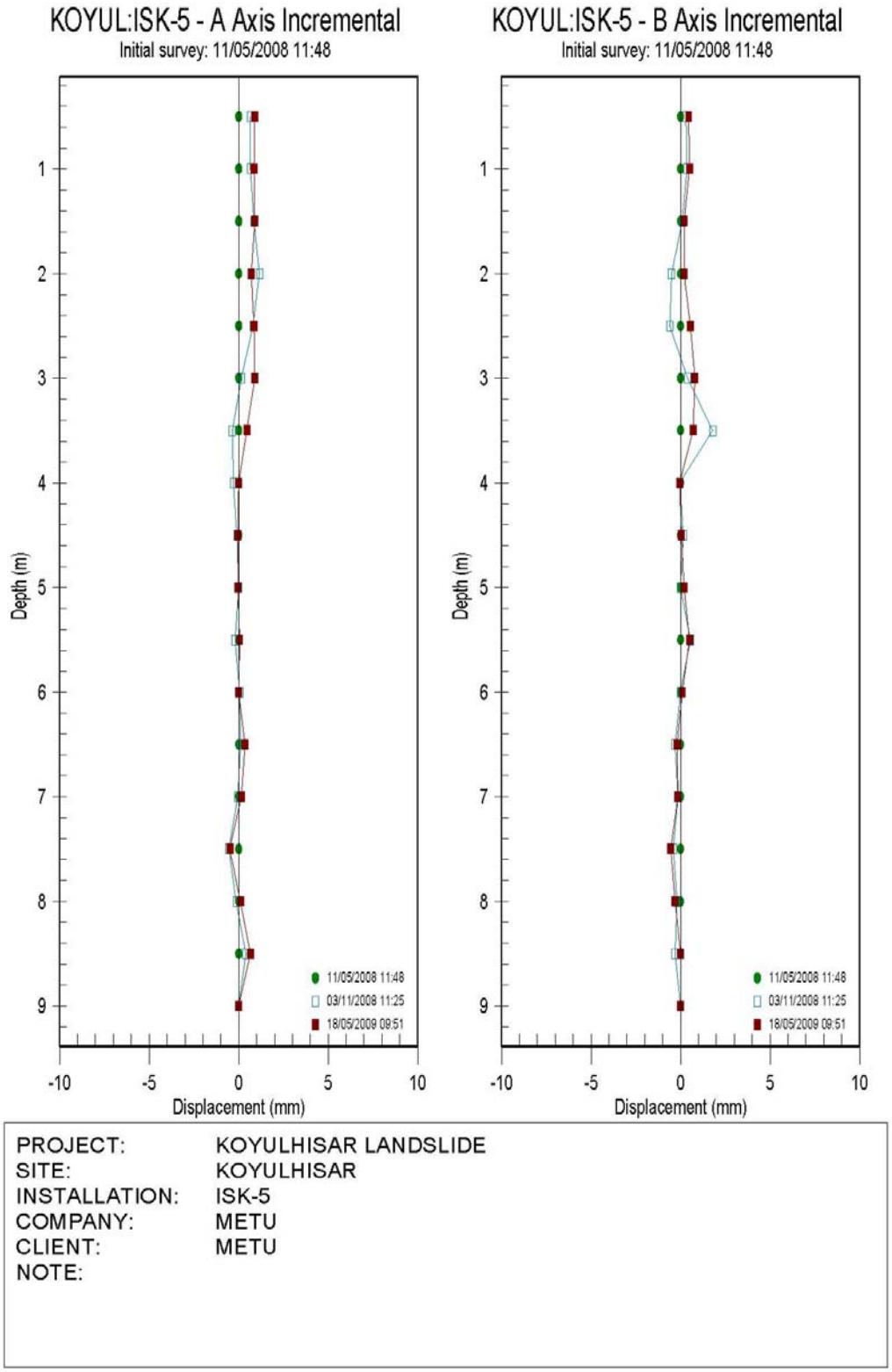

Figure B.15 Incremental plot of ISK-5 borehole

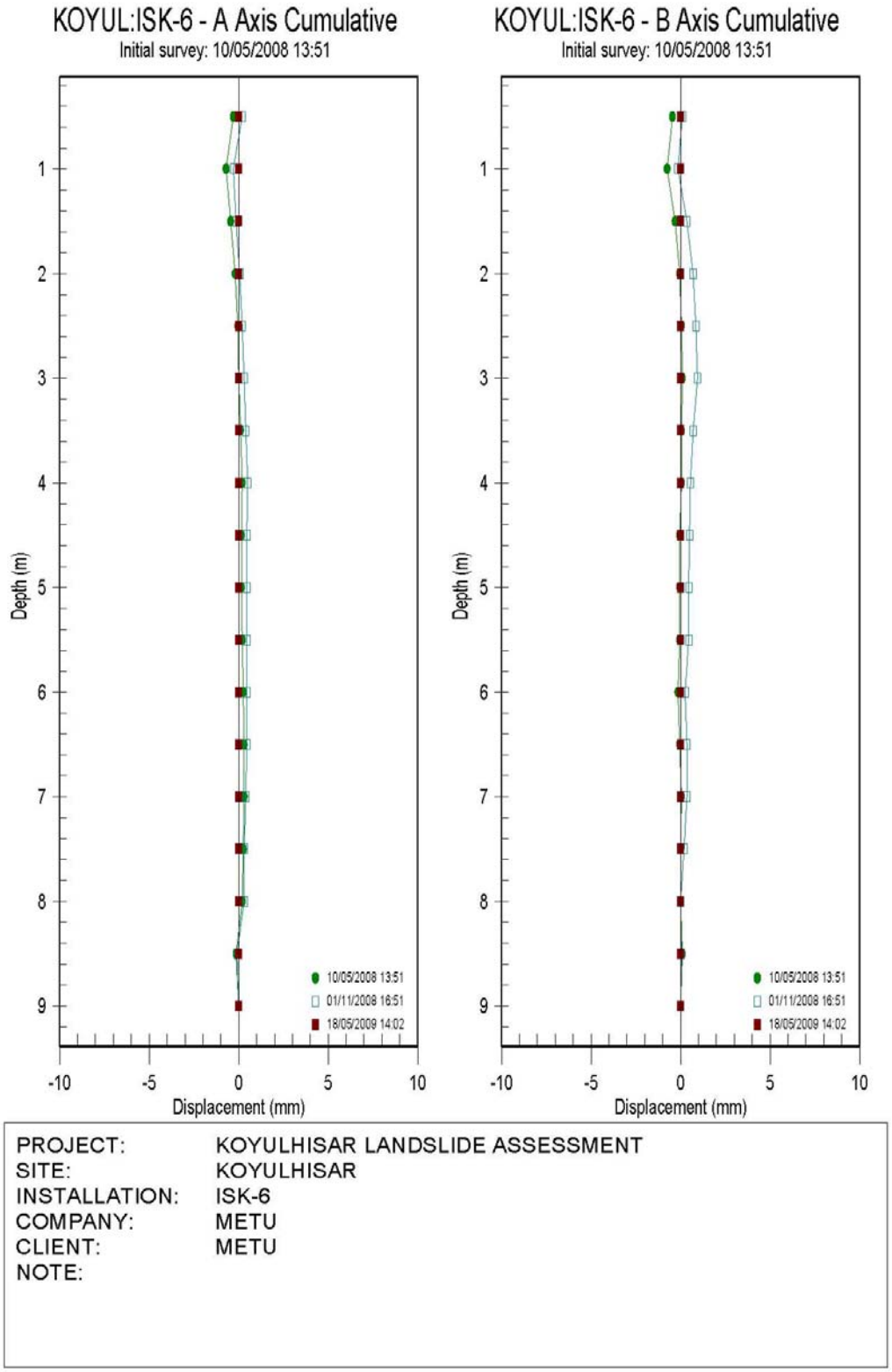

Figure B.16 Cumulative plot of ISK-6 borehole

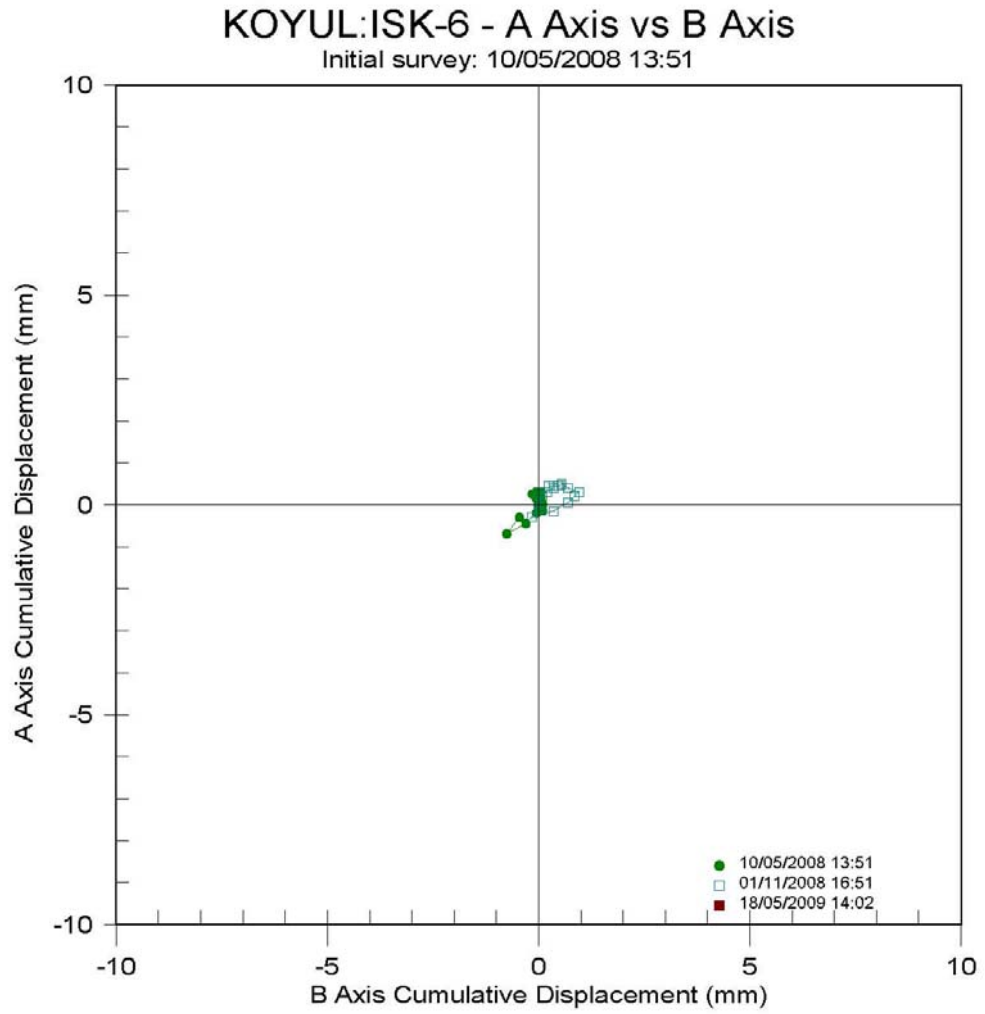

PROJECT:	KOYULHISAR LANDSLIDE ASSESSMENT
SITE:	KOYULHISAR
INSTALLATION:	ISK-6
COMPANY:	METU
CLIENT:	METU
NOTE:	

Figure B.17 Plan view plot of ISK-6 borehole

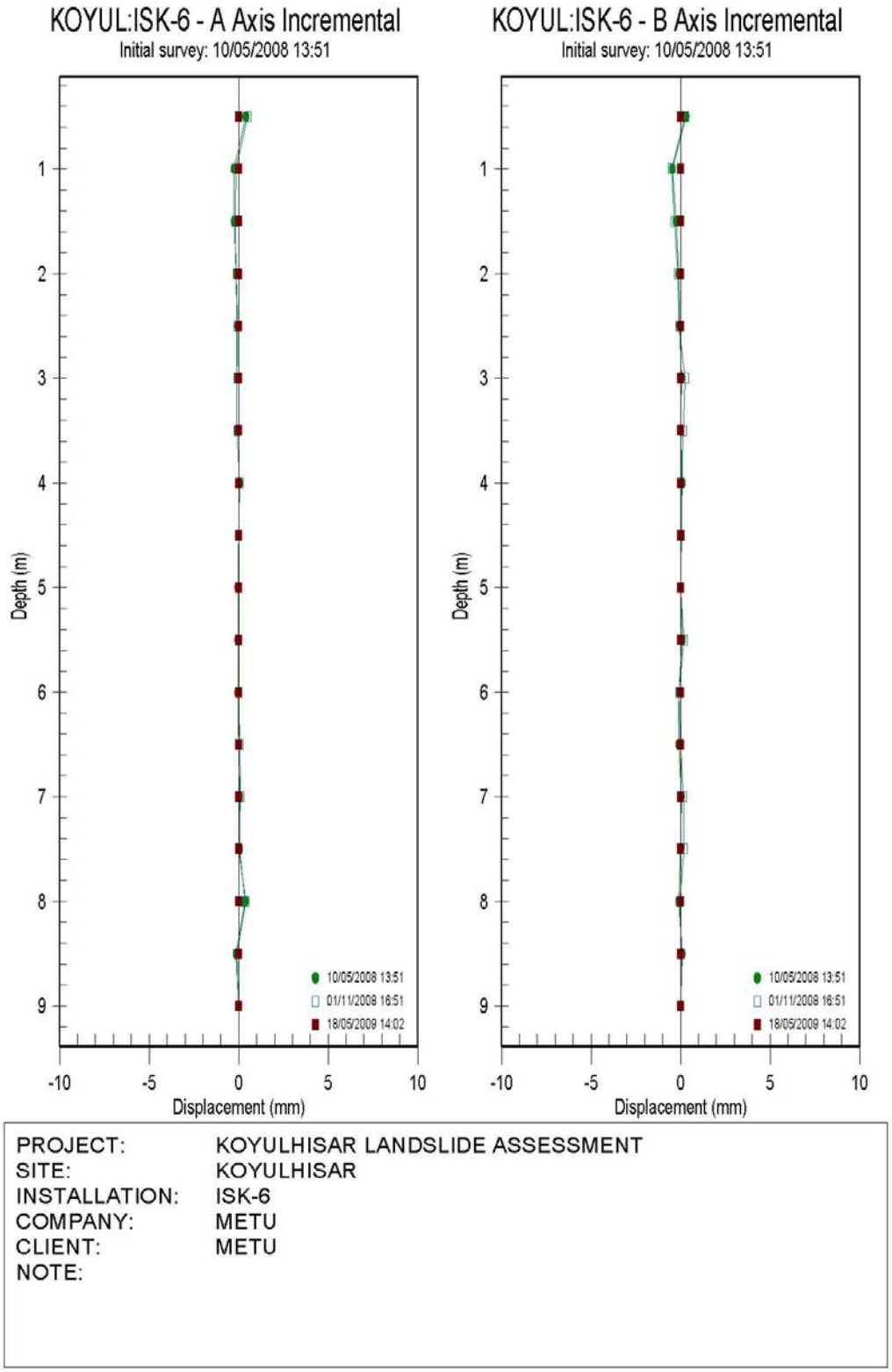

Figure B.18 Incremental plot of ISK-6 borehole

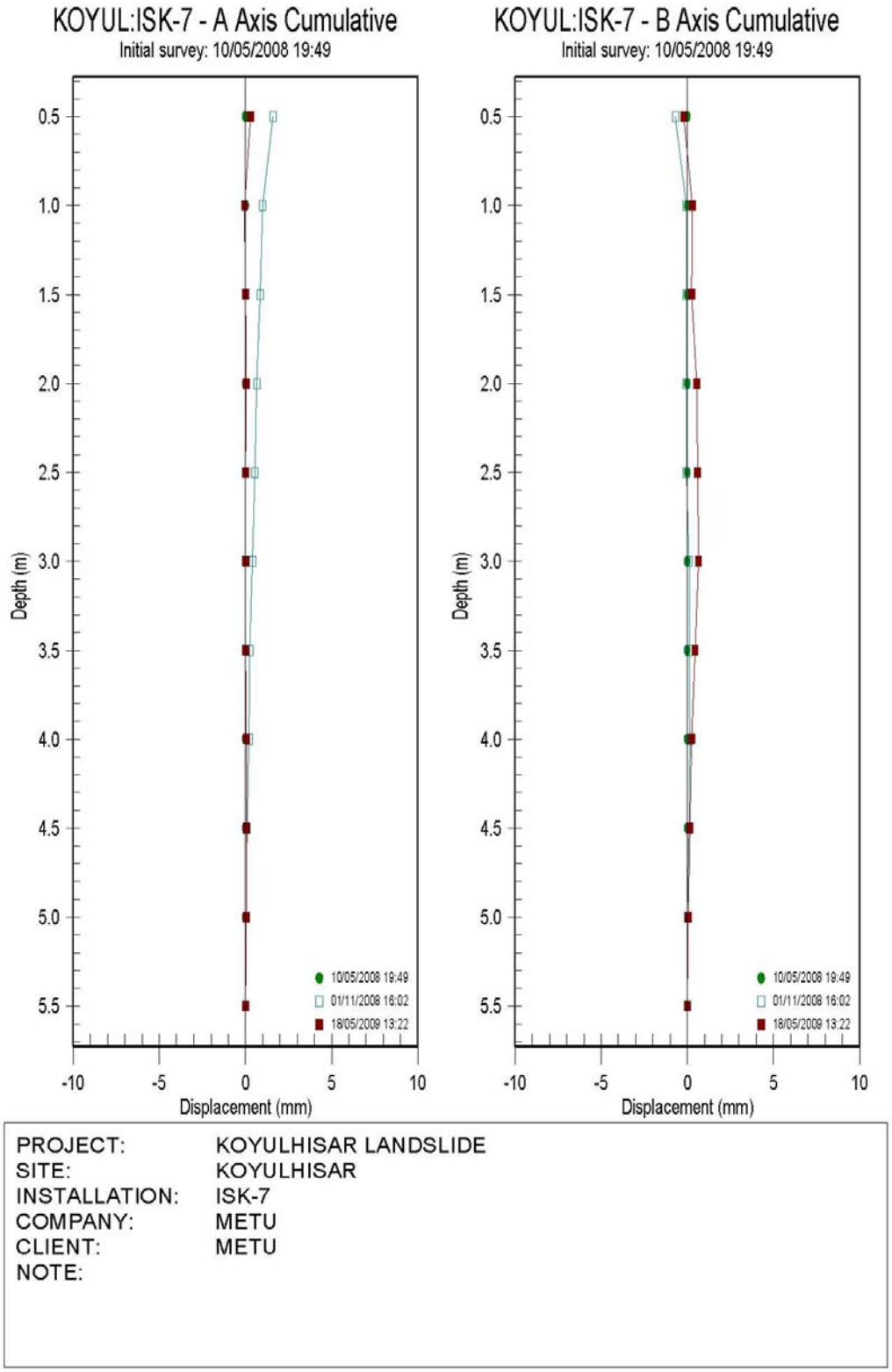

Figure B.19 Cumulative plot of ISK-7 borehole

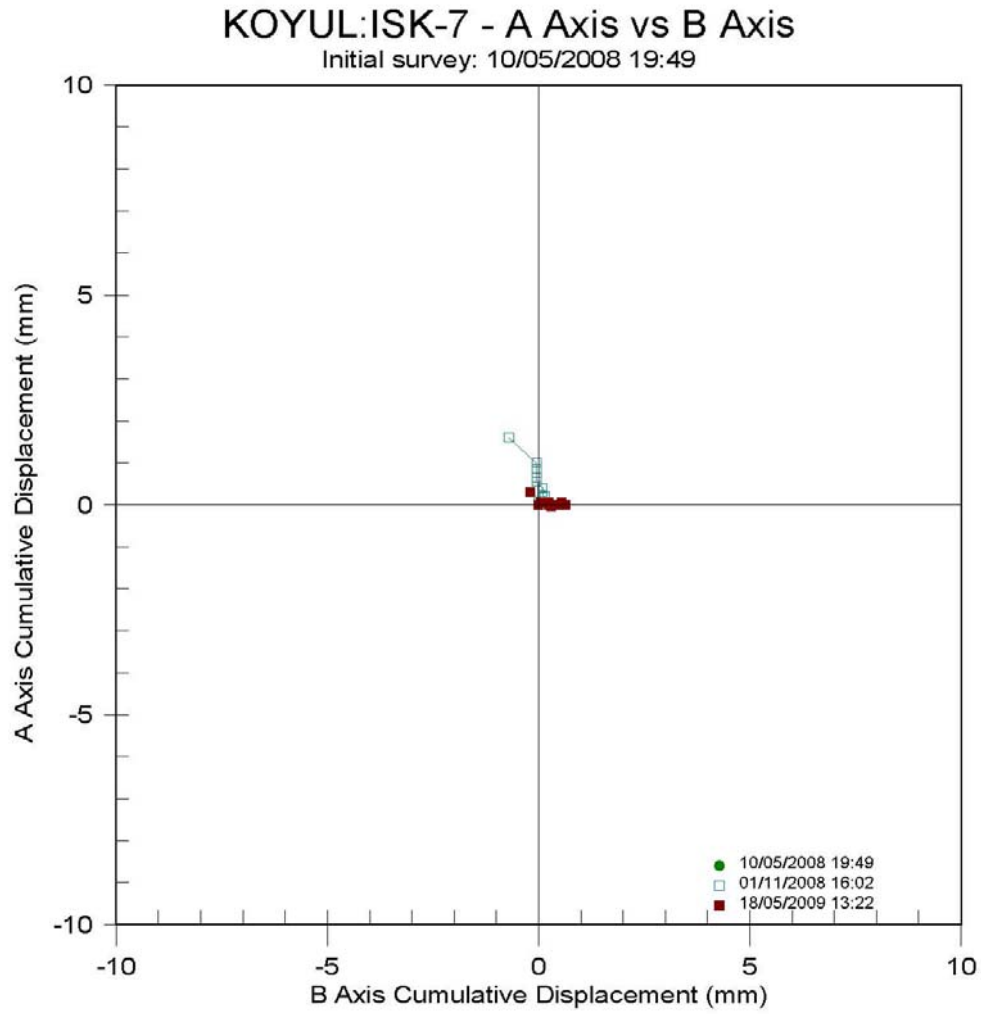

PROJECT:	KOYULHISAR LANDSLIDE
SITE:	KOYULHISAR
INSTALLATION:	ISK-7
COMPANY:	METU
CLIENT:	METU
NOTE:	

Figure B.20 Plan view plot of ISK-7 borehole

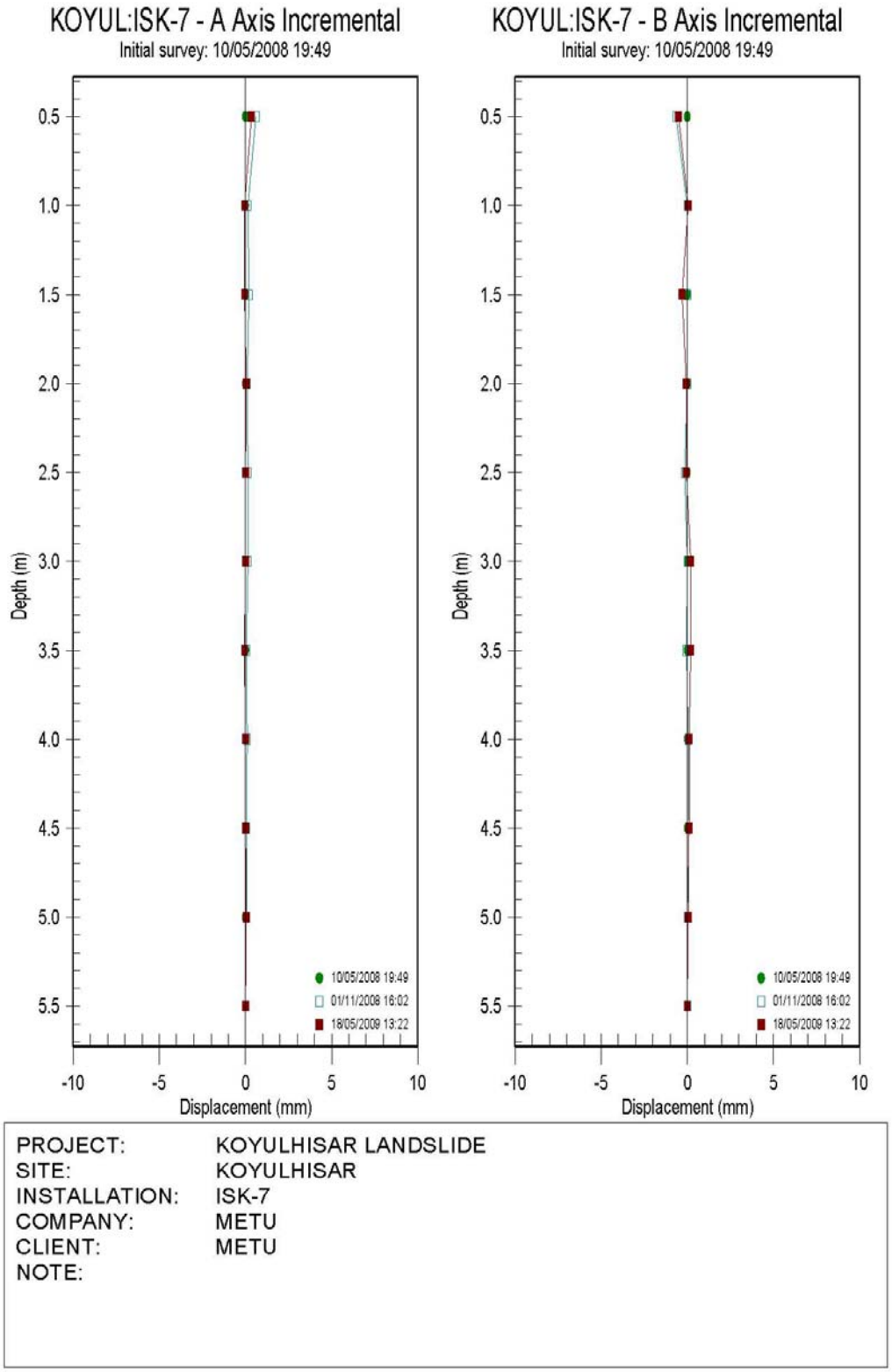

Figure B.21 Incremental plot of ISK-7 borehole

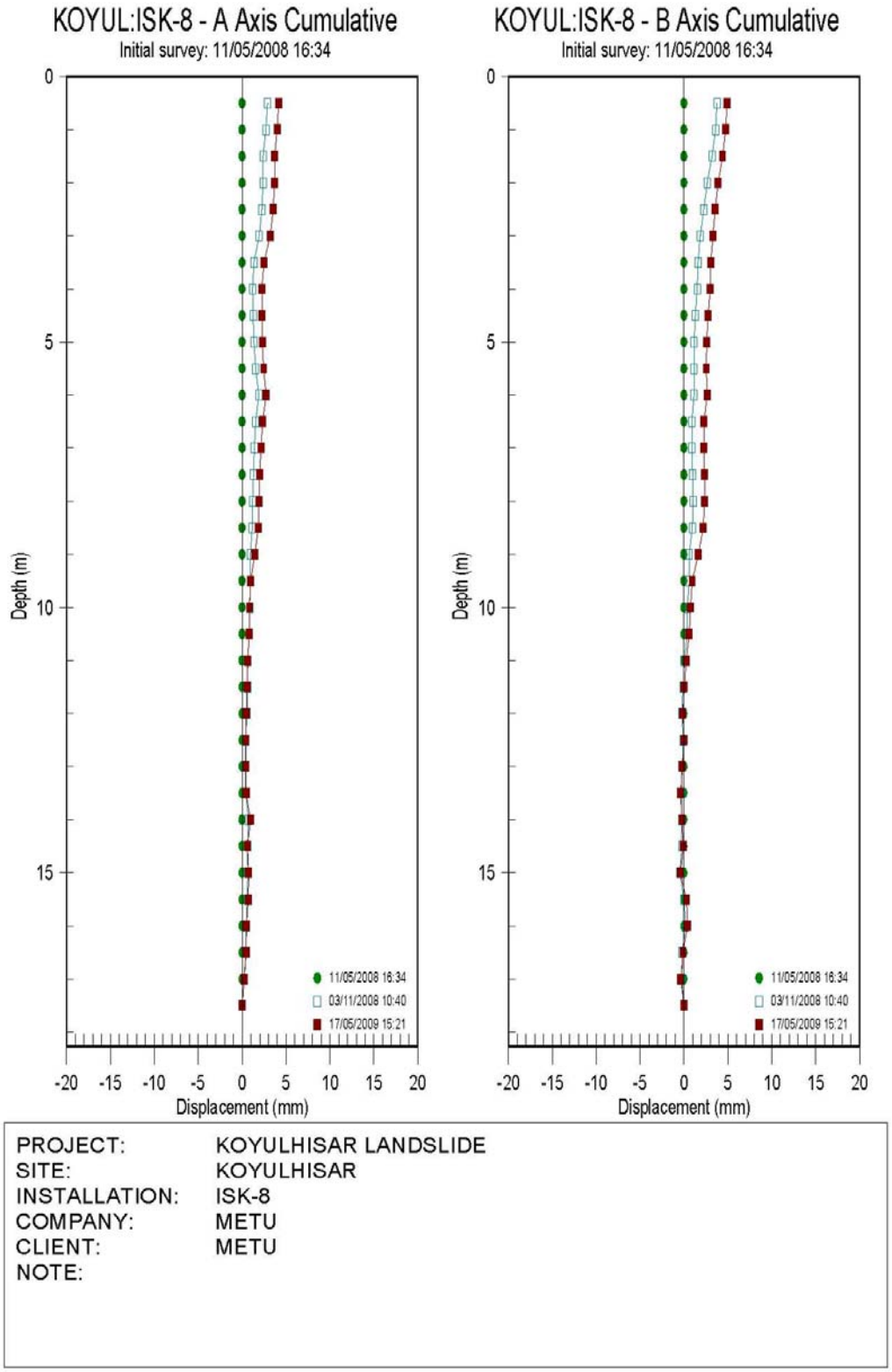

Figure B.22 Cumulative plot of ISK-8 borehole

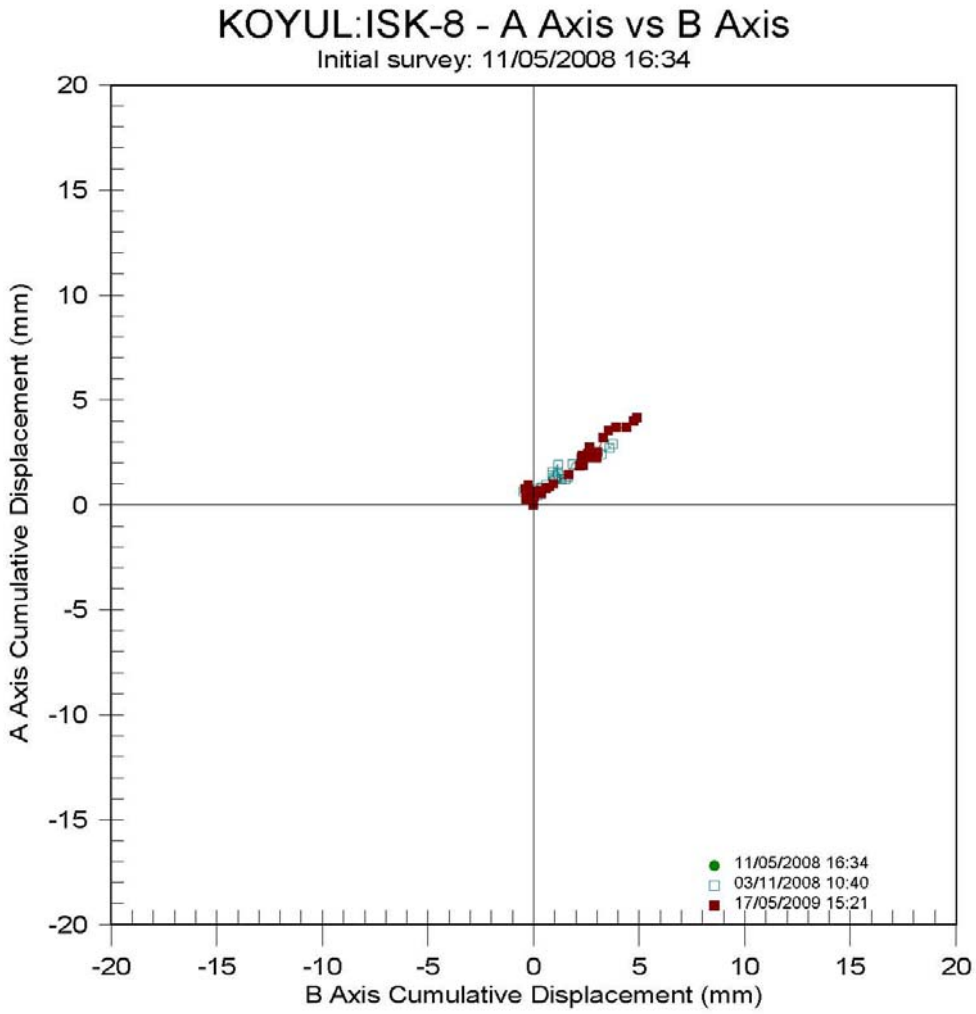

PROJECT:	KOYULHISAR LANDSLIDE
SITE:	KOYULHISAR
INSTALLATION:	ISK-8
COMPANY:	METU
CLIENT:	METU
NOTE:	

Figure B.23 Plan view plot of ISK-8 borehole

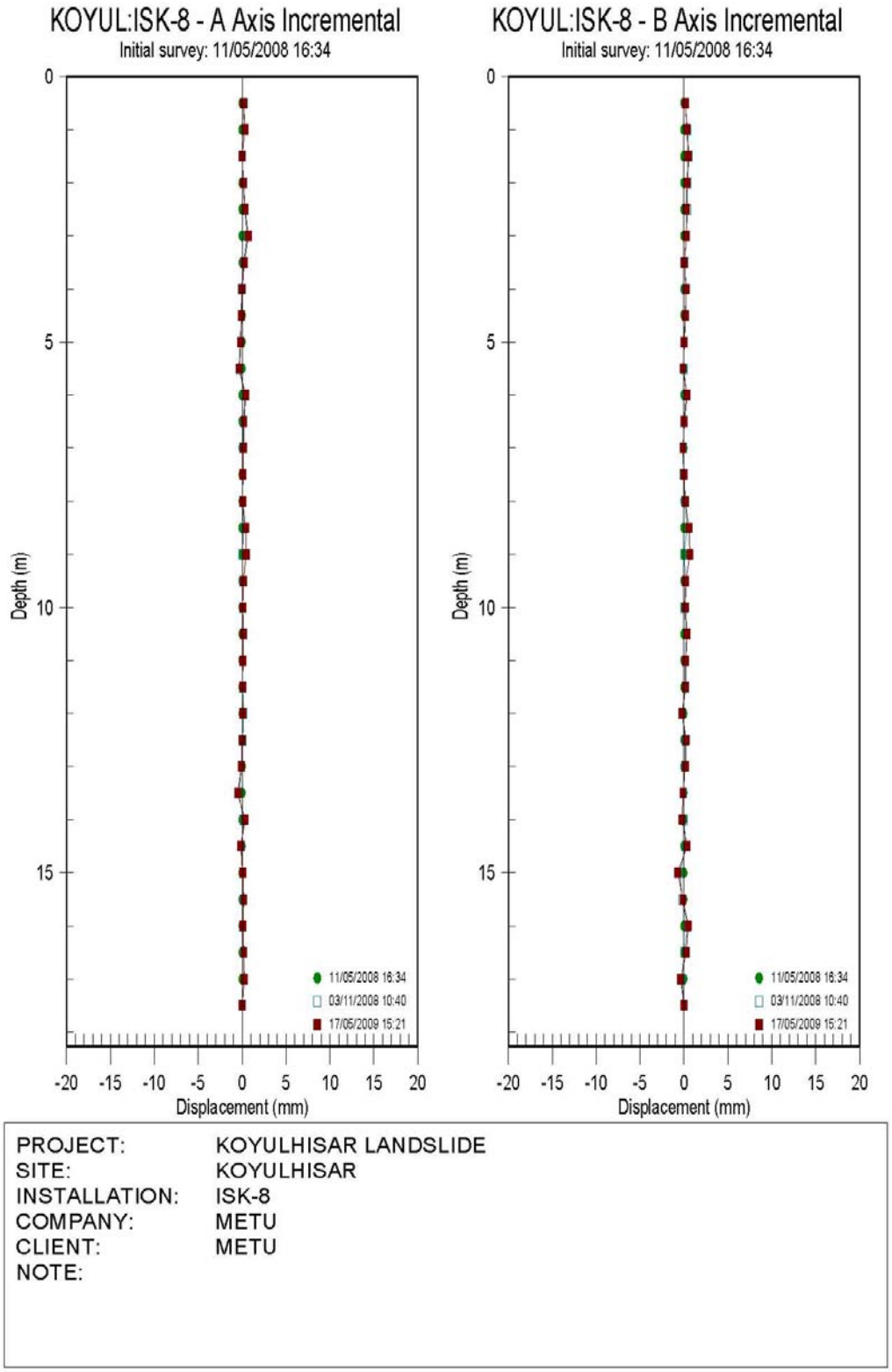

Figure B.24 Incremental plot of ISK-8 borehole

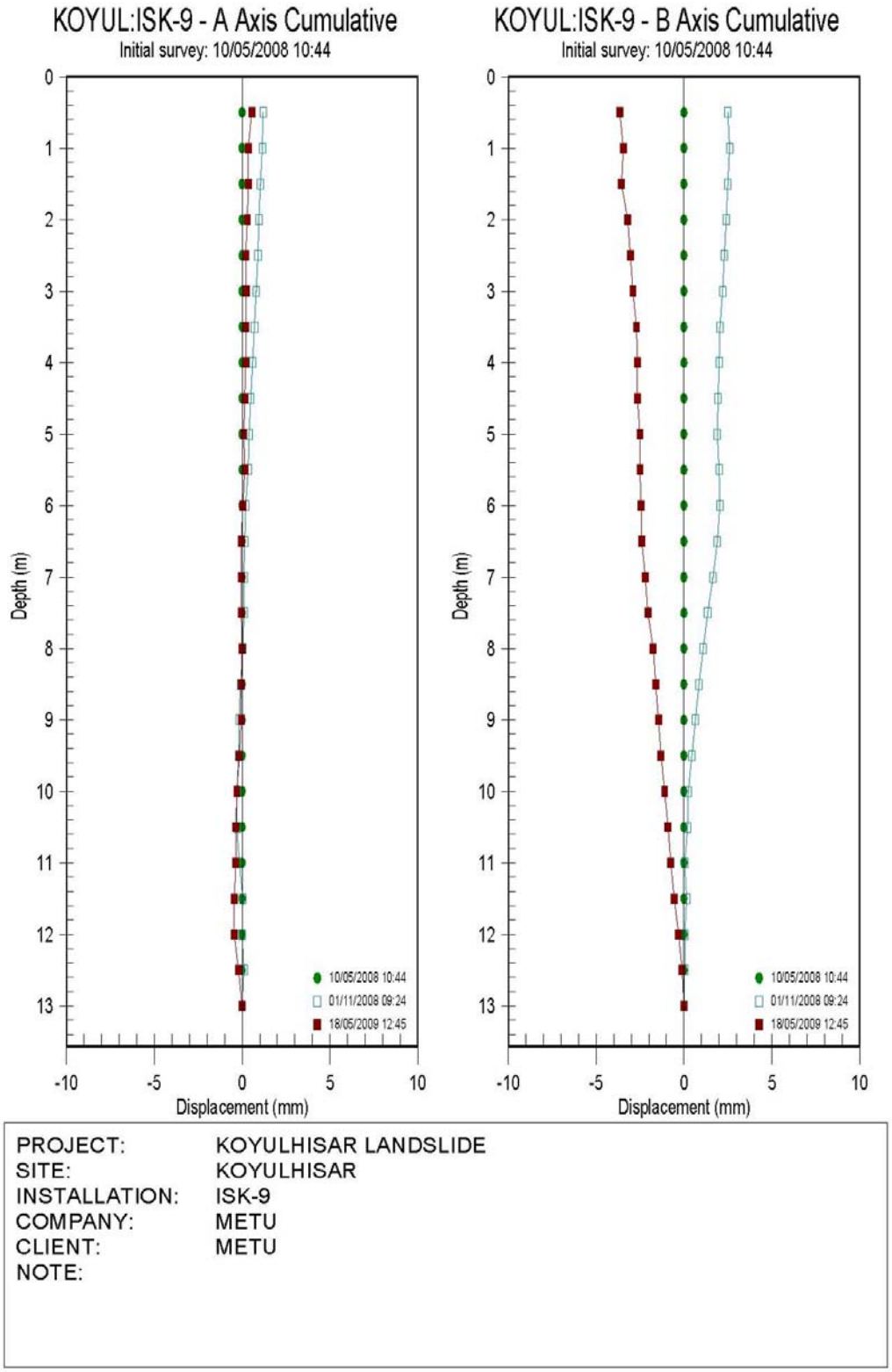

Figure B.25 Cumulative plot of ISK-9 borehole

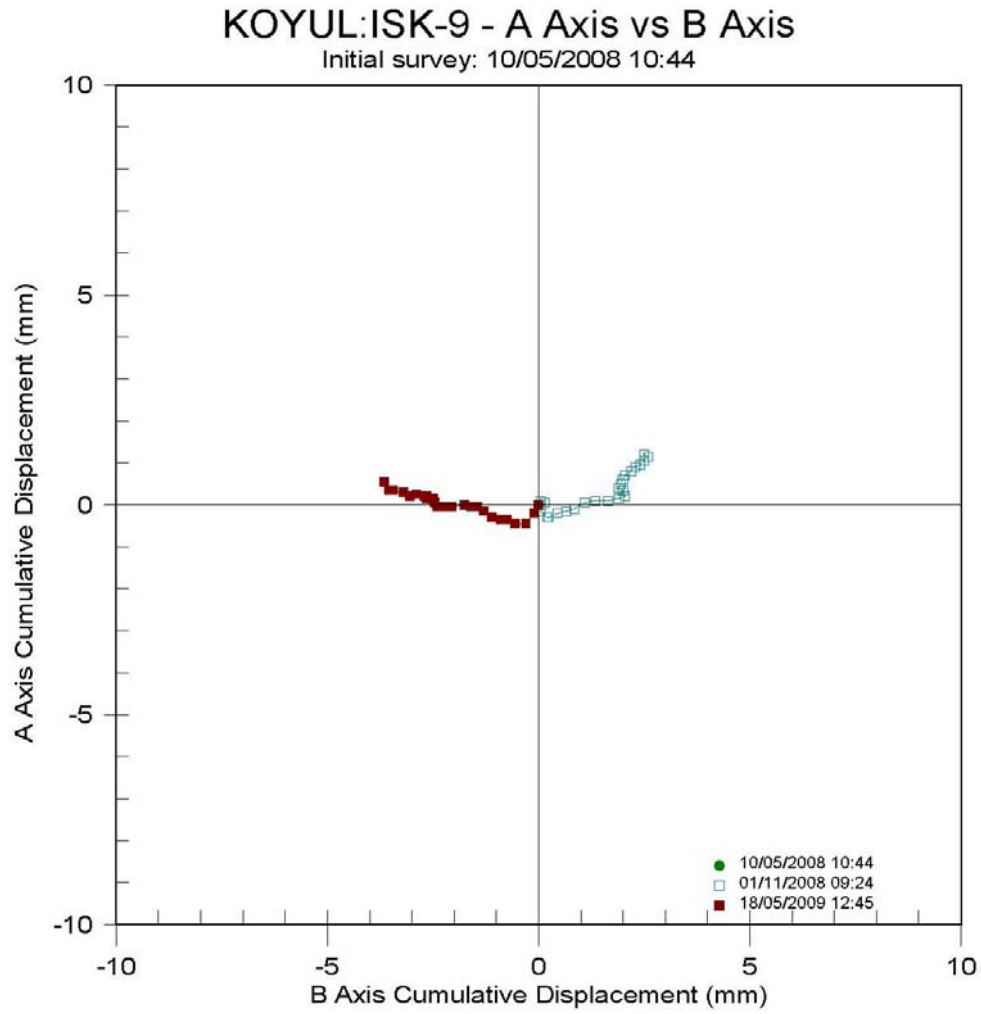

PROJECT:	KOYULHISAR LANDSLIDE
SITE:	KOYULHISAR
INSTALLATION:	ISK-9
COMPANY:	METU
CLIENT:	METU
NOTE:	

Figure B.26 Plan view plot of ISK-9 borehole

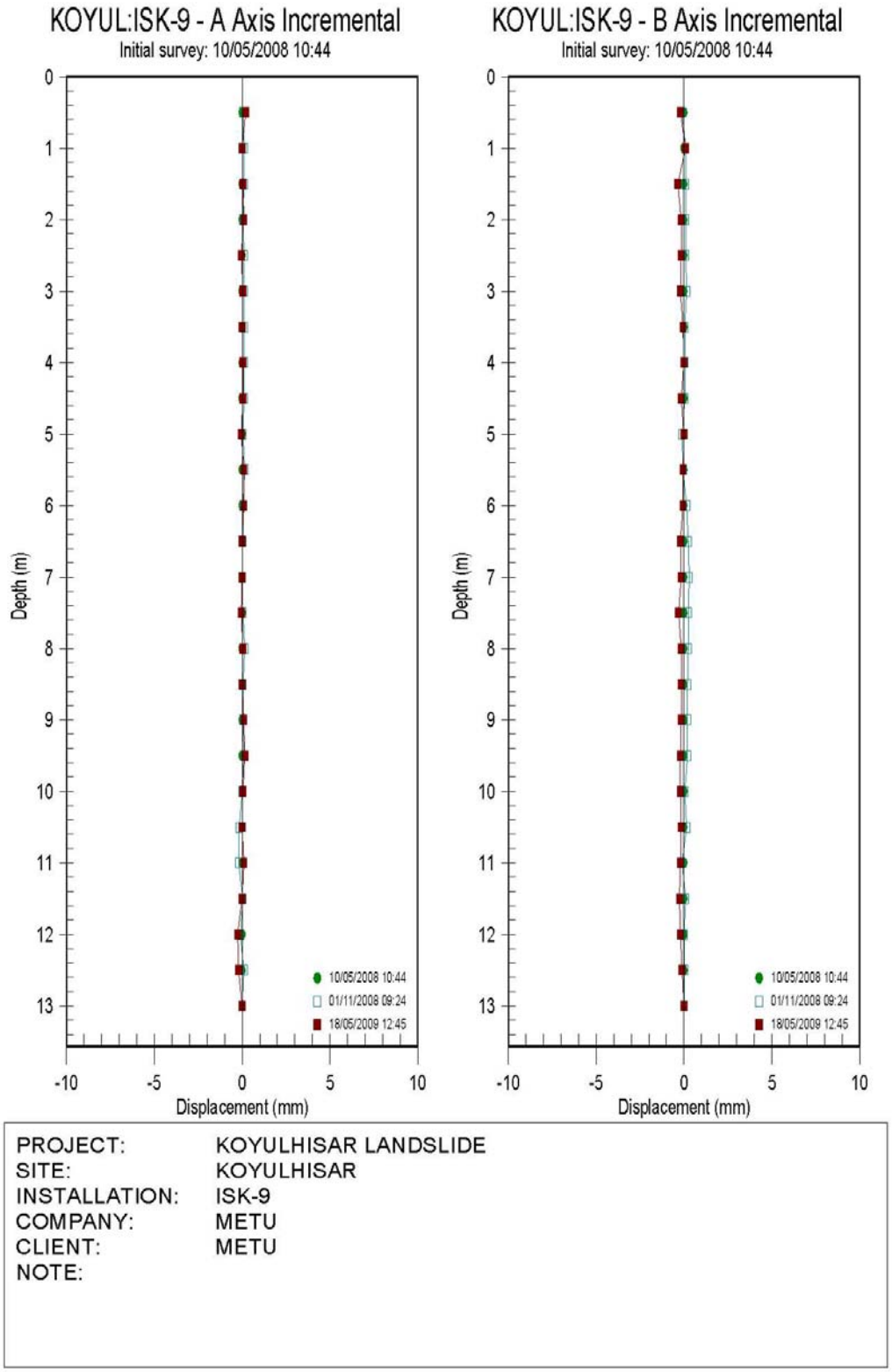

Figure B.27 Incremental plot of ISK-9 borehole

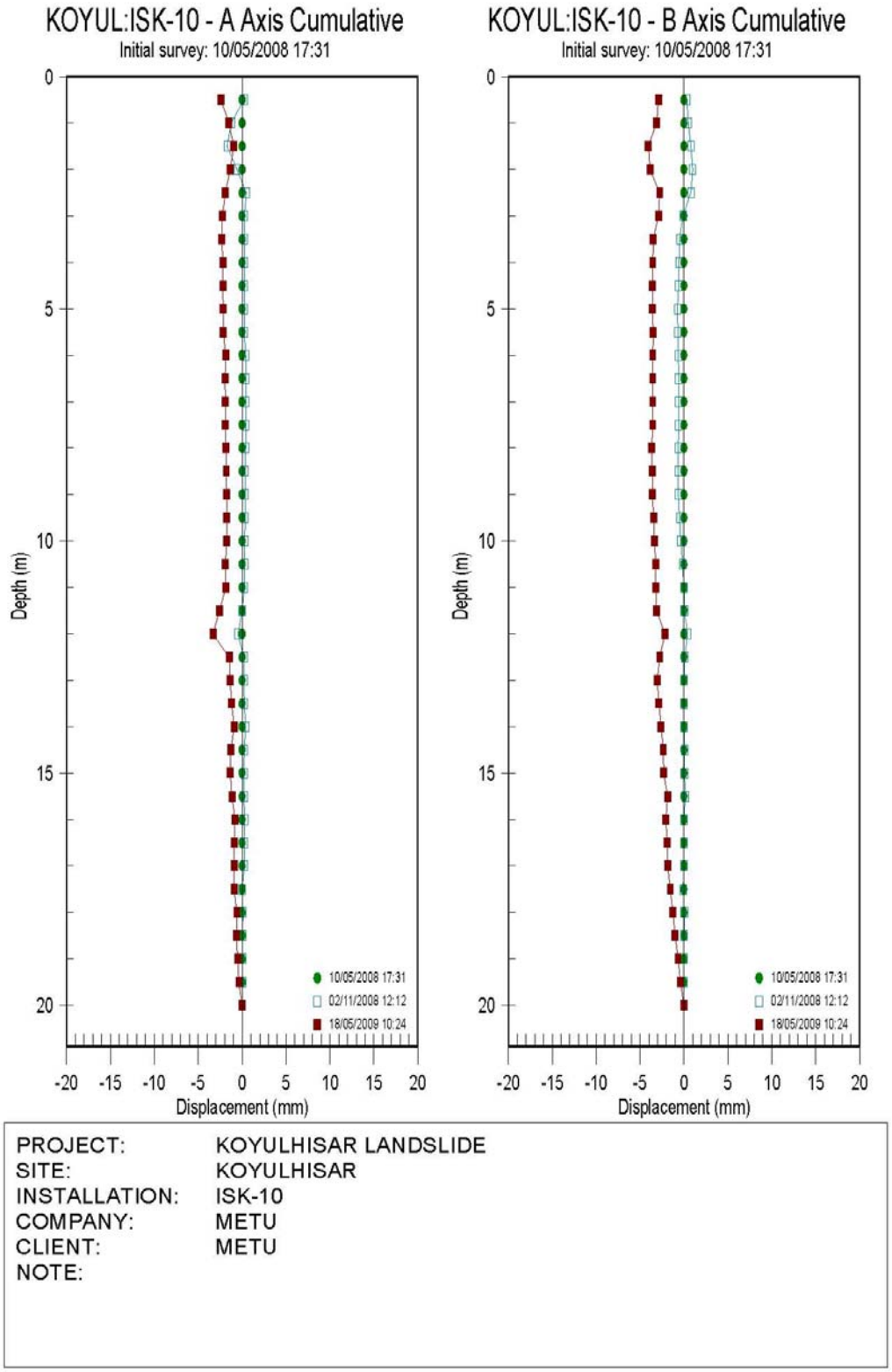

Figure B.28 Cumulative plot of ISK-10 borehole

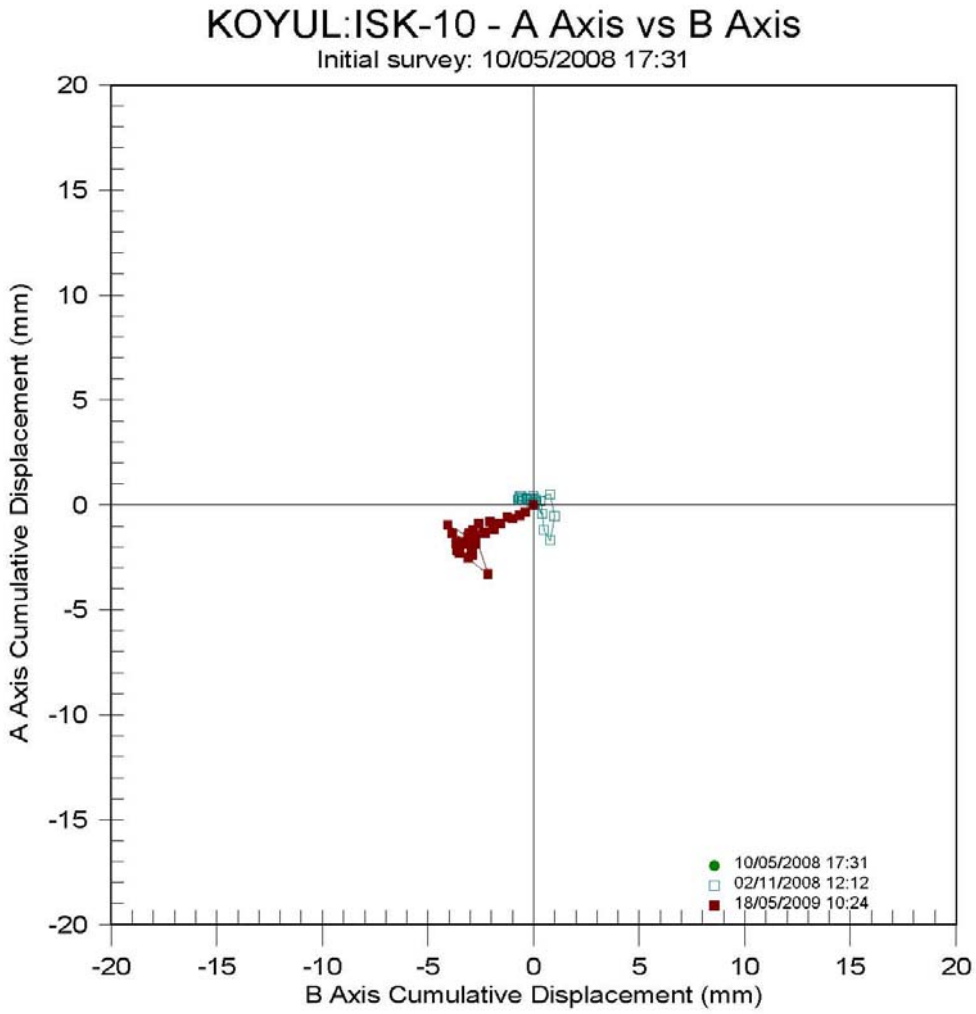

PROJECT:	KOYULHISAR LANDSLIDE
SITE:	KOYULHISAR
INSTALLATION:	ISK-10
COMPANY:	METU
CLIENT:	METU
NOTE:	

Figure B.29 Plan view plot of ISK-10 borehole

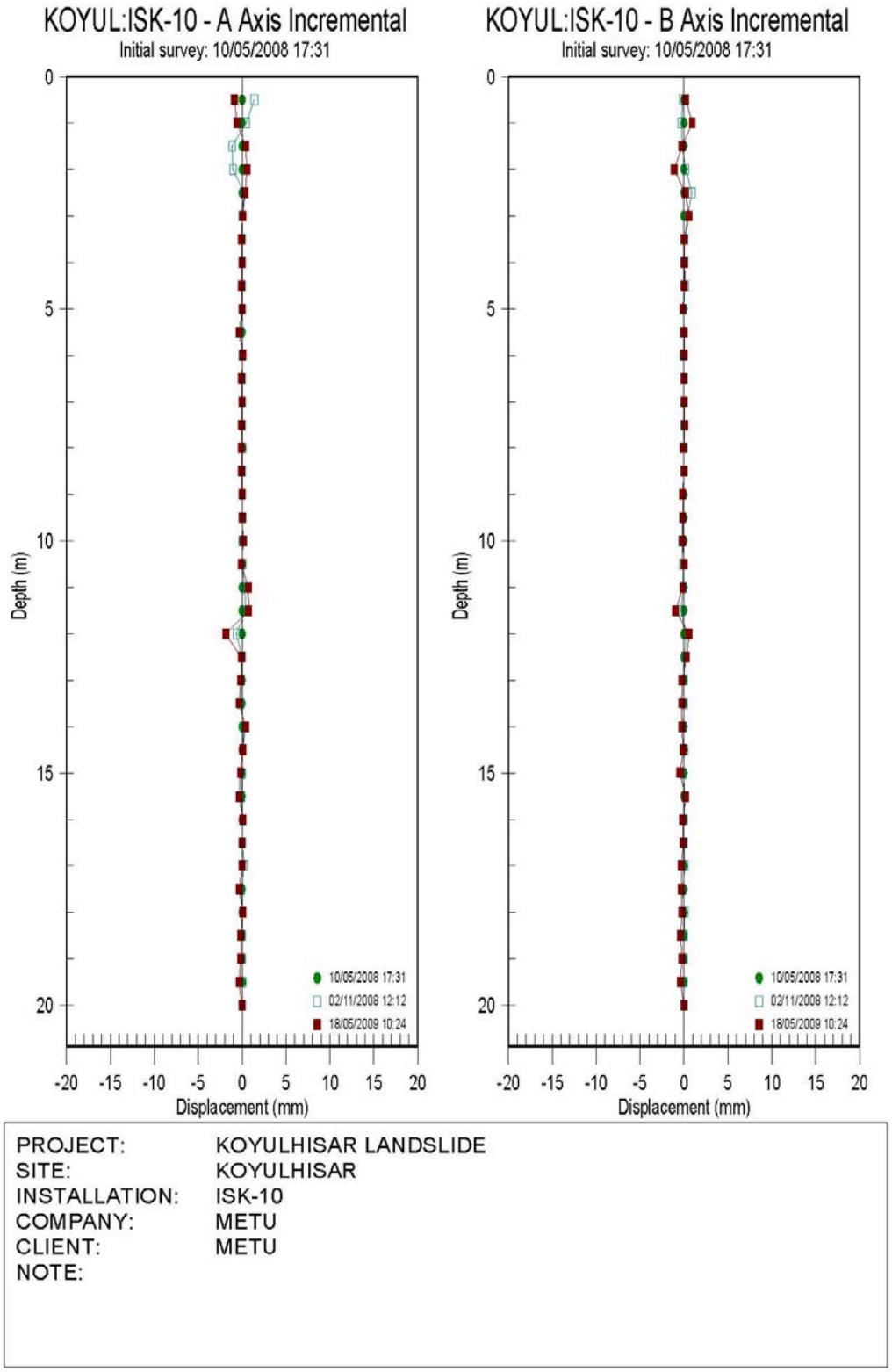

Figure B.30 Incremental plot of ISK-10 borehole

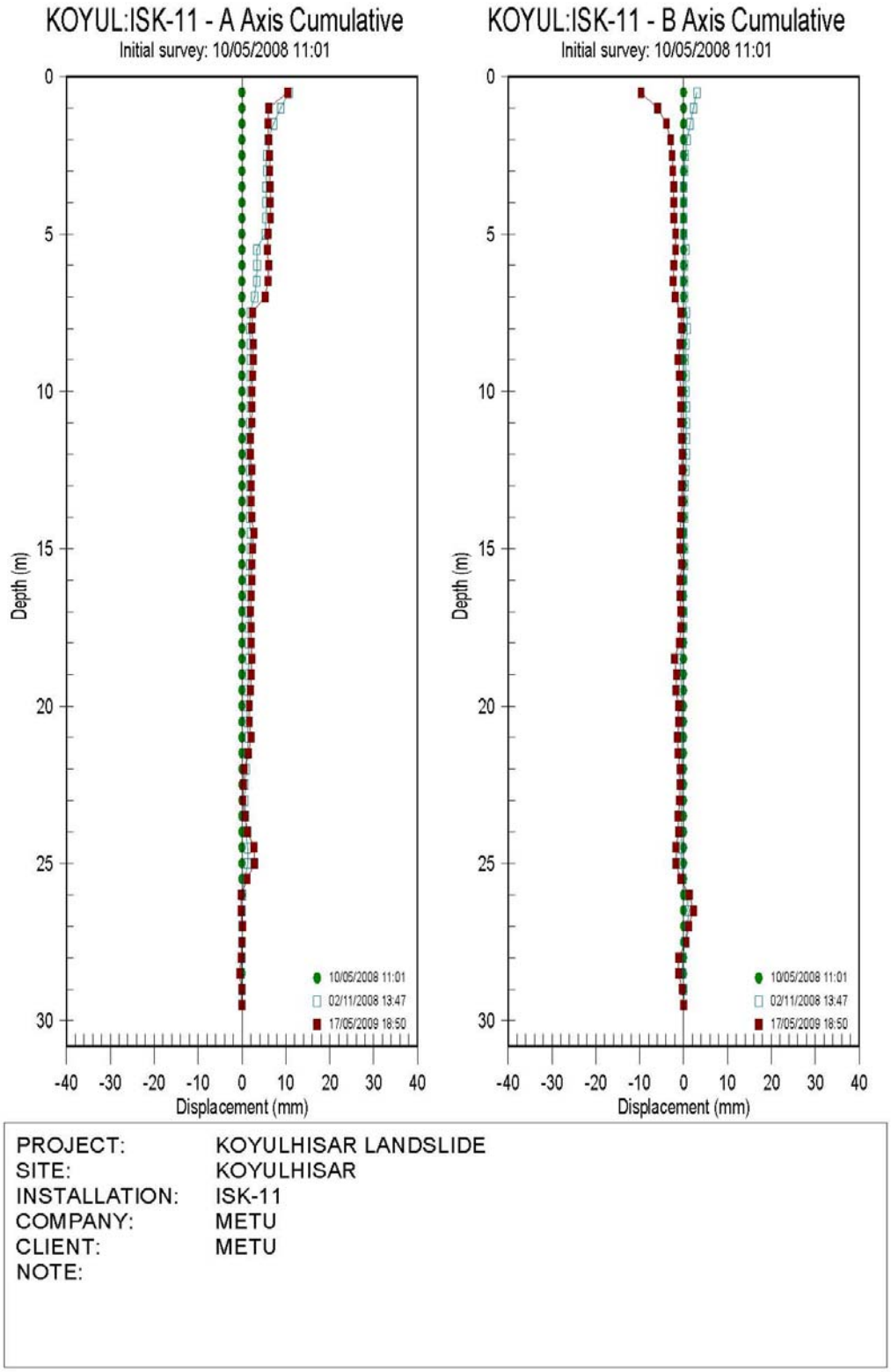

Figure B.31 Cumulative plot of ISK-11 borehole

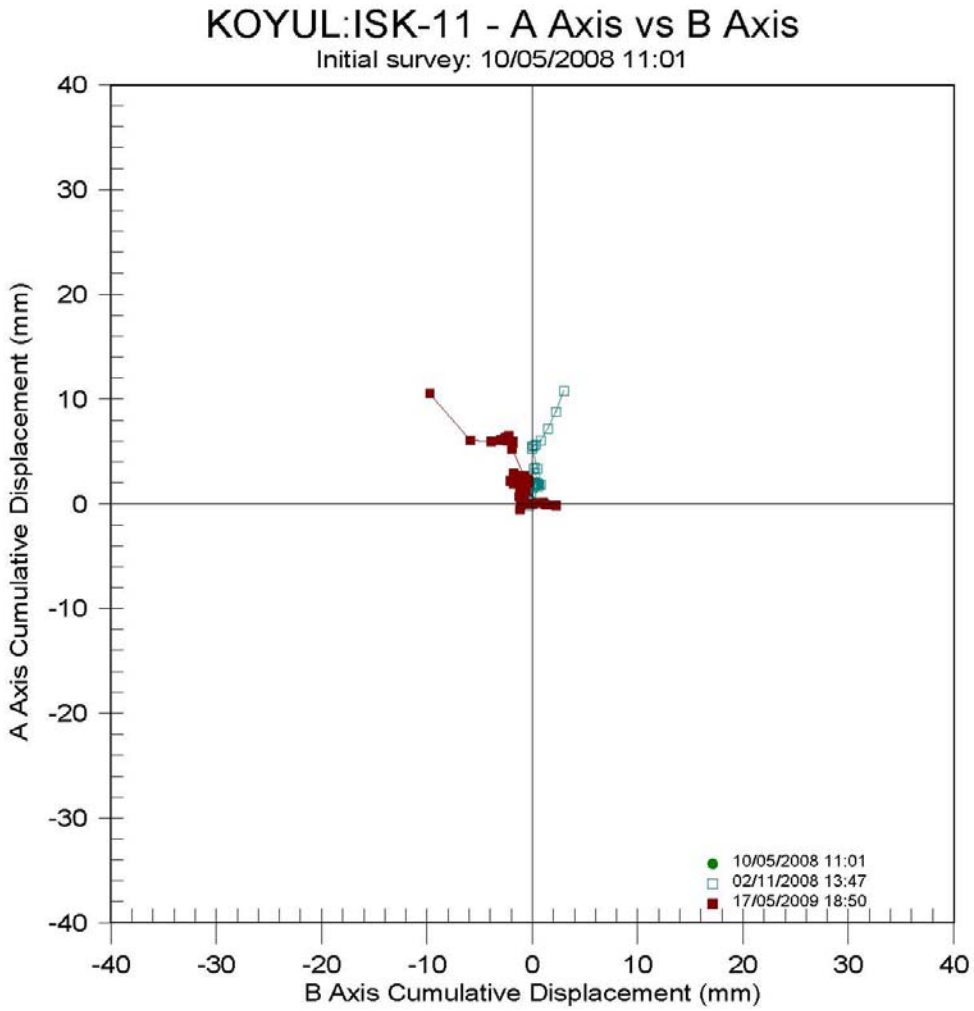

PROJECT:	KOYULHISAR LANDSLIDE
SITE:	KOYULHISAR
INSTALLATION:	ISK-11
COMPANY:	METU
CLIENT:	METU
NOTE:	

Figure B.32 Plan view plot of ISK-11 borehole

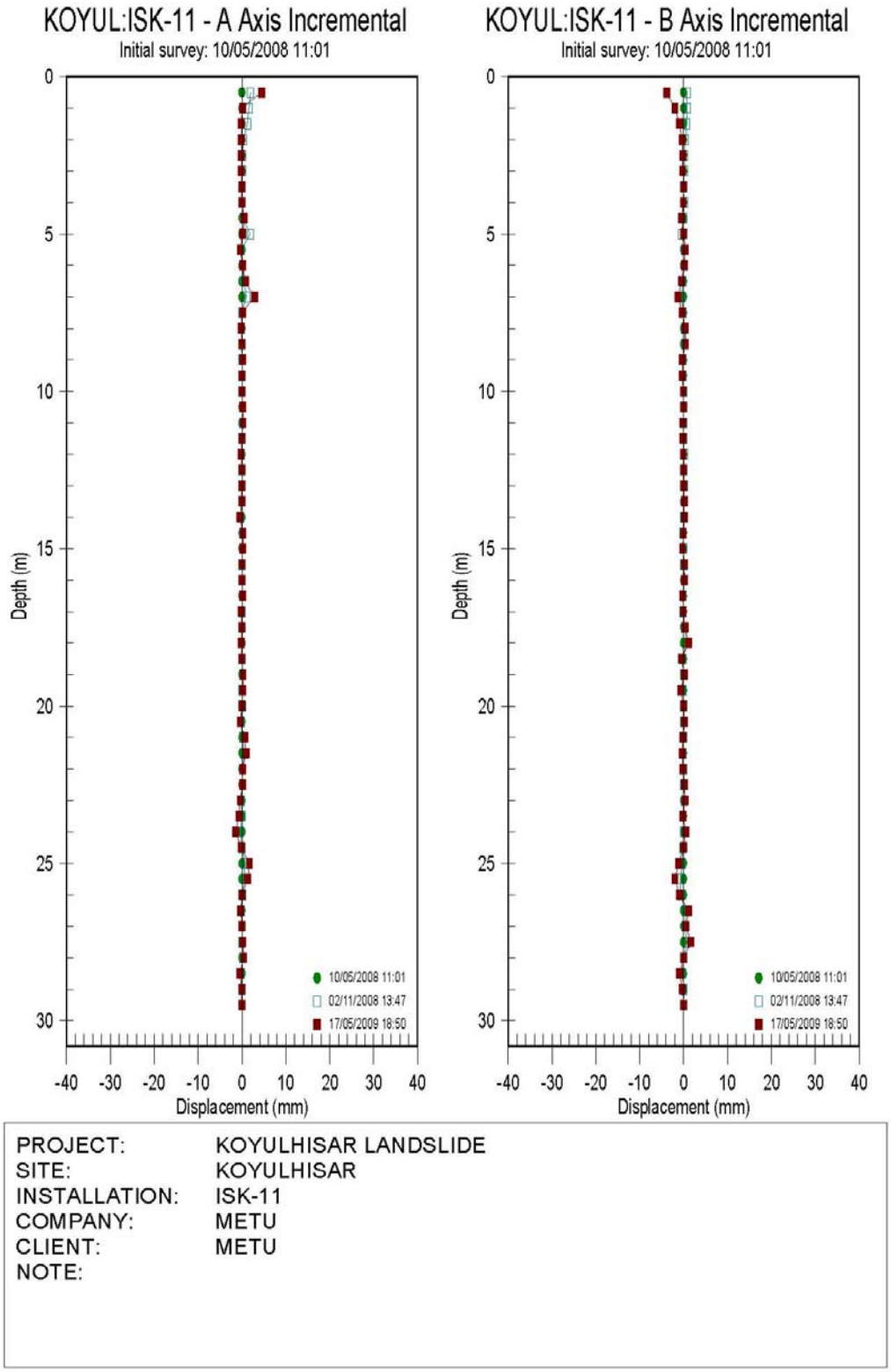

Figure B.33 Incremental plot of ISK-11 borehole

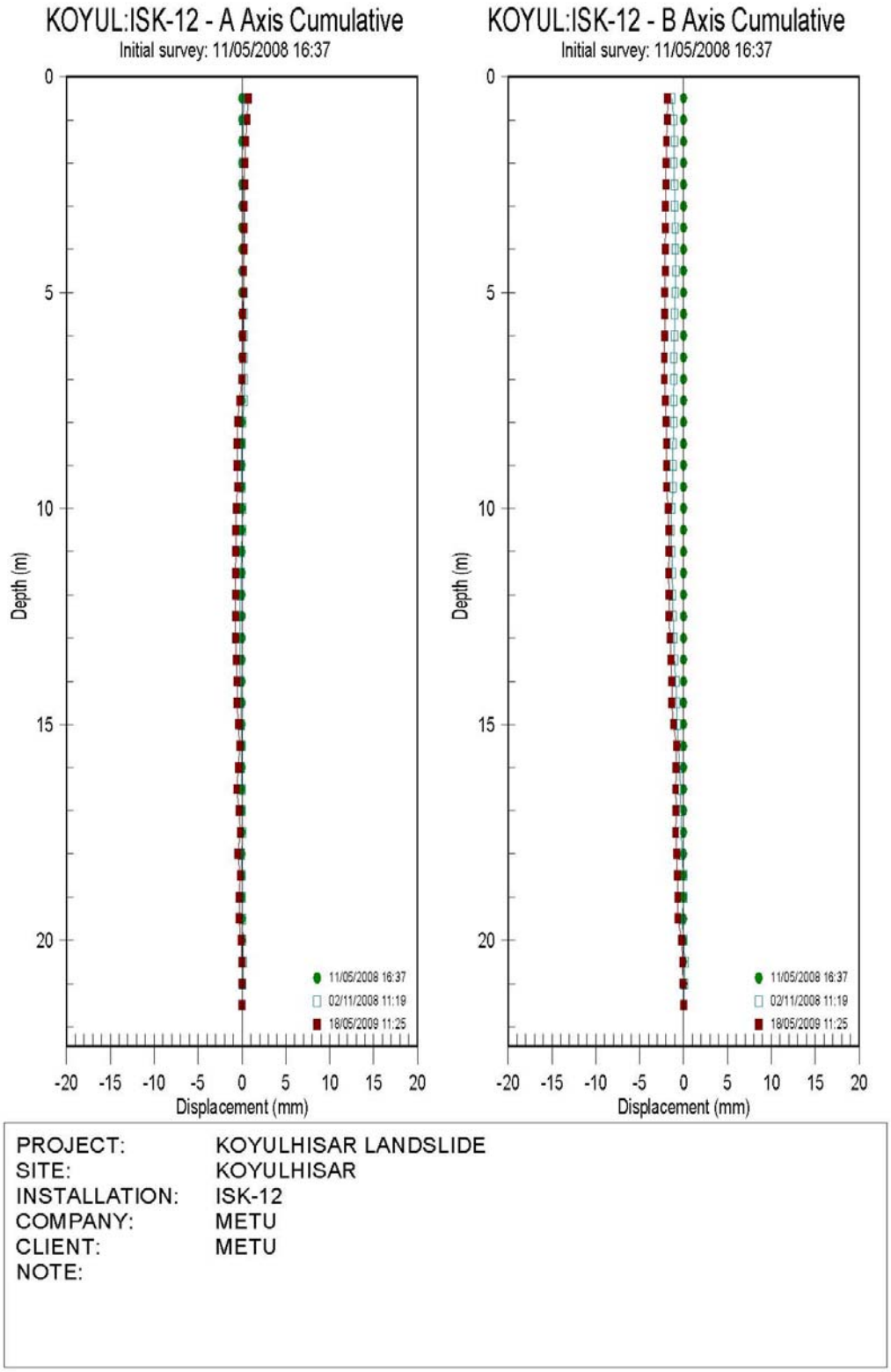

Figure B.34 Cumulative plot of ISK-12 borehole

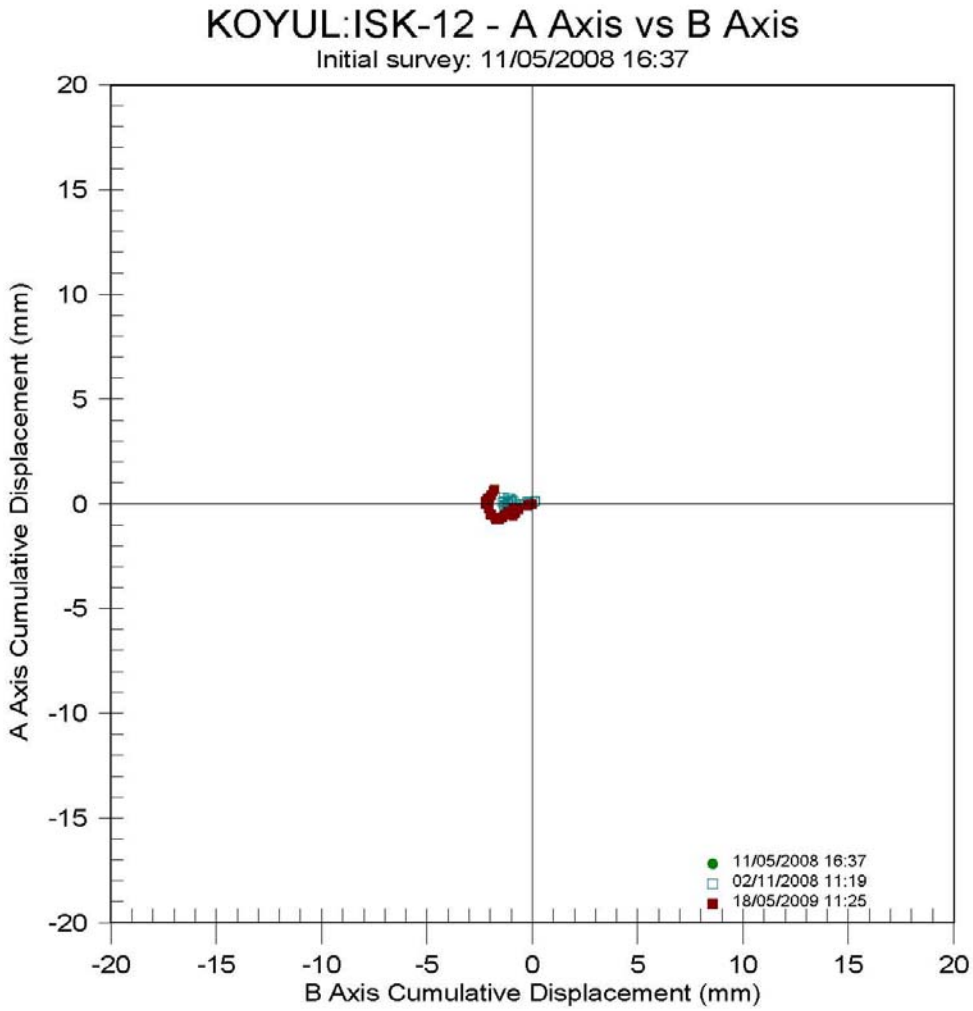

PROJECT:	KOYULHISAR LANDSLIDE
SITE:	KOYULHISAR
INSTALLATION:	ISK-12
COMPANY:	METU
CLIENT:	METU
NOTE:	

Figure B.35 Plan view plot of ISK-12 borehole

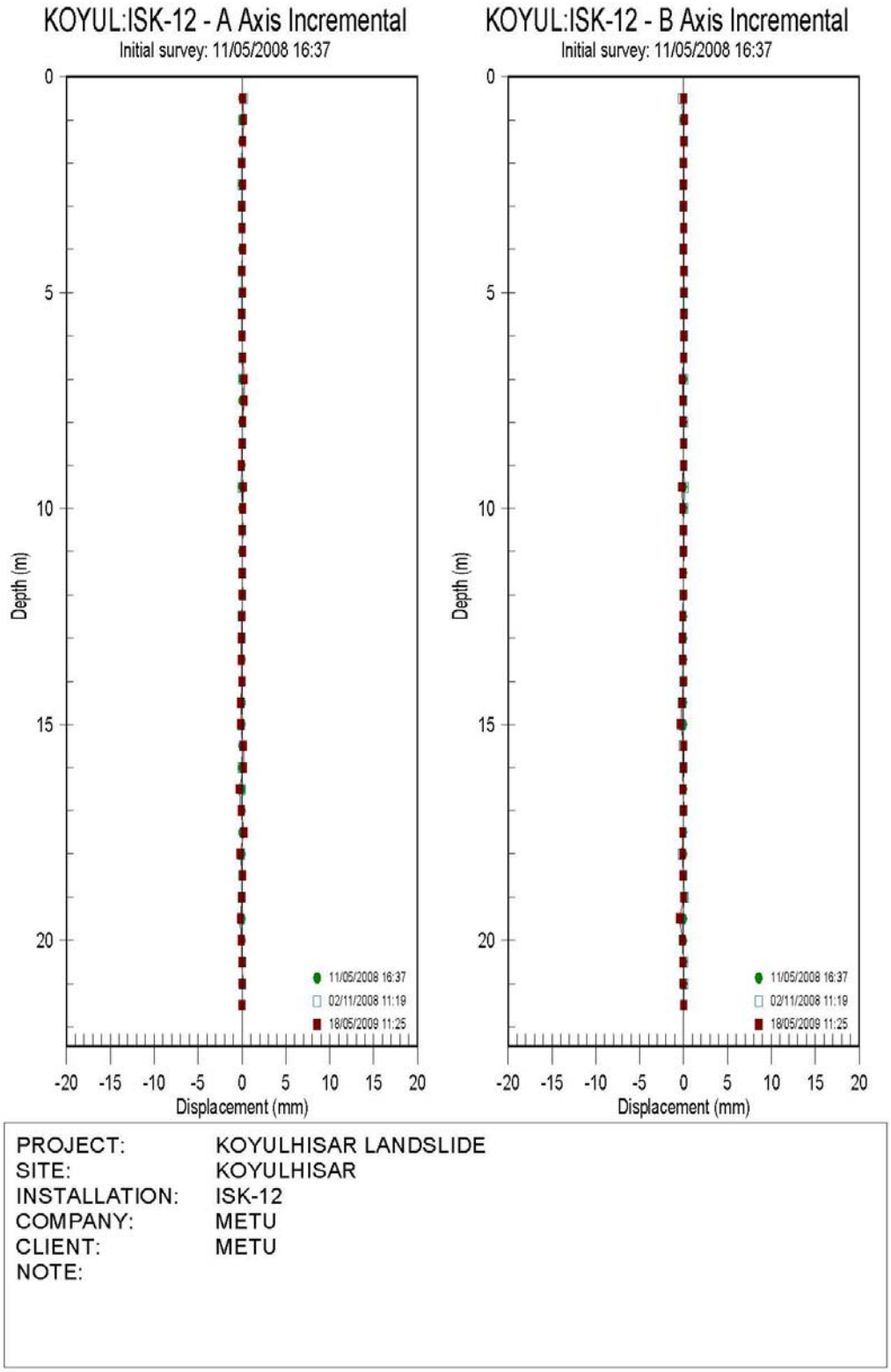

Figure B.36 Incremental plot of ISK-12 borehole

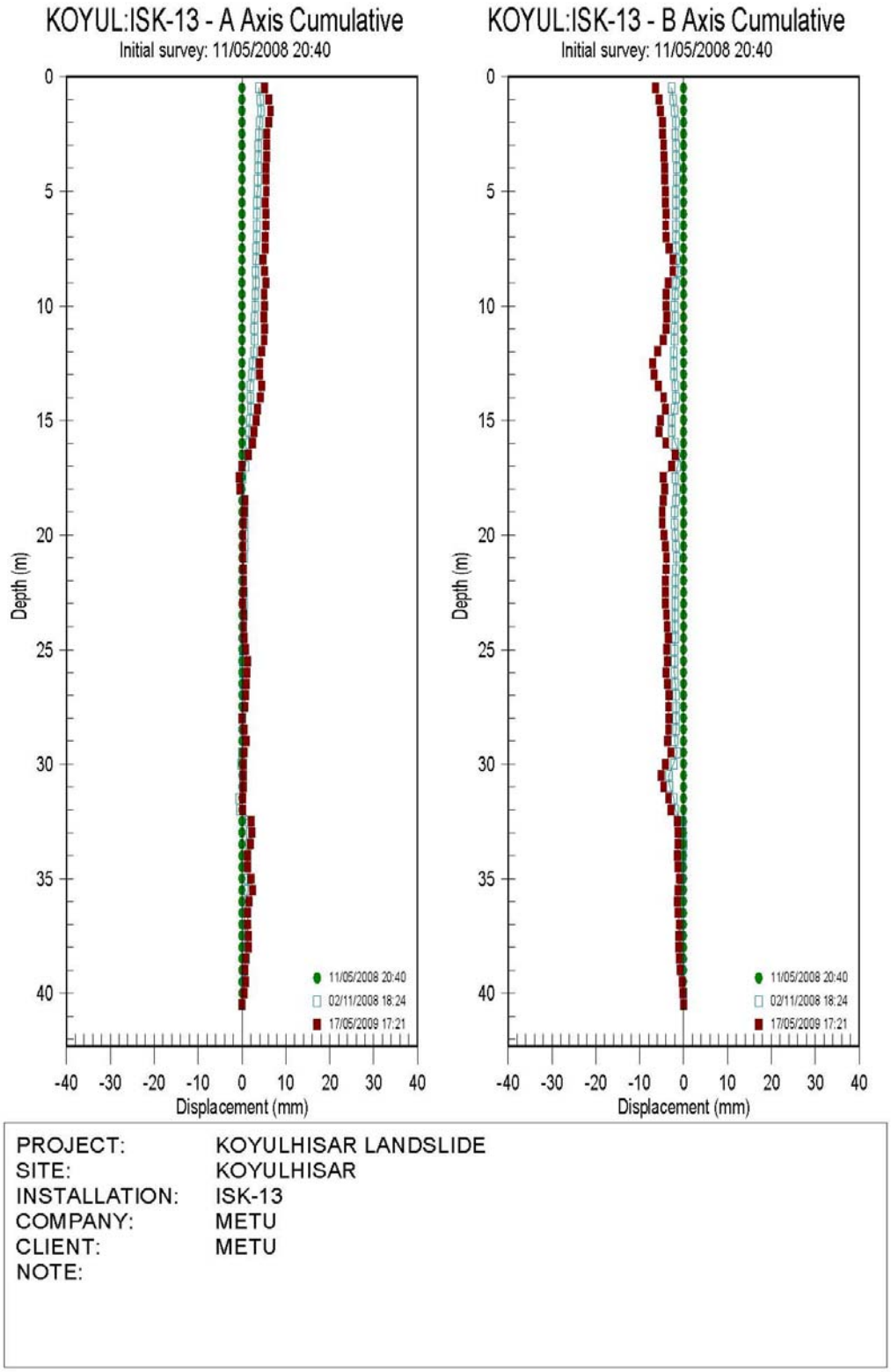

Figure B.37 Cumulative plot of ISK-13 borehole

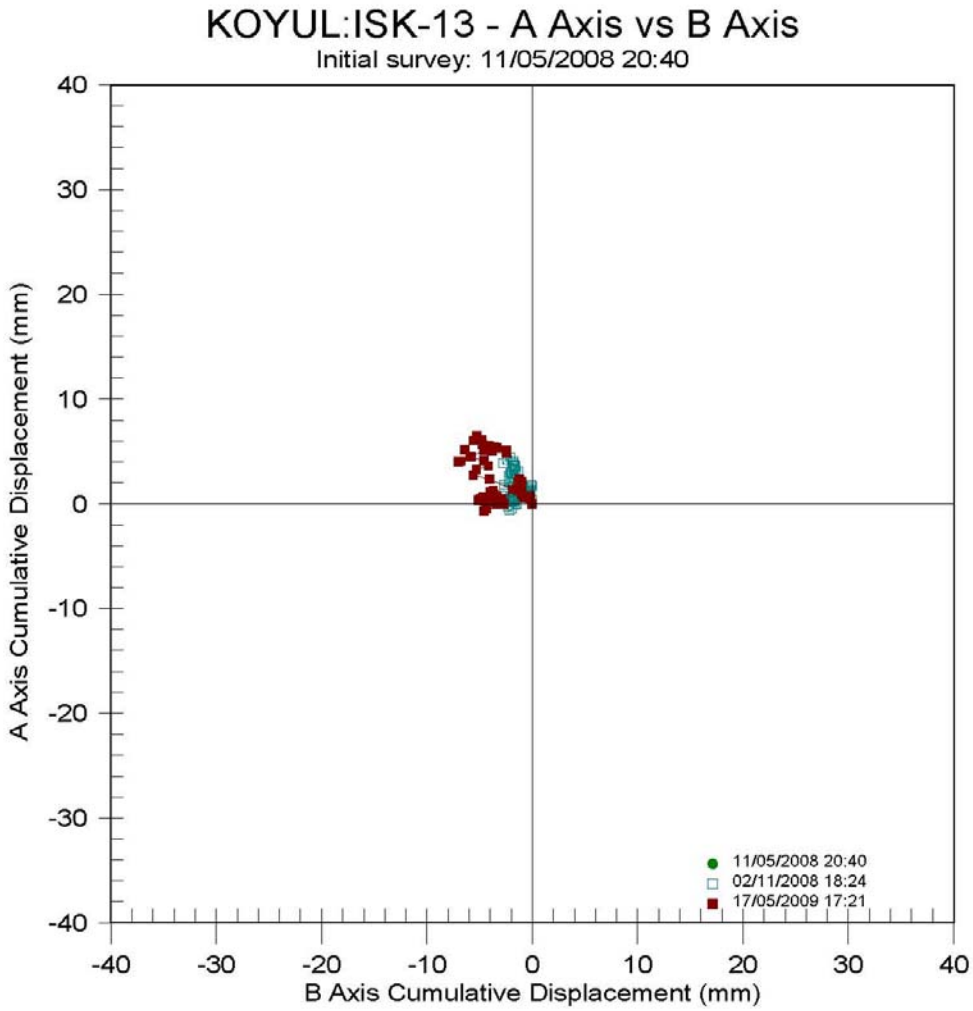

PROJECT:	KOYULHISAR LANDSLIDE
SITE:	KOYULHISAR
INSTALLATION:	ISK-13
COMPANY:	METU
CLIENT:	METU
NOTE:	

Figure B.38 Plan view plot of ISK-13 borehole

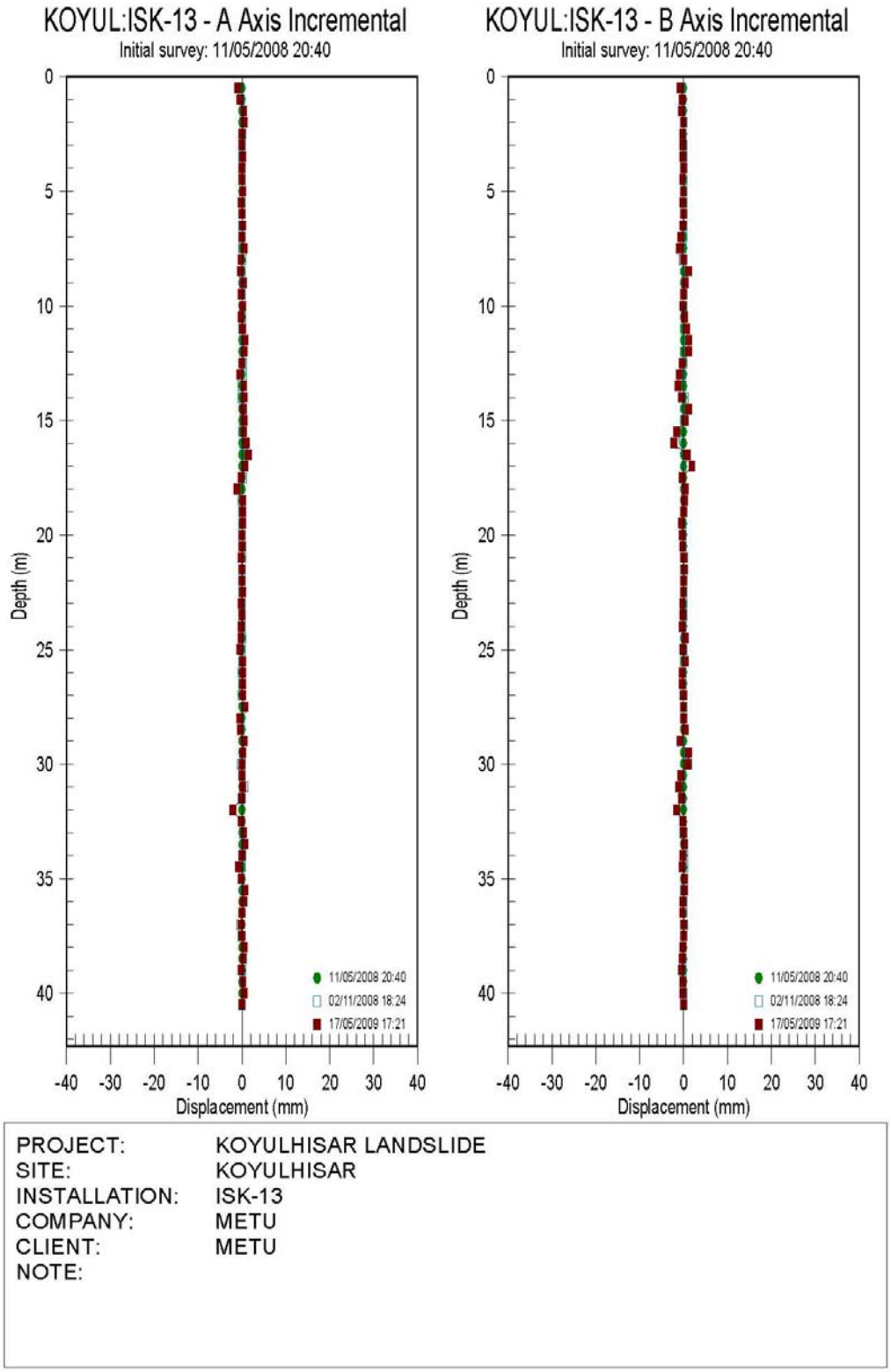

Figure B.39 Incremental plot of ISK-13 borehole

APPENDIX C

LABORATORY TEST RESULTS

Table C.1 Laboratory test results

Drilling No.	Specimen No.	Depth (m)	Water Content (%)	Unit Weight (KN / m3)	Dry Unit Weight (g/cm3)	Specific Gravity (g/cm3)	Hydrometer	Sieve Analysis		Atterberg Limits			Soil Class	Residual Direct Shear		Triaxial Test (UU)		Consolidation Test	
								Retained from No. 4 (%)	Pass from No. 200 (%)	LL (%)	PL (%)	PI (%)		Max. Shear Strength (kgf/cm2)	Min. Shear Strength (kgf/cm2)	c (kgf/cm2)	f (o)	Swelling Percentage	Swelling Pressure (kgf/cm2)
SK-1	SPT-1	1,50	29,5				✓	0,5	71,8	61,8	25,2	36,6	CH						
SK-1	SPT-2	3,00	25,7				✓	0,0	85,7	59,6	25,2	34,4	CH						
SK-1	SPT-3	4,50	16,9				✓	0,0	66,3	41,8	22,2	19,6	CL						
SK-1	SPT-4	6,00	23,0				✓	21,5	52,4	52,7	22,8	29,9	CH						
SK-1	SPT-5	7,50	22,0					38,3	41,5	40,3	19,9	20,4	GC						
SK-1	SPT-6	9,00	8,8					44,3	33,7	32,4	15,7	16,7	GC						
SK-1	SPT-7	10,50	23,3				✓	0,0	87,3	23,0	19,8	3,2	ML						
SK-1	SPT-8	12,00	22,4				✓	0,0	73,8	37,3	19,8	17,5	CL						
SK-1	SPT-9	13,50	20,8				✓	3,2	51,6	37,8	19,8	18,0	CL						
SK-1	SPT-10	15,00	9,2					43,6	17,1	36,8	16,2	20,6	GC						
SK-1	SPT-11	16,50	1,6					65,3	13,8		NP		GM						
SK-1	SPT-12	18,00	17,7					64,5	7,8		NP		GM						
SK-1	SPT-13	19,50	14,7					50,3	11,0		NP		GM						
SK-1	SPT-14	21,00	20,6					23,1	15,5		NP		SM						

Table C.1 (Continued)

SK-1	SPT-15	22,50	13,1					44,4	16,9		NP		GM						
SK-1	UD-3	3,50	24,2	17,81	14,34	2,65	✓	0,3	68,7	48,5	23,8	24,7	CL	**1,155**	**0,224**			1,13	0,120
SK-1	UD-9	9,50	21,7	17,58	14,44	2,65	✓	0,0	82,1	48,6	23,4	25,2	CL	**1,401**	**0,216**			1,24	0,129
SK-1	UD-12	12,50	23,3	17,47	14,17	2,67	✓	0,0	89,6	48,8	20,1	28,7	CL	**1,483**	**0,211**			0,93	0,098
SK-1	UD-15	15,50	22,7	17,67	14,40	2,71	✓	0,0	90,9	72,1	26,3	45,8	CH	**1,298**				1,54	0,160
SK-2	SPT-1	1,50													**0,198**				
SK-2	SPT-2	3,00																	
SK-2	SPT-3	4,50																	
SK-2	SPT-4	6,00																	
SK-2	SPT-5	7,50																	
SK-2	SPT-6	9,00																	
SK-2	SPT-7	10,50																	
SK-2	SPT-8	12,00																	
SK-2	SPT-9	13,50																	
SK-2	SPT-10	15,00																	
SK-3	SPT-1	1,50																	
SK-3	SPT-2	3,00	20,1				✓	1,9	68,7	34,4	18,0	16,4	CL						
SK-3	SPT-3	4,50																	
SK-3	SPT-4	6,00	18,2				✓	0,0	59,1	31,7	15,8	15,9	CL						
SK-3	SPT-5	7,50																	
SK-3	SPT-6	9,00	21,3				✓	0,7	73,7	52,0	23,3	28,7	CH						

Table C.1 (Continued)

SK-3	SPT-7	10,50																	
SK-3	SPT-8	12,00	12,6				✓	0,0	85,5	35,1	17,2	17,9	CL						
SK-3	SPT-9	13,50																	
SK-3	SPT-10	15,00	22,1				✓	0,0	85,7	71,5	29,1	42,4	CH						
SK-3	SPT-11	16,50																	
SK-3	SPT-12	18,00	38,1				✓	2,2	61,6	61,5	27,3	34,2	CH						
SK-3	SPT-13	19,50																	
SK-3	SPT-14	21,00	32,8				✓	4,0	58,3	58,4	26,8	31,6	CH						
SK-3	SPT-15	22,50																	
SK-3	SPT-16	24,00	43,6				✓	0,9	72,3	63,3	25,9	37,4	CH						
SK-3	UD-3	3,50																	
SK-3	UD-9	9,50																	
SK-3	UD-	12,50																	
SK-3	UD-	15,50																	
SK-4	SPT-1	1,50																	
SK-4	SPT-2	3,00	10,1					48,1	17,1	27,6	17,9	9,7	GC						
SK-4	SPT-3	4,50	10,1					30,2	25,7	24,4	16,0	8,4	SC						
SK-4	SPT-4	6,00	6,0					34,5	20,8	25,4	16,7	8,7	SC						
SK-4	SPT-6	9,00	15,6				✓	1,0	66,3	33,4	15,6	17,8	CL						
SK-4	UD-3	3,50																	
SK-4	UD-6	6,50																	

Table C.1 (Continued)

SK-5	SPT-1	1,00	25,2				✓	3,8	52,5	35,3	18,0	17,3	CL					
SK-5	SPT-2	2,00	18,4					18,4	48,2	36,2	17,7	18,5	SC					
SK-5	SPT-3	3,00	18,4				✓	4,1	51,3	33,5	17,2	16,3	CL					
SK-5	SPT-4	4,00	18,3				✓	3,2	51,5	36,4	17,8	18,6	CL					
SK-5	SPT-5	5,00	18,1				✓	10,4	52,9	33,5	17,2	16,3	CL					
SK-5	SPT-6	6,00	17,8					19,8	23,9		NP		SM					
SK-5	SPT-7	7,00	19,0					11,2	41,7		NP		SM					
SK-5	SPT-8	8,00	17,1					11,3	39,7		NP		SM					
SK-5	SPT-9	9,00	18,6					16,3	39,8		NP		SM					
SK-5	SPT-10	10,00	13,9					32,9	33,9	33,4	14,5	18,9	SC					
SK-5	SPT-11	11,00	12,9				✓	10,9	53,4	30,4	15,0	15,4	CL					
SK-5	SPT-12	12,00	17,8				✓	5,3	51,9	31,3	14,5	16,8	CL					
SK-5	SPT-13	13,00	12,6					19,3	40,9	31,3	14,9	16,4	SC					
SK-5	SPT-14	14,00	15,4				✓	7,7	52,4	28,2	14,6	13,6	CL					
SK-5	SPT-15	15,00	9,9					53,1	24,9		NP		GM					
SK-6	SPT-1	1,50	23,3				✓	0,0	86,5	49,6	21,1	28,5	CL					
SK-7	SPT-1	1,50																
SK-7	SPT-2	3,00	20,8				✓	2,2	61,9	39,1	20,0	19,1	CL					
SK-7	SPT-3	4,50	13,8					16,6	40,9	30,1	19,0	11,1	SC					
SK-7	SPT-4	6,00	11,5					38,1	25,8	38,2	19,0	19,2	GC					
SK-7	SPT-5	7,50	7,6					26,3	6,6	35,4	16,8	18,6	SC					

Table C.1 (Continued)

SK-7	SPT-6	9,00	16,2				✓	24,8	47,9	38,7	15,0	23,7	SC						
SK-7	SPT-7	10,50	9,4					43,4	9,6	53,4	20,5	32,9	SC						
SK-7	SPT-8	12,00	26,6				✓	0,8	71,6	51,1	22,0	29,1	CH						
SK-7	SPT-9	13,50	18,9				✓	26,1	44,5	34,3	14,4	19,9	SC						
SK-7	SPT-10	15,00	13,0					32,7	30,7	37,6	18,3	19,3	SC						
SK-7	UD-3	3,50	23,0	18,08	14,70	2,69	✓	1,5	57,8	51,3	23,6	27,7	CH	**1,505**	**0,280**			1,17	0,132
SK-7	UD-6	6,50	28,6	17,90	13,92	2,70	✓	0,5	71,1	63,9	25,4	38,5	CH	**1,108**	**0,233**			1,44	0,154
SK-8	SPT-1	1,50																	
SK-8	SPT-2	3,00	24,7				✓	0,0	77,1	60,1	22,3	37,8	CH						
SK-8	SPT-3	4,50																	
SK-8	SPT-4	6,00	22,2				✓	0,0	92,4	59,2	18,1	41,1	CH						
SK-8	SPT-5	7,50																	
SK-8	SPT-6	9,00	14,1				✓	0,4	64,0	59,8	22,9	36,9	CH						
SK-8	SPT-7	10,50																	
SK-8	SPT-8	12,00	12,3				✓	2,2	56,3	27,6	12,4	15,2	CL						
SK-8	SPT-9	13,50																	
SK-8	UD-3	3,50	16,2				✓	0,0	91,4	49,9	19,8	30,1	CL						
SK-8	UD-6	6,50	20,3				✓	0,0	86,2	49,4	19,4	30,0	CL						
SK-9	SPT-1	1,50																	
SK-9	SPT-2	3,00	22,6				✓	0,0	89,6	44,0	21,9	22,1	CL						
SK-9	SPT-3	4,50																	

Table C.1 (Continued)

SK-9	SPT-4	6,00	3,7				✓	14,6	50,5		NP		ML						
SK-9	SPT-5	7,50																	
SK-9	SPT-6	9,00	32,5					39,1	13,0		NP		SM						
İSK-1	SPT-1	1,50	26,7				✓	3,3	53,6	40,5	19,0	21,5	CL						
İSK-1	SPT-3	3,50	22,2				✓	2,3	64,9	37,6	18,9	18,7	CL						
İSK-1	SPT-5	5,50	15,9				✓	12,6	55,0	41,7	20,2	21,5	CL						
İSK-1	SPT-7	7,50	9,6					24,8	45,8	31,0	15,8	15,2	SC						
İSK-1	SPT-9	9,50	13,3				✓	0,0	85,2	53,2	22,6	30,6	CH						
İSK-1	SPT-11	11,50	21,6				✓	2,1	61,0	35,4	17,3	18,1	CL						
İSK-1	SPT-13	13,50	18,6					17,3	26,5	43,3	21,8	21,5	SC						
İSK-2	SPT-2	2,50	18,2				✓	0,8	71,9	48,6	23,7	24,9	CL						
İSK-2	SPT-4	4,50	15,5				✓	0,0	92,1	64,3	25,5	38,8	CH						
İSK-2	SPT-6	6,50	19,7				✓	0,0	89,6	63,4	30,0	33,4	CH						
İSK-2	SPT-8	8,50	29,9				✓	0,0	78,9	73,3	27,3	46,0	CH						
İSK-2	SPT-10	10,50	31,2				✓	0,0	86,3	63,9	27,1	36,8	CH						
İSK-2	SPT-12	12,50	21,9				✓	0,0	92,6	55,6	23,7	31,9	CH						
İSK-2	SPT-14	14,50	19,1				✓	0,5	73,6	53,6	23,9	29,7	CH						
İSK-2	SPT-16	16,50	19,4				✓	0,5	74,7	67,4	23,4	44,0	CH						
İSK-2	SPT-18	18,50	18,7				✓	0,0	92,9	66,2	27,3	38,9	CH						
İSK-2	SPT-20	20,50	11,1					24,4	40,5	33,1	16,2	16,9	SC						
İSK-2	SPT-22	22,50	15,0				✓	0,0	92,4	61,2	25,1	36,1	CH						

Table C.1 (Continued)

İSK-2	UD-7	7,00	7,8			2,55		33,4	39,1	35,9	26,9	9,0	GM						
İSK-3	SPT-2	2,50	26,1				✓	0,8	71,7	67,8	26,9	40,9	CH						
İSK-3	SPT-3	3,50	23,8				✓	1,9	74,6	58,6	22,7	35,9	CH						
İSK-3	UD-4	4,00	24,2	17,81	14,34	2,71	✓	0,0	91,9	67,7	23,8	43,9	CH					1,77	0,188
İSK-3	SPT-4	4,50	19,5				✓	0,0	88,6	78,8	24,1	54,7	CH						
İSK-3	SPT-5	5,50	13,3				✓	1,3	61,5	35,6	16,9	18,7	CL						
İSK-3	SPT-6	6,50	29,1				✓	0,4	75,3	56,7	23,8	32,9	CH						
İSK-3	SPT-8	8,50	19,0				✓	3,6	51,2	52,3	27,1	25,2	CH						
İSK-3	SPT-10	10,50	17,9				✓	0,0	88,3	80,4	26,6	53,8	CH						
İSK-3	SPT-12	12,50	17,3				✓	0,0	86,6	76,2	23,0	53,2	CH						
İSK-3	SPT-14	14,50	25,6				✓	0,0	83,1	45,3	22,6	22,7	CL						
İSK-3	SPT-16	16,50	32,0				✓	3,3	61,8	65,2	28,9	36,3	CH						
İSK-3	SPT-18	18,50	28,2				✓	1,0	65,8	42,0	24,2	17,8	CL						
İSK-3	SPT-20	20,50	33,7				✓	0,0	92,6	66,1	33,2	32,9	MH						
İSK-3	SPT-22	22,50	24,1				✓	0,0	78,6	53,6	21,5	32,1	CH						
İSK-3	SPT-24	24,50	20,4				✓	0,0	89,6	54,4	23,9	30,5	CH						
İSK-3	SPT-26	26,50	10,8					9,1	34,0	56,0	23,3	32,7	SC						
İSK-4	UD-2	2,00	21,0	18,10	14,96	2,66	✓	4,8	67,5	38,3	21,1	17,2	CL	**1,535**	**0,276**			0,73	0,076
İSK-4	SPT-2	2,50	20,6					36,4	14,9	36,9	16,4	20,5	SC						
İSK-4	SPT-4	4,50	15,3					17,5	38,4		NP		SM						
İSK-4	SPT-6	6,50	19,9					37,5	15,4	50,2	25,6	24,6	SC						

Table C.1 (Continued)

İSK-4	SPT-8	8,50	3,8					48,0	12,5		NP		GM						
İSK-5	UD-3	3,00	25,1	17,88	14,30	2,70	✓	0,0	86,6	54,8	26,5	28,3	CH	**1,246**	**0,233**			1,23	0,130
İSK-5	SPT-3	3,50	21,9				✓	0,0	80,9	42,1	19,0	23,1	CL						
İSK-5	SPT-4	4,50	22,3				✓	0,0	82,1	44,3	19,9	24,4	CL						
İSK-5	SPT-5	5,50	5,6					73,9	9,3		NP		GM						
İSK-5	SPT-7	7,50	15,6					42,1	18,5		NP		GM						
İSK-6	SPT-2	2,50	12,4					0,0	35,6	33,5	17,4	16,1	SC						
İSK-6	UD-3	3,00																	
İSK-6	SPT-4	4,50	18,0				✓	1,9	59,1	43,2	25,8	17,4	CL						
İSK-6	SPT-6	6,50	8,9					50,9	23,5	35,2	18,1	17,1	GC						
İSK-7	SPT-2	2,50	11,8				✓	0,7	61,9	40,8	19,0	21,8	CL						
İSK-7	UD-3	3,00	20,9	18,15	15,01	2,65	✓	2,3	59,1	47,9	22,3	25,6	CL	**1,319**	**0,237**			1,04	0,109
İSK-7	SPT-4	4,50	8,5					44,7	38,2	35,0	17,3	17,7	GC						
İSK-7	SPT-6	6,50	9,9					61,5	14,7		NP		GM						
İSK-8	SPT-2	2,50	27,5				✓	0,0	83,7	72,5	23,2	49,3	CH						
İSK-8	UD-3	3,00	21,0	17,95	14,84	2,69	✓	1,9	65,3	51,9	21,8	30,1	CH	**1,235**	**0,220**			1,31	0,137
İSK-8	SPT-3	3,50	20,8				✓	1,3	66,2	51,7	20,6	31,1	CH						
İSK-8	UD-4	4,00																	
İSK-8	SPT-4	4,50	35,0				✓	0,6	65,7	51,2	22,2	29,0	CH						
İSK-8	SPT-5	5,50	22,2				✓	0,0	90,6	48,6	21,2	27,4	CL						
İSK-8	UD-6	6,00																	

Table C.1 (Continued)

İSK-8	SPT-6	6,50	15,8				✓	0,0	76,6	31,3	16,1	15,2	CL					
İSK-8	SPT-7	7,50	16,6				✓	0,0	91,9	56,7	17,4	39,3	CH					
İSK-8	SPT-8	8,50	23,2				✓	2,3	65,9	61,0	20,7	40,3	CH					
İSK-8	SPT-12	12,50	11,9					36,7	32,7	29,0	14,8	14,2	GC					
İSK-8	SPT-14	14,50	19,0				✓	0,0	83,0	40,1	20,0	20,1	CL					
İSK-8	SPT-16	16,50	18,7				✓	0,0	89,5	41,4	21,1	20,3	CL					
İSK-8	SPT-18	18,50	18,4				✓	0,0	85,3	37,4	20,2	17,2	CL					
İSK-9	SPT-2	2,50	19,5				✓	0,0	85,2	51,4	25,5	25,9	CH					
İSK-9	SPT-4	4,50	20,6				✓	0,8	64,3	40,5	21,2	19,3	CL					
İSK-9	SPT-6	6,50	3,0					7,8	41,7		NP		SM					
İSK-10	SPT-2	2,50	19,6				✓	2,4	60,6	54,9	23,0	31,9	CH					
İSK-10	SPT-4	4,50	17,6				✓	3,2	57,2	34,9	19,5	15,4	CL					
İSK-10	SPT-6	6,50	10,7				✓	1,3	71,9	33,6	16,0	17,6	CL					
İSK-10	SPT-8	8,50	10,7					36,7	23,7	30,1	14,5	15,6	SC					
İSK-10	SPT-10	10,50	25,1				✓	1,5	65,8	59,6	21,7	37,9	CH					
İSK-10	SPT-12	12,50	27,8				✓	0,0	87,3	64,7	20,4	44,3	CH					
İSK-10	SPT-14	14,50	29,2				✓	0,0	89,1	53,6	23,6	30,0	CH					
İSK-10	SPT-16	16,50	21,2				✓	0,0	87,6	69,6	23,7	45,9	CH					
İSK-10	SPT-18	18,50	22,3				✓	0,0	91,6	44,4	21,6	22,8	CL					
İSK-10	SPT-20	20,50	24,8				✓	0,0	90,6	56,4	22,6	33,8	CH					
İSK-11	SPT-2	2,50	14,2				✓	0,0	81,1	61,6	24,9	36,7	CH					

Table C.1 (Continued)

İSK-11	UD-3	3,00																	
İSK-11	SPT-3	3,50	21,8				✓	0,6	74,4	61,4	28,7	32,7	CH						
İSK-11	SPT-4	4,50	22,3				✓	0,0	75,6	70,4	25,9	44,5	CH						
İSK-11	SPT-5	5,50	24,5				✓	0,0	82,1	73,4	24,7	48,7	CH						
İSK-11	UD-6	6,00																	
İSK-11	SPT-6	6,50	23,5				✓	0,0	82,6	52,6	21,8	30,8	CH						
İSK-11	SPT-7	7,50	27,6				✓	0,0	91,9	74,4	25,9	48,5	CH						
İSK-11	SPT-8	8,50	18,9				✓	0,8	66,6	60,2	23,3	36,9	CH						
İSK-11	SPT-9	9,50	11,4				✓	2,6	57,5	37,1	18,4	18,7	CL						
İSK-11	SPT-10	10,50	19,9				✓	0,4	72,6	61,4	25,8	35,6	CH						
İSK-11	SPT-11	11,50	18,7				✓	0,0	89,2	65,2	25,8	39,4	CH						
İSK-11	SPT-12	12,50	19,0				✓	0,0	84,2	69,8	22,7	47,1	CH						
İSK-11	SPT-13	13,50	10,0				✓	4,7	51,2	40,0	17,3	22,7	CL						
İSK-11	SPT-14	14,50	27,4				✓	0,0	82,3	58,9	25,6	33,3	CH						
İSK-11	SPT-15	15,50	17,6				✓	1,5	73,6	55,8	22,9	32,9	CH						
İSK-11	SPT-16	16,50	17,5				✓	0,0	91,9	44,2	21,0	23,2	CL						
İSK-11	SPT-17	17,50	20,2				✓	0,0	82,2	61,4	30,6	30,8	CH						
İSK-11	SPT-18	18,50	17,0				✓	0,0	87,5	67,9	23,8	44,1	CH						
İSK-11	SPT-19	19,50	26,5				✓	0,9	69,9	59,1	22,6	36,5	CH						
İSK-12	SPT-2	2,50	16,2					29,0	47,6	43,8	21,6	22,2	GC						
İSK-12	SPT-4	4,50	27,5					6,7	47,4	50,6	24,2	26,4	SC						

Table C.1 (Continued)

İSK-12	SPT-6	6,50	17,0					41,4	24,4	41,2	20,7	20,5	GC					
İSK-12	SPT-8	8,50	18,4				✓	4,7	52,2	37,0	19,6	17,4	CL					
İSK-12	SPT-10	10,50	15,9				✓	2,8	57,9	41,2	19,6	21,6	CL					
İSK-12	SPT-14	14,50	0,8					10,2	33,9		NP		SM					
İSK-12	SPT-16	16,50	12,1					40,9	29,5	40,2	21,4	18,8	GC					
İSK-12	SPT-18	18,50	24,5				✓	1,1	70,2	59,7	27,6	32,1	CH					
İSK-12	SPT-20	20,50	13,3					47,1	17,6	37,3	18,4	18,9	GC					
İSK-12	SPT-22	22,50	22,2				✓	0,0	81,7	77,4	25,9	51,5	CH					
İSK-13	SPT-2	2,50	17,2				✓	3,2	59,9	39,6	18,3	21,3	CL					
İSK-13	UD-3	3,00																
İSK-13	SPT-3	3,50	24,6				✓	0,0	81,0	53,2	24,6	28,6	CH					
İSK-13	UD-4	4,00																
İSK-13	SPT-4	4,50	22,3				✓	1,9	70,0	48,4	22,6	25,8	CL					
İSK-13	SPT-5	5,50	15,9				✓	2,4	69,9	51,1	21,5	29,6	CH					
İSK-13	UD-6	6,00																
İSK-13	SPT-6	6,50	8,0					37,8	27,8	34,9	16,9	18,0	GC					
İSK-13	SPT-7	7,50	9,2				✓	14,9	69,0		NP		ML					
İSK-13	SPT-8	8,50	10,5					36,8	27,2	27,6	13,1	14,5	GC					
İSK-13	SPT-9	9,50	36,0				✓	0,0	89,5	65,5	27,3	38,2	CH					
İSK-13	SPT-10	10,50	24,7				✓	0,8	72,3	46,0	20,9	25,1	CL					
İSK-13	SPT-11	11,50	30,5				✓	3,1	56,7	50,2	21,4	28,8	CH					

Table C.1 (Continued)

İSK-13	SPT-12	12,50	21,9				✓	1,5	65,0	39,4	21,3	18,1	CL					
İSK-13	SPT-13	13,50	21,8				✓	0,0	80,0	37,4	20,0	17,4	CL					
İSK-13	SPT-14	14,50	21,5				✓	1,9	69,1	52,0	20,1	31,9	CH					
İSK-13	SPT-15	15,50	21,3				✓	0,0	83,8	45,2	21,7	23,5	CL					
İSK-13	SPT-16	16,50	22,1				✓	0,0	86,8	52,6	21,9	30,7	CH					
İSK-13	SPT-17	17,50	22,2				✓	0,8	68,0	39,2	19,5	19,7	CL					
İSK-13	SPT-18	18,50	22,3				✓	1,0	69,7	46,9	19,0	27,9	CL					
İSK-13	SPT-19	19,50	24,0				✓	1,1	69,8	45,8	23,7	22,1	CL					
İSK-13	SPT-20	20,50	21,1				✓	0,0	91,9	68,7	22,8	45,9	CH					
İSK-13	SPT-21	21,50	25,7				✓	2,2	63,1	44,4	20,1	24,3	CL					
İSK-13	SPT-22	22,50	26,6				✓	0,9	65,0	48,2	23,0	25,2	CL					
İSK-13	SPT-23	23,50	24,6				✓	1,0	73,1	65,1	19,9	45,2	CH					
İSK-13	SPT-24	24,50	24,2				✓	0,0	81,6	61,4	22,6	38,8	CH					
İSK-13	SPT-31	31,50	24,6				✓	0,0	81,8	66,0	23,8	42,2	CH					

APPENDIX D

CONSOLIDATION TEST RESULTS AND PLOTS

CONSOLIDATION TEST RESULTS (4 kg Load)

CONSOLIDATION MEASUREMENTS			
Dial Gauge Measurement		Square root time	Reference Points
0,00	0	0,000	6000
145,00	1450	0,316	4550
150,00	1500	0,548	4500
151,00	1510	0,707	4490
153,00	1530	1,000	4470
154,00	1540	1,118	4460
155,00	1550	2,000	4450
156,00	1560	2,500	4440
156,60	1566	3,000	4434
157,00	1570	4,000	4430
157,40	1574	5,000	4426
157,90	1579	6,000	4421
158,20	1582	7,000	4418
158,60	1586	8,000	4414
158,90	1589	9,000	4411
159,20	1592	10,000	4408
159,80	1598	11,000	4402
160,00	1600	15,492	4400
161,00	1610	23,238	4390
162,00	1620	37,947	4380

TIME CALCULATION		
Second	Minute	Square root time
0	0	0
6	0,10	0,316
18	0,30	0,548
30	0,50	0,707
60	1,00	1
75	1,25	1,118
240	4,00	2
375	6,25	2,5
540	9,00	3
960	16,00	4
1500	25,00	5
2160	36,00	6
2940	49,00	7
3840	64,00	8
4860	81,00	9
6000	100,00	10
7260	121,00	11
14400	240,00	15,492
32400	540,00	23,238
86400	1440,00	37,947

A= 2,4	
B= 2,8	B=(A*1,15)
C= 1,5	Intersection Point
D= 135,0	D=(C²*60)
T90= 135,0	

t50=T90/4,28
tf=50*T50
dr=df/tf
dr=0,0076

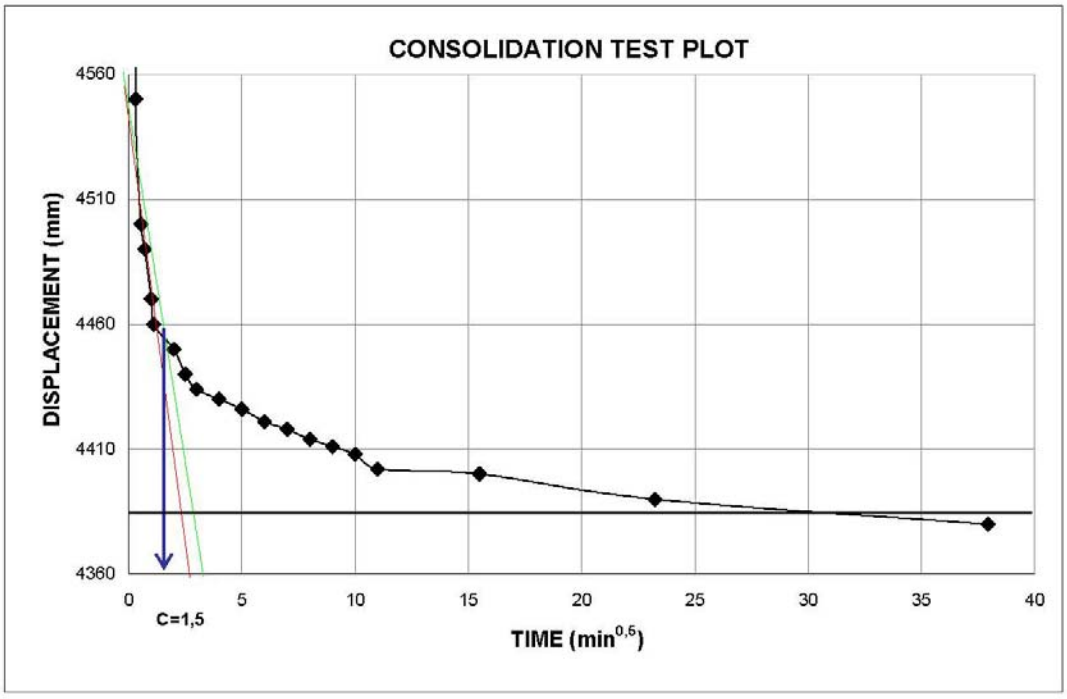

Figure D.1 Consolidation test results and plot for 4 kg

CONSOLIDATION TEST RESULTS (8 kg Load)

CONSOLIDATION MEASUREMENTS			
Dial Gauge Measurement		Square root time	Reference Points
0,00	0	0,000	6000
252,00	2520	0,316	3480
257,40	2574	0,548	3426
261,50	2615	0,707	3385
266,96	2670	1,000	3330
267,10	2671	1,118	3329
269,10	2691	2,000	3309
269,80	2698	2,500	3302
270,20	2702	3,000	3298
271,20	2712	4,000	3288
272,80	2728	5,000	3272
273,90	2739	6,000	3261
275,10	2751	7,000	3249
276,60	2766	8,000	3234
277,00	2770	9,000	3230
278,40	2784	10,000	3216
279,60	2796	11,000	3204
280,10	2801	15,492	3199
280,90	2809	23,238	3191
281,60	2816	37,947	3184

TIME CALCULATION		
Second	Minute	Square root time
0	0	0
6	0,10	0,316
18	0,30	0,548
30	0,50	0,707
60	1,00	1
75	1,25	1,118
240	4,00	2
375	6,25	2,5
540	9,00	3
960	16,00	4
1500	25,00	5
2160	36,00	6
2940	49,00	7
3840	64,00	8
4860	81,00	9
6000	100,00	10
7260	121,00	11
14400	240,00	15,492
32400	540,00	23,238
86400	1440,00	37,947

A= 1,5	
B= 1,8	B=(A*1,15)
C= 1,2	Intersection Point
D= 86,4	D=(C²*60)
T90= 86,4	

t50=T9O/4,28
tf=50*T50
dr=df/tf
dr=0,0019

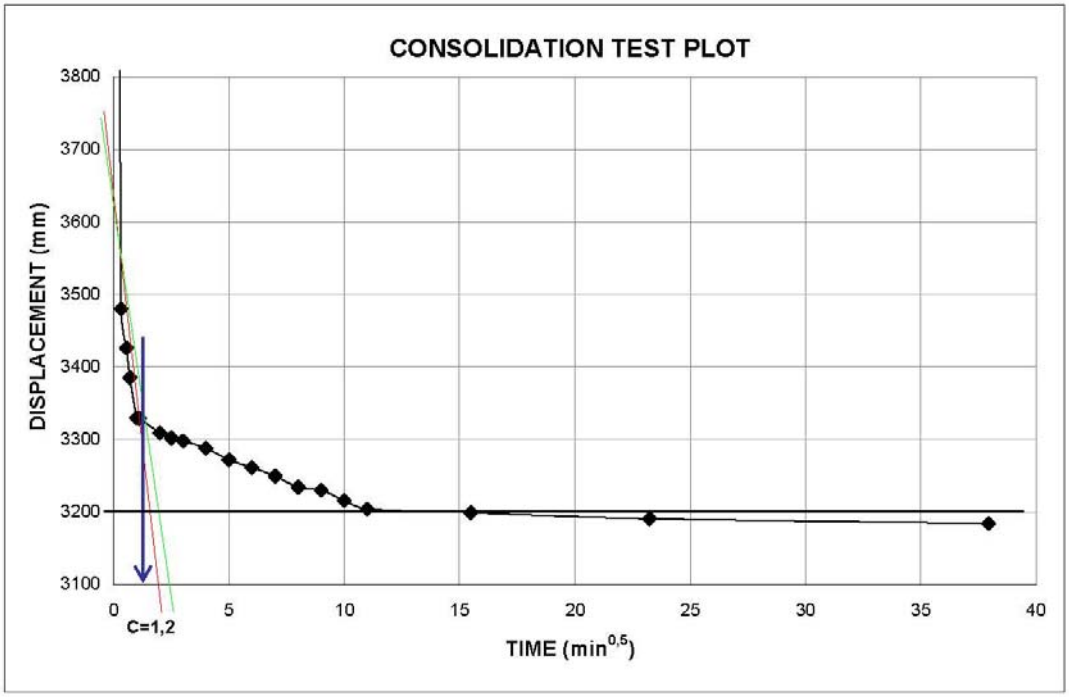

Figure D.2 Consolidation test results and plot for 8 kg

CONSOLIDATION TEST RESULTS (16 kg Load)

CONSOLIDATION MEASUREMENTS			
Dial Gauge Measurement		Square root time	Reference Points
0,00	0	0,000	5000
361,10	3611	0,316	2389
367,80	3678	0,548	2322
373,20	3732	0,707	2268
375,80	3758	1,000	2242
378,50	3785	1,118	2215
381,50	3815	2,000	2185
384,00	3840	2,500	2160
385,90	3859	3,000	2141
386,60	3866	4,000	2134
387,50	3875	5,000	2125
389,90	3899	6,000	2101
392,20	3922	7,000	2078
394,60	3946	8,000	2054
396,60	3966	9,000	2034
397,80	3978	10,000	2022
398,80	3988	11,000	2012
399,90	3999	15,492	2001
400,10	4001	23,238	1999
400,80	4008	37,947	1992

TIME CALCULATION		
Second	Minute	Square root time
0	0	0
6	0,10	0,316
18	0,30	0,548
30	0,50	0,707
60	1,00	1
75	1,25	1,118
240	4,00	2
375	6,25	2,5
540	9,00	3
960	16,00	4
1500	25,00	5
2160	36,00	6
2940	49,00	7
3840	64,00	8
4860	81,00	9
6000	100,00	10
7260	121,00	11
14400	240,00	15,492
32400	540,00	23,238
86400	1440,00	37,947

A= 2,1	
B= 2,4	B=(A*1,15)
C= 1,1	Intersection Point
D= 72,6	D=(C²*60)
T90= 72,6	

t50=T9O/4,28
tf=50*T50
dr=df/tf
dr=0,0014

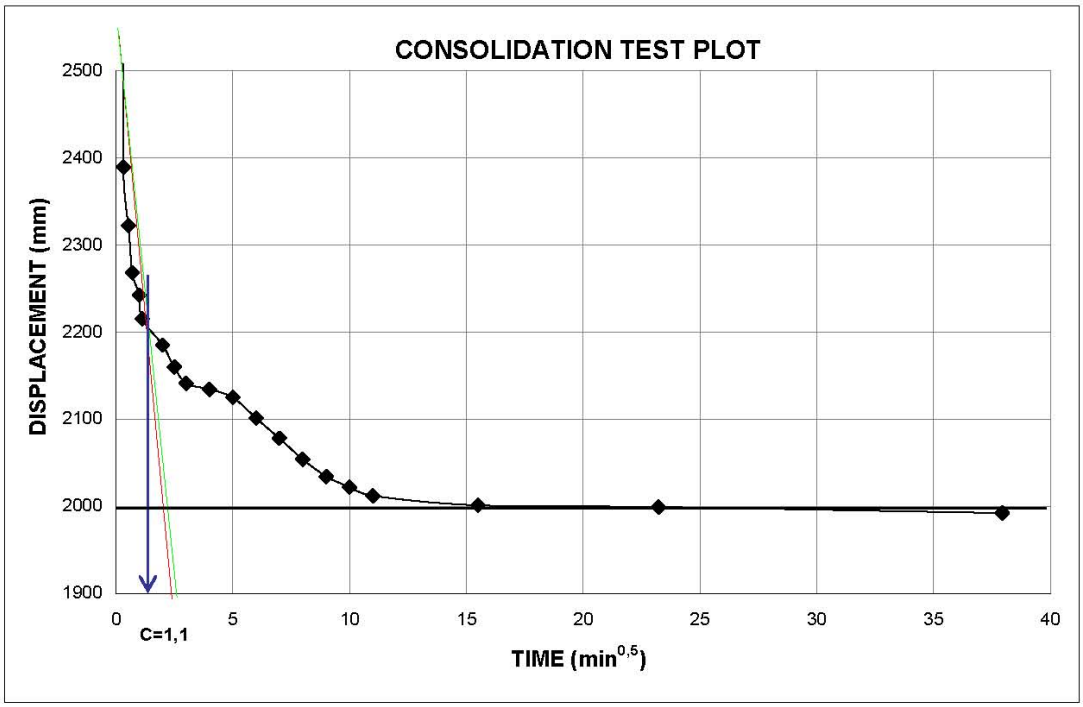

Figure D.3 Consolidation test results and plot for 16 kg